



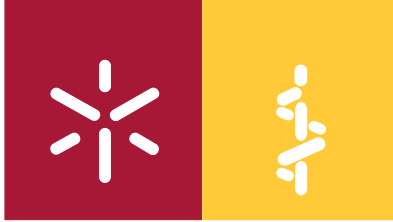
Universidade do Minho
Escola de Ciências da Saúde

Ana Maria Macedo Mesquita

New insights into the effects of caloric restriction on *Saccharomyces cerevisiae* chronological lifespan

Novas perspectivas no efeito da restrição calórica na longevidade cronológica em *Saccharomyces cerevisiae*





Universidade do Minho

Escola de Ciências da Saúde

Ana Maria Macedo Mesquita

New insights into the effects of caloric restriction on *Saccharomyces cerevisiae* chronological lifespan

Novas perspectivas no efeito da restrição calórica na longevidade cronológica em *Saccharomyces cerevisiae*

Tese de Doutoramento em Ciências da Saúde
Especialidade de Ciências da Saúde

Trabalho efectuado sobre a orientação da
Doutora Paula Cristina da Costa Alves Monteiro Ludovico
Professora Auxiliar da Escola de Ciências da Saúde
Universidade do Minho

e co-orientação do
Doutor Fernando José dos Santos Rodrigues
Professor Auxiliar da Escola de Ciências da Saúde
Universidade do Minho

Julho de 2011

Nome: Ana Maria Macedo Mesquita

Endereço electrónico: ammesquita@ecsau.de.uminho.pt

Telefone: +351 962783734

N.º do Bilhete de Identidade: 10843852

Título da Tese de Doutoramento:

New insights into the effects of caloric restriction on *Saccharomyces cerevisiae* chronological lifespan

Novas perspectivas no efeito da restrição calórica na longevidade cronológica em *Saccharomyces cerevisiae*

Orientador:

Doutora Paula Cristina da Costa Alves Monteiro Ludovico

Co-orientador:

Doutor Fernando José dos Santos Rodrigues

Ano de conclusão: 2011

Ramo de Conhecimento do Doutoramento:

Ciências da Saúde

DE ACORDO COM A LEGISLAÇÃO EM VIGOR, NÃO É PERMITIDA A REPRODUÇÃO DE QUALQUER PARTE DESTA TESE/TRABALHO

Universidade do Minho, 01/07/11

Assinatura: _____



A tese de doutoramento aqui apresentada foi desenvolvida no âmbito de financiamento pela Fundação para a Ciência e Tecnologia (FCT) através de uma bolsa individual de doutoramento, com a referência SFRH/BD/32464/2006 no âmbito do QREN - POPH - Tipologia 4.1 - Formação Avançada, participado pelo Fundo Social Europeu e por fundos nacionais do MCTES. O trabalho aqui apresentado foi realizado com o co-financiamento da FCT (PTDC/BIA-MIC/114116/2009).

AGRADECIMENTOS / ACKNOWLEDGMENTS

A elaboração desta tese não teria sido possível sem a colaboração, estímulo e amizade de diversas pessoas. Gostaria, por este facto, de expressar toda a minha sincera gratidão e apreço a todos aqueles que, directa ou indirectamente, contribuíram para a concretização deste trabalho.

À Professora Doutora Paula Ludovico, que prontamente aceitou a orientação deste trabalho. Agradeço todo o apoio, ensinamentos e disponibilidade, bem como a confiança que depositou em mim no decorrer destes anos. Muito obrigada Paula!

Ao meu co-orientador Professor Doutor Fernando Rodrigues, que desde início aceitou fazer parte deste projecto. Agradeço todos os ensinamentos e sugestões partilhados no decorrer deste percurso.

Um agradecimento especial é devido à Professora Doutora Cecília Leão, directora do Instituto de Investigação em Ciências da Vida e da Saúde da Universidade do Minho, pela oportunidade de realizar o meu trabalho nesta instituição de excelência. Agradeço todo o apoio, o incentivo, a confiança e a amizade que sempre demonstrou para comigo.

Ao Professor Doutor Vítor Costa, pela colaboração, apoio e incentivo, bem como pelo modo como prontamente me acolheu e integrou no seu grupo no IBMC onde vivi momentos muito enriquecedores.

I would like to acknowledge Professor William Burhans for collaborating and sharing his expertise with us. Professor Bill, it was a real pleasure working with you!

À Professora Doutora Elsa Logarinho, por todo o apoio e colaboração, pelo incentivo e especialmente pela amizade que sempre demonstrou.

À Fundação para a Ciência e Tecnologia por me ter concedido a bolsa de doutoramento com a referência SFRH/BD/32464/2006 que me financiou durante estes 4 anos.

A todos os professores, funcionários e colegas do ICVS e do IBMC, em especial aos colegas do ID9, I3.01, MIRD's e MCA's, pelo apoio e bons momentos partilhados ao longo destes anos. Obrigada a todos!

Especialmente a vocês, queridos amigos e família, pela presença nos momentos mais exigentes que marcaram estes anos. Sob pena de não conseguir transmitir toda a minha gratidão nesta frase, terei todo o prazer em retribuir a vossa amizade, carinho e amor ao longo das nossas vidas! Obrigada mãe!

ABSTRACT / RESUMO

ABSTRACT

The aging of the population is one of the major transformations being experienced by most developed countries over the last century. Although the increase in lifespan expectancy can be seen as a success story for public health policies and for socio-economic development, it also challenges the society to adapt and promote health and functional capacity of older people. In this scenario, the understanding of human aging has become one of the most relevant challenges in the modern science. The study of aging has been wrapped up in several theories that attempt to identify the primary causes of the stereotypic changes that are observed with age trying to explain the dynamic nature of the aging process. Conventionally, aging is seen as a process of progressive decline of homeostasis caused by genetic and environmental events. However, the degree to each theoretical cause contributes to elucidate the primary cause of aging has been difficult to establish and, instead, aging is considered an extremely complex process driven by a variety of different mutually interacting mechanisms.

According to the leading and longstanding "Free Radical Theory of Aging" proposed by Denham Harman, in 1956, aging is the result of the damage caused by free radical reactions that occur in the cell. In support to this theory, several studies have shown that increases in lifespan, mediated by genetic and environmental manipulations, are associated with decreases in the levels of intracellular reactive oxygen species (ROS) and oxidative stress. However, it has also been suggested that lifespan extension may be associated with increases in the intracellular levels of ROS and oxidative stress and that the overexpression of antioxidant defences does not always result in a significant extension of lifespan. Thus, increasing evidence started to challenge Harman's theory and have proposed a puzzling involvement of ROS and/or oxidative stress in the aging process.

A particularly active area of aging research has been the influence of diet on longevity and age-related diseases. Since the pioneering work of McCay in 1935 in rodents, caloric restriction (CR) has repeatedly been shown to extend lifespan and to promote beneficial health effects in several model systems. The predictable results of CR in primate models, and inclusively in humans, have supported the potential of alternatives to CR in the improvement of health and longevity including the rapidly growing area of calorie restriction mimetics (CRM) research. However, despite all the background for the benefits observed with CR, the molecular mechanisms underlying the CR effects in lifespan extension and aging delay remain enigmatic.

The use of simple systems with short lifespan, considerable genetic plasticity and easy manipulation of diet still remains an advantage towards the study of highly conserved

genes/pathways that underlie the effects of CR. By providing two aging paradigms, *Saccharomyces cerevisiae* stands for a unique opportunity to compare and contrast the aging processes of both proliferating and non-proliferating cells in a simple single-celled organism and, thus, to understand the aging mechanisms of mitotic and post-mitotic tissues in higher organisms. The rapidity with which lifespan can be assessed in yeast cells as well as their easy manipulation, has allowed the identification of a lifespan regulatory network. In this context, longevity regulation has been suggested to involve parallel but partially connected signaling pathways controlled by sirtuins, nutrient-sensing signaling pathways and intracellular oxidative status. Nevertheless, the mechanistic details underlying such regulation in the CR-mediated extension of yeast lifespan are far from being established.

This work aimed to study the involvement of ROS and oxidative stress in the chronological lifespan (CLS)-extending effects of CR in *S. cerevisiae*. The results obtained show that the CLS-extending effects of CR are coupled to increase, rather than decrease, in the accumulation of intracellular ROS. Furthermore, CR or inactivation of catalases were shown to promote ROS accumulation in the form of H₂O₂, which increased longevity despite the oxidative damage of macromolecules. Upon CR or inactivation of H₂O₂-detoxifying systems, H₂O₂ levels induced superoxide dismutases which reduce the levels of O₂⁻. Increased oxidative stress during CR in the form of H₂O₂ was also suggested by the high sensitivity to H₂O₂ treatment observed in wild type-CR cells. Nevertheless, the exposure of non-CR wild type cells to non-toxic concentrations of H₂O₂ resulted in CLS extension. A pro-longevity role for H₂O₂ was also suggested to be independent of the activation of protective cellular processes by nutrient-sensing pathways signaling. For instance, in $\Delta rim15$ cells the CLS-extending effect of CR was also shown to be promoted by H₂O₂ increases and O₂⁻ reduction comparatively to wild type cells. A different approach in which CR was modelled by the inactivation of specific steps of the glycolytic pathway also revealed that CLS extension occurred in parallel with increases in H₂O₂ and decreases in O₂⁻ levels. However, a strain displaying reduced glucose uptake showed CLS extension associated with decreases in the accumulation of intracellular ROS levels, rather than an increase in H₂O₂, and increases in oxidative stress resistance.

Overall, results herein presented challenge the validity of Harman's theory and provide a different paradigm for understanding how oxidative stress, and specific forms of ROS, may impact on the aging process. It is proposed that CR may mediate an hormesis-like response in which H₂O₂ might be positively acting as second messenger molecule in other pathways operating under yeast CLS extension. In this scenario, *S. cerevisiae* re-emerges as a suitable model by adding new insights into the understanding of aging in more complex organisms.

RESUMO

O envelhecimento da população é um processo que tem sido observado na maioria dos países desenvolvidos ao longo do último século. O aumento da esperança de vida pode ser visto como resultado do sucesso das políticas de saúde pública e do desenvolvimento socio-económico, no entanto, desafia também a sociedade a adaptar-se e a promover melhores condições de saúde bem como a capacidade funcional dos idosos. Neste âmbito, o estudo do envelhecimento tornou-se um dos desafios mais relevantes para a ciência moderna. Várias teorias têm procurado identificar a principal causa do envelhecimento e das alterações fisiológicas observadas com a idade. Convencionalmente, o envelhecimento é visto como um processo de declínio progressivo da homeostasia celular regulado por factores genéticos e ambientais. No entanto, a contribuição de cada teoria na identificação de uma causa primordial do envelhecimento tem sido difícil de estabelecer e, desta forma, o envelhecimento é considerado um processo complexo governado pela interacção de diferentes processos. De acordo com a "Teoria dos Radicais Livres" proposta por Denham Harman, em 1956, o envelhecimento resulta dos danos celulares resultantes da acção dos radicais livres. Diversos estudos suportam essa teoria tendo demonstrado que o aumento da longevidade, promovido por manipulações genéticas e ambientais, está associado à diminuição dos níveis intracelulares de espécies reactivas de oxigénio (ROS) e de stresse oxidativo. No entanto, tem sido também sugerido que a extensão da longevidade pode estar associada a um aumento dos níveis de ROS e de stresse oxidativo, e que a sobre-expressão de defesas antioxidantes nem sempre resulta num aumento significativo da longevidade. Estes estudos desafiam a teoria de Harman propondo um novo envolvimento dos ROS e do stresse oxidativo no processo de envelhecimento.

O estudo da influência da dieta na longevidade e no aparecimento de doenças associadas à idade tem sido uma área de intensa investigação. Desde o trabalho pioneiro de McCay em 1935, inúmeros estudos sugerem que a restrição calórica (CR) pode prolongar a longevidade e ter efeitos benéficos na saúde de vários organismos modelo. Estudos em primatas, incluindo humanos, sugerem que abordagens que mimetizam a CR (CRM, *caloric restriction mimetics*) poderão constituir estratégias relevantes na melhoria da saúde e no aumento da longevidade. No entanto, os mecanismos moleculares que regulam os efeitos da CR no aumento da longevidade e no atraso do envelhecimento permanecem ainda enigmáticos.

O uso de seres menos complexos com ciclos de vida curtos e de fácil manipulação genética é considerado uma vantagem no estudo de genes/vias filogeneticamente conservados e que regulam os efeitos da CR. Apresentado dois modelos de envelhecimento, a levedura *Saccharomyces*

cerevisiae representa um modelo único para comparar e contrastar os processos de envelhecimento de células proliferativas e não proliferativas e, por extrapolação, compreender os mecanismos de envelhecimento em tecidos mitóticos e pós-mitóticos de organismos superiores. *S. cerevisiae* permitiu a identificação de vários mecanismos envolvidos na regulação da longevidade que são controlados por sirtuínas, cinases de resposta aos nutrientes e pelo estado redox da célula. No entanto, os efeitos da CR na extensão da longevidade estão ainda pouco estabelecidos.

Neste âmbito, o presente trabalho teve como objectivo estudar o envolvimento dos ROS e do stress oxidativo durante o aumento da longevidade cronológica na levedura *S. cerevisiae*, promovida pela CR. Os resultados obtidos sugerem que os efeitos da CR no aumento da longevidade estão associados a um aumento, e não a uma diminuição, dos níveis intracelulares de ROS. Demonstrou-se que a CR bem como a inactivação de catalases, apesar de induzirem um aumento de ROS na forma de H_2O_2 , promovem a longevidade. Por outro lado, observou-se que o aumento dos níveis de H_2O_2 promove a actividade das superóxido dismutases e consequente redução dos níveis de O_2^- . Apesar de a CR ter conferido às células uma maior sensibilidade ao stress oxidativo sob a forma de H_2O_2 , verificou-se que concentrações não tóxicas de H_2O_2 promovem um aumento da longevidade em células não sujeitas a CR. Estudos adicionais mostraram ainda que o envolvimento do H_2O_2 na extensão da longevidade é independente da activação de processos celulares de defesa mediada por cinases de resposta aos nutrientes. neste contexto, os resultados demonstraram que, à semelhança do que foi observado em células de tipo selvagem, o efeito da CR no aumento da longevidade está também está associado a aumentos nos níveis de H_2O_2 e à redução nos níveis de O_2^- em células $\Delta rim15$. A extensão da longevidade associada a aumentos dos níveis de H_2O_2 e diminuição de O_2^- foi também ainda observada quando a CR foi induzida pela inibição genética de etapas específicas da via glicolítica. No entanto, o efeito da CR induzido pela redução do transporte de glucose através da célula mostrou estar associado a uma diminuição dos níveis dos ROS, e não a um aumento dos níveis de H_2O_2 , bem como a um aumento da resistência ao stress oxidativo. Deste modo, os resultados apresentados sugerem que a CR pode mediar um efeito hormético do H_2O_2 que, actuando na sinalização de processos celulares específicos, é um factor determinante na regulação da longevidade cronológica na levedura. Desta forma, é questionada a teoria de Harman e sugere-se um paradigma diferente para a compreensão do envolvimento do stress oxidativo, e de formas específicas de ROS, na regulação da longevidade. Neste cenário, *S. cerevisiae* mostrou, mais uma vez, ser um modelo adequado e promissor na compreensão do envelhecimento em organismos mais complexos.

CONTENTS

List of tables and figures.....	xvii
Abbreviations list.....	xxi
Objectives and outline of the thesis.....	1
Chapter 1. Introduction.....	5
1. Study of aging: lessons from model systems.....	7
1.1 Longevity regulation by the conserved nutrient-sensing signaling pathways.....	10
2 Theories of aging.....	16
2.1 "Free Radical Theory of Aging".....	21
3. Longevity regulation by caloric restriction.....	25
3.1 CR effects in longevity: linking nutrient-sensing and antioxidant defences.....	28
3.2 Caloric restriction effects in <i>S. cerevisiae</i> life span extension.....	30
3.3 Calorie restriction mimetics (CRM)	33
Chapter 2. Materials and methods.....	35
1. Strains.....	37
1.1 Generation of <i>rho0</i> strains and verification by DAPI staining.....	38
2. Media.....	38
3. Chronological lifespan assay.....	38
4. Construction of the <i>CTA1</i> overexpressing and <i>CTA1CTT1</i> double mutant strains.....	39
5. Pharmacological inhibition treatments.....	39
6. FACS analysis of intracellular reactive oxygen species.....	40
7. Protein extract preparation, superoxide dismutase, and catalase activity assays.....	41
8. Western-blot analysis.....	42
9. Determination of oxidative damage.....	42
10. Epifluorescence and confocal microscopy.....	43
11. Statistical analysis.....	43
Chapter 3. Results and discussion.....	45
1. CR extends CLS associated with increases in ROS.....	48
1.1 CR extends <i>S. cerevisiae</i> CLS associated with increases in H ₂ O ₂	49
1.2 Peroxisomes and mitochondria are involved in the CLS-extending effects of CR.....	52
1.3 Inactivation of catalases mimics the CLS extending effects of CR.....	59
1.4 Increased H ₂ O ₂ induces superoxide dismutase activity	69
1.5 Increased H ₂ O ₂ is associated with oxidative damage to macromolecules.....	73
1.6 Ectopic exposure of cells to H ₂ O ₂ mimics CLS-extending effects of CR.....	75
2. CLS extension by CR mimetics might be associated with increases in ROS	79
2.1 Reduced glucose uptake extends CLS associated with decreases in ROS.....	82
2.2 Inactivation of specific glycolytic steps CLS associated with increases in H ₂ O ₂	87
2.3 Reduced growth signaling extends CLS associated with increases in H ₂ O ₂	88
Chapter 4. Concluding remarks and future perspectives.....	93
References.....	101
Attachments.....	117

LIST OF TABLES AND FIGURES

LIST OF TABLES AND FIGURES

Pg. CHAPTER 1 - Introduction

- 10 **Figure 1** - Two aging paradigms in yeast cells.
- 12 **Figure 2** - Longevity is regulated by major nutrient-sensing signaling pathways including TOR-S6K, RAS-AC-PKA and the insulin/insulin growth factor 1-like (Ins/IGF-1-like) pathway.
- 18 **Figure 3** - In the last century, different theories have been presented in the light of the existing discoveries from evolutionary, genomic and molecular genetic studies on aging and longevity.
- 20 **Figure 4** - Aging is regulated by a multiplicity of mechanisms which operate at different biological levels.
- 21 **Figure 5** - Sources of reactive oxygen species (ROS), key metabolic pathways, enzymes for these species and resulted cellular damage.
- 26 **Figure 6** - Experiments on dietary restriction and genetic or chemical alteration of nutrient-sensing signaling pathways have been shown to extend lifespan from yeast to humans.
- 27 **Figure 7** - A caloric restriction diet promotes a healthier phenotype when compared to normal diet conditions.

CHAPTER 2 - Materials and Methods

- 37 **Table 1** - *Saccharomyces cerevisiae* strains used in this study.

CHAPTER 3 - Results and discussion

- 68 **Table 1** - pH of aging cultures
- 50 **Figure 1** - CR (0.05% and 0.5% glucose) extends *S. cerevisiae* CLS comparatively to non-CR conditions (2% glucose).
- 51 **Figure 2** - The CLS-extending effects of CR occur in parallel with increased levels of intracellular ROS accumulation in *S. cerevisiae* wild type cells.
- 53 **Figure 3** - CR extends CLS of *S. cerevisiae* BY4742 *rho0* cells in SC medium associated with increased intracellular ROS levels
- 55 **Figure 4** - Impaired peroxisomal function extends *S. cerevisiae* CLS associated with increases in intracellular ROS levels, in severe (0.05% glucose) and non-CR (2% glucose), but not in moderate CR (0.5% glucose).
- 57 **Figure 5** - Cta1p is not co-localized to mitochondria during the *S. cerevisiae* CLS-extending effects of CR.
- 59 **Figure 6** - CR promotes increases in the ratio of Pex14p/Porin protein expression in *S. cerevisiae* cells.
- 60 **Figure 7** - CR induces the activity of both peroxisomal (Cta1p) and cytosolic catalase (Ctt1p) in wild type, *rho0*, $\Delta pex13$, $\Delta pex14$ and oleate grown *S. cerevisiae* cells (BY4742 background) during CLS, although more evident in severe CR (0.05% glucose).
- 61 **Figure 8** - Genetic and pharmacological inactivation of catalases extends *S. cerevisiae* CLS by increasing intracellular levels of ROS.
- 62 **Figure 9** - The deletion of Cta1p (peroxisomal catalase) in W303 cells (A) or of both Cta1p and Ctt1p (cytosolic catalase) in BY4742 cells (B) extends *S. cerevisiae* CLS.
- 63 **Figure 10** - CR induces the activity of the peroxisomal catalase Cta1p, as well as the cytosolic catalase Ctt1p.
- 64 **Figure 11** - CR shortens *S. cerevisiae* CLS of *CTA1* overexpressing wild-type cells.
- 65 **Figure 12** - Inactivation of glutathione peroxidase (GpX) with BSO extends *S. cerevisiae* CLS in wild type (A), but not in $\Delta cta1$ (B) or $\Delta ctt1$ (C) cells.
- 67 **Figure 13** - The longevity-promoting effects of high intracellular H_2O_2 levels induced by CR or inactivation of catalases are accompanied by a reduction in the chronological age-dependent accumulation of O_2^- .
- 68 **Figure 14** - Mutational inactivation of *CTT1* or of both catalases *CTA1* and *CTT1* mimics the CLS extending effects of CR in parallel with high intracellular H_2O_2 levels and reduction in the chronological age-dependent accumulation of superoxide anions (O_2^-).
- 69 **Figure 15** - CR-induced increases in intracellular H_2O_2 accompanied by a reduction in the accumulation of O_2^- occurs independently of changes in levels of acetic acid as demonstrated in cells cultured in buffered medium.
- 70 **Figure 16** - Superoxide dismutase activity is induced by intracellular H_2O_2 in stationary phase wild type and $\Delta cta1$ cells.
- 71 **Figure 17** - Superoxide dismutase activity is induced by intracellular H_2O_2 in stationary phase wild type

and $\Delta ctt1$ cells.

- 72 **Figure 18** - Induction of *SOD1* and *SOD2* mRNA expression by intracellular H_2O_2 .
- 74 **Figure 19** - Effects of increased H_2O_2 induced by CR or by inactivation of *CTA1* on oxidative damage to macromolecules.
- 75 **Figure 20** - Effects of increased H_2O_2 induced by CR or by inactivation of *CTT1* on oxidative damage to macromolecules.
- 76 **Figure 21** - Ectopic exposure cells to non-toxic concentrations of H_2O_2 promotes *S. cerevisiae* CLS extension.
- 76 **Figure 22** - Ectopic exposure of non-CR *S. cerevisiae* cells to H_2O_2 promotes the induction of Sod2p, but not Sod1p, activity in wild type cells.
- 82 **Figure 23** - Decreased glucose uptake into the cell (strain KOY.TM6*P) promotes CLS extension of cells when compared to cells displaying intermediate/high and high glucose uptake.
- 83 **Figure 24** - Reduced glucose uptake into the cells (KOY.TM6*P) promotes CLS extension associated with decreased intracellular ROS accumulation.
- 84 **Figure 25**- CR modelled by decreased glucose uptake (KOY.TM6*P) promotes resistance to both (A) oxidative and (B) acid stresses when compared to higher glucose uptake conditions.
- 86 **Figure 26** - Genetic inactivation of specific enzymes involved in glucose metabolism extends *S. cerevisiae* CLS by increasing intracellular H_2O_2 levels and decreasing O_2^- levels.
- 87 **Figure 27** - Genetic inactivation of specific enzymes involved in glucose metabolism promotes resistance to both oxidative and acid stresses.
- 89 **Figure 28** - Pharmacological inactivation of RAS, PKA and TOR kinases with manumycin, wortmannin and rapamycin, respectively, extends CLS in BY4742 wild type cells cultured in 2% glucose, comparatively to non-treated cells.
- 91 **Figure 29** - The inhibition of the growth signaling pathway Rim15p promoted increases in H_2O_2 and a reduction in the intracellular O_2^- accumulation.

CHAPTER 4 - Concluding remarks and future perspectives

- 99 **Figure 1** - The CLS-extending effects of CR may be independent of the established CR signaling through the conserved Sch9p-, Tor1p-, and RAS-dependent pathways and of the induction of oxidative stress defences by Rim15p

ABBREVIATIONS LIST

ABBREVIATIONS LIST

2-DOG	2-deoxyglucose
3-AT	3-Amino-1,2,4-triazole
BSO	L-buthionine sulfoximine
c.f.u.	Colony forming units
CLS	Chronological lifespan
CRM	Caloric restriction mimetics
DHE	Dihydroethidium
CR	Caloric restriction
d	Day
DCF	Dichlorofluorescein
DHR	Dihydrorhodamine
DNA	Deoxyribonucleic acid
DMSO	Dimethyl sulfoxide
DR	Dietary restriction
EDTA	Ethylenediaminetetraacetic acid
FACS	Fluorescence Activated Cell Sorting
GAPDH	Glyceraldehyde-3-phosphate dehydrogenase
GFP	Green fluorescence proteins
GH	Growth hormone
GLUT	Glucose transporter
H₂O₂	Hydrogen peroxide
HXT	Hexose transporter
H XK	Hexokinase
NO	Nitric oxide
O₂[•]	Superoxide anion
OH[•]	Hydroxyl radical
PBS	Phosphate buffered saline

PCR	Polymerase chain reaction
PDC	Pyruvate dehydrogenase
PFK	Phosphofructokinase
PKA	Protein kinase A
PMSF	Phenylmethanesulfonylfluoride
PVDF	Poly-vinylidene fluoride
RLS	Replicative lifespan
ROS	Reactive oxygen species
RT-PCR	Reverse transcription polymerase chain reaction
r.p.m.	Rotations per minute
SC	Synthetic complete
SEM	Standard error of the mean
SD	Standard deviation
SDS-PAGE	Sodium dodecyl sulphate polyacrilamide gel electrophoresis
Sods	Superoxide dismutases enzymes
SODs	Genes coding for superoxide dismutases
TOR	Target of rapamycin
YEPD	Yeast Extract Peptone Dextrose
YEPG	Yeast Extract Peptone Glycerol
YPD	Yeast Peptone Dextrose

OBJECTIVES AND OUTLINE OF THE THESIS

OBJECTIVES AND OUTLINE OF THE THESIS

Over the last decades, researchers have looked for a single theory that could explain the aging process. A leading and longstanding theory posits that aging is a result of the accumulation of oxidative damage to macromolecules as organisms age over time [1]. However, a direct cause-effect has been difficult to establish between reactive oxygen species (ROS) accumulation in the cell and its effect on aging. The budding yeast *Saccharomyces cerevisiae* is considered a valious model in aging-related research. Among several advantages, the relative easy and short time with which longevity can be quantified in yeast has allowed rapid progress in defining the molecular mechanisms of aging in this organism and the identification of important aging regulators. Even though some features of yeast aging are specific to these cells, numerous important features have been evolutionarily conserved and, thus, enrich the understanding of such regulation in more complex organisms. In this context, we aimed to get new insights on the involvement of ROS and oxidative stress in the chronological lifespan-extending effects of caloric restriction (CR) in *S. cerevisiae*.

With the intention to drive the reader through the main achievements, this thesis was organized in four chapters:

In chapter 1, an introduction to the theme is made focusing in the main contribution of the aging models and theories to the identification of the conserved longevity regulators. A special attention is given to the "Free Radical Theory of Aging" and to the use of *S. cerevisiae* in the study of the chronological lifespan-extending effects of CR, particularly in which concerns to its effects on ROS and oxidative stress.

In chapter 2, all the materials and methods used in this work are referred.

In chapter 3, results are presented and discussed in two sections. The results presented in the section 3.1 show evidence indicating that the CR-effects on *S. cerevisiae* CLS extension are intimately associated with the intracellular accumulation of specific forms of ROS suggesting that specifically H₂O₂ might be a primordial player of an hormetis-like process in the aging process. The involvement of ROS and oxidative stress in CLS was further demonstrated within CR mimetics, achieved by targeting glucose metabolism, transport and sensing signaling, in section 3.2.

In chapter 4, the main concluding remarks and future perspectives are pointed out.

CHAPTER1.

INTRODUCTION

The proportion of aged people is growing faster than any other age group. Such trend is a reflex of the advances in sanitation, housing and nutrition conditions that took place over the last century. The discovery of vaccines and antibiotics has contributed to a reduction in premature mortality from many infectious and chronic diseases. Although population aging can be seen as a success story for public health policies and for socioeconomic development, it also challenges society to adapt in order to maximize the health and functional capacity of the increasing older people. Data from the *World Health Organization (WHO)* show that in 2000 the global population of people aged 60 and over was 600 million; by 2025 there will be 1.2 billion and, by 2050, almost 2 billion. In this scenario, and as proposed by *WHO*, society must promote “age-friendly” environments that encourage “active aging by optimizing opportunities or health, participation and security in order to enhance quality of life as people age”. The practice of a healthy diet and exercise, having a good social environment, not using drugs or alcohol and avoiding stress are considered important behaviours that may lead to a healthy aging. However, the prolongation of human lifespan with quality is much more than just a lifestyle issue being governed by biological processes, heredity, health conditions or disease. Specific disciplines including microbiology, physiology, and genetics have suggested new strategies for efficient intervention in aging model systems that, ultimately, may be used to prevent aging and age-related diseases in humans. Nevertheless, and despite such multidisciplinary efforts, the understanding of aging mechanisms remains one of the most relevant challenges for the modern science.

1.1 STUDY OF AGING: LESSONS FROM MODEL SYSTEMS

Over the last century much of the challenge in understanding human aging has been wrapped up in an attempt to identify the primary causes of the stereotypic changes that are observed with age. Increasing evidence from aggregation studies in centenarians suggest a genetic predisposing for longer longevity and survival advantage [2, 3]. However, humans age in unique ways depending on several factors including gender, cultural background, lifestyle, geographical location and whether they live in industrialized or developing countries. In this scenario, studying such a multifactorial biological process in humans still represents a major challenge in the aging field.

Relevant findings in human aging have been gleaned from clinical observations of people with premature aging syndromes, the progerias. For instance, studies conducted in patients with Hutchinson Gilford progeria syndrome (HGPS) have revealed that several cellular and molecular alterations observed during the course of this disease are also detected during the so-called *normal* aging including genome instability, telomere attrition, premature senescence and altered stem cell homeostasis [4]. Such studies, together with genetic and epidemiological association studies in different age groups, may represent an opportunity to identify genetic and environmental key determinants in the regulation of human aging and longevity. However, ethical concerns as well as the duration of human's lifespan still represent major limitations for the development of this type of approaches. In this scenario, research on non-human primates have obvious benefits to take aging research closer to human and provide a more reliable and worthwhile knowledge than non-primates models [5-7]. Nevertheless, the expensiveness of their maintenance as well as their extended lifespan may limit their utility in aging research. As an alternative, studies in more simple mammals, such as rodents, which display genetic plasticity and close position to humans on the evolutionary scale, may represent an advantage in aging research when compared to simpler models. Yet, the duration of their lifespan may be still considered a limitation for their utilization in aging research.

Despite aging studies with humans [4] and primates [5] are currently being performed the ultimate causes of aging stay largely unknown. Important clues of aging regulation have resulted from the integration of several models and theories. Over the last decades, the use of model systems has been extremely revealing in predicting how changes in specific genetic and environmental factors may modulate longevity and affect the aging process. Much of the understanding of the aging process have resulted from studies conducted in simple and short-lived systems including mice [8], nematodes (*Caenorhabditis elegans*) [4], the fruit fly (*Drosophila melanogaster*) [5, 6] and the single-celled budding yeast (*Saccharomyces cerevisiae*) [9]. When compared to mammals, these systems have shorter lifespans, are easily maintained in laboratory conditions, are smaller and have simpler physiology. In addition, the advanced genetic tools available for these models have made possible the identification of an ever-growing number of pathways that govern longevity. For instance, *C. elegans* was one of the first organisms linking growth signaling to longevity by showing that mutations in the insulin/insulin growth factor-1 (Ins/IGF-1) receptors, or in downstream components

of the phosphatidylinositol 3-Kinase (PI3K)-PDK-Akt pathway, promote longevity (reviewed in [10, 11]). Relative to more simple systems such as yeast, the nematode model has been particularly useful in unravelling the pathways regulating the aging process of specific cell types and organs [11]. The fly model has also been particularly important in the establishment of the evolutionary conservation of mechanisms regulating tissue-specific aging, particularly in which concerns to sex-specific events [12].

Of the invertebrate eukaryotic model organisms, the single-celled yeast *S. cerevisiae* is the simpler and most amenable microorganism to genetic and molecular manipulations. Supporting its utilization for aging research, accumulating evidence indicate that a subset of pathways influencing longevity in yeast are evolutionary conserved among eukaryotes, including the sirtuins which were firstly linked to aging in this model [13]. Yeast cells divide very fast, have short lifespan and present amenable genetic manipulation. Thus, a large amount of biological material for physiological, biochemical, molecular and genetic analysis can be easily and rapidly obtained. On the other hand, being at the same time a cell and an organism, key insights into the genetic and environmental factors that can control cellular and organismal aging have resulted from studies in this model [10, 14-16]. Two different models can be assessed during yeast aging; the replicative lifespan (RLS) and the chronological lifespan (CLS) (Fig. 1) (reviewed in [17]). RLS measures the number of mitotic events that an individual mother cell can undergo before senescence assuming that the probability of a yeast cell to divide again decreases exponentially [18, 19]. On the other hand, CLS measures the time that non-dividing yeast cells maintain their viability in a depleted culture or in water [20, 21]. Studies focusing these two paradigms stand for a unique opportunity to compare and contrast the aging processes of both proliferating and non-proliferating cells and, thus, be used as a model to study the aging mechanisms of mitotic and post-mitotic tissues in higher organisms.

The extrapolation for mammals based on considerably short-lived systems developed for laboratory research may be awkward. Despite the inherent risk, the use of simple model systems have revealed to be of particular relevance in the identification of a number of genes/pathways involved in longevity [22-24], that are evolutionary conserved among the eukaryotic kingdom and, ultimately, are the basis for research into aging in mammals and particularly humans [25-27].

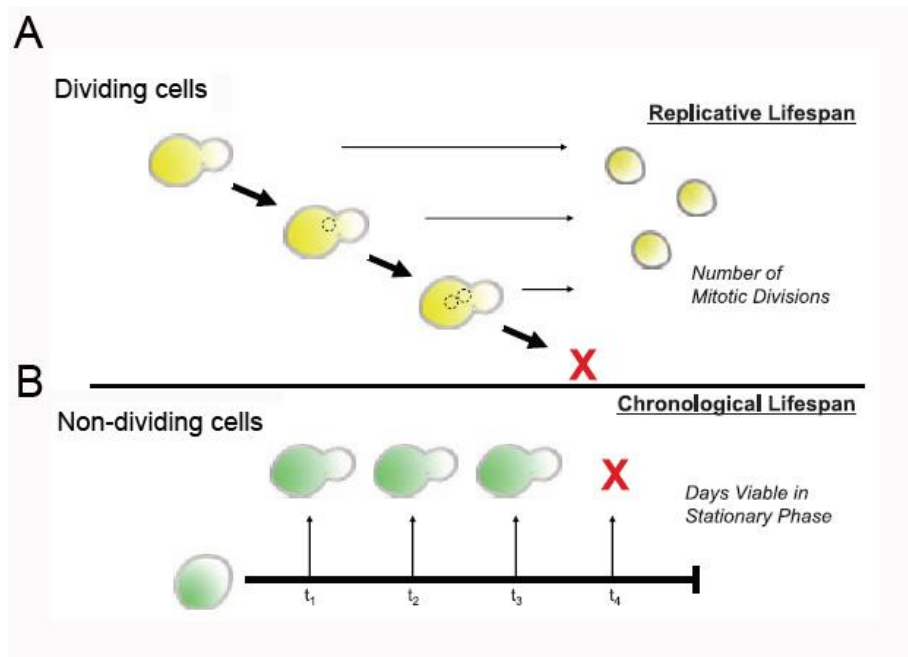


Figure 1 - Two aging paradigms exist in yeast cells. The replicative lifespan (A) is a measure of the proliferative capacity of a cell, taking advantage of the asymmetric division in which a daughter cell can be easily differentiated from the mother. Chronological lifespan (B) measures the time that a yeast cell can maintain viability in the culture medium in a post-replicative state. (Figure from [17] with adaptations).

1.1.1 LONGEVITY REGULATION BY THE CONSERVED NUTRIENT-SENSING SIGNALING PATHWAYS

The capacity of organisms to deal with changes in their environment is essential to their survival and reproductive success. Changes in environmental factors such as food supply, require an adaptation in energetic processes including growth, metabolism and reproduction. Evidence from genetic studies conducted in different model systems have implicated specific nutrient-sensing signaling pathways in lifespan regulation and suggest that mechanisms modulating aging are evolutionary conserved (reviewed in [22, 25]). In the presence of nutrients and growth factors three major conserved nutrient-sensing signaling pathways are activated including the Ins/IGF-1-like, the TOR-S6K (TOR, target of rapamycin) and the RAS-AC-PKA (AC, adenylate cyclase; PKA, protein kinase A) (Fig. 2). Conversely, growth factors/nutrients restriction in dietary

regimens (DR, dietary restriction) or a specific reduction in calories intake (CR, caloric restriction) have been shown to promote a decrease in the activity of those major pathways and their activation of specific transcription factors in higher eukaryotes (e.g. the Forkhead FoxO transcription factor FOXO) and in yeast (e.g. Msn2p, Msn4p and Gis1p) which, in turn, regulate the expression of enzymes and proteins involved in protective and metabolic activities that extend lifespan (Fig. 2).

Pioneering studies in the nematode model have linked growth/nutrient-sensing signaling to longevity through a major axis of longevity regulation, the conserved Ins/IGF-1 pathway (reviewed in [11]). It has been shown that, in response to food restriction and crowding, the Ins/IGF-1 pathway mediates the formation of long-lived dauers which exhibit arrested development, reproductive immaturity and resistance to oxidative stress. Conversely, when food or stress conditions are re-established dauers become fertile adults with normal lifespan. This mechanism was shown to involve the reduction in the activity of the Ins/IGF-1 receptor homolog, Daf-2, as well as the recruitment and activation of the insulin-PI3K, resulting in the activation of several downstream kinases and specific transcription factors such as FOXO-like transcription factor Daf-16 [28] known to regulate genes involved in several cellular protective processes including stress response, antimicrobial activity and detoxification of xenobiotics and free radicals (reviewed in [29]) (Fig. 2). Reduced levels of IGF-1 and of the downstream targeted Akt/PKB kinases have also been demonstrated to mediate cellular protection mechanisms and the extension of lifespan in more complex eukaryotes including flies and mammals (reviewed in [11, 22, 29]) (Fig. 2). It was recently shown that *Drosophila* mutants for specific insulin-like peptides in neuroendocrine cells of the brain are significantly longer-lived than controls [30]. Also, flies carrying mutations in the insulin-like receptor (InR) are sterile dwarfs and females show increased lifespan [31]. In mammals, growth hormone (GH) and insulin-like pathways have linked hormonal control to aging in association with an increase of antioxidant defences and increased stress resistance (reviewed in [32]). Although not displaying any growth defects, lack of insulin-receptor in adipose tissue was also shown to promote lifespan in mice [33]. In humans, either mutations that impair IGF-1 receptor function and genetic variants in the insulin receptor gene were found to be more frequent in a cohort of centenarians [34]. On the other hand, long-lived Japanese men were shown to share a genetic variation within the *FOXO3A* gene, that functions in the conserved IGF-1 signaling pathway [3]. This genetic association was replicated in a

caucasian population from Germany showing that it is not population specific [2]. However, more studies are needed to establish the beneficial effects of manipulating the Ins/IGF-1 pathway in humans.

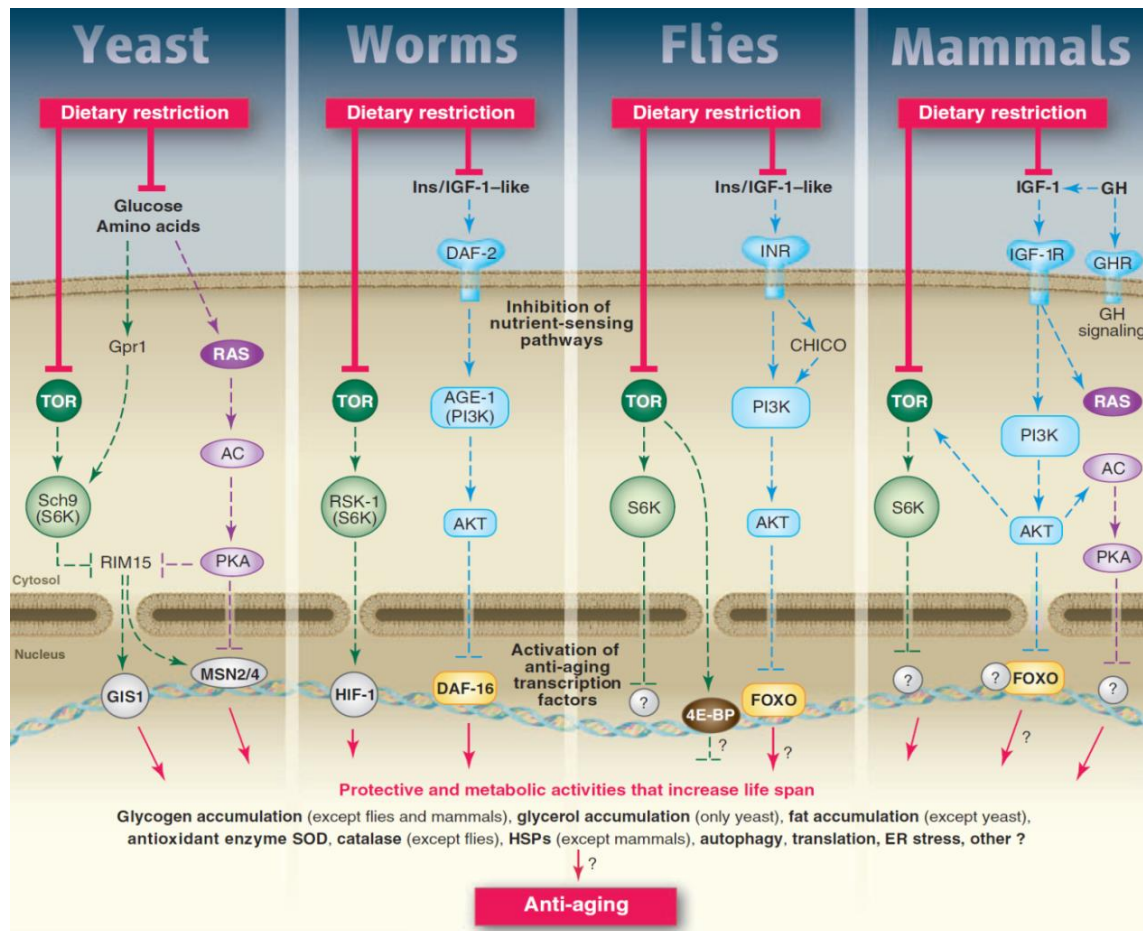


Figure 2 - Longevity is regulated by major nutrient-sensing signaling pathways including TOR-S6K, RAS-AC-PKA and the insulin/insulin growth factor 1-like (Ins/IGF-1-like) pathway. A decrease in the activity of these pathways upon dietary restriction (nutrient/calorie restriction) culminates in the activation of specific transcription factors (e.g. GIS1, MSN2/4, HIF-1, DAF-16 and FOXO) that regulate protective and metabolic activities that increase lifespan involving, for instance, heat shock proteins (HSPs); endoplasmatic reticulum (ER) stress and autophagy proteins; apoptosis; xenobiotic metabolism; translation regulation and antioxidant enzymes such as superoxide dismutase and catalase [22, 35] (Figure from [22]).

In response to nutrients and growth factors the Ins/IGF-1 pathway and its downstream components of the PI3K-PDK-Akt pathway interconnect with another major pathway linked to longevity regulation, the conserved TOR-S6K pathway [36,

37] (Fig. 2). The TOR kinase is a phosphatidylinositol-related kinase specifically inhibited by the macrolide rapamycin and known to regulate various cellular processes, including initiation of mRNA translation, ribosome synthesis, expression of metabolism-related genes and autophagy [38]. In *C. elegans*, the worm ortholog of the mammalian mTOR-interacting protein Daf-15 has been shown to integrate the Ins/IGF-1 and TOR signaling pathways in the regulation of larval development, metabolism and longevity [36]. In mammals and flies, TOR functions downstream of the Ins-PI3K pathway and cooperates in the regulation of cell growth and proliferation in response to growth factors, hormones and cytokines [39, 40]. An extension of lifespan was also observed in flies when TOR pathway was pharmacological inactivated with rapamycin or upon overexpression of dominant-negative dTOR variant or TOR-inhibitory dTsc1/2 proteins [41, 42]. In mammals, the inhibition of the mTOR pathway has also been associated with lifespan extension and reduced incidence of age-related diseases including immune and motor dysfunction as well as insulin resistance [43]. In yeast TOR signaling pathway has been associated to amino acid sensing in a PI3K-independent manner [37]. In this model two mTOR homologous, TOR1 and TOR2 kinases complexes, have been identified [44]. While TORC1 mediates the growth-related signaling in a rapamycin-sensitive manner, TORC2 signaling is rapamycin-insensitive and is required for controlling the cell-cycle-dependent organization of actin cytoskeleton [44]. Inhibition of the TOR1 with rapamycin was firstly shown to increase yeast CLS [45] and has recently been found to increase lifespan in mice [46]. A high throughput assay to measure the CLS of individual yeast deletion mutants identified several long-lived strains carrying deletions of genes implicated in the TOR pathway [45, 47]. The downregulation of TOR and Sch9p, a ribosomal S6 kinase homologue in yeast which shares high sequence identity with the mammalian kinases Akt/PKB (protein kinase B), have been shown to operate in a pathway downstream of nutrient availability to extend CLS [20]. Deletion of *SCH9* has since been shown to increase yeast RLS similarly, and to increase longevity in nematodes, flies and mice [48].

Studies in yeast have revealed that, together with TOR-Sch9p, the RAS-AC-PKA pathway is another key nutrient-sensing pathway involved in longevity regulation [20, 49, 50]. This pathway has been involved in the regulation of several downstream processes including ribosome biogenesis and translation, changes in the metabolism of amino acid/carbon source utilization, autophagy and stress response (reviewed in [22, 51, 52]). A decrease in the activity of TOR-Sch9p and RAS-AC-PKA pathways is

known to drastically increase yeast lifespan by converging in the activation of the Rim15p kinase and in the induction of several cellular defence processes [20, 45, 53-57] (Fig. 2). Mutations in *CYR1* or *RAS2*, which operate within the RAS-AC-PKA pathway, were shown to extend yeast CLS [20, 21]. *CYR1* encodes for adenylate cyclase (AC) which, in turn, stimulates cyclic adenosine monophosphate (cAMP)-dependent PKA activity, required for cell cycle progression and growth. Decreased activity of PKA pathway has also been implicated in yeast RLS extension [49]. However, whereas the effect of the cAMP/PKA pathway on CLS was suggested to require Msn2p/Msn4p and Sod2p and to be associated with increased stress resistance, its effect on RLS appears to be independent from stress resistance and dependent on the expression of the Sir2p deacetylase, an important aging regulator [56]. Nevertheless, the deletion of *SOD1* or of both *SOD1* and *SOD2* has been shown to dramatically decrease yeast CLS [58] and RLS [59]. Mutations in the *RAS2* gene, triggering loss of function have been described as doubling yeast CLS [60]. Although deletion of *SCH9* or downregulation of proteins of the PKA signaling pathway were shown to extend both RLS and CLS in yeast [20, 49, 61], there are a number of genetic manipulations that increase CLS and do not increase the RLS. For instance, the deletion of *RAS2* extends the CLS whereas it shortens RLS, in contrast to the RLS-extending effects of the deletion of *RAS1* [50]. However distinct, the mechanisms that regulate yeast CLS and RLS may be interconnected as suggested by the reduction in RLS in chronologically aged cells [62]. On the other hand, and contrary to most long-lived mutants in higher eukaryotes, long-lived *RAS2*-null yeast cells show a small increase in cell size comparatively to wild type cells [54], suggesting that lifespan extension may be not associated with dwarfism in response to nutrients [25]. Nevertheless, together with Akt, RAS proteins have also been shown to promote aging in mammals being one of the key mediators of IGF-I signaling [63, 64]. Similar to what has been observed in yeast cells, disruption of type 5 adenylate cyclase (AC5) in mice, which is predominantly expressed in the heart and brain, also promotes stress resistance and longevity [65].

A valious contribution of the yeast model in aging research relies on the fact that these cells established, for the first time, a link between specific NAD⁺-dependent protein deacetylases, the sirtuins, and aging. In yeast, Sir2p is a key determinant of longevity [13]. The activity of these proteins were shown to extend yeast RLS by inhibiting the progressive enlargement and fragmentation of the nucleoli in old cells resulting from the accumulation of toxic extrachromossomal ribosomal DNA circles

(ERCs) [13]. ERCs self-replicate and are retained by the mother-cell nucleus leading to an exponential increase in their copy number during aging [66]. Subsequent discoveries have revealed that activation of Sir2p orthologues can as well extend lifespan in nematodes and flies and sirtuin activators are being explored for their beneficial effects in several disease models (reviewed in [11, 67]). For instance, in *C. elegans*, the over-expression of the sirtuin gene *SIR-2.1* extends lifespan by activating DAF-16/FOXO which mediates an oxidative stress response [68]. In *Drosophila*, the over-expression of *SIR2* has been associated with the prevention of cell death [69], however, further studies are needed to elucidate the role of sirtuins in flies longevity. In mammals, sirtuins have gained significant attention for their impact on mammalian physiology, since they may provide novel targets for treating age-related diseases and, perhaps, extend human lifespan (reviewed in [70]). A proper cause-effect relationship between sirtuins and lifespan has been difficult to achieve, however, studies in mice have suggested that anti-aging effects of resveratrol, a plant polyphenolic compound, may occur through sirtuin-dependent processes [71]. Despite the fact that the effects of resveratrol in delaying the onset of several mammalian diseases are associated with sirtuins, the aspects of such relationship remain contradictory [72]. It has been recently shown that resveratrol requires the NAD⁺-dependent deacetylase sirtuin 1 (SIRT1) to induce the pro-longevity effects of autophagy in human cells and in *C. elegans* [73]. On the other hand, similar lifespan-extending and autophagy-inducing effects observed under treatment with spermidine, a polyamine found in citrus and soybean which inhibits acetylases, were shown to be independent of *SIR-2.1* (nematodes) and *SIR2* (yeast) and associated with the inhibition of acetylases [74]. These studies suggest that these two agents may trigger autophagy through distinct primary targets, however, they can synergistically induce autophagy by stimulating convergent (de)acetylation reactions and, thus, balancing the acetylproteome [74]. Nevertheless, the effective downstream targets of these kinases are still difficult to identify due to their overlapping roles in regulating several cellular responses to nutrient exposure. In yeast cells, it has been recently suggested that sirtuins may extend RLS by avoiding H4 lysine 16 acetylation and loss of histones at specific subtelomeric regions [75]. However, the contradictory findings regarding involvement of sirtuins in lifespan extension still suggest that there are additional and yet unknown pathways regulating aging [76].

The yeast model has allowed the identification of yeast-specific molecules that modulate aging, particularly concerning the effects of two by-products of alcohol

fermentation ; acetic acid (pro-aging) and glycerol (anti-aging) [77, 78]. Mutations in the TOR-Sch9p and RAS-AC-PKA pathways have been shown to extend yeast CLS by mediating the accumulation of glycerol or by reducing the toxic effects of acetic acid that promotes cell death [78-80]. However, the identification of specific metabolic products, such as acetic acid, as limiting factors of yeast CLS under standard conditions may rise questions regarding the validity of this system as a model for studying aging in higher eukaryotes [77, 78].

Overall, studies conducted in different model systems have shown that mutations in genes affecting endocrine signalling, metabolism, stress response and telomeres increase the life span, providing the identification of the major evolutionary conserved players underlying the mechanistic regulation of the aging process.

1.2. THEORIES OF AGING

A key question remains related with the different regulators of aging and longevity. Why living systems age? Over the last century, several theories have contributed to answer this question (Fig. 3). In the late 19th century, and soon after the development of the Darwin's theory of evolution in 1858, August Weismann proposed an evolutionary approach to the problem of aging by hypothesizing that a limited lifespan should be viewed as an evolutionary advantage for the species (reviewed in [81]). In this context, specific death mechanisms of natural selection would determine death of older members of a population to avoid competition for supplies with younger counterparts. Following theories by Peter Medawar ("Mutation Accumulation Theory"), George Williams ("Antagonist Pleiotropy Theory") and Thomas Kirkwood ("Disposable Soma Theory") have further supported a role of natural selection in determining aging (reviewed in [82]) (Fig. 3). According to Medawar aging would result from the accumulation of mutations that are not subjected to natural selection throughout life. On the other hand, Williams hypothesized that natural selection would favour genes that confer short-term benefits to the organism in detriment of genes with long term benefits. In this line of thought, Kirkwood suggested that natural selection would favour a strategy that ensure continued reproductive success early in life; investing less resources in the maintenance of somatic cells and tissues after reproduction. However, evidence have emerged suggesting that the antagonism reproduction/longevity may not be absolute. For instance, no loss in reproductive capacity has been observed in long-lived *Drosophila*

[83]. Also, in eusocial insects the switch during adult life from a normal worker to a reproductive gamergate has been shown to be associated with significant increase in lifespan [84].

The evolutionary theories may explain the evolution of aging through the interaction between mutations and natural selection that would result in the elimination of the oldest and less-competitive members of a population. However, over the last century, several other causes have been proposed and aging was viewed as a result of the accumulation of damage/errors at molecular, cellular and system levels which, in turn, may have evolutionary implications for reproduction and survival (Fig. 4) (reviewed in [82]). According to the "Gene Regulation Theory" senescence is a result of changes in gene expression [85]. Many genes have been associated to aging and some have shown lifespan-extending effects on animal models, however, their associations with human aging are far from validated. A genetic predisposing for increased longevity and survival advantage has also been suggested in humans. For instance, a genome-wide scan of linkage study carried out in American centenarians and their siblings has revealed that exceptional old age may be associated with predisposing loci in chromosome 4 at D4S1564 [86]. On the other hand, aging may be seen as a reflex of the accumulation of errors and a decline of the fidelity in the genetic machinery and resulted altered proteins over time ("Error Catastrophe Theory") [87]. For instance, altered DNA replication as a result of the loss of helicase function has been demonstrated in patients with premature aging disorders [88].

Several cellular processes have also been associated with age including programmed cell death (PCD) in aged tissues ("Apoptosis Theory") and the accumulation of normal injury ("Wear-and-tear Theory") (reviewed in [82]) (Fig. 3 and 4). For instance, neuronal cell death has been associated with age-related neurodegenerative diseases [89]. Apoptotic events have also been demonstrated in both muscle and fat tissue during *Drosophila* aging [90] and in chronologically aged yeast cells [91]. However, it was suggested that mutation in pro-apoptotic caspase genes has no effect in *C. elegans* lifespan extension [92] and that the over-expression of caspase inhibitors results in the reduction of adult *Drosophila* lifespan [93]. Therefore, suggesting that other cellular processes should also be considered in the aging process.

Much of the comprehension of the aging process has resulted from the work by Leonard Hayflick and Paul Moorhead, in 1965, suggesting that cell's senescence is a reflex of the limited replicative lifespan ("Cell Senescence Theory of Aging") (Fig. 3).

Moreover, some decades later, in 1998, Andrea Bodnar and colleagues proposed a mitotic clock that signals cell senescence which is determined by the loss of telomeric DNA through incomplete replication of the chromosome ends ("Telomere Theory of Aging") (Fig. 3). Ever since, increasing evidence have implicated telomeres in aging and different age-related phenotypes (reviewed in [94]). Pioneering findings on the first cloned sheep, that died at the age of six, demonstrated that telomeres were found to be shorter than those expected for its age [95]. Studies in engineered mice have shown that longer telomeres are associated with lifespan extension [96]. However, and unless genetically modified, such mice do not resist to cancer.

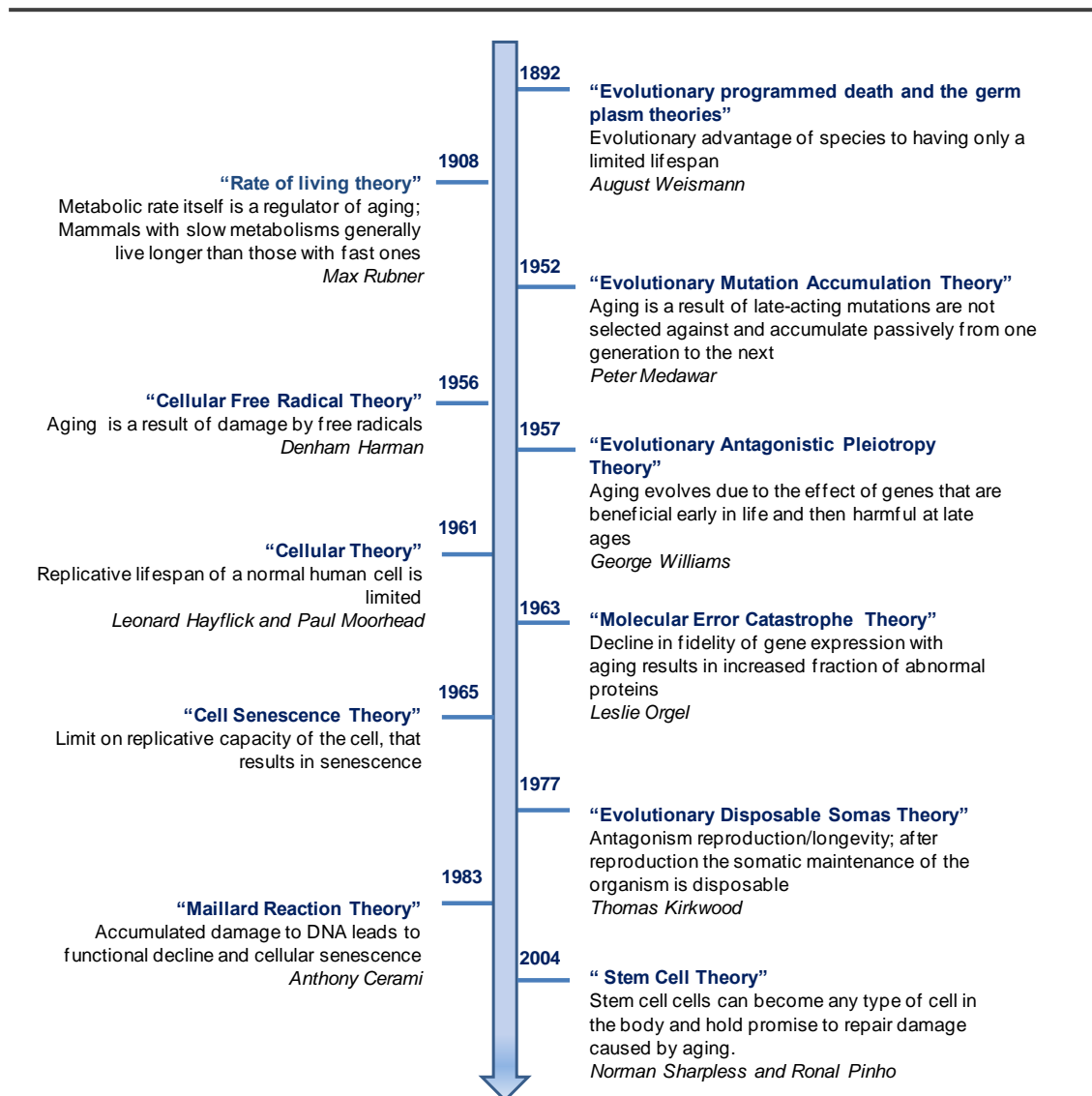


Figure 3. In the last century different theories have been presented in the light of the existing discoveries from evolutionary, genomic and molecular genetic studies on aging and longevity [82, 94, 97].

The shortening of telomeres has also been demonstrated in humans with progeria when compared with healthy individuals of the same age [98]. Taking into consideration that progerias may not faithfully reproduce the process of natural aging, such evidence remain controversial. A major role for telomeres in aging has also been associated with the restorative capacity of tissue stem cells and, ultimately, their fate [97], leading the formulation of the "Stem Cell Theory of Aging" (Fig. 3 and 4). Overall, increasing evidence support the involvement of telomere biology of aging and human diseases. In this context, new insights into the telomere biology outcomes in the aging process have recognized Elizabeth Blackburn, Carol Greider and Jack Szostak with the attribution of the *2009 Nobel Prize in Physiology or Medicine*, for their pioneering research showing that telomerase, the enzyme that adds telomeres to the end of the chromosome, might have a critical role in protecting telomere shortening associated with the aging process and with multiple aging-associated diseases and conditions.

Despite a tune regulation of specific molecular and cellular processes, aging has also been suggested to be determined by changes at a more complex physiological level, including alterations in metabolism (Fig. 4). For instance, changes in the neuroendocrine control of homeostasis or a decline of immune function, have been associated with aging (reviewed in [82]) (Fig. 4). Growth hormone (GH), known to promote growth in children and to play a central role in adult metabolism, has been already described as a key player in delaying aging and age-related phenotype (reviewed in [22]). Also, changes in energy metabolism have been suggested to mediate the aging process. This idea was firstly suggested early in the 20th century by Max Rubner who, by comparing long (tortoises) and short-lived (mice) species, proposed the "Rate of Living Theory of Aging" (Fig. 3 and 4). According to Rubner and followers, the faster an organism uses oxygen the shorter it lives and, thus, aging would be promoted by increased metabolism upon increased nutrient availability [99]. Nevertheless, it has also been suggested that metabolic rates, when correctly normalized for body size, do not correlate with maximum lifespan in mammals [100]. Despite such controversial evidence, this theory has later provided a background for explaining the lifespan-extending effects of restricted diet regimens in several organisms [101-105]. In this context, a decrease in nutritive/caloric availability would extend lifespan by promoting a decrease in the amount of energy metabolized. Some decades later, in

1956, Denham Harman provided a molecular basis for Rubner's theory by suggesting that a decrease in energy metabolism would prevent aging by avoiding the intracellular accumulation of free radicals and its cumulative damage to the cell [1] and, ultimately, to the organism (reviewed in [82]) (Fig. 3 and 4). Ever since, the longstanding "Free Radical Theory of Aging" of Harman has supported a involved role for free radicals in aging and longevity regulation. This topic will be focused with further detail in the next section.

Overall, a number of theories have been proposes in order to identify the causes of aging and of the onset of several age-related phenotypes throughout life. However, the degree to each theory contributes to elucidate the primary cause of aging is still a topic of strong research. Therefore, the difficulty in identifying a single or primordial cause for aging suggests that aging is a very complex and multifactorial process.

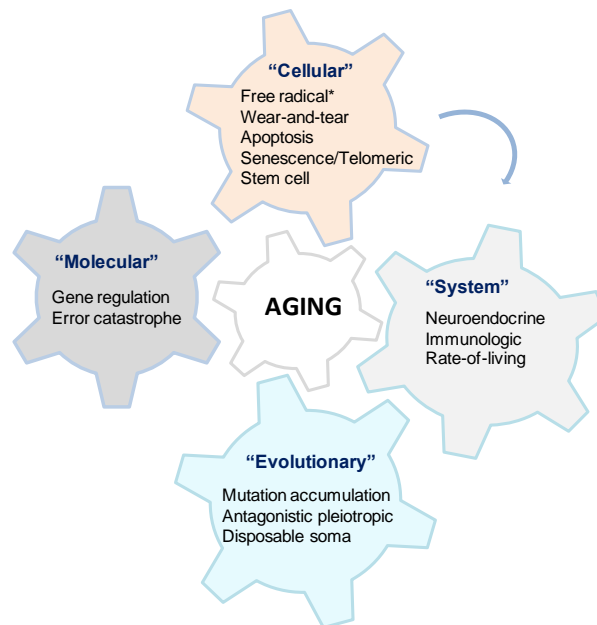


Figure 4. Aging is regulated by a multiplicity of mechanisms which operate at different biological levels. Different molecular events may culminate in specific cellular alterations which, in turn, may contribute to a decline at organ/system level with evolutionary repercussions for reproduction and longevity [82, 94, 97].

1.2.1 "FREE RADICAL THEORY OF AGING"

One of the most plausible and acceptable explanations for the mechanistic basis of aging is the longstanding "Free Radical Theory of Aging", proposed by Denham Harman in the mid-1950s which hypothesizes that aging and age-related diseases are the consequence of free radical-induced damage to cellular macromolecules throughout life [1, 106] (Figs. 3 and 4). A multiplicity of cellular endogenous and exogenous sources of reactive oxygen species (ROS) generation are considered including mitochondrial and peroxisomal metabolism, and chemical and environmental insults (Fig. 5) ([107, 108]; reviewed in [109]).

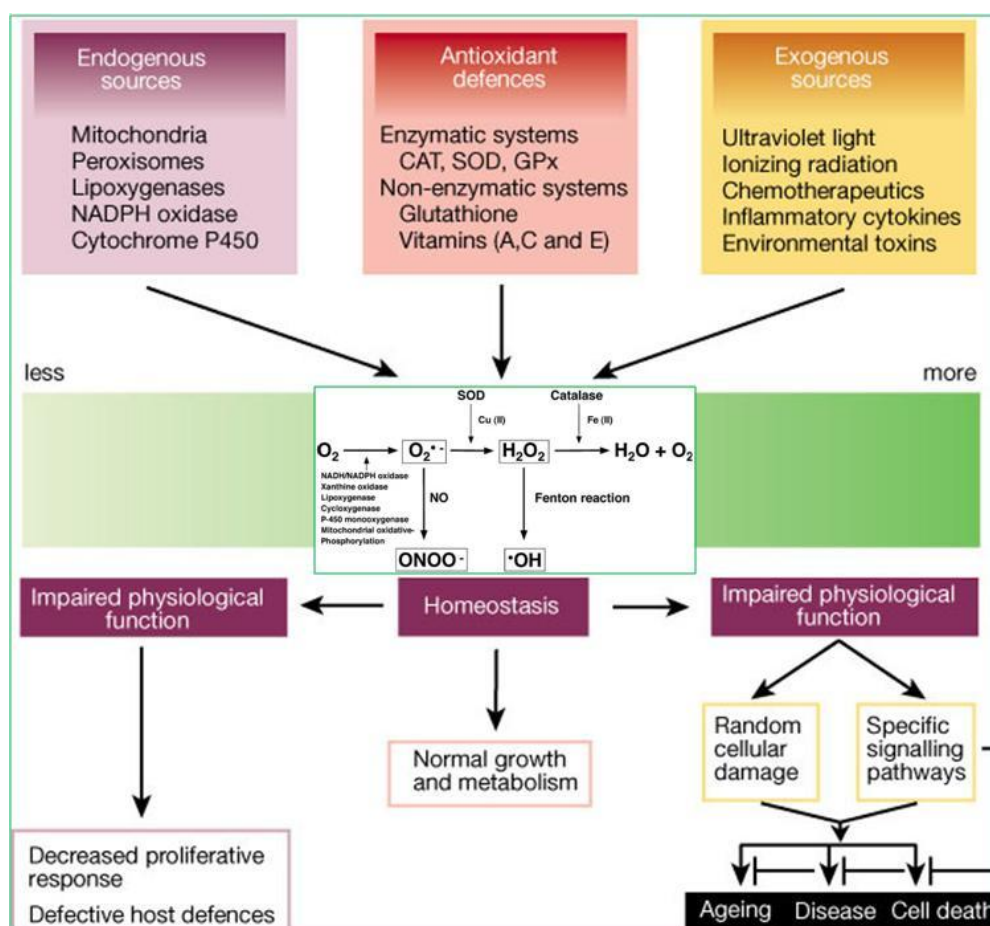


Figure 5 – Sources of reactive oxygen species (ROS), key metabolic pathways, enzymes for these species and resulted cellular damage. $O_2^{\bullet-}$, superoxide anion radical; H_2O_2 , hydrogen peroxide; $\bullet OH$, hydroxyl radical; $ONOO^-$, peroxynitrite; SOD, superoxide dismutase; CAT, catalase; GPx, glutathione peroxidase). (Figure from [107] and [108] with adaptations).

Different cellular enzyme systems are possible sources such as NAD(P)H oxidase, xanthine oxidase, uncoupled endothelial nitric oxide (NO) synthase (eNOS), arachidonic acid metabolizing enzymes including cytochrome P-450 enzymes, lipoxygenase and cyclooxygenase, and the mitochondrial respiratory chain [107, 110, 111] (Fig. 5). Although mitochondrial respiration originates most intracellular ROS in the majority of mammalian cells types (reviewed in [112]), peroxisomes are ubiquitous organelles that also control the synthesis and degradation of ROS and, thus, contribute to the maintenance of cellular ROS homeostasis [113, 114]. Even though peroxisomes probably do not generate near the amount of ROS that mitochondria their contribution to oxidative imbalance during aging has not been discarded. In this scenario, recent findings suggest that biochemical processes ruled by peroxisomes, such as hydrogen H_2O_2 turnover by a major H_2O_2 -detoxifying system, catalase, may also play a critical role in regulating cellular aging (reviewed in [115]).

In mitochondria, ROS are generated as by-products of respiration during the electron transport through respiratory chain complexes and are formed as necessary intermediates of metal catalyzed oxidation reactions. Under conditions in which the activity of the complexes I and/or III is highly reduced, a significant proportion of electrons are directly diverted to molecular oxygen, leading to the formation of the radical superoxide anion (O_2^-). As a membrane impermeable and charged molecule, O_2^- represents a particular damaging molecule. However, O_2^- may be rapidly converted to H_2O_2 by copper/zinc superoxide dismutase (Cu/ZnSod, Sod1p) in the cytoplasm and in the mitochondrial intermembranar space; and by manganese superoxide dismutase (MnSod, Sod2p) in the mitochondrial matrix [116] (Fig. 5). Relative to other ROS species, H_2O_2 is more stable, long-lived and less reactive, however, it may diffuse from mitochondria leading to a cumulative oxidative damage effect [117]. H_2O_2 may be converted to water by catalase and glutathione peroxidase (GPx) systems [116] or can also be transformed in other ROS such as hydroxyl anions (HO^-), singlet oxygen (1O_2) and hypochlorite (ClO^-). In addition it may react with nitrogen-derived free radicals such as nitric oxide (NO) to produce peroxynitrite ($ONOO^-$). In the presence of transition metals (e.g., copper and iron), H_2O_2 can generate the highly reactive OH via the Fenton reaction or the Haber-Weiss reaction, which is short-lived, highly reactive, and contribute significantly to local damage.

In addition to antioxidant enzymes, there are several non-enzymatic small antioxidant molecules that play a role in detoxification including vitamins C and E and

glutathione. A primary mechanism to reduce H_2O_2 and lipid peroxides to water and corresponding alcohols, respectively, uses reduced glutathione (GSH) and is mediated by glutathione peroxidase. Therefore, the ratio of the oxidized form of glutathione (GSSG) and the reduced form (GSH) is considered a dynamic indicator of the oxidative stress of an organism. However, and despite these defences, sustained high levels of ROS surpassing the antioxidant capacity of the cell results in oxidative stress and, ultimately, in the indiscriminate damage to cellular components (lipids, DNA, proteins, mitochondrial components) compromising cell function and promoting cellular aging and death (reviewed in [107]) (Fig. 5).

In 1972, Harman extended his original hypothesis proposing that mitochondria, by generating and consuming most of the intracellular oxygen, may control lifespan [118]. Several studies have supported the oxidative damage theory by establishing correlations between aging, oxidative stress and levels of antioxidant defences including superoxide dismutases (Sods) and, to a slighter extent, of catalases (reviewed in [119]). Due to the established emphasis of oxidative damage theory in O_2^- most studies have focused on *SOD* genes. For instance, in long-lived worms, a genetic link between stress responsiveness and lifespan has also been established based on their resistance to oxidative stress and age-dependent increase of Sods and catalase activities [120]. In addition, lack of peroxisomal catalase was shown to induce a progeric phenotype in this organism [121]. Also, interventions extending *C. elegans* lifespan have been associated with induced mitochondrial respiration and increased oxidative stress resistance [122, 123]. However, it has also been demonstrated that loss of Cu/ZnSOD1 gene does not to reduce lifespan [124] and that its overexpression does not promote significant increases in *C. elegans* lifespan [125]. In the fly model, the overexpression of either Cu/ZnSOD [126, 127] or MnSOD [128] has been shown to promote a slight extension of lifespan. An extension of lifespan was also demonstrated in transgenic *Drosophila* expressing *SOD* [129] alone, or in combination with catalase [130]. However, as in the nematode model, a direct relationship between mitochondrial ROS production longevity has been difficult to establish in the fly model [131, 132]. A similar controversy has been suggested in mice. For instance, it has been reported that individuals expressing mitochondrially-targeted catalase display a 21% increase in lifespan [133]. However, the overexpression of Cu/ZnSOD, MnSOD, catalase or a combination of Cu/ ZnSOD and MnSOD, or Cu/ZnSOD and catalase had no effect in mice lifespan [134]. Furthermore, it has been demonstrated that a decrease in MnSOD activity gene causes

increased levels of DNA damage, but does not accelerate aging in mice [135]. On the other hand, in the exceptional long-lived mole rats several markers of oxidative damage have been described in all tissues, comparatively to mice or rats whose lifespans are much shorter [136]. A recent study conducted in ants suggests that increased stress resistance displayed by the oldest reproducing gamergates and socially isolated workers, is not coupled to increased catalase activity or glutathione levels [84]. Therefore suggesting that, as already demonstrated for other organisms, increased lifespan may be not directly coupled to higher levels of antioxidants systems. Overall these data support pioneering studies in the yeast model which have shown, for more than a decade ago, that the deletion of *SOD1* or of both *SOD1* and *SOD2* dramatically reduces CLS [58] and RLS [137]. However, and as observed in other model systems, a controversial involvement of antioxidant defences in longevity has also been demonstrated in yeast. For instance, the overexpression of both *SOD1* and *SOD2* or catalase promote a minor increase in mean survival, indicating that many other systems such as DNA-repair genes may important in yeast longevity modulation [20, 79]. Therefore, although the abrogation of antioxidant defence systems promote yeast aging [61, 138], the corresponding overexpression of these systems appear to have no significant effect in increasing maximum longevity survival.

Overall, studies conducted in different model systems that intended at dropping oxidative damage through manipulations of antioxidant enzyme systems have yielded inconclusive results so far being difficult to establish if this process promotes aging in complex organisms. There is considerable evidence from a variety of model systems indicating that in vivo oxidative damage is highly correlated with biological aging, nevertheless, increasing evidence have emerged challenging and failing to support the longstanding inverse relationship between ROS/oxidative stress and the aging process [109, 136, 139, 140]. In contrast to the pro-aging effects assigned to ROS, recent evidence indicate that specific forms of ROS may alter gene/protein expression and act as secondary messenger molecules in varying intracellular signaling pathways that modulate several cellular processes [36, 49]. For instance, low concentrations of H_2O_2 have been associated with the extension of human skin keratinocytes lifespan, being this effect accompanied by an increase in telomere length [141]. Moreover, although O_2^- may inhibit telomere elongation [142] it has been demonstrated that SODs can extend mammalian cells lifespan by promoting telomere maintenance [143]. In the long-lived Ames dwarf mice it has been suggested that vascular endothelial cells produce more

H₂O₂ than those of normal littermates [144]. Increases in the intracellular steady-state production of H₂O₂ by *SOD2* overexpression have also been shown to block the activation of cellular processes required for programmed cell death [145]. These findings suggest that ROS-mediated mechanisms may act as a pro-survival response or contribute to death. A paradoxical induction of a stress response to increased metabolism has also been referred in mice suggesting that it might also be relevant to multicellular eukaryotes for reasons widely unresolved [146, 147]. However, few studies exist providing a molecular explanation for this paradoxical involvement of ROS in aging regulation, being still uncertain whether ROS are a cause or a consequence of the aging process.

1.3 LONGEVITY REGULATION BY CALORIC RESTRICTION

Over the last decades, studies conducted in model organisms have produced a wealth of knowledge showing an interaction between gene variants and environment in determining longevity. After the pioneering studies in rats by McCay, in 1935, showing that rats fed with a restricted diet dramatically extends mean and maximum lifespan [102], different dietary restriction (DR) protocols were shown to promote longevity and delay the onset of several age-related diseases including cancer, diabetes and cardiovascular disease in rats and mice [148]. Ever since DR, and specifically caloric restriction (CR), is well established as nutritional manipulation known to increase lifespan in all model systems (Fig. 6) and to delay the onset or reduce the frequency of several age-related diseases in mammals including diabetes, cancer and cardiovascular disorders (reviewed in [22, 149]).

As previously referred (Section 1.1.1), many of the mutations that extend lifespan have been shown to decrease the activity of the nutrient-sensing signaling pathways such as Ins/IGF-like and TOR pathways. DR has been proposed to act by reducing the activity of various signal transduction pathways either directly or through the decrease in the activity of nutrient-sensing pathways (reviewed in [22, 29]) (Figs. 2 and 6). For instance, in yeast, the CLS-extending effects of CR have been demonstrated either by reducing asparagine or glutamate levels in the culture medium [45]; by transferring cells from medium to water (reviewed in [21]) or by mutational inactivation of Shc9p and Tor1p [20, 45] as well as of proteins involved in RAS protein signal transduction (Cyr1p and Ras2p [61]). The RLS-extending effects of CR have also been observed

under reduction in the glucose [56, 76] and amino acids [150] levels in the culture media; and by mutational inactivation of proteins involved in glucose metabolism (e.g. Hxk2p [56]) and glucose/nutrients-mediated signaling (e.g. Gpa2p [56]; Sch9p and Tor1p [53]) (reviewed in [151]). In the nematode model, CR can be imposed by reducing the bacterial food in the medium or mutating genes involved in feeding behaviour (e.g. *EAT2*) (reviewed in [152]). In flies, DR may be imposed by reducing the availability of live yeast in the diet or by the dilution of nutrients in the medium (reviewed in [153]). In this case, lifespan is extended by DR and, thus, without a specific reduction in calories content. In mice and rats, DR can be imposed by alternate day feeding (reviewed in [154]) or by a reduction in food/nutrient intake [148].







		Life-span increase	
		Dietary restriction	Mutations/ drugs
	Yeast	3-fold	10-fold (with starvation/ DR)
	Worms	2- to 3-fold	10-fold
	Flies	2-fold	60–70%
	Mice	30–50%	30–50% (~100% in combination with DR)
	Monkeys	Trend noted	Not tested
	Humans	Not determined	Not determined (GHR-deficient subjects reach old age)

Figure 6 - Experiments on dietary restriction and genetic or chemical alteration of nutrient-sensing signaling pathways have been shown to extend lifespan from yeast to humans. Little is known about the long-term effects in humans. (Figure from [22]).

CR studies in primates are still underway and CR effects has been suggested to promote beneficial health effects similar to rats and mice [148]. A study conducted in *rhesus* monkeys, in the Wisconsin National Primate Research Center, has shown that animals submitted to a low-calorie diet have a healthier life and may possibly live longer than their normal dieting counterparts [7] (Figs. 6 and 7). Monkeys on a restricted diet looked visibly younger, with eyes less sunken, coats thicker and posture less cramped when compared with those in normal diet conditions (Fig. 6). In humans, studies on CR longevity are already ongoing and it seems that, as for CR-rodents, this intervention may reduce the risk factors of many age-related diseases including cardiovascular disease and cancer and provides important and sustained beneficial effects against obesity, insulin resistance, inflammation, oxidative stress and hypertension (reviewed in [22, 155]). Also, an association between low-calorie diet, lifestyle and beneficial health along with longevity has already been suggested in Okinawan centenarians [156]. However, despite the existing studies pointing to a positive effect of CR on lifespan and risk factors for age-related diseases, the direct effect of CR on extension of longevity and in the amelioration of the age-related markers in humans are still under strong debate.

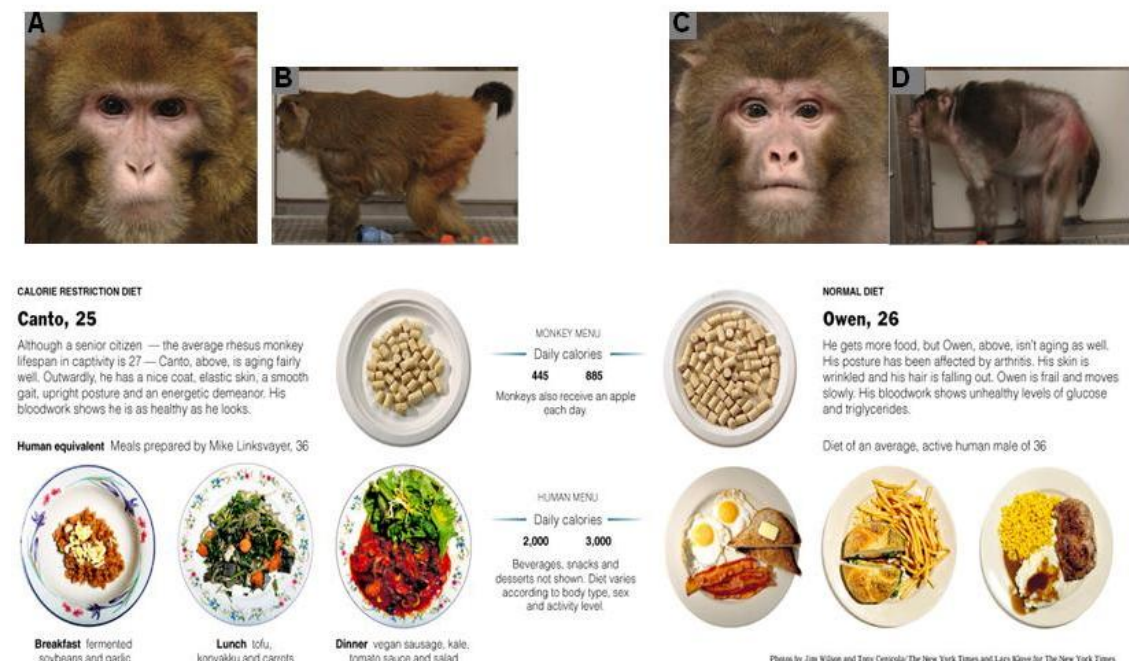


Figure 7 - A caloric restriction diet promotes a healthier phenotype (A, B) when compared to normal diet conditions (C, D). Monkeys on a restricted diet looked visibly younger, with eyes less sunken, coats

thicker and posture less cramped when compared with their dieting counterparts. Study that has been conducted in Wisconsin National Primate Research Center. (Figure from [6] with adaptations).

Overall, studies focused in DR and reduced activity of nutrient-sensing signaling pathways suggest that they may delay aging by similar mechanisms, that have been evolutionary conserved (Fig. 2). Yet, the metabolic and molecular mechanisms that underlie the different effects of CR on aging and longevity remain to be further clarified.

1.3.1 CR EFFECTS IN LONGEVITY: LINKING NUTRIENT-SENSING AND ANTIOXIDANT DEFENCES

An unifying aspect of the conserved nutrient-sensing signaling pathways is the activation of stress responses and particularly the induction of antioxidant defences (reviewed in [22]). For instance, in worms, Daf-16 regulates genes involved the detoxification of xenobiotics and free radicals (reviewed in [29]) (Fig. 2). In mammals, GH and insulin pathways have linked hormonal control to aging in association with an increase antioxidant defences (reviewed in [32]). For instance, in mice, mutations that promote deficits in Ins/IGF-1-like signaling have been shown to extend lifespan and to increase oxidative stress resistance [157, 158]. In *Drosophila*, the accumulation of sestrins which are induced by the chronic TOR activation was shown to be inhibited by the expression of the ROS scavengers including catalase and peroxiredoxin [159]. A decrease in nutrient-sensing signaling by TOR-Sch9p and RAS-AC-PKA pathways has also been shown to drastically increase yeast lifespan by converging in the induction of *SOD2* by Rim15p activation ([54], reviewed in [22]) (Fig. 2). Overall, these evidence support to the Harman's theory of aging [106] and suggest that the ability that cells have to cope appropriately with the effects of oxidative stress may underlie the CR effects mediated by decreased nutrient-sensing signaling. However, CR has also been shown to further increase the lifespan of the already long-lived mice [160] or of Ins/IGF-1 signaling-impaired flies [161], raising the possibility that CR may implicate other pro-survival mechanisms not exclusively focused in nutrient-sensing.

It has been demonstrated that CR induces ROS scavenging activity by inducing catalase activity [162] and the transcripts levels of *SOD1* and *SOD2* in rodents [163]. In yeast, CR reduces ROS production despite the increased respiratory activity in such conditions [164]. Nevertheless, CR was also shown to promote ROS production [165-167]. On the other hand, it has been demonstrated that changes in ROS production or in antioxidant defence systems fail to regulate lifespan in various model organisms including *C. elegans* [125] mice [168] and naked mole rats [136]. In *Drosophila* CR is not capable of a primary decrease in ROS production [132], suggesting no correlation between mitochondrial ROS production and lifespan in this organism. These findings suggest a link between increased respiration, high ROS production and an adaptive ROS defence response, supporting the notion that CR may promote longevity based on a secondary response to ROS-related stress originated in mitochondria, defined as mitochondrial hormesis [169]. Moreover, it is suggested that ROS itself may promote ROS defence and ultimately increase lifespan. This idea was further supported by a study in *C. elegans* showing that co-treatment of animals with different antioxidants fully abolished the life-extending effects of CR [139]. Interestingly, this study provided a direct evidence for a crucial role of increased ROS formation in lifespan extension.

In addition to targeting nutrient-sensing signaling or inducing a hormesis-like mechanism CR effects in longevity may also be explained in the light of an evolutionary theory. According "Disposable Soma Theory" (reviewed in [82],[170]), individuals with genomes that respond to food shortages by directing energy expenditure to somatic maintenance rather than reproduction, would have an increased ability to survive. Based on this assumption, CR would induce a response that reflects an evolutionary advantage with respect to survival during periods of unpredictable, short-term food shortage. In addition, and taking into consideration that survival also depends on the ability to cope with several stresses induced by the unpredictable food shortages in wild, it may also be reasonable that such evolutionary adaptation would be in line with the hormesis hypothesis.

Despite the different hypotheses proposed, the underlying mechanisms for the CR effects in delaying aging and promoting longevity are still elusive. Oxidative stress may play a major role in aging, however, it is still necessary to understand how CR mediates the involvement of antioxidant defences and of specific forms of ROS in longevity regulation. Therefore, a more detailed knowledge of the role of redox regulation and

mitochondrial function in CR in simple model systems may be of particular interest and may contribute to advances in the biology of aging.

1.3.2 CALORIC RESTRICTION EFFECTS ON *S. cerevisiae* LIFESPAN EXTENSION

CR is the most efficient manipulation known to extend lifespan in several species from yeast to mammals [151]. In yeast, CR can be modelled by reducing the glucose concentration in the culture media, from 2% to 0.5%, or by different genetic models of CR which are suggested to mimic the physiologic response of the cell under glucose limitation [56, 171]. Although reduction of the glucose content in the media culture from 2% to 0.5% results in both RLS and CLS extension [56, 76, 172-176] there is still some controversy concerning the optimal level of restriction imposed and its effects on yeast lifespan extension [177, 178]. In this scenario, it has been suggested that a more severe CR approach (0.05% glucose) mediates lifespan extension by the induction of a separate set of genes comparatively to moderate CR conditions [53, 76, 179]. In addition to glucose limitation, a different CR protocol refers the reduction of amino acid availability in the culture medium which has also been found to increase yeast RLS [150]. Overall, studies using both RLS and CLS models suggest an interesting parallel linking CR to longevity by overlapping, but distinct, molecular pathways.

Studies conducted in different yeast backgrounds have shown that CR may promote a 30-50% RLS extension [56, 76, 172-174, 180, 181]. Although the mechanisms by which CR extends yeast RLS are far from being completely understood, it has been initially suggested that CR delays aging by activating Sir2p and, thus, protecting mother cells from nucleolar damage by the accumulation of toxic rDNA circles [56]. This suggestion was further supported by studies showing that the deletion of *SIR2* prevents lifespan extension by growth on low glucose [181] or in genetic models of CR including mutants in hexokinase 2 gene (*HXK2*) and in glucose-sensing genes involved in RAS-AC (*GPR1* and *GPA2*) and cAMP-PKA signaling (*CDC35*) [181]. On the other hand, the overexpression of *SIR2* was shown to be sufficient to increase RLS [13]. A role for sirtuins in yeast lifespan has also been associated with the fact that upon glucose limitation *S. cerevisiae* shifts from fermentation to respiration, resulting in increased transcription of respiratory genes and a higher rate of oxygen consumption. It has been suggested that in yeast cells, after exhaustion of glucose, Sir2p activation is induced either by increasing cellular NAD⁺ levels [172] or decreasing

cellular NADH [182]. On the other hand, it has also been reported that CR may not change NAD⁺ levels [174]. The additive effect in lifespan extension observed in yeast cells overexpressing *SIR2* and grown in glucose restriction conditions suggest that CR effects in lifespan may be independent of Sir2p and regulated by parallel pathways still undefined [76].

A role for oxidative damage in limiting yeast RLS has also been suggested. It has been shown that deletion of *SOD1* shortens RLS [137]. Upon low glucose conditions, the overexpression of the antioxidants methionine sulfoxide reductases has also been shown to extend yeast RLS [183]. In the presence of oxygen these reductases were shown to increase RLS independently of the RLS-extending effects of CR. However, under complete anaerobic conditions RLS was reduced, not affected by reductase activity and further reduced by CR. As most ROS ultimately result from oxygen, it is suggested that ROS may not limit yeast RLS. On the other hand, an age-related accumulation of oxidative damage to macromolecules by ROS, such as protein carbonylation, has also been described during replicative aging [184]. During chronological aging the interaction between ROS, antioxidants and efficiency of energy production in lifespan regulation has also been investigated and considerable evidence exist that oxidative stress limits yeast CLS. For instance, protein carbonyls have been shown to accumulate and to depend on the rate of mitochondrial ROS production [185, 186]. On the other hand, as previously referred, CLS has been shown to be reduced upon deletion of the antioxidant genes *SOD1* and *SOD2* [58, 187] or by the activation of Sod2p associated with the lifespan-extending effects of nutrient-sensing signaling pathways [20, 60].

Although a limited role for oxidative stress in RLS has been suggested, most evidence suggest that it is an important determinant in CLS. Such a different impact of oxidative stress and ROS production in both replicative and chronological aging paradigms may be viewed as reflex of differences in mitochondrial respiration. In effect, a yeast mutant lacking *SOD2* was shown to grow as well as wild-type strain in logarithmic phase on glucose medium, in which mitochondrial electron flux is lower and the consequent production of ROS is not physiologically significant [58, 187]. On the other hand, cells lacking *SOD2* were shown to die more rapidly comparatively to wild-type cells in the postdiauxic phase [58, 187]. ROS production during increased mitochondrial metabolism may induce cellular and systemic damage, remaining as the underlying cause of aging [1].

CR also has been shown to be capable of preventing the longevity limitations associated with the absence of mitochondrial DNA as demonstrated by the RLS-extending effects of CR in respiratory-deficient yeast [177]. On the other hand, the compensatory signaling pathway that responds to loss of mitochondrial function through alterations in nuclear gene expression, the retrograde response, has been implicated in yeast RLS extension [188]. TOR signaling inhibition has been suggested to involve retrograde response through changes in nuclear gene expression [189]. For instance, the inhibition of TOR signaling with rapamycin has been shown to upregulate respiration by the induction of the expression of tricarboxylic acid cycle (TCA) enzymes and proteins involved in oxidative phosphorylation [190, 191]. However, whether TOR signaling or other CR model extends lifespan through this mechanism is still a matter of debate [192].

As previously referred in Section 1.1.1, a decrease in the activity of the conserved nutrient-sensing signaling pathways is known to extend lifespan extension in response to nutrient limitation. In this context, many of the mutations in TOR-Sch9p and RAS-AC-PKA pathways have been demonstrated to represent genetic mimetics of CR. For instance, deletion of *SCH9* [61, 171] or reduced PKA activity [49] are known to promote RLS extension. A similar decrease in the activity of Sch9p and PKA has been associated with the lifespan extending effects of CR modelled by growth on glucose restriction [171]. It has also been suggested that CR and a decrease in TOR signaling may act in the same pathway to regulate yeast longevity [53]. In effect, a genome-wide study has involved the nutrient-sensing kinases Tor1p and Tor2p in RLS in response to nutrients [53, 151] which regulate some of the downstream targets of Sch9p and PKA, including genes involved in autophagy, cell cycle progression and the stress-responsive transcription factors Msn2p/Msn4p [193]. The requirement of a Msn2/Msn4p-mediated stress response to extend lifespan during CR has been suggested by evidence showing that the deletion of *MSN2* or *MSN4* does not fail to prevent RLS extension in these conditions [49]. Also, a reduction in protein translation or ribosome production has been suggested as essential for the CR effects in RLS, as demonstrated by the RLS extension upon deletion of individual ribosomal protein genes [53]. On the other hand, the decreased activity of these two pathways is known to drastically increase yeast lifespan by converging in the activation of the Rim15p kinase and its induction of antioxidant systems [20, 45, 53-57].

The budding yeast *S. cerevisiae* has been extensively used as a model system allowing the identification of important lifespan regulators and the enrichment understanding of such regulation in multicellular organisms [10, 14]. Taking into consideration the evolutionary conservation in longevity determinants and signaling pathways from yeast to mammals, studying aging in a simple model system as *S. cerevisiae* represents a valious opportunity to a better knowledge to human aging and age-related diseases. The recent finding that highly conserved nutrient-sensing signaling kinases modulate aging in both replicative and non-replicative yeast cells through different downstream elements suggest a possible mechanism by which CR might delay aging in both mitotic and post-mitotic cell of higher eukaryotes. An investment in the identification of genes and alternative mechanism(s) that operate in parallel with the components of the nutrient-sensing signaling pathways in this simple model will provide direction for research in the CR. For instance, it is still necessary to identify additional mediators of redox regulation during CR effects in complex organisms and, ultimately, in humans.

1.3.3 CALORIE RESTRICTION MIMETICS (CRM)

Important advances have been made searching for calorie restriction (CR) mimetics (CRM) that would develop the same biological pathways without requiring people to go on severe diets for prolonged periods. Although the field of CRM is still in its youth the identification of CRM candidates may be a promising strategy to target the metabolic and stress response pathways affected by CR. Therefore it is possible to produce the CR-like effects on longevity without dropping food intake or restricting calories (reviewed in [194]).

Extended longevity and improved health conditions may be obtained in response to a perceived reduction in energy production (reviewed in [195]). It has been suggested that inhibiting energy utilization as far upstream as possible might offer a broader range of CR-like effects. In this context, the inhibition of glycolysis has emerged as a strategy to mimic the metabolic effects of CR [194]. Pioneering studies in this field have identified 2-deoxyglucose (2-DOG), a glycolytic inhibitor, as a candidate for developing CRM by providing a remarkable phenotype of CR [194]. More recently it was shown that application of 2-DOG extends lifespan in *C. elegans* [139] and in yeast [172]. Deletion of *HXK2*, which encodes the glycolytic enzyme hexokinase II, has also

been suggested to promote yeast RLS [49]. *HXX2* has also been associated with longevity control based on its involvement in a signaling pathway important for maintaining glucose repression [196]. Moreover, the pretreatment of cultured fetal hippocampal neurons with iodoacetate, which inhibits the glycolytic enzyme glyceraldehyde-3-phosphate (GAPDH), has also shown potential as a CRM strategy providing protection against several stresses [197]. On the other hand, many different targets for CRM development have been proposed at more downstream steps including sirtuin activators and mTOR inhibitors (reviewed in [195]).

The use of antioxidants as CRM has also been suggested as having benefits to human health. For instance, it has been shown that the p53 tumour suppressor controls the expression of antioxidant genes and that p53 null mice display increased oxidative stress [198]. In addition, lifespan and carcinogenesis in p53 null mice has been shown to be rescued by the administration of pharmacological doses of the antioxidants [198]. Therefore, it is suggested that rather than manipulating antioxidant enzymes, it would be particularly interesting to manipulate the signaling pathways that control intracellular ROS levels. But, is it prudent to artificially modulate the fragile balance between oxidative stress and antioxidants? Results from ongoing clinical trials and additional studies will be necessary to extend our knowledge on the impact of antioxidant supplements on human health. Meanwhile, a major question remains to be answered: is oxidative stress the main cause of aging and age-related diseases or rather a consequence? Ideally, we should have more data to address these questions.

CHAPTER2.

MATERIALS AND METHODS

2. MATERIALS AND METHODS

2.1 STRAINS

Saccharomyces cerevisiae strains BY4742, CEN.PK and W303 as well as the respective knockouts in the studied genes used in this study are represented in Table 1.

Table1 - *Saccharomyces cerevisiae* strains used in this study.

Strain	Genotype/phenotype	Source
BY4742 wt	MAT α his3 Δ 1 leu2 Δ 0 lys2 Δ 0 ura3 Δ 0	Euroscarf
BY4742 <i>Acta1</i>	Mat α ; his3 Δ 1; leu2 Δ 0; lys2 Δ 0; ura3 Δ 0; YDR256c::kanMX4	Euroscarf
BY4742 <i>Actt1</i>	Mat a; his3 Δ 1; leu2 Δ 0; lys2 Δ 0; ura3 Δ 0; YGR088w::kanMX4	Euroscarf
BY4742 <i>Acta1Actt1</i>	Mat a; his3 Δ 1; leu2 Δ 0; lys2 Δ 0; ura3 Δ 0; YGR088w::kanMX4::cta1::URA3	V. Costa
BY4742 <i>CTA1</i> oex	MAT α his3 Δ 1 leu2 Δ 0 lys2 Δ 0 ura3 Δ 0::pUG35CTA1	This study
BY4742 <i>CTA1</i> (empty vector)	MAT α his3 Δ 1 leu2 Δ 0 lys2 Δ 0 ura3 Δ 0::pUG35	This study
BY4742 <i>Apex13</i>	Mat a; his3 Δ 1; leu2 Δ 0; lys2 Δ 0; ura3 Δ 0; YLR191w::kanMX4	Euroscarf
BY4742 <i>Apexx14</i>	Mat a; his3 Δ 1; leu2 Δ 0; lys2 Δ 0; ura3 Δ 0; YGL153w::kanMX4	Euroscarf
BY4742 CEN.PK113-7D wt	BY4742 <i>rho0</i> MATa, prototrophic	This study P.Koetter
W303-1A wt	MATa ura3-1 leu2-3,112 his3-11,15 trp1-1 can1-100 ade2-1 ade3::hisG	V. Costa
W303-1A <i>Acta1</i>	alpha leu2 ura3 his3 trp1	V. Costa
BY4742 <i>Δhxx2</i>	Mat a; his3 Δ 1; leu2 Δ 0; lys2 Δ 0; ura3 Δ 0; YGL253w::kanMX4	Euroscarf
BY4742 <i>Δpfk2</i>	Mat a; his3 Δ 1; leu2 Δ 0; lys2 Δ 0; ura3 Δ 0; YMR205c::kanMX4	Euroscarf
BY4742 <i>Δtdh2</i>	Mat a; his3 Δ 1; leu2 Δ 0; lys2 Δ 0; ura3 Δ 0; YJR009c::kanMX4	Euroscarf
BY4742 <i>Δtdh3</i>	Mat a; his3 Δ 1; leu2 Δ 0; lys2 Δ 0; ura3 Δ 0; YGR192c::kanMX4	Euroscarf
BY4742 <i>Δpdc1</i>	Mat a; his3 Δ 1; leu2 Δ 0; lys2 Δ 0; ura3 Δ 0; YLR044c::kanMX4	Euroscarf
CEN.PK	MATa MAL2-8c SUC2; auxothrophic	L.Gustafsson
KOY.PK21C83 wt	Strain displaying high glucose transport characteristics *	
CEN.PK	Strain displaying low glucose transport characteristics *	L.Gustafsson
KOY.TM6*P		
CEN.PK	Strain displaying high/intermediate glucose transport characteristics *	L.Gustafsson
KOY. HXT 7P		
BY4742 <i>Δrim15</i>	Mat a; his3 Δ 1; leu2 Δ 0; lys2 Δ 0; ura3 Δ 0; YFL033c::kanMX4	Euroscarf

* Strains producing functional chimeras between the hexose transporters Hxt1 and Hxt7 and with altered glucose transport/uptake characteristics (strains description in [199]).

(Wt, wild type; oex, overexpression).

2.1.1 GENERATION OF *rho0* STRAINS

The BY4742 *rho0* strain used for lifespan analysis and fluorescence microscopy was generated by treatment with ethidium bromide. In a standard experiment cells are washed with sterile 10 mM KPO₄, pH 7 and inoculated into 10 ml of 10 mM KPO₄ phosphate, pH 7 buffer containing 10 µg/ml ethidium bromide. After incubation for 1 hour with shaking (150rpm) at 26°C cells are spread on YPD plates for single colonies growth. Small colonies should correspond to respiratory deficient mutants. Each experiment was determined for more than one *rho0* isolate in order to verify the observed phenotype. Absence of mitochondrial DNA was verified by fluorescence microscopy of log phase cells stained with DAPI and by the absence of growth on the non-fermentable carbon source, glycerol.

2.2. MEDIA

Cells were maintained in YEPD agar medium consisting of 0.5% yeast extract, 1% peptone, 2% agar and 2% glucose. All experiments were performed in synthetic complete (SC) medium containing 0.67% yeast nitrogen base without amino acids (Difco Laboratories, Detroit, MI) supplemented with the appropriate amino acids and bases for which the strains were auxotrophic (50µg ml⁻¹ histidine, 50µg ml⁻¹ lysine, 300µg ml⁻¹ leucine, 100µg ml⁻¹ uracyl, 100µg ml⁻¹ tryptophan and 100µg ml⁻¹ adenine). Calorie restriction (CR) was accomplished by reducing the glucose concentration from 2% to 0.5% or to 0.05% in the initial culture medium. In a standard experiment, overnight cultures were grown in either media and inoculated into flasks with a ratio volume/medium of 3:1 at 26°C with shaking at 150 rpm. Growth was monitored by measuring the turbidity of the culture at 640 nm (OD₆₄₀) on a spectrophotometer (Genesys 20/Thermo Spectronic) and viability was determined by counting colony-forming units (CFUs) after 2 d of incubation at 26 °C on YEPD agar plates. For growth in buffered medium, a citrate phosphate buffer (64.2 mM Na₂HPO₄ and 17.9 mM citric acid) adjusted to pH 6.0 was added to the medium before inoculation.

2.3 CHRONOLOGICAL LIFESPAN ASSAY

Yeast chronological lifespan (CLS) was measured as previously described [46-48]. In a standard experiment, overnight cultures were grown in SC medium containing different concentrations of glucose and then inoculated into flasks containing medium with the same concentration of glucose at a volume ratio of 1:3. These cultures were then incubated at 26 °C with shaking at 150 rpm. Cultures reached stationary phase 2–3 d later and this was considered day 0 of CLS. Survival was assessed by counting colony-forming units (CFUs) after 2 d of incubation of culture samples at 26 °C on YEPD agar plates beginning at day 0 of CLS (when viability was considered to be 100%) and then again every 2–3 d until less than 0.01% of the cells in the culture were viable.

2.4 CONSTRUCTION OF THE *CTA1* OVEREXPRESSING AND *CTA1CTT1* DOUBLE MUTANT STRAINS

To construct the *CTA1* overexpressing strain, *CTA1* was amplified by PCR with the following primers: F (CCGGTCTAGAATGTCGAAATTGGGACAAGA) and R (CCGGAAGCTTGGAGTTACTCGAAAGCTCAG) using genomic DNA isolated from *Saccharomyces cerevisiae* wild-type cells as template. The resulting fragment was cloned into the XbaI–HindIII site of the plasmid pUG35 (EUROSCARF), producing the plasmid pUG35*CTA1*. The wild-type *S. cerevisiae* strain BY4742 was transformed by the lithium acetate method with plasmid pUG35*CTA1* to produce the strain overexpressing *CTA1* (“MET-*CTA1*”) or with the plasmid pUG35 to produce the “empty-vector” control strain. Double *CTA1CTT1* mutant cells were obtained by *CTT1* disruption in the Δ *cta1* strain. A deletion fragment, containing URA3 gene and *CTT1* flanking regions, was amplified by PCR using genomic DNA isolated from W303 Δ *ctt1*::URA3 cells and the following primers: F (ATGGGGATAGAACCTCCGTTAT) and R (GAATTTAAAGTTTTCTCTGCTGG). Cells were transformed by electroporation and Δ *cta1ctt1* mutants were selected in minimal medium lacking uracil. Gene disruption was confirmed by the analysis of catalase activity in a native gel. Double mutants lacking both Cta1p and Ctt1p activity were selected.

2.5 PHARMACOLOGICAL TREATMENTS

Pharmacological inhibition of catalases was accomplished by treating cells at day 0 of CLS with 10 mM 3-amino-1,2,4-triazole (3AT) (Sigma), which binds covalently to the active center of the active tetrameric heme-containing form of catalases [200, 201]. Pharmacological inhibition of glutathione synthesis was accomplished by treating cells at day 0 of CLS with 1 mM L-buthionine-sulfoximine (BSO) (Sigma), which indirectly inhibits glutathione synthesis by interacting with γ -glutamylcysteine synthetase [202, 203].

The study of the ectopic effects of hydrogen peroxide (H_2O_2) on CLS was performed by treating non-CR (2% glucose) wild-type cells with 0, 0.2, 0.3, and 1 mM H_2O_2 (Merck) beginning at day 0 of CLS and survival was measured as described before. For hydrogen peroxide (H_2O_2) treatment, yeast cells were grown until mid-log phase in liquid media and then harvested and suspended (10^6 cells/ml) in fresh medium followed by the addition of 0, 0.5, 1, 1.5 and 2 mM H_2O_2 and incubation for 200 minutes at 26°C with stirring (150 r.p.m.) in the dark, as previously described [204]. For acetic acid treatment yeast cells were grown until mid-log phase in liquid media and then harvested and suspended (10^6 cells/ml) in fresh medium followed by the addition of 0, 80, 120, 160 and 180 mM of acetic acid and incubation for 200 minutes at 26°C with stirring (150 r.p.m.) in the dark, as previously described [80]. After treatments, approximately 300 cells were spread on YPD agar plates and viability was determined by counting colony-forming-units (c.f.u.) after 2 days of incubation at 26°C.

The pharmacological inactivation of nutrient-sensing signalling pathways was performed treating cells with 10 μ M manumycin, 3 μ M wortmannin and 1 μ M rapamycin (for RAS, PKA and TOR inhibition, respectively). A diluted solution of each compound was directly administrated to cells at day 7 of CLS.

2.6 FACS ANALYSIS OF INTRACELLULAR REACTIVE OXYGEN SPECIES

Levels of intracellular ROS were measured using dihydrorhodamine 123 (DHR) or 2',7'-dichlorodihydrofluorescein diacetate (H_2DCFDA) (Molecular Probes), compounds that are capable of detecting H_2O_2 [205]. Briefly, aliquots were taken at selected time points and DHR was added to a final concentration of 15 μ g/mL and cells were incubated for 90 min at 26 °C. For H_2DCFDA staining cells were incubated with a final concentration of 10 μ M for 90 min at 30 °C. Cells were then washed twice in PBS and analyzed by flow cytometry. FACS analysis used an EPICS XL-MCL

(Beckman– Coulter) flow cytometer equipped with a 15 mW argon laser emitting at 488 nm. The green fluorescence was collected through a 488-nm blocking filter, a 550-nm long-pass dichroic with a 525 nm band pass. Data acquired from a minimum of 30,000 cells per sample at low flow rate were analyzed with the Multigraph software included in the system II software for the EPICS XL-MCL version 1.0. Intracellular superoxide anions were measured using dihydroethidium (DHE) (Molecular Probes). Aliquots of cells were collected at indicated time points and DHE was added to a final concentration of 5 μ M from a 5-mM stock in DMSO. After incubation for 10 min at 30 °C, cells were washed once with 0.5 mL PBS, resuspended in 50 μ L PBS, and added to 1 mL PBS. After briefly sonicating the suspension, DHE signals were measured using a FACSCaliber2 flow cytometer (BD-Biosciences) with a 488-nm excitation laser. Signals from 25,000 cells/sample were captured in FL3 (>670 nm) at a flow rate of 5,000 cells/s. For specific experiments, DHR signals were measured using a FACSCaliber flow cytometer to capture signals in FL1 (530 nm \pm 15 nm) from 25,000 cells/sample at a flow rate of 5,000 cells/s. Data collected with the FACSCaliber2 flow cytometer were processed with Flowjo software (Tree Star) and quantified with WinList software (Verity Software House).

2.7 PROTEIN EXTRACT PREPARATION, SUPEROXIDE DISMUTASE, AND CATALASE ACTIVITY ASSAYS

For determination of catalase and superoxide dismutase activities, yeast extracts were prepared in 25 mM Tris buffer (pH 7.4) containing a mixture of protease inhibitors. Protein content of cellular extracts was estimated by the method of Lowry using BSA as a standard. Briefly, for determination of catalase activity 30 μ g of proteins were separated by native PAGE and catalase activity was analyzed in situ in the presence of 3,3'-diaminobenzidine tetrahydrochloride (Sigma), using the H₂O₂/peroxidase system [206]. The gel was incubated in horseradish peroxidase (Sigma) (50 μ g/ mL) in 50 mM potassium phosphate buffer (pH 6.7) for 45 min. H₂O₂ was then added to a final concentration of 5 mM and incubation was continued for 10 min. The gel was then rapidly rinsed twice with distilled water and incubated in 0.5 mg/mL diaminobenzidine in 50 mM potassium phosphate buffer until staining was complete. Superoxide dismutase activities were measured on the basis of their ability to inhibit reduction of nitro blue tetrazolium to formazan in nondenaturing polyacrylamide

gels [207]. Sod2p activity was distinguished from Sod1p activity on the basis of the ability of 2 mM cyanide to inhibit Sod1p, but not Sod2p. Quantification of band intensities was performed by densitometry using Quantity One Basic software from Bio-Rad.

2.8 WESTERN-BLOT ANALYSIS

For detection of protein levels by Western-blot total cell extracts, aged cells were collected and disrupted using glass beads and lysis buffer [1% v/v triton X-100, 120 mM NaCl, 50 mM Tris-HCl pH 7.4, 2mM EDTA, 10% v/v glycerol, 1mM PMSF and Complete Mini protease inhibitor cocktail (Roche, Germany)]. Of total protein, 40 µg was resolved on a 10% SDS gel and transferred to a nitrocellulose membrane for 90 min at 100V. Membranes were then probed with the following antibodies: polyclonal rabbit anti-Pex14p (1:5000), monoclonal mouse anti-porin (1:5000) (Invitrogen) and monoclonal goat anti-actin (1: 5000). Correspondent HRP-conjugated IgG secondary antibodies were used at a dilution of 1:5000 and detected by enhanced chemiluminescence. The anti-Pex14p and anti-actin antibodies were kindly supplied by Prof. Wolfgang Girzalsky and Prof. Campbell Gourlay, respectively.

2.9 DETERMINATION OF OXIDATIVE DAMAGE

To measure levels of carbonylated proteins, samples of total cell protein were derivatized by mixing aliquots with one volume of 12% (wt/vol) SDS and two volumes of 20 mM 2,4-dinitrophenylhydrazine in 10% (vol/vol) trifluoroacetic acid (a blank control was treated with two volumes of 10% (vol/vol) trifluoroacetic acid alone) [208]. After incubation for 30 min at room temperature in the dark, samples were neutralized and proteins (0.15 µg) were slot blotted onto a poly-vinylidene fluoride membrane (Hybond-PVDF, GE Healthcare). The PVDF membrane was probed with rabbit IgG anti-DNP (Dako) (1:5,000 dilution) and goat anti-rabbit IgG linked to horseradish peroxidase (Sigma) (1:5,000 dilution) by standard techniques. Detection of derivatized proteins was accomplished by chemiluminescence, using reagents contained in a RPN 2109 kit (GE Healthcare). The membranes were exposed to a Hybond- ECL film (GE Healthcare) for 15 s to 1 min, and the film was developed. Quantitative analysis of carbonyls was performed by densitometry using Quantity One Basic software from Bio-

Rad. Autofluorescence signals indicating oxidative damage to proteins and lipids were collected from 25,000 cells/sample using a FACSCaliber2 flow cytometer as described above for DHE measurements, except that cells were not stained with DHE after the PBS wash step.

2.10 EPIFLUORESCENCE AND CONFOCAL MICROSCOPY

Epifluorescence microscopy was performed using an Olympus BX61 microscope equipped with a high-resolution DP70 digital camera and an Olympus PlanApo 60 \times /oil objective, with a numerical aperture of 1.42. Total magnification 600 \times . (Bar, 5 μ m.) Yeast cells either expressing Cta1p–GFP and DsRedSKL were washed twice with PBS buffer (pH 7.4) and subsequently examined using a confocal laser-scanning microscope.

2.11 STATISTICAL ANALYSIS

Data are reported as mean values of at least three independent assays and presented as mean \pm SD or mean \pm SEM. The arithmetic means are given with SD with 95% confidence value. Statistical analyses were carried out using Student's t-test. *P < 0.05 was considered statistically significant.

CHAPTER3.

RESULTS AND DISCUSSION

SECTION 3.1

**CALORIC RESTRICTION EXTENDS *Saccharomyces cerevisiae*
CHRONOLOGICAL LIFESPAN ASSOCIATED WITH INCREASES
IN REACTIVE OXYGEN SPECIES ACCUMULATION**

The results presented in this section were partially published as follow:

Mesquita A., Weinberger M., Silva A., Sampaio-Marques B., Almeida B., Leão C., Costa V., Rodrigues F., Burhans W.C., Ludovico P. Caloric restriction or catalase inactivation extends yeast chronological lifespan by inducing H₂O₂ and superoxide dismutase activity. Proc Natl Acad Sci U S A. 2010 Aug 24;107(34):15123-8.

National congresses:

- Mesquita, A., Silva, A., Sampaio-Marques, B., Logarinho E., Leão, C., Rodrigues, F. and Ludovico, P. 2010. Reactive oxygen species generation during chronological lifespan in *Saccharomyces cerevisiae*. XVIII Jornadas de Biologia das leveduras "Professor Nicolau van Uden", Lisboa, Portugal. (Oral communication by Mesquita, A.)
- Mesquita, A., Silva, A., Sampaio-Marques, B., Logarinho E., Leão, C., Rodrigues, F. and Ludovico, P. 2009. Oxidative stress during chronological lifespan in *Saccharomyces cerevisiae*. MicroBiotec09, Vilamoura, Portugal. (Oral communication by Mesquita, A.).

3.1. CALORIC RESTRICTION EXTENDS *Saccharomyces cerevisiae* CHRONOLOGICAL LIFESPAN ASSOCIATED WITH INCREASES IN REACTIVE OXYGEN SPECIES ACCUMULATION

3.1.1 CALORIC RESTRICTION EXTENDS *S. cerevisiae* CHRONOLOGICAL LIFESPAN ASSOCIATED WITH AN INCREASED FRACTION OF CELLS DISPLAYING HIGH INTRACELLULAR LEVELS OF REACTIVE OXYGEN SPECIES, PARTICULARLY H₂O₂

While CR in worms, flies and mammals usually requires a complex food source limitation, in yeast, moderate CR is commonly modelled by reducing the glucose content in the media culture from 2% to 0.5% [56, 76, 172-175]. However, there is still some controversy in the optimal level of restriction imposed and its effects on lifespan extension [177, 178]. A more severe glucose restriction (0.05%), associated with a fully respiratory metabolism and lower specific growth rates (Fig. 1B), has been suggested to induce a separate set of genes that also mediate lifespan extension [53, 76, 179]. In this study, and taking into consideration that these two CR approaches may signal different CLS regulation pathways, cells were grown in either 0.5% and 0.05% glucose concentrations in specific CR experiments described hereafter. As expectable, CLS measured by the survival of non-dividing stationary phase *S. cerevisiae* cells was clearly extended by CR (0.5% and 0.05% glucose) comparatively to cells grown in non-CR conditions (2% glucose) [56, 76, 172-175], being this effect independent of the genetic background (Fig. 1A-D). In addition, CLS extension was dependent on the level of glucose restriction, being higher in cells upon severe restriction (0.05% glucose) comparatively to cells grown in moderate glucose restriction (Fig. 1A-D). Therefore, using different genetic backgrounds, these results established the CLS-extending effects of both CR approaches in the budding yeast *S. cerevisiae*.

A leading hypothesis on the mechanisms through which CR prevents aging is that it decreases reactive oxygen species (ROS) generation and therefore their oxidative damage effects [209-211]. Therefore, CR is suggested to mitigate the destructive effects of ROS which, according to the free radical theory proposed by Harman, are primordial aging promoters [1]. In this scenario, and taking into consideration that ROS and oxidative stress have also been previously suggested as crucial negative regulators of yeast CLS [187, 212, 213], we evaluated whether the *S. cerevisiae* CLS-extending

effects of CR are linked with increases of ROS production. To answer this question, CLS experiments were followed by measurements of the intracellular ROS levels by

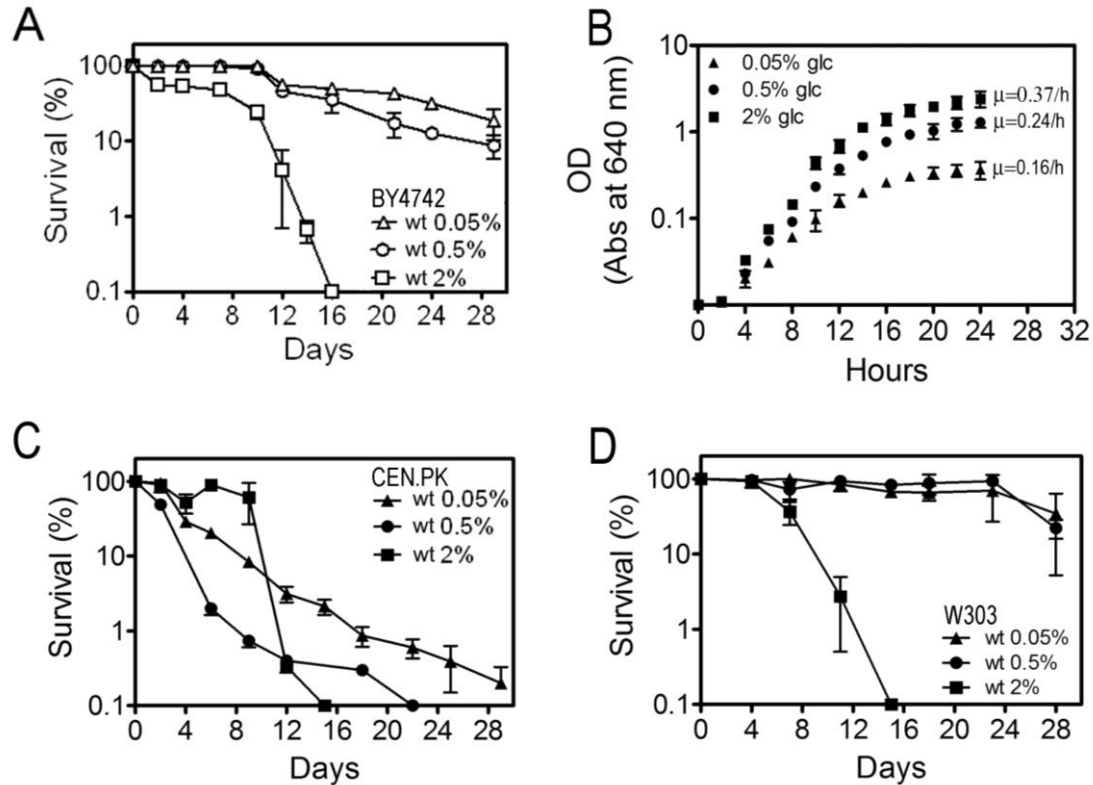


Figure 1 - CR (0.05% and 0.5% glucose) extends *S. cerevisiae* CLS comparatively to non-CR conditions (2% glucose). Survival of BY4742 (A), CEN.PK (C) and W303 (D) cells was measured by cell viability over time beginning the day cultures reached stationary phase (day 0) and expressed as % of survival compared with survival at day 0 (100%). (B) Growth curves, specific growth rates (μ) and glucose concentrations of BY4742 cells cultured in SC medium upon severe (0.05% glucose), moderate (0.5% glucose) and non-CR conditions (2% glucose). Values are means \pm SD of three independent experiments.

flow cytometry and epifluorescence microscopy techniques, using dihydrorhodamine 123 (DHR) and 2',7' dichlorodihydrofluorescein diacetate (DCF); two probes commonly employed for detection of hydroperoxides, lipid hydroperoxides, peroxynitrites and hydroxyl radicals [214-217]. However, because DCF fluorescence is known to be modulated in an artifactual manner by changes in cellular pH or by cytosolic esterases which hydrolyze the acetate groups of the probe, rather than by oxidation [Molecular Probes], DHR was preferentially used in most of the experiments described hereafter. Surprisingly, and differently from what has been mostly suggested [187, 212, 213], our results revealed that the CLS-extending effects of CR occur in parallel with increases, rather than decreases, in the intracellular ROS levels (Fig. 2), as detected by staining

cells with both the fluorescent probes DHR (DHR positive cells) (Fig. 2A-D) and DCF (DCF positive cells) (Fig. 2E, F). Furthermore, the intracellular levels of ROS accumulation were dependent on the level of glucose restriction, being higher in cells upon severe conditions (0.05% glucose) comparatively to moderate conditions (0.5% glucose) (Fig. 2A).

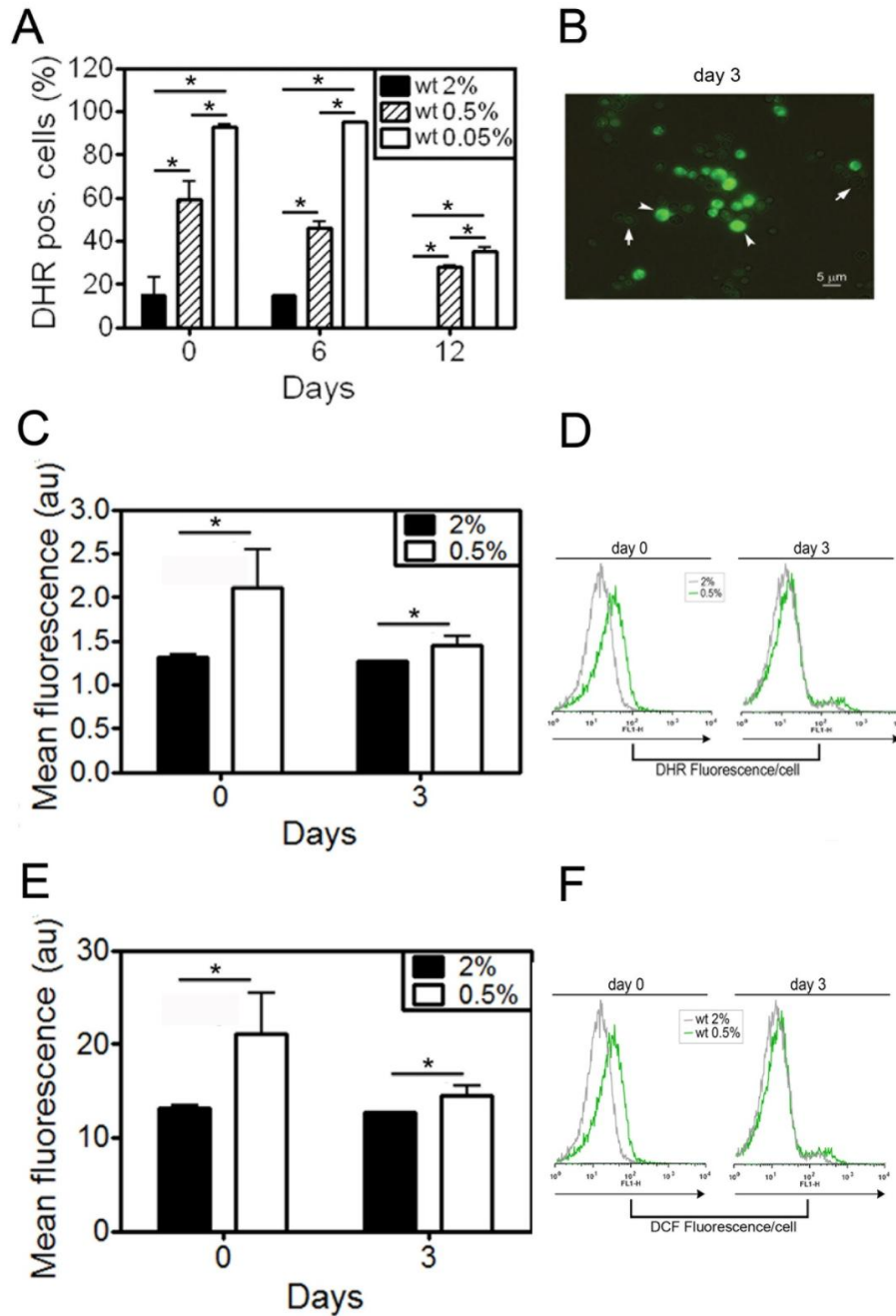


Figure 2 - The CLS-extending effects of CR occur in parallel with increased levels of intracellular ROS accumulation in *S. cerevisiae* wild type cells. Intracellular ROS accumulation detected by FACS

measurements of fluorescence of the probes dihydrorhodamine 123 (DHR) (A, C and -D) and 2',7'-dichlorodihydrofluorescein diacetate (DCF) (E,F). (B) Photomicrograph of *S. cerevisiae* DHR-stained wild-type cells at day 3 of CLS during moderate CR conditions (0.5% glucose). Arrowheads indicate cells displaying bright green fluorescence and correspond to cells with high intracellular ROS levels, designated DHR positive cells. Arrows indicate cells that did not stain with DHR. Cells were visualized by epifluorescence microscopy using an Olympus BX61 microscope equipped with a high-resolution DP70 digital camera and an Olympus PlanApo 60×/oil objective, with a numerical aperture of 1.42. Total magnification 600×. (Bar, 5 μm.) Three to five biological replicas of each experiment were performed. Statistical significance (*P < 0.05) was determined by Student's t-test. Bar graphs indicate mean ± SEM (%) or ± SD fluorescence/cell (% or arbitrary units, respectively) measured in 30,000 cells/sample in three independent experiments. ROS levels were evaluated both by the number of stained cells (% of cells displaying high ROS accumulation) and by the concentration of probe per cell (mean channel fluorescence).

As these two probes are not oxidized by superoxide (O_2^-) to any significant extent [216, 218], increases in the fluorescent product could be interpreted, at a first glance, as intracellular changes in hydrogen peroxide (H_2O_2). These results are supported by recent studies that challenge and fail to support the longstanding inverse relationship between ROS/oxidative stress and the aging process [109, 136, 139, 140]. For instance, higher levels of oxidative stress were suggested in long-lived naked mole rats comparatively to physiologically age-matched mice [136]. In the nematode model *Caenorhabditis elegans*, it has also been suggested that the lifespan-extending effects of CR occur in parallel with the induction of mitochondrial respiration and increases in oxidative stress [139]. In mammals specific forms of ROS have been shown to function as essential secondary messengers in several intracellular signaling pathways [109] and specifically H_2O_2 has been recently implicated as a cell-survival signaling molecule [140]. These controversial data suggest that new experimental designs should be performed to a better understanding of the involvement of specific forms of ROS in the CLS-extending effects of CR.

3.1.2 PEROXISOMES AND MITOCHONDRIA ARE INVOLVED IN THE CLS-EXTENDING EFFECTS OF CR ASSOCIATED WITH HIGH INTRACELLULAR ROS

Having in mind the previously results suggesting a dual role for ROS in the CLS-extending effects of CR we next focused on the involvement of mitochondria, a major

organelle implicated in ROS production and scavenging. As mitochondria are a major source of ROS in the cell, we next asked whether diminishing mitochondrial function compromises CLS and its effects on CLS extension by CR. For that, we produced an isogenic wild type strain lacking mitochondrial DNA (*rho0* cells) and assessed for its survival in both CR and non-CR conditions (Fig. 3A). In addition, measurements of intracellular ROS accumulation were performed (Fig. 3B and C).

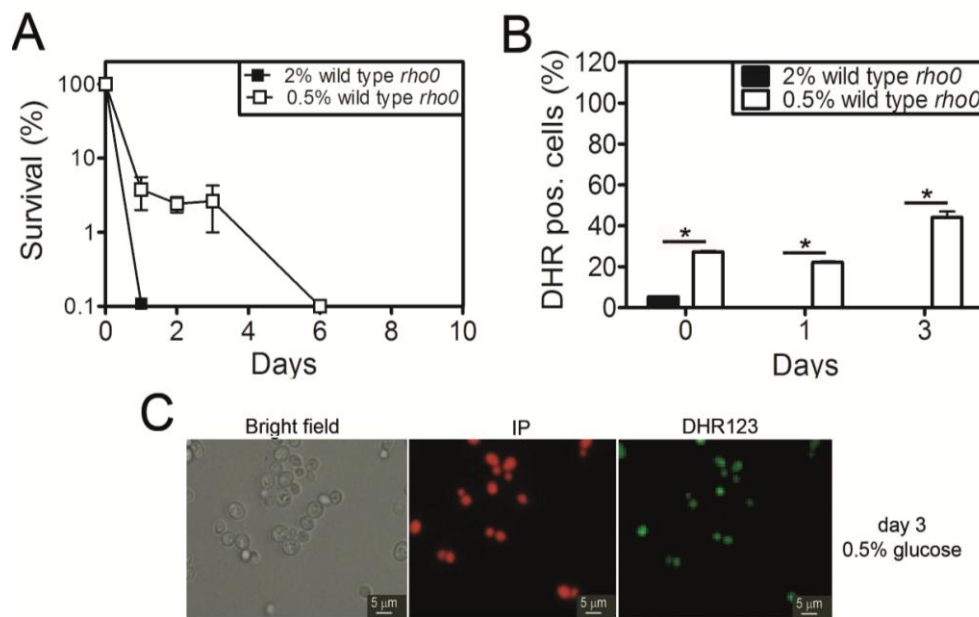


Figure 3 - CR extends CLS of *S. cerevisiae* BY4742 *rho0* cells in SC medium associated with increased intracellular ROS levels. (A) Survival of BY4742 *rho0* cells measured by cell viability at 2- to 3-d intervals beginning the day cultures reached stationary phase (day 0) and expressed as % of survival compared with survival at day 0 (100%). (B) Intracellular ROS accumulation in wild type *rho0* cells detected by FACS measurements of fluorescence of the probe dihydrorhodamine 123 (DHR). (C) Photomicrograph of *S. cerevisiae* DHR-stained BY4742 *rho0* cells at day 3 of CLS during moderate CR conditions (0.5% glucose). Cells displaying bright green fluorescence correspond to cells with high intracellular ROS levels, designated DHR positive cells. Cells were also stained with propidium iodide (red fluorescence) to have an indication of cell survival, as it is excluded by viable cells but can penetrate cell membranes of dying or dead cells. Cells were visualized by epifluorescence microscopy using an Olympus BX61 microscope equipped with a high-resolution DP70 digital camera and an Olympus PlanApo 60 \times /oil objective, with a numerical aperture of 1.42. Total magnification 600 \times . (Bar, 5 μ m.) Three to five biological replicas of each experiment were performed. Statistical significance (* $P < 0.05$) was determined by Student's t-test. Bar graphs indicate mean \pm SEM (%) measured in 30,000 cells/sample in three independent experiments.

The results revealed that lack of functional mitochondria resulted in a reduction of CLS (Fig. 3A) comparatively to the correspondent wild type cells (Fig. 1A), consistently with the essential pro-longevity role [138]. However, CR was still able to promote a clear extension of CLS in *rho0* cells (Fig. 3A) associated with increased levels of intracellular ROS accumulation (Fig. 3B). Altogether, these data pointed to the hypothesis that the CLS-extending effects of CR were not exclusively dependent of mitochondria, or mitochondrial-derived ROS, and could be associated with an extramitochondrial source of ROS.

Cellular ROS generation results from a number of processes and organelles besides mitochondria which are critical for normal cell function (reviewed in [109]). Peroxisomes are ubiquitous organelles that, by being able to control the synthesis and degradation of ROS, contribute to the maintenance of cellular ROS homeostasis [113, 114]. Following this line of thought, we hypothesised that peroxisomal production of ROS was contributing to the CLS-extending effects of CR previously observed. In a first approach we aimed to address the effect of compromising peroxisomal function in the CLS-extending effect of CR. To tackle this task, we used two strains mutated in *PEX13* and *PEX14*, which encode proteins involved in the peroxisomal import system, and thus with altered peroxisomal function [219]. The results obtained revealed an extension of CLS in $\Delta pex13$ and $\Delta pex14$ cells comparatively to wild type cells under non-CR conditions (Fig. 4A and C). In addition, the longer CLS observed in $\Delta pex13$ and $\Delta pex14$ cells was accompanied by an increased fraction of cells containing high ROS levels under non-CR conditions from day 6 on (Fig. B and D). However, mutations in *PEX13* and *PEX14* resulted in a decrease in CLS during moderate CR conditions (0.5% glucose) comparatively to wild type cells (Fig. 4A and C). On the other hand, the shorter CLS observed in $\Delta pex13$ and $\Delta pex14$ cells under moderate CR conditions was accompanied by a decreased fraction of cells containing high ROS levels (Fig. 4A and C). Thus, suggesting that functional peroxisomes or, at least, peroxisomal-derived ROS may be required for the CLS-extending effects of moderate CR observed in wild type cells. Similar to non-CR conditions, the severest CR conditions (0.05% glucose) promoted an extension of CLS in both $\Delta pex13$ and $\Delta pex14$ (Fig. 4A and C) associated with increases in the intracellular ROS levels at day 12 (Fig. 4B and D), probably reflecting the increase of mitochondrial ROS production associated with a fully respiratory metabolism.

In an opposite approach, peroxisome's biogenesis was promoted in wild type cells and its effects in CLS were addressed (Fig. 4E). The results showed that CLS was promoted in wild type cells cultured in peroxisome's biogenesis inducing media (0.5% oleate and Tween 80 as energy and carbon sources) comparatively to those grown in 2% glucose (Fig. 4E). However, the CLS-extending effects of oleate were not so drastic as those promoted by both CR conditions (Fig. 4E). Overall, the findings herein described raise the hypothesis that peroxisomes or, at least, peroxisomes-derived ROS may be involved in the CLS-extending effect of CR. Interestingly, recent findings suggest that biochemical processes ruled by peroxisomes, such as hydrogen H_2O_2 turnover, may also play a critical role in regulating cellular aging (reviewed in [115]). It has also been suggested that pexophagy, an autophagy-related process for selective degradation of oxidatively damaged and dysfunctional peroxisomes, may have a key role in the maintenance of the population of peroxisomes during the aging process [220, 221].

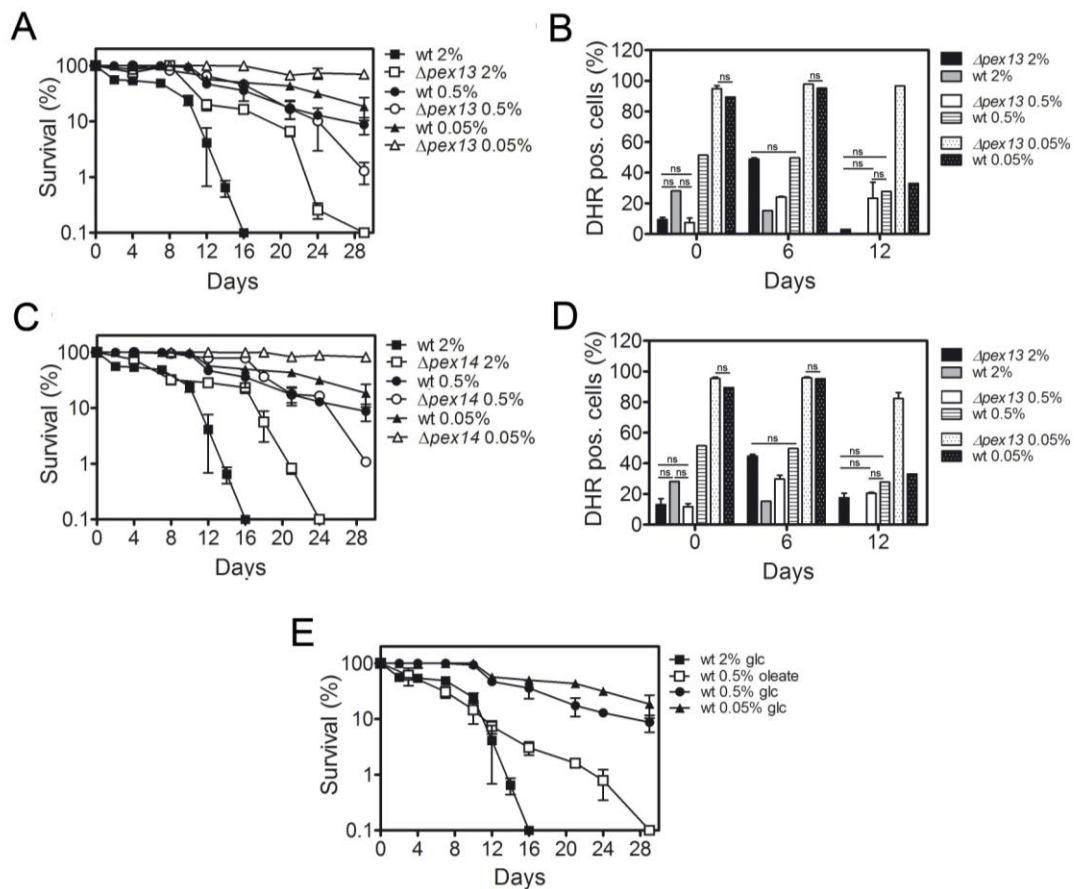


Figure 4 - Impaired peroxisomal function extends *S. cerevisiae* CLS associated with increases in intracellular ROS levels, in severe (0.05% glucose) and non-CR (2% glucose), but not in moderate CR (0.5% glucose). Survival of BY4742 $\Delta pex13$ (A), $\Delta pex14$ (C) and oleate (0.5%) grown cells (E)

measured by cell viability at 2- to 3-d intervals beginning the day cultures reached stationary phase (day 0) and expressed as % of survival compared with survival at day 0 (100%). (B) Intracellular ROS accumulation in $\Delta pex13$ and $\Delta pex14$ cells detected by FACS measurements using dihydrorhodamine 123 (DHR). Values are means \pm SD of three independent experiments. Statistical significance (* $P < 0.05$) was determined by Student's t-test. As for most of the comparative groups differences are statistically significant, only not significant (ns) are marked.

Based on the approaches used we may speculate about a specific positive role of peroxisomes, or a pro-longevity role of H_2O_2 in the CLS-extending effects of CR. On the other hand, and as peroxisome's biogenesis also resulted in CLS extension, it may be reasonable to consider that it may be a result of the great increase in ROS production or, at least, a result of a pexophagy process that protects cells from aged and damaged peroxisomes. Therefore, peroxisomes could elicit an anti-aging cellular program based on the hypothesis that H_2O_2 levels are maintained below a specific threshold level that may induce an adaptative response to oxidative stress. In this context, these findings may provide new insights into the role of peroxisomes, and H_2O_2 , leading us to speculate about a "pexo-hormesis" mechanism by which CR extends CLS in *S. cerevisiae*.

Taking into account that peroxisomes contribute to the maintenance of extraperoxisomal ROS levels and the suggestion that they might be involved in the *S. cerevisiae* CLS-extending effects of CR, we attempted to investigate the involvement of a major H_2O_2 -metabolizing enzyme present in this organelle, the peroxisomal catalase (Cta1p). It has been suggested that Cta1p may not be only targeted to peroxisomes but also efficiently co-imported into mitochondria, when cells are cultivated under respiratory growth conditions where Cta1p functions as scavenger of mitochondrial derived H_2O_2 [222]. In this line of thought, we raised the question of the relevance of Cta1p localization to the observed CLS-extending effects of CR. For that purpose, we used a wild type strain in which Cta1p was fused to GFP and harbouring a plasmid with dsRED target to mitochondria. Similar to wild type cells (Fig. 1A) CR was demonstrated to extend CLS in cells expressing Cta1p-GFP (Fig. 5A). The confocal microscopic analysis revealed that, in non-CR conditions, Cta1p is not co-localized to mitochondria being imported to peroxisomes during the first days of CLS (Fig. 5B). In this conditions Cta1p was barely detected after day 6, probably as a result of the compromised trafficking into peroxisomes during the aging process [223].

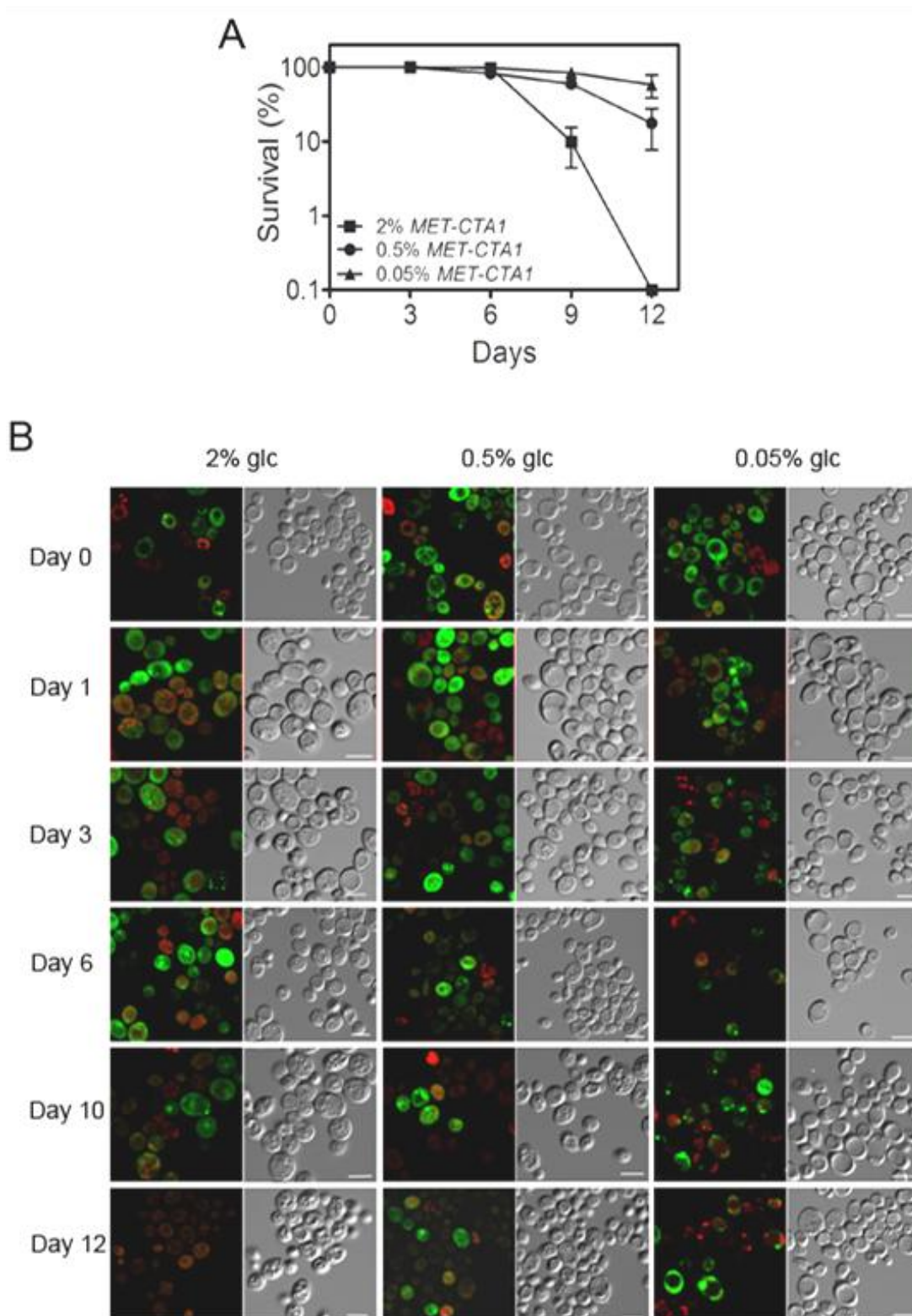


Figure 5 - Cta1p is not co-localized to mitochondria during the *S. cerevisiae* CLS-extending effects of CR. (A) Survival of a wild type strain co-expressing Cta1p-GFP and DsRed, measured by cell viability at selected time points and beginning the day cultures reached stationary phase (day 0) and expressed as % of survival compared with survival at day 0 (100%). Values are means \pm SD of three independent experiments. (B) Confocal microscopy of a wild type strain co-expressing Cta1p-GFP and DsRed for

mitochondrial localization, at the selected time points. Insets are 200% magnifications; upper inset- mitochondria, lower inset- catalase.

In CR conditions (0.5%), and in contrast to what others have suggested for cells grown under respiratory or respiratory/fermentative conditions [222], no co-localization of Cta1p was observed in mitochondria. The co-localization of Cta1p in mitochondria was only observed in some cells under severe CR conditions (0.05%) (Fig. 5B), probably as a result of the fully respiratory growth conditions where Cta1p may function as scavenger of mitochondrial derived H_2O_2 . Overall, these results discarded the contribution of peroxisomes to the CLS-extending effects of CR exclusively based on the mitochondrial co-localization of Cta1p. However, it is still necessary to confirm the involvement of peroxisomes in the CLS extension as previously suggested by growing cells in the peroxisome's induction media (oleate) (Fig. 4E).

To further understand the involvement of peroxisomes in CLS, we investigated whether the CLS-extending effects of CR could be coupled to an increase in peroxisomal biogenesis relative to mitochondria. For that we evaluated, in CR and non-CR conditions, the expression levels of Pex14p and Porin, two membrane proteins present in peroxisome and in mitochondria, respectively (Fig.6). The results demonstrated that both moderate and severe CR (0.5% and 0.05% glucose, respectively) promote the induction of Pex14p expression (Fig. 6A and B) suggesting an increase in the biogenesis of peroxisomes, rather than an increase in the mitochondria mass (Fig. 6A and C). Similar results were obtained in severe CR conditions (0.05% glucose). However, the increase in the ratio Pex14/Porin expression relative to non-CR conditions was not so evident as for moderate CR (0.5% glucose). This result may explain the great increase in mitochondria mass associated with the fully respiratory metabolism of these severe CR-restricted cells, particularly from day 6 on (Fig. 6A-C). These results obtained raise the possibility that peroxisomes, despite their negative role previously suggested in non-CR conditions (Fig. 4A and C), may have a positive contribution to the CLS-extending effects of CR in *S. cerevisiae* (Fig. 4A, C and E; Fig. 6). Or, at least, the negative effects of aged peroxisomes may be counteracted in CR conditions. Such positive contribution was suggested to be associated with increased levels of peroxisomes-derived ROS, further supporting a more complex role of ROS in the aging process and challenging the free-radical theory of aging [1]. Moreover, a major role for

Cta1p in the CLS-extending effects of CR, based on its co-localization in mitochondria, was discarded

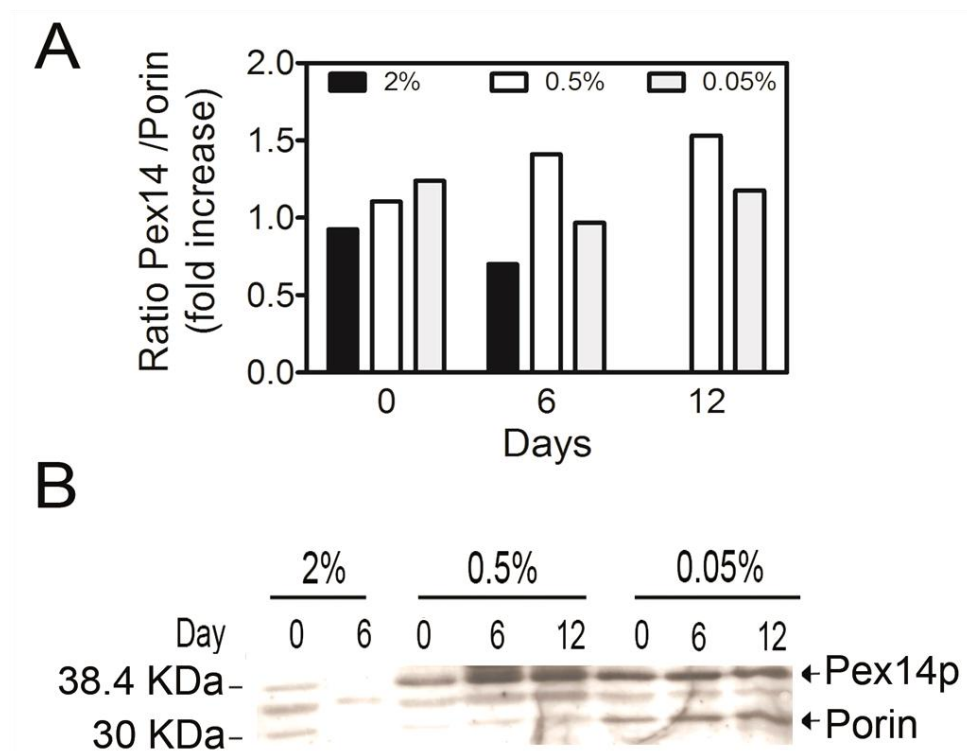


Figure 6 - CR promotes increases in the ratio of Pex14p/Porin protein expression in *S. cerevisiae* cells. (A) Quantification of band intensity by densitometry (BioRad Quantity One Software). (B) Western-blot analysis of the levels of Pex14p of chronological aged cells. The Western blot results shown represent the results from a number of attempts which showed similar trends. The expression levels was normalized by the expression level of actin.

3.1.3 INACTIVATION OF CATALASES MIMICS THE CLS-EXTENDING EFFECTS OF CR BY PROMOTING AN INCREASE IN H_2O_2 LEVELS

Although our previous results did not suggest a major involvement of Cta1p in the CLS-extending effects of CR, we further aimed to test the involvement of catalases in such process. In *C. elegans*, it has been demonstrated that the specific loss of peroxisomal catalase resulted in a progeric phenotype associated with alterations in ROS generation, changes in peroxisome morphology and reduction in the organism's lifespan [121]. The same study showed similar effects in *S. cerevisiae* strains in which

lack of Cta1p, but not cytosolic catalase (Ctt1p), decreased the viability of yeast by ~15-fold [121]. On the other hand, loss of Ctt1p was suggested to have a moderate effect on *S. cerevisiae* CLS, even though its levels are highly induced during the stationary phase of growth [58]. Even though catalases do not seem to be important under fermentative growth conditions, their involvement in cellular survival under extreme conditions, such as oxidative stress, has been suggested in respiratory growth conditions [224, 225].

In a first approach we evaluated the impact of CR in the activity of both Cta1p and Ctt1p, the two main H₂O₂-scavenging enzymes present in *S. cerevisiae* cells (Fig. 7).

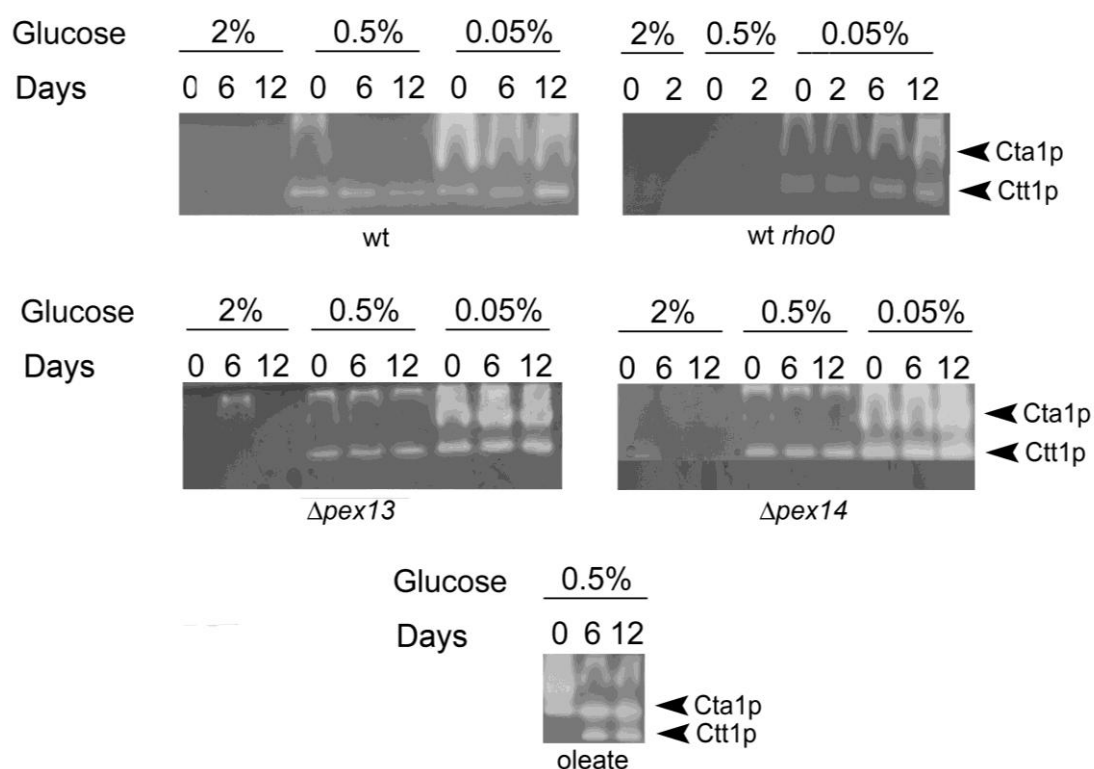


Figure 7 - CR induces the activity of both peroxisomal (Cta1p) and cytosolic catalase (Ctt1p) in wild type, *rho0*, $\Delta pex13$, $\Delta pex14$ and oleate grown *S. cerevisiae* cells (BY4742 background) during CLS, although more evident in severe CR (0.05% glucose). Results shown represent the results from a number of attempts, which showed similar trends.

The results showed that the CLS-extending effects of CR observed in wild type, *rho0*, $\Delta pex13$, $\Delta pex14$ and oleate grown cells (Figs. 3 and 4) are associated with increased activity of both Cta1p and Ctt1p, comparatively to non-CR conditions (Fig. 7). However, and despite the higher activity of peroxisomal catalase observed in these

strains in CR conditions, we previously shown that they still display increases in intracellular ROS, specifically H_2O_2 accumulation (Fig. 2; Fig 3B and C; Fig. 4B and D). Thus, suggesting that their increased antioxidant activity may not be primarily determinant in the CLS-extending effects of CR in *S. cerevisiae*. This hypothesis was further supported as CLS was also extended by mutational inactivation of *CTA1* (Fig. 8A).

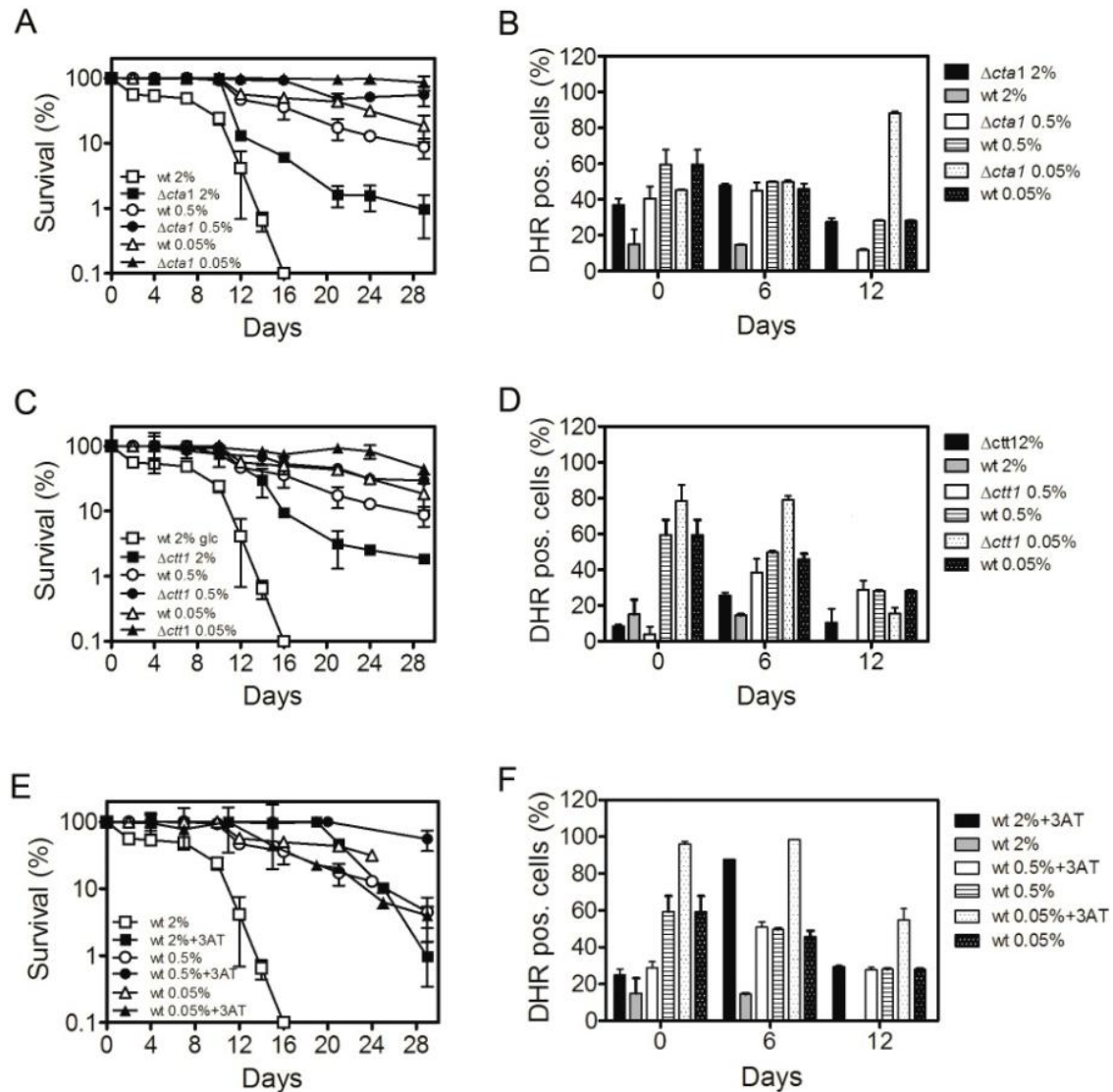


Figure 8 - Genetic and pharmacological inactivation of catalases extends *S. cerevisiae* CLS by increasing intracellular levels of ROS. Survival of Δcta , $\Delta ctt1$ and 3AT-treated cells (A, C and E, respectively) was measured at 2- to 3-d intervals beginning the day cultures reached stationary phase (day 0) and is expressed as % of survival compared with survival at day 0 (100%). Percentage of Δcta , $\Delta ctt1$ and 3AT-treated cells (B, D and F, respectively) exhibiting high levels of intracellular ROS was detected by FACS measurements using DHR123. Values are means \pm SD of three independent experiments. Statistical significance (* $P < 0.05$) was determined by Student's t-test. Due to the number of comparative group

showed in each graphic, none of the statistic differences are noted. Globally, genetic and pharmacological inactivation of catalases in non-CR conditions resulted in a statistically significant increase in intracellular ROS accumulation (with the exception of the following comparative group: $\Delta ctt1$ 2%/wt2% at day 0).

Furthermore, the longer CLS of $\Delta cta1$ cells was further extended by CR (Fig. 8A), suggesting that other mechanism(s), rather than the H_2O_2 -detoxifying capacity of catalase, may be contributing to the CR effect in *S. cerevisiae* CLS extension. Similar results were obtained using the *CTT1* knockout strain and by pharmacological inhibition of catalases with 10 mM 3-amino-1,2,4-triazole (3AT) (Fig. 8C and E, respectively). The CLS-extending effects of inactivating catalases was further confirmed in a different background (W303), although more moderated when compared with BY4742 background, and upon deletion of both *CTA1* and *CTT1* genes in BY4742 background (Fig. 9). The manipulation of catalase activity was further confirmed by the abolishment of catalase activity in CR-cells treated with 3AT and by the induction of its activity in cells overexpressing *CTA1*, particularly evident in non-CR conditions (Fig. 10).

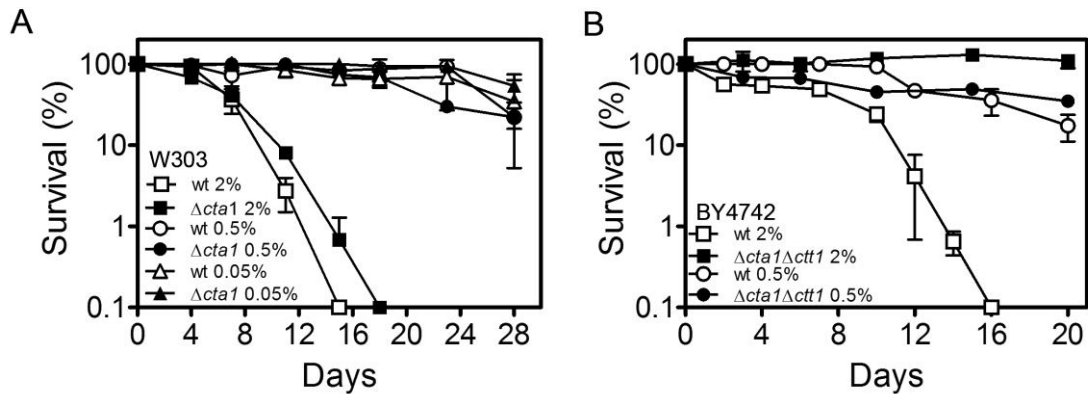


Figure 9 - The deletion of Cta1p (peroxisomal catalase) in W303 cells (A) or of both Cta1p and Ctt1p (cytosolic catalase) in BY4742 cells (B) extends *S. cerevisiae* CLS. Cells viability was measured at 2- to 3-d intervals beginning the day cultures reached stationary phase (day 0) and is expressed as % of survival compared with survival at day 0 (100%). Values are means \pm SD of three independent experiments.

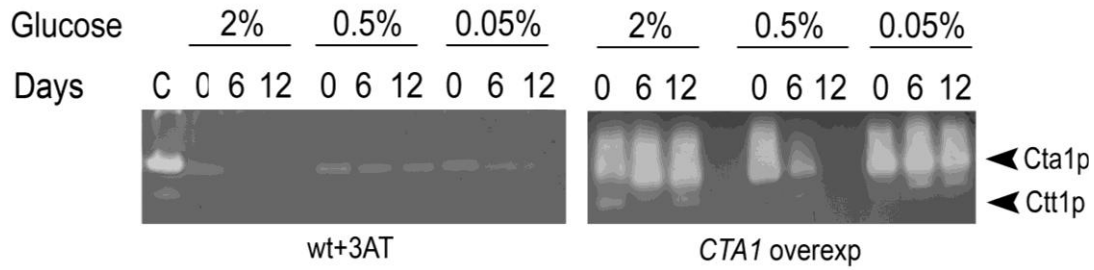


Figure 10 - CR induces the activity of the peroxisomal catalase Cta1p, as well as the cytosolic catalase Ctt1p. The pharmacological inhibition of catalase with 10 mM 3-amino-1,2,4-triazole (3AT) resulted in complete inhibition of CR-induced Cta1p and Ctt1p activity. Overexpression of *CTA1* resulted in a substantial increase in Cta1p activity in CR and non-CR conditions. Results shown represent the results from a number of attempts, which showed similar trends.

According to the free radical theory, CR may revert aging by decreasing ROS generation and oxidative damage to cellular components [209-211]. However, our results have shown that CLS extension by CR is associated with increases in ROS levels. These results corroborate, however, similar trends obtained in yeast [166] and in *C. elegans* [139] in which it was shown that glucose availability promotes survival rates in parallel with formation of ROS, induction of catalase activity and posterior increases of oxidative stress resistance [139, 166]. As suggested by those studies, our results might raise the hypothesis that ROS, and specifically H₂O₂, may activate a cell anti-aging program or trigger a pro-aging route at concentrations beyond a specific threshold.

Despite the increases in catalase activity in CR conditions our results propose that catalases may exert detrimental effects on *S. cerevisiae* CLS, challenging the well described effects of these enzymes in the promotion of lifespan in other models [58, 121, 226, 227]. In this context, to further study the involvement of catalases in CLS, we simultaneously investigated the intracellular ROS levels associated within the manipulation of these enzymes during the CLS-extending effects of CR (Fig. 8). The results obtained show that the longer CLS of $\Delta cta1$ cells was accompanied by an increased fraction of cells containing high levels of intracellular ROS under non-CR conditions (Fig. 8A and B). Under CR conditions, the fraction of $\Delta cta1$ cells exhibiting high intracellular ROS levels was similar to CR wild-type cells or non-CR $\Delta cta1$ cells at day 6 and lower at day 12 (Fig. 8B). A similar increase in intracellular ROS levels were also detected in $\Delta ctt1$ compared with wild-type cells and in 3AT treated cells (Fig. 8F).

Thus, suggesting that both CR and catalases inactivation might promote yeast CLS by similar mechanism involving increases in intracellular ROS levels or, at least, in H₂O₂. This hypothesis was further supported by the overexpression of *CTA1* in wild type cells which had effects opposite to those associated with inactivation of catalases, resulting in decreased CLS in non-CR and CR cells (Fig. 11A) and reduced the fraction of cells containing high levels of intracellular ROS (Fig. 11B). The fraction of cells containing high intracellular levels of ROS was also reduced (albeit to a lesser extent) in cells harbouring the empty vector, which may be a reflex of the specificity of different medium content required to maintain plasmids in these but not other experiments.

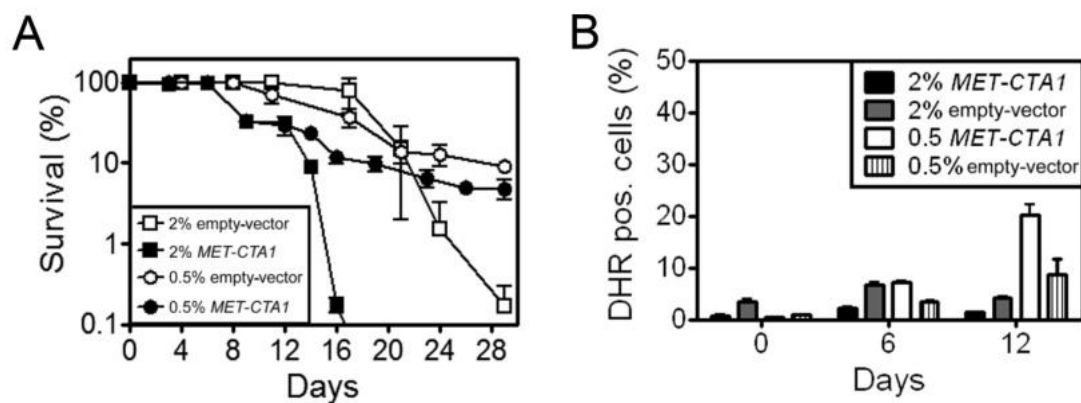


Figure 11 - CR shortens *S. cerevisiae* CLS of *CTA1* overexpressing wild-type cells. (A) CLS is extended in of *CTA1* overexpressing cells (“MET-*CTA1*”) comparatively to cells transformed with an empty vector and is this effect is associated with low levels of intracellular ROS (B), as detected by FACS measurements using DHR123. Cells viability was measured at 2- to 3-d intervals beginning the day cultures reached stationary phase (day 0) and is expressed as % of survival compared with survival at day 0 (100%). Values are means \pm SD of three independent experiments. Statistical significance (* $P < 0.05$) was determined by Student’s t-test.

An involvement of H₂O₂ in the CLS-extending effects of CR was also suggested by the pharmacological inhibition of the synthesis of glutathione with 1mM buthionine sulfoximine (BSO) in wild type cells and, thus, upon H₂O₂-induced glutathione synthesis (Fig. 12). As for catalases inactivation (Fig. 8A, C and E), treatment of wild type cells with BSO promoted a drastic extension of CLS, particularly demonstrated under non-CR conditions (Fig. 12A). However, treatment of Δ *cta1*(Fig.12B) and Δ *ctt1*

(Fig.12C) cells with BSO did not result in the extension of CLS suggesting, once more, that increases in the H_2O_2 levels are crucial for CLS extension.

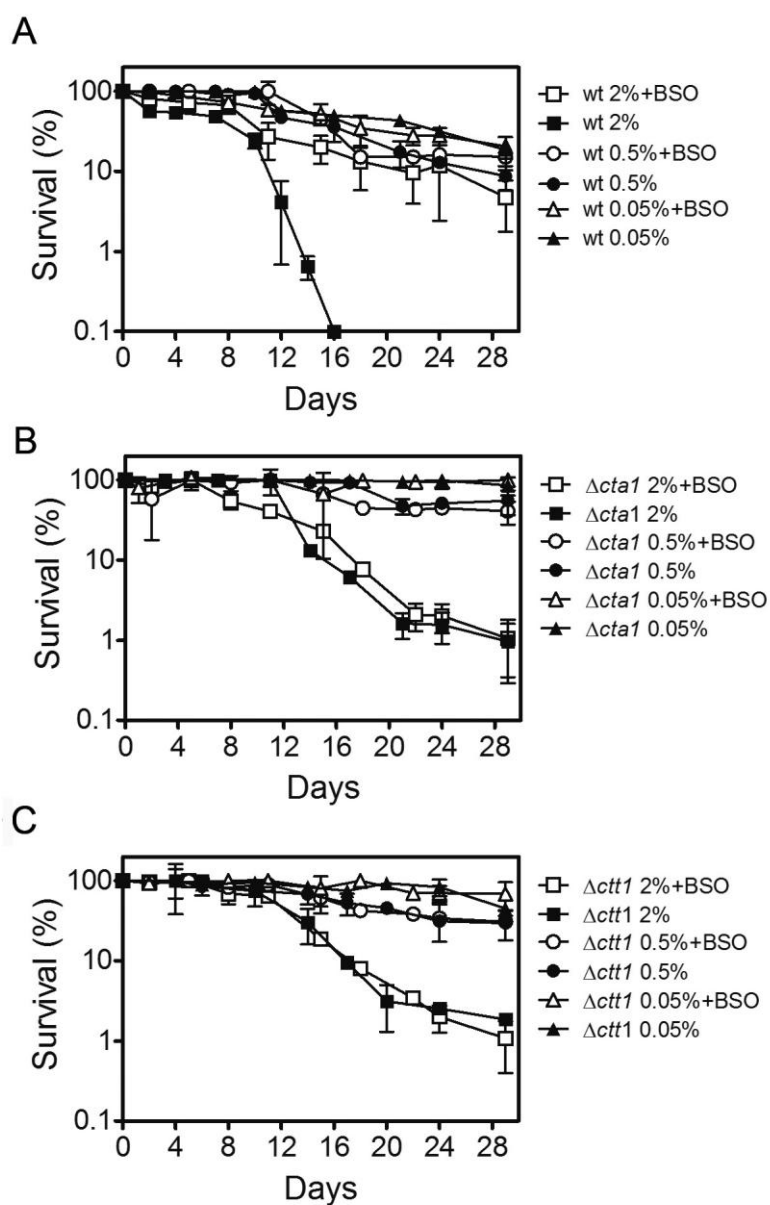


Figure 12 - Inactivation of glutathione peroxidase (GpX) with BSO extends *S. cerevisiae* CLS in wild type (A), but not in Δcta (B) or $\Delta ctt1$ (C) cells. Cell viability was measured at 2- to 3-d intervals beginning the day cultures reached stationary phase (day 0) and is expressed as % of survival compared with survival at day 0 (100%). The percentage of cells exhibiting high levels of intracellular ROS was detected by FACS measurements of fluorescence of 123 (DHR). Values are means \pm SD of three independent experiments.

Overall, the results based on the genetic and pharmacological inactivation of H_2O_2 -metabolizing systems, catalases and GPx, combined with the specificity of the probes used for ROS detection, pointed to a pro-longevity role of H_2O_2 in CLS extension by CR. However, it is well established that superoxide anion (O_2^-) is generated during CLS and plays a major role in the age-associated death of yeast and other eukaryotic [213]. Following this line of thought, during the CLS experiments described hereafter we simultaneously evaluated the intracellular levels of O_2^- associated to the CLS-extending effects of CR. For that purpose, we used dihydroethidium (DHE), which detects this form of ROS [228]. The results obtained show that, in non-CR conditions, O_2^- levels increased in wild-type cells from day 0 to day 3 of stationary phase, whereas H_2O_2 levels remained unchanged (Fig. 13A). However, in CR conditions, a significant reduction in O_2^- levels compared with levels in non-CR cells was detected, despite a pronounced increase in H_2O_2 in the same cells. Similar to the effects of CR in wild-type cells, O_2^- levels were decreased and H_2O_2 levels were increased in Δcta1 compared with wild-type cells at day 0 and day 3 of stationary phase (Fig. 13A). Accordingly, treatment of wild-type cells with 3AT (Fig. 13B) or upon mutational inactivation of both *CTA1* and *CTT1* ($\Delta\text{cta1ctt1}$ cells) (Fig. 14A and B), also promoted a reduction in O_2^- levels at the same time that it increased intracellular H_2O_2 levels in the same cells. Therefore, these results suggest that the longevity-promoting effects of intracellular H_2O_2 during CR or catalase inactivation are related to inhibition of the accumulation of O_2^- .

The role of ROS in processes that lead cells to acid and oxidative-induced programmed cell death is well recognized [204, 213, 229]. Extrinsic factors such as acetic acid are known to cause oxidative stress and, during chronological aging [78, 79, 230, 231]. Acetic acid toxicity is considered a primary cause of chronological senescence under standard growth conditions [78]. In this context, we speculated whether the CLS-extending effects of increased H_2O_2 levels induced by CR could rely on changes in acetic acid levels. Thus, we eliminated the effect of acetic acid by buffering the aging medium (Table 1) and measured ROS levels during CLS experiments. The results revealed that the CR effects of CR in CLS are also associated with increases in H_2O_2 as well as a reduction of O_2^- levels in buffered medium (Fig. 15). In accordance, the inhibition of the accumulation of O_2^- levels was observed in buffered medium in wild-type cells in stationary phase [77]. Therefore, suggesting that in the

studied conditions other mechanism (s) signalled by glucose, rather than acetic acid, may be underlying the CR effects in *S. cerevisiae* CLS extension.

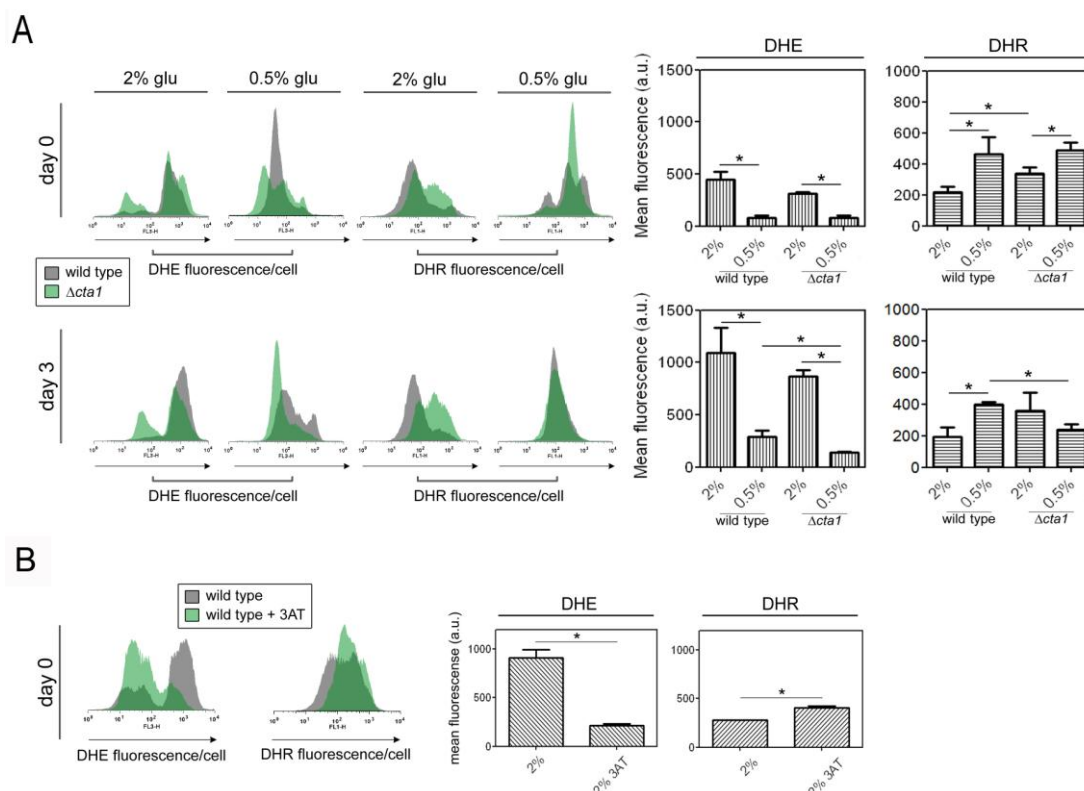


Figure 13 - The longevity-promoting effects of high intracellular H_2O_2 levels induced by CR or inactivation of catalases are accompanied by a reduction in the chronological age-dependent accumulation of O_2^- . (A) FACS measurements of O_2^- using dihydroethidium (DHE) in parallel with measurements of H_2O_2 using DHR123 in wild-type (gray histograms) and $\Delta cta1$ (green histograms) cells at day 0 and day 3 of stationary phase. Bar graphs indicate mean \pm SD fluorescence/cell (arbitrary units) measured in 25,000 cells/sample in three independent experiments. (B) FACS measurements of O_2^- (DHE) and H_2O_2 (DHR123) in wild-type cells in the absence (gray histograms) or presence (green histograms) of the catalase inhibitor 3AT at day 0 of stationary phase. Bar graphs indicate mean \pm SD fluorescence/cell (arbitrary units) of three independent experiments. Statistical significance (* $P < 0.05$) was determined by Student's t-test.

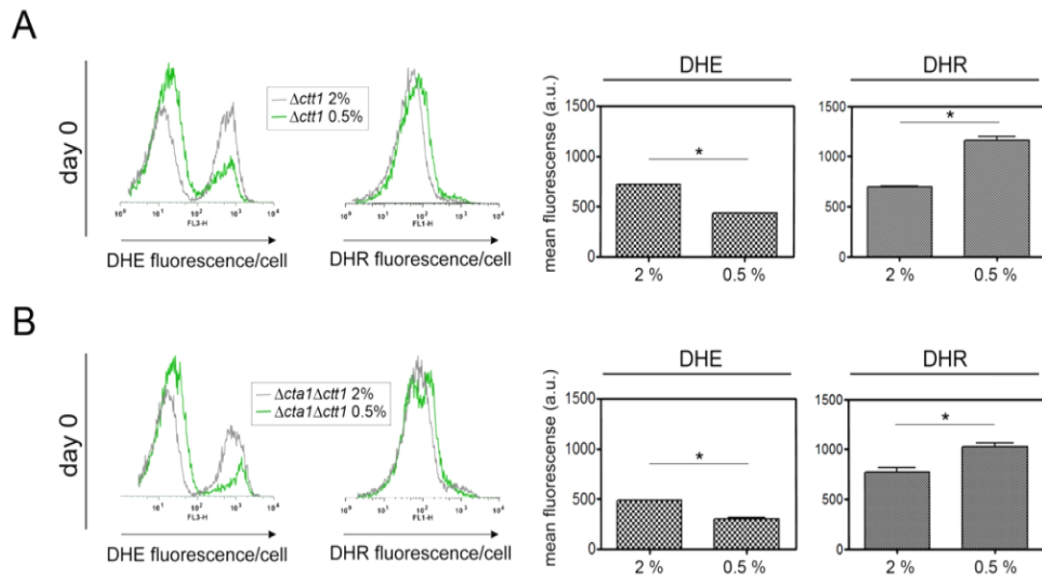


Figure 14 - Mutational inactivation of *CTT1* or of both catalases *CTA1* and *CTT1* mimics the CLS extending effects of CR in parallel with high intracellular H_2O_2 levels and reduction in the chronological age-dependent accumulation of superoxide anions (O_2^-). FACS measurements of O_2^- using DHE in parallel with measurements of H_2O_2 using DHR123 at day 0 of CLS in $\Delta ctt1$ (A) and $\Delta cta1\Delta ctt1$ (B) cells. Bar graphs indicate mean \pm SD fluorescence/cell (arbitrary units) measured in 30,000 cells/sample in three independent experiments. Statistical significance (* $P < 0.05$) was determined by Student's t-test.

Table 1 – pH of aging cultures

	SC 2%	SC 0.5%
BY4742	2.95 (\pm 0.02)	3.16 (\pm 0.02)
BY4742 $\Delta cta1$	2.93 (\pm 0.01)	3.10 (\pm 0.03)
BY4742 $\Delta ctt1$	2.93 (\pm 0.00)	3.26 (\pm 0.06)
BY4742 $\Delta cta1\Delta ctt1$	2.96 (\pm 0.00)	3.16 (\pm 0.01)

Cells were inoculated into the indicated medium and pH was measured at 72 hours of aging. Data is presented as mean pH of three biological replicates with standard deviation in parentheses.

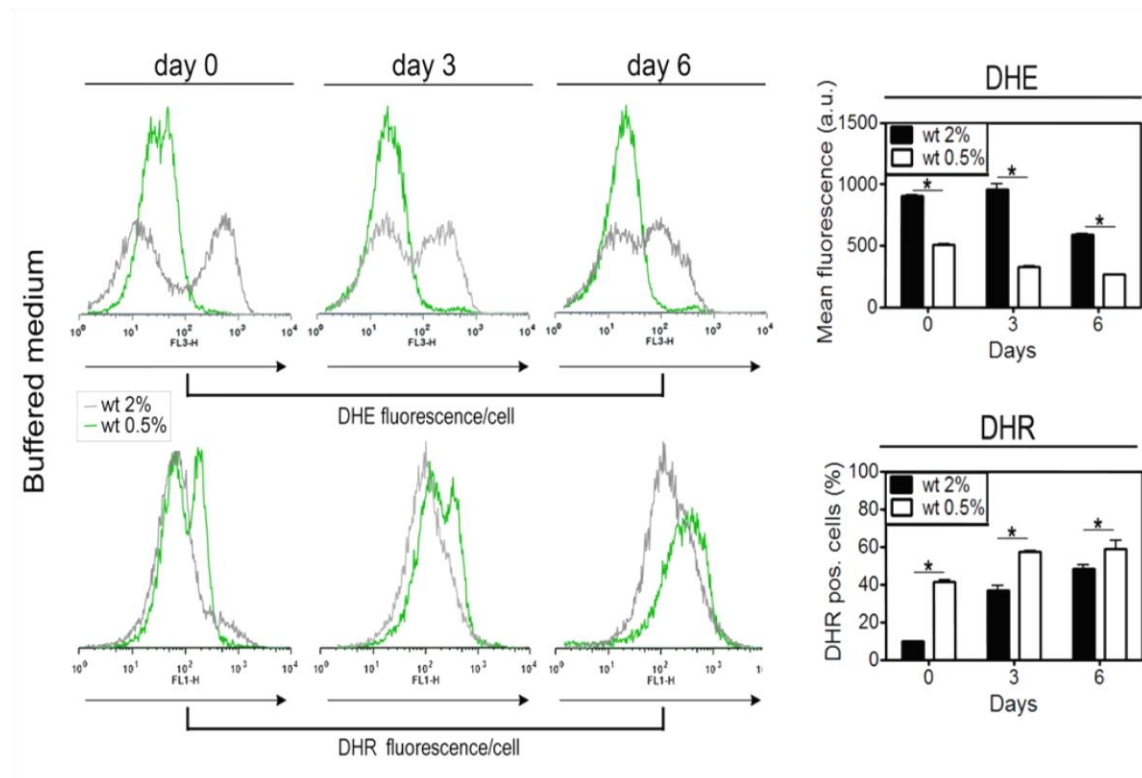


Figure 15 - CR-induced increases in intracellular H_2O_2 accompanied by a reduction in the accumulation of O_2^- occurs independently of changes in levels of acetic acid as demonstrated in cells cultured in buffered medium. FACS measurements of superoxide anions using dihydroethidium (DHE) in parallel with measurements of H_2O_2 using dihydrorhodamine 123 (DHR) in wild-type cells cultured in buffered medium (citrate phosphate buffer, pH 6.0) at days 0, 3, and 6 of stationary phase. Bar graphs indicate mean \pm SD fluorescence/cell (arbitrary units) measured in 30,000 cells/sample in three independent experiments. Statistical significance (*P < 0.05) was determined by Student's t test.

3.1.4 INCREASED H_2O_2 , INDUCED BY CR OR CATALASE INACTIVATION, INDUCES SUPEROXIDE DISMUTASE ACTIVITY

In *S. cerevisiae*, most evidence provided until now based on the overexpression of superoxide dismutases (Sods), which scavenge O_2^- [61, 138, 232] is still favouring ROS, and particularly O_2^- , as important determinants of chronological aging. Also, the induction of the transcription of both *SOD1* and *SOD2* genes [233, 234], as well as increases in levels of the corresponding proteins [233], have been suggested upon ectopic application of sublethal concentrations of H_2O_2 . In this context, we explored whether the reduction in O_2^- levels that accompanies increases in intracellular H_2O_2 is triggered by the induction of superoxide dismutases (Sods) activity. For that, we measured the activities of Sod1p and Sod2p, as well as the mRNA expression levels of *SOD1* and *SOD2* under CR and non-CR conditions in wild type and in catalases

mutants. The results showed that CR or *CTA1* deletion resulted in minor increases in Sod1p activity at day 0 that were not detected at day 3 of stationary phase (Fig. 16 A and B). Nevertheless, at day 6 both CR and deletion of *CTA1* increased the activity of Sod1p (Fig. 16A and B).

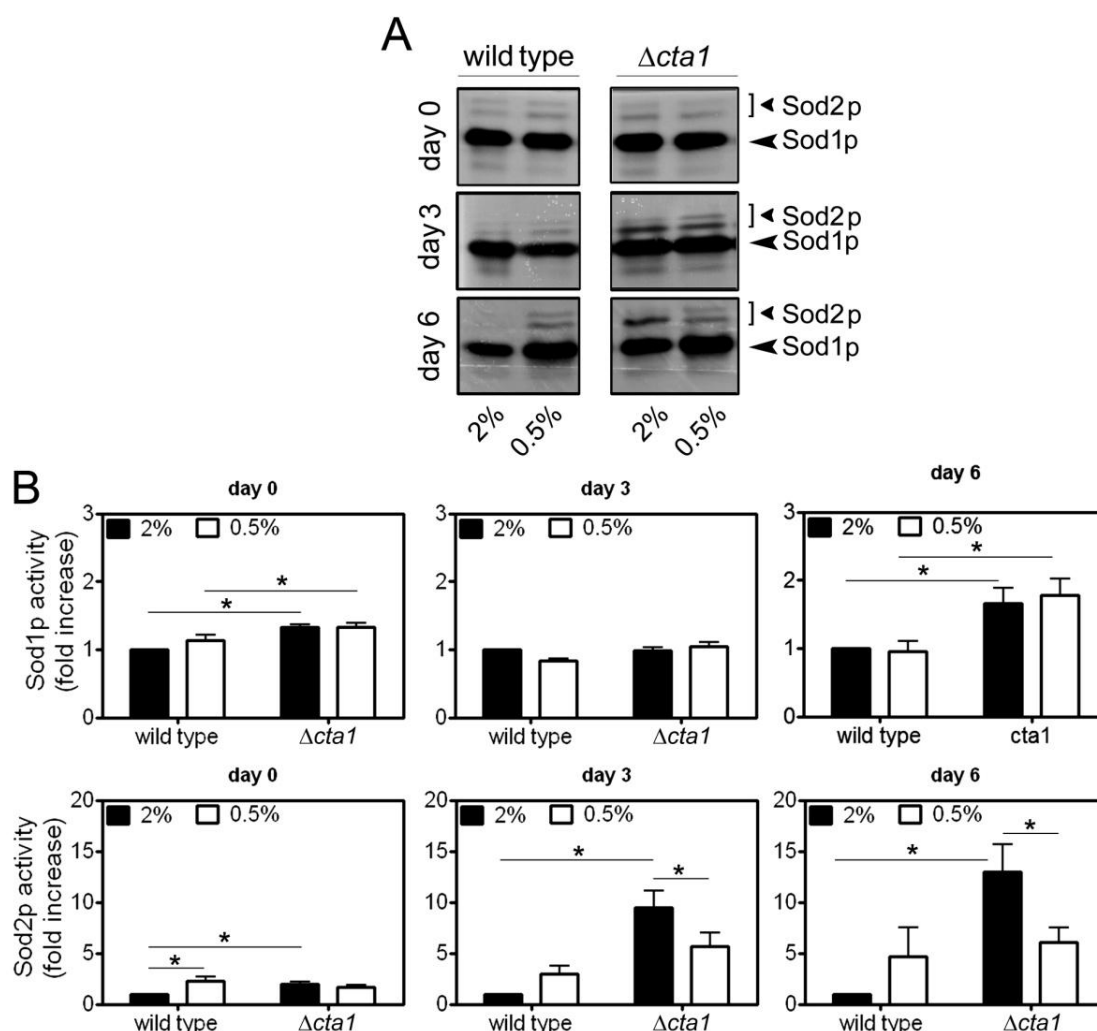


Figure 16 - Superoxide dismutase activity is induced by intracellular H_2O_2 in stationary phase wild type and $\Delta cta1$ cells. (A) In situ determination of superoxide dismutases (Sods) activity as measured as previously described. (B) Quantification of fold increases in Sod1p (Cu,ZnSOD) and Sod2p (MnSOD) activity under indicated conditions in wild-type and $\Delta cta1$ cells. Sod1p and Sod2p activity at each time point was normalized to activity in wild-type cells under non-CR conditions (2% glucose). Values indicate mean \pm SEM from three independent experiments. Statistical significance (* $P < 0.05$) was determined by Student's t-test.

CR or deletion of *CTA1* increased the activity of Sod2p at day 0 compared with wild-type cells in non-CR conditions. Larger increases in Sod2p activity were induced by CR conditions in wild-type cells at day 3 and day 6. Deletion of *CTA1* also induced large increases in Sod2p activity at day 3 and day 6 under non-CR conditions and under CR conditions at day 3 (Fig. 16A and B). Thus, suggesting that H_2O_2 may reduce O_2^- by inducing Sod activity, as further confirmed similar observations in $\Delta ctt1$ cells at these same time points (Fig. 17).

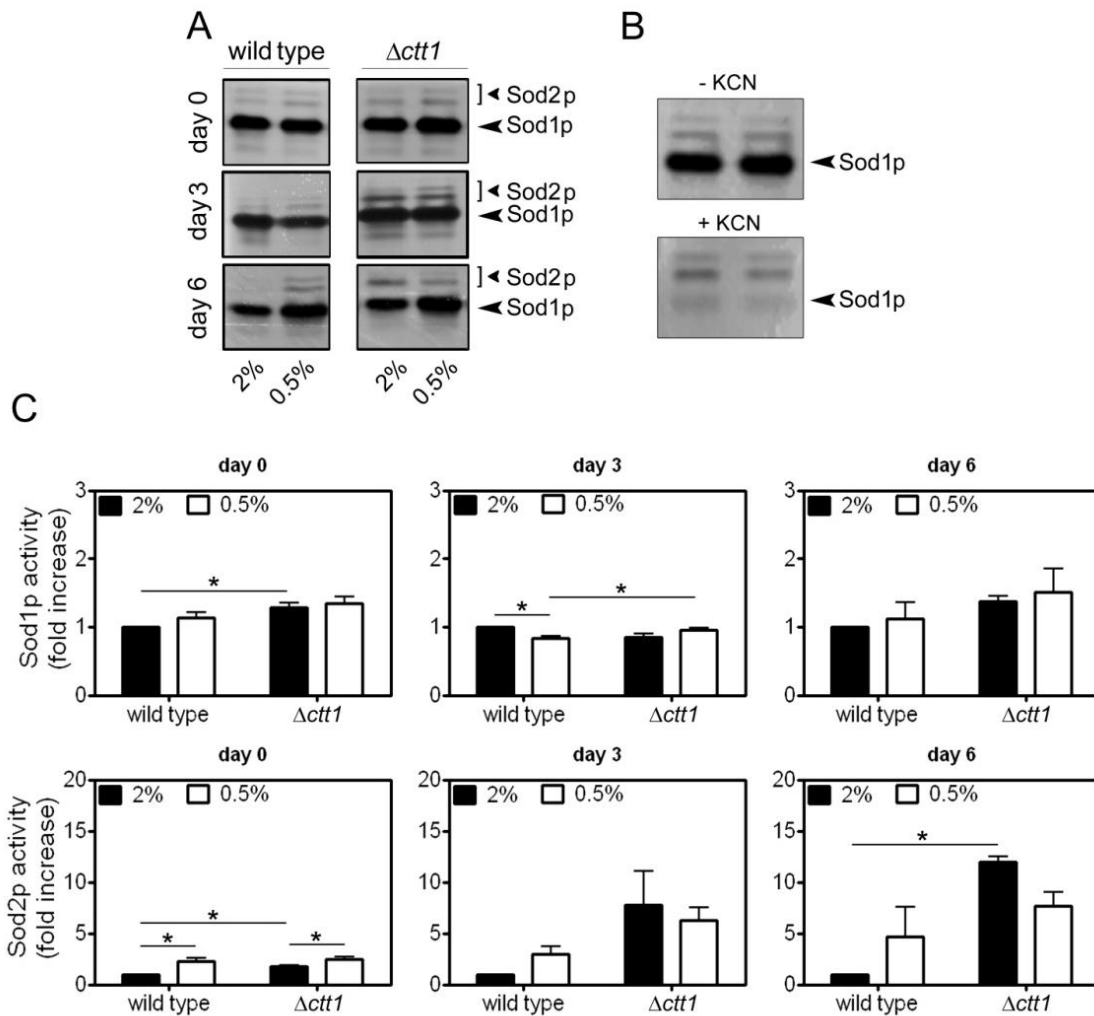


Figure 17 - Superoxide dismutase activity in induced by intracellular H_2O_2 in stationary phase wild type and $\Delta ctt1$ cells. (A) In situ determination of Sods activities in stationary phase wild-type and $\Delta ctt1$ cells. (B) MnSOD (Sod2p) activity detected in the presence of 2 mM potassium cyanide, which inhibits Sod1p activity. (C) Quantification of fold increase in Sod1p and Sod2p activity in wild-type and $\Delta ctt1$ cells. Sod1p and Sod2p activities measured at each time point were normalized to the activity of wild-type cells under non-CR conditions (2% glucose). Values indicate mean \pm SEM from three independent experiments. Statistical significance (* $P < 0.05$) was determined by Student's t test.

The contribution of Sods was further studied by analyzing the expression levels of both *SOD1* and *SOD2* (Fig. 18). Although not conclusive for the effects of catalase mutation in *SOD* genes expression, a similar trend was observed from day 3 on for *SOD2* expression being observed increased levels of *SOD2* expression in CR conditions (Fig. 18). These results probably reflect the fact that overexpressing a gene that encodes a Sodp can potentially generate detrimental or beneficial effects [232].

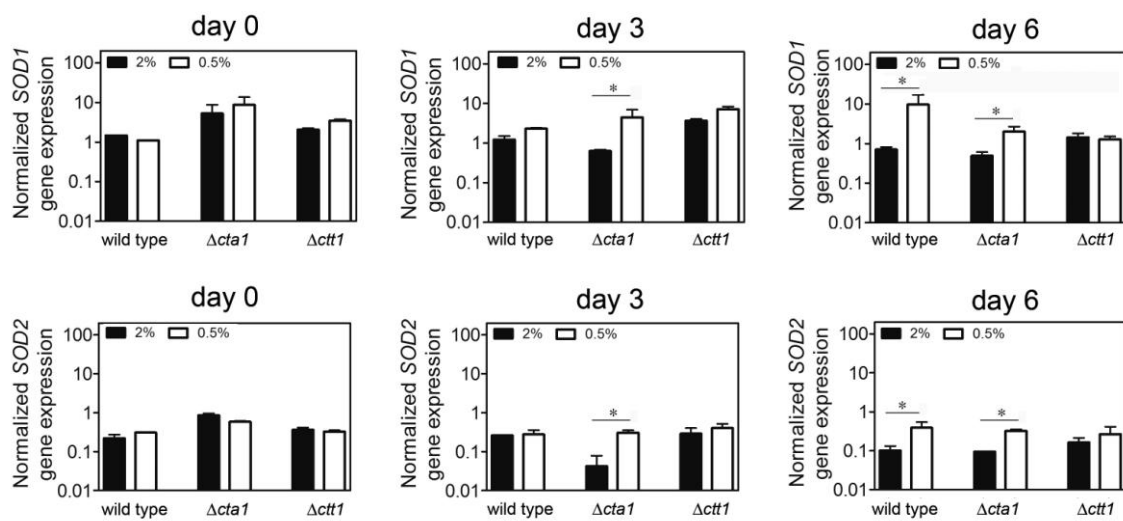


Figure 18 - Induction of *SOD1* and *SOD2* mRNA expression by intracellular H_2O_2 . *SOD1* and *SOD2* expression at each time point was normalized to activity in wild-type cells under non-CR conditions (2% glucose). Values indicate mean \pm SEM from three independent experiments. Statistical significance (* $P < 0.05$) was determined by Student's t-test.

In general, these findings point out that intracellular H_2O_2 induced by CR or by inactivation of catalase activity induces Sods activity in budding yeast, especially Sod2p activity. Furthermore, and consistent with our results, others have shown that ectopic exposure to H_2O_2 induces higher levels of Sod2p compared with Sod1p [233, 235, 236]. Consistently with our results, it has already been suggested that inhibition of O_2^- by H_2O_2 may be a conserved feature of the quiescent state that is enhanced by CR. For instance, reduced levels of O_2^- were also detected in parallel with elevated levels of H_2O_2 in wild-type but not *SOD2*-defective mouse cells driven into quiescence by contact inhibition [237]. Also, it was recently reported that in a mouse model of inflammatory responses in the lung, genetic or pharmacological inactivation

of catalase in neutrophils induces intracellular H_2O_2 that inhibits the superoxide-dependent inflammatory responses of these cells [238, 239]. It is proposed that H_2O_2 exerts its anti-inflammatory effects in mouse neutrophils by inducing Sodp activity and leading to a reduction in levels of O_2^- that promote inflammation.

Overall, and consistently with other studies, our findings in *S. cerevisiae* cells suggest that H_2O_2 , by inducing Sodp activity and, therefore, reducing O_2^- levels may contribute to the understanding of important aspects of aging.

3.1.5 INCREASED H_2O_2 , INDUCED BY CR OR CATALASE INACTIVATION, IS ASSOCIATED WITH OXIDATIVE DAMAGE TO MACROMOLECULES

According to the Harman's free radical theory oxidative damage to macromolecules is a primary factor in the aging process [1]. In yeast, many interventions that increase CLS were shown to promote resistance to oxidative stress, avoiding the damage to proteins and mitochondria that is known to accumulate in chronological-aged cells [240, 241]. Our observations showed that under different experimental conditions, H_2O_2 levels are increased while O_2^- levels are decreased in the same cells (Fig. 13). To determine the overall impact these divergent changes in different types of ROS have on oxidative damage, we examined levels of protein carbonylation, which is a form of oxidative damage, already shown to accumulate during chronological aging [185, 186]. Our results revealed that protein carbonylation was increased in Δcta1 cells compared to wild type cells at day 0 of CLS (Fig. 19A). In addition, CR promoted an increase in protein carbonylation in wild type cells at day 0. A similar increase in protein carbonylation was observed in Δctt1 cells at this time point (Fig. 20). Nevertheless, CR conditions decreased protein carbonylation in wild type and Δcta1 cells at day 6 (Fig. 19A). We also measured changes in cellular autofluorescence as an indication of global oxidative damage to proteins and lipids [242, 243] (Fig. 19B). Similar to the increased protein carbonylation detected in Δcta1 compared to wild type cells (Fig. 19A), autofluorescence of Δcta1 cells was increased at day 0 and day 3 (Fig. 19B). In contrast, CR led to a reduction in autofluorescence of wild type cells at these time points (Fig. 20B), similar to the effects of CR on protein carbonylation in wild type cells at day 6 (Fig. 20A). CR also reduced the autofluorescence of Δcta1 (Fig. 19B) and Δctt1 cells (Fig. 20B).

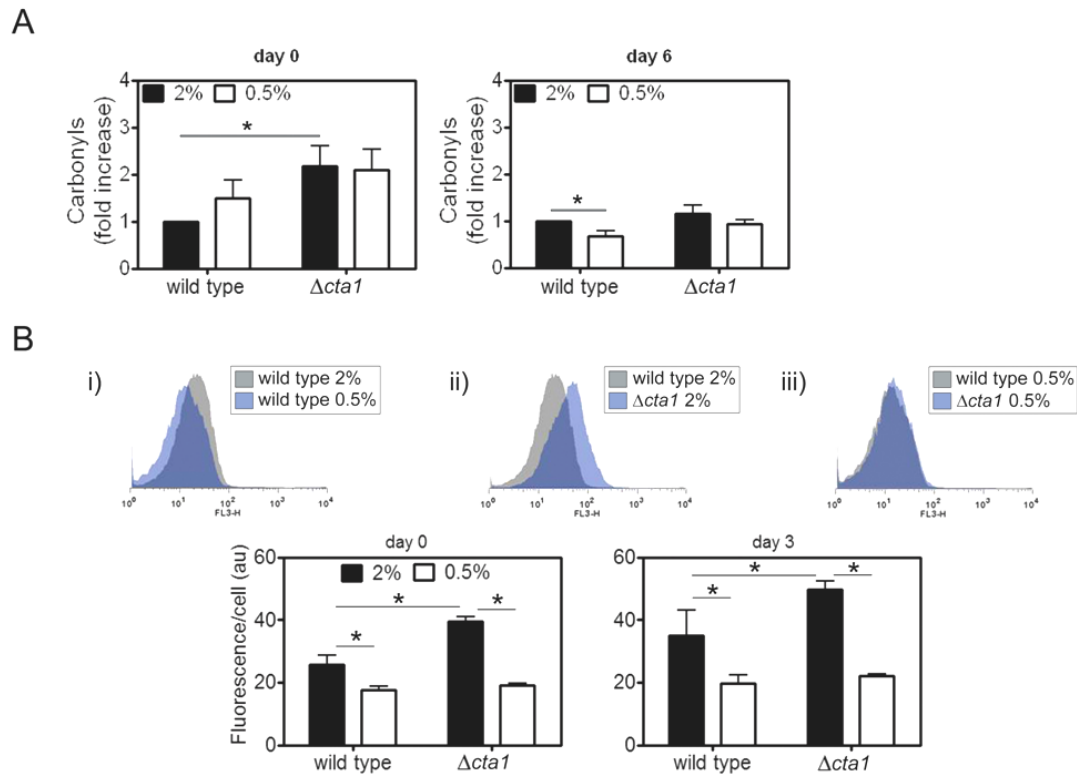


Figure 19 - Effects of increased H_2O_2 induced by CR or by inactivation of *CTA1* on oxidative damage to macromolecules. (A) Oxidative damage was assessed by measuring levels of oxidized proteins (carbonyls) in stationary phase wild-type and $\Delta cta1$ cells under non-CR and CR conditions. Levels of carbonyls were normalized at each time point to wild-type cell values under non-CR conditions (2% glucose). (B) Oxidative damage to proteins and lipids measured as autofluorescence of stationary phase wild-type and $\Delta cta1$ cells under non-CR and CR conditions. Histograms are representative of data collected at day 3. Values indicate mean \pm SEM from three independent experiments. Statistical significance (* $P < 0.05$) was determined by Student's t-test.

Together, the results from oxidative damage assessment established that CR extends *S. cerevisiae* CLS in parallel with a reduction in oxidative damage to macromolecules despite the induction of higher levels of H_2O_2 . In contrast, the CLS-extending effects of inactivating catalases are accompanied by parallel increases in levels of both H_2O_2 and oxidative damage, especially under non-CR conditions. Despite the observed increase in oxidative damage to macromolecules, our findings propose that both CR or inactivation of catalases induce oxidative stress in the form of H_2O_2 which, by inducing superoxide dismutases (Sods) that reduce levels of O_2^- , promote *S. cerevisiae* longevity.

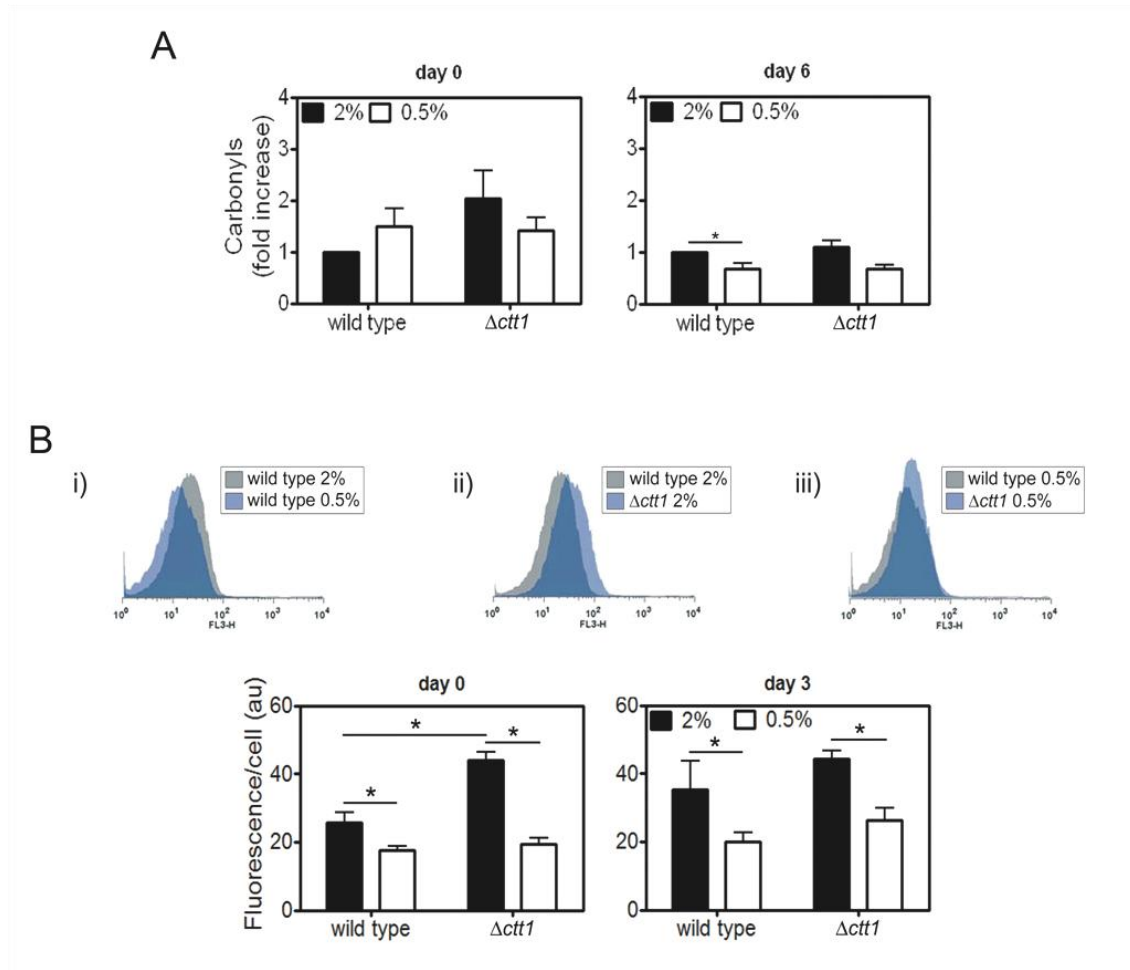


Figure 20 - Effects of increased H_2O_2 induced by CR or by inactivation of *CTT1* on oxidative damage to macromolecules. (A) Oxidative damage was assessed by measuring levels of oxidized proteins (carbonyls) in stationary phase wild-type and $\Delta ctt1$ cells under non-CR and CR conditions. Levels of carbonyls were normalized at each time point to wild-type cell values under non-CR conditions (2% glucose). (B) Oxidative damage to proteins and lipids measured as autofluorescence of stationary phase wild-type and $\Delta ctt1$ cells under non-CR and CR conditions. Histograms are representative of data collected at day 3. Values indicate mean \pm SEM from three independent experiments. Statistical significance (* $P < 0.05$) was determined by Student's t-test.

3.1.5 ECTOPIC EXPOSURE OF *S. CEREVISIAE* CELLS TO H_2O_2 MIMICS THE CLS-EXTENDING EFFECTS OF CR

Based on the results previously described, the pro-longevity role for H_2O_2 is clearly recognized. However, we further asked whether the ectopic application of H_2O_2 would extend CLS of non-CR wild-type cells. Given that H_2O_2 is a well established inducer of programmed cell death in yeast [204], cells were treated with a range of

concentrations that are likely to be far less than those that induce toxic effects. Exposure of wild type cells to the lowest H_2O_2 concentrations tested did not alter CLS compared with cells that were not exposed to H_2O_2 (Fig. 21A).

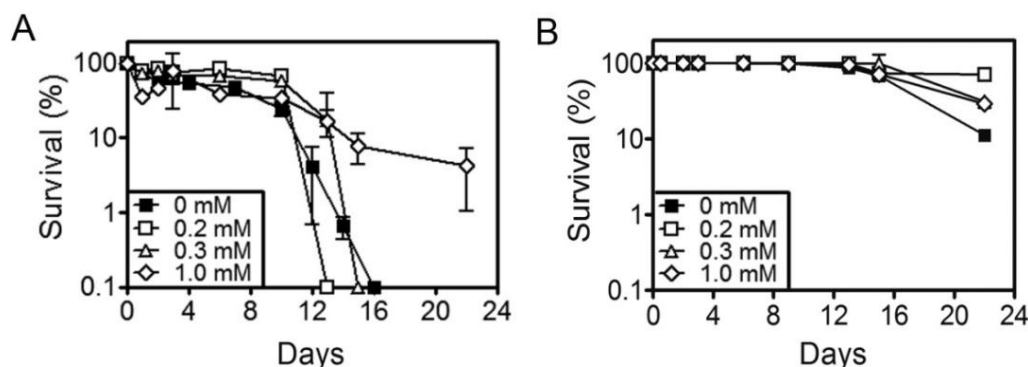


Figure 21 - Ectopic exposure cells to non-toxic concentrations of H_2O_2 promotes *S. cerevisiae* CLS extension. Wild type (A) and $\Delta act1$ (B) cells, cultured in 2% glucose medium, were treated with H_2O_2 over a range of concentrations from 0mM to 1mM. Cell viability was measured at 2- to 3-d intervals beginning the day cultures achieved stationary phase (day 0) and is expressed as % survival compared with survival at day 0 (100%). Values indicate mean \pm SEM from three independent experiments. Statistical significance (* $P < 0.05$) was determined by Student's t-test.

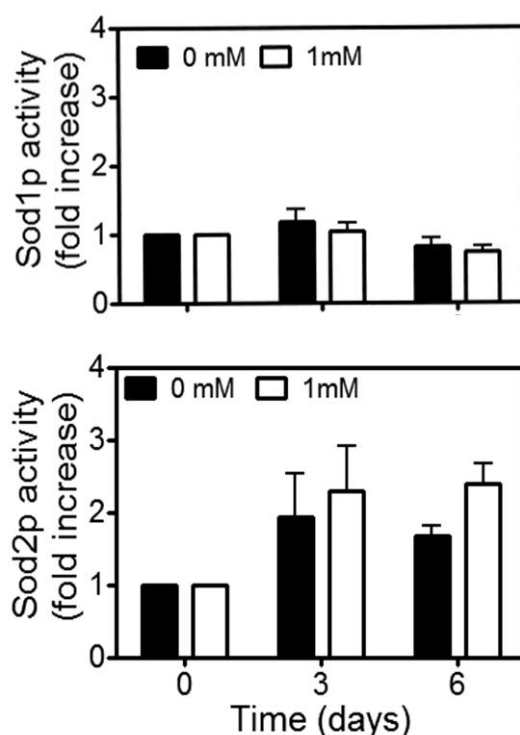


Figure 22 - Ectopic exposure of non-CR *S. cerevisiae* cells to H_2O_2 promotes the induction of Sod2p, but not Sod1p, activity in wild type cells. Sod1p and Sod2p activity at each time point was normalized to

activity in wild-type cells under non-CR conditions (2% glucose). Values indicate mean \pm SEM from three independent experiments. Statistical significance (* $P < 0.05$) was determined by Student's t test.

However, the exposure of wild type cells to 1 mM H_2O_2 resulted in a significant increase of CLS. The effects of H_2O_2 were also observed in $\Delta cta1$ cells for all the concentrations used, although in a lower extent (Fig. 21B). In addition, exposure of wild type cells to 1mM H_2O_2 also resulted in an increase in Sod2p but not Sod1p activity (Fig. 22), similar to what was observed in CR or upon catalases inactivation. Therefore, despite the resulting oxidative stress, specific concentrations of H_2O_2 were suggested to mediate a "hormesis-like" induction of stress resistance response by Sods.

The approaches described in this section aimed to better understand how CR impacts oxidative stress and longevity in the model system *S. cerevisiae*. We showed that either CR or inactivation of catalases promote CLS extension by increasing H_2O_2 levels which, in turn, activate Sods and inhibit the intracellular accumulation of O_2^- . In addition, we demonstrated that the increases in H_2O_2 in catalase-deficient cells extend CLS despite parallel increases in oxidative damage. As a result, we suggest a role for hormesis effects of H_2O_2 in promoting longevity. According to the hormesis theory, little doses of a toxin might have a long-term useful consequences as a way of conditioning the organisms toward more efficient stress responses [244]. Although this results may challenge the free radical theory of aging, it has already been suggested that ROS may be lifespan promoters mediating a secondary stress resistance response and, ultimately, extending lifespan. For instance, a study conducted in *C. elegans* has shown that a decrease in glucose availability, by glycolysis inhibition with DOG, increases respiration and ROS production, induces the activity of antioxidant enzymes and extends lifespan [139]. Also, food restriction was shown to promote mitochondrial biogenesis by inducing the expression of endothelial nitric oxide synthase (eNOS) in rodents, suggesting that NO may also play an essential role in CR-induced mechanisms and may be involved in the extension of lifespan in mammals [245]. In *S. cerevisiae*, glucose reduction in the media culture is known to promote a shift from fermentation to respiration, described as resulting in increased resistance to ROS and in extend lifespan extension [172]. Interestingly, it was recently shown that the pre-treatment of *S. cerevisiae* cells with the oxidant menadione promotes an adaptative response in which Sod1p activity is increased, resulting in CLS extension [246]. Overall, our findings

challenge the free radical theory of aging, which posits oxidative damage to macromolecules as a primary determinant of lifespan, and mark out a beneficial hormesis-like role of H_2O_2 in promoting longevity and, thus, opening new perspectives for the understanding aging and age-related diseases in humans. For instance, the administration of antioxidants is becoming a matter of debate and it has already been suggested that antioxidants may abrogate the beneficial effects of physical exercise in healthy humans, through inhibition of the ROS-mediated activation of endogenous antioxidant capacity [247]. Therefore, interventions aimed at reducing intracellular ROS accumulation may not necessarily promote longevity and may rather shorten lifespan in eukaryotes.

SECTION 3.2

Saccharomyces cerevisiae CHRONOLOGICAL LIFESPAN
EXTENSION BY CALORIC RESTRICTION MIMETICS MIGHT BE
ASSOCIATED WITH INCREASES IN REACTIVE OXYGEN SPECIES
ACCUMULATION

The results presented in this section were partially published as follow:

Almeida B., Buttner S., Ohlmeier S., Silva A., Mesquita A., Sampaio-Marques B., Osório N.S., Kollau A., Mayer B., Leão C., Laranjinha J., Rodrigues F., Madeo F., Ludovico P.. NO-mediated apoptosis in yeast. *J Cell Sci.* 2007 Sep 15;120(Pt 18):3279-88.

Weinberger M., Mesquita A., Carroll T., Marks L., Yang H., Zhang Z., Ludovico P., Burhans W.C.. Growth signaling promotes chronological aging in budding yeast by inducing superoxide anions that inhibit quiescence. *Aging (Albany NY).* 2010 Oct;2(10):709-26.

The results described in this section were presented in the following national or international congresses:

National congresses:

- Mesquita, A., Almeida, B., Silva, A., Leão, C., Rodrigues, F. and Ludovico, P.. 2007. Oscilações glicolíticas e resposta ao stresse em *Saccharomyces cerevisiae*. XV Jornadas de Biologia de das leveduras "Professor Nicolau van Uden", Porto. Portugal. (Oral communication by Mesquita, A.)
- Almeida, B., Buttner, S., Ohlmeier, S., Silva, A., Mesquita, A., Sampaio-Marques, B., Osório, N., Kollau, A., Mayer, B., Leão, C., Rodrigues, F., Madeo, F. and Ludovico, P.. 2007. Óxido nítrico como mediador da apoptose em *Saccharomyces cerevisiae*. XV Jornadas de Biologia de das leveduras "Professor Nicolau van Uden", Porto, Portugal. (Oral communication by Almeida, B. A.)

International congresses:

- Mesquita, A., Leão, C., Rodrigues, F. and Ludovico, P.. 2010. *Saccharomyces cerevisiae* cells with decreased glucose transport capacity present increased resistance to stress and extension of chronological lifespan. "Yeast: an evergreen model system. Tribute to P. Slonimski", Rome, Italy. (Oral communication by Mesquita, A.).
- Almeida, B., Silva, A., Mesquita, A., Sampaio-Marques, B., Leão C., Rodrigues, F. and Ludovico, P.. 2008. Glyceraldehyde-3-phosphate dehydrogenase as a crucial mediator of *Saccharomyces cerevisiae* apoptotic cell death, 6th International Meeting on Yeast Apoptosis, Leuven, Belgium. (Poster presentation by Mesquita, A.).
- Mesquita, A., Almeida, B., Silva, A., Leão, C., Rodrigues, F. and Ludovico, P.. 2007. Glycolytic oscillations and stress response in *Saccharomyces cerevisiae*. SMYTE - 25th Small Meeting in Yeast Transport and Energetic, Bahia, Brazil. (Oral communication by Mesquita, A.).
- Almeida, B.A, Buttner, S., Ohlmeier, S., Silva, A., Mesquita, A., Sampaio-Marques, B., Osório, N., Kollau, A., Mayer, B., Leão, C., Laranjinha, J., Rodrigues, F., Madeo, F. and Ludovico, P.. 2007. Evidence for NO-mediated apoptosis in yeast. XXIIIrd International Conference on Yeast Genetics and Molecular Biology. Melbourne, Australia. (Oral communication by Almeida, B. A.)

SECTION 3.2 *Saccharomyces cerevisiae* CHRONOLOGICAL LIFESPAN EXTENSION BY CALORIC RESTRICTION MIMETICS MIGHT BE ASSOCIATED WITH INCREASES IN REACTIVE OXYGEN SPECIES ACCUMULATION

The length of restriction required for an effective antiaging strategy for humans is still considered a challenge, due to unpleasant side effects and health disadvantages [248]. In order to accomplish these limitations, the identification of CR mimetics (CRM) candidates has emerged as a new strategy to target the metabolic and stress response pathways affected by CR and, thus, producing the CR-like effects on longevity (reviewed in [194]). Based on this perspective, our aim in this section was to contribute to a better comprehension of the impact of ROS/oxidative stress in *S. cerevisiae* CLS using different CRM approaches. For that, we tested whether manipulating glucose uptake, specific enzymatic steps of glycolysis and glucose-sensing signaling also impacts oxidative stress and its involvement in the CLS-extending effects of CR.

3.2.1 REDUCED GLUCOSE UPTAKE EXTENDS *S. cerevisiae* CLS ASSOCIATED WITH DECREASES IN INTRACELLULAR ROS

In a first approach, and as we aimed to target glucose uptake into the cell, we used three strains producing functional chimeras between the hexose transporters Hxt1p and Hxt7p each of which displaying distinct glucose transport characteristics [199]. In the following experiments we used three strains described as displaying low (KOY.TM6*P), intermediate/high (KOY.HXT7P) and high (KOY.PK2IC83) glucose uptake [199]. The results showed that a reduction in the glucose uptake into the cell (strain KOY.TM6*P) resulted in CLS extension, comparatively to intermediate/high (KOY.HXT7P) and high (KOY.PK2IC83) glucose uptake and higher growth rates (Fig. 23A and B). Thus, modelling CR by interfering with glucose uptake had similar effects in CLS to those observed upon reduction of glucose concentration in the culture media (Fig.1, Section 1).

Simultaneously, we evaluated the intracellular ROS accumulation in these cells. In accordance to Harman's theory [209-211], but in contrast to our results presented in Section 1, the CLS-extending effects observed upon reduction of glucose uptake into

the cell were associated with decreases in both the intracellular levels of H_2O_2 and O_2^- (Fig. 24 A-C), as determined by staining cells with DHR and DHE, respectively.

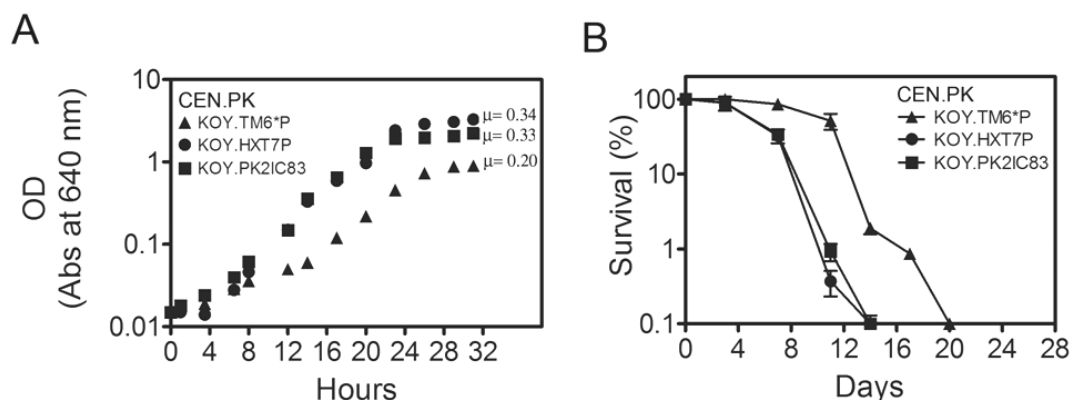


Figure 23 - Decreased glucose uptake into the cell (strain KOY.TM6*P) promotes CLS extension of cells when compared to cells displaying intermediate/high (strain KOY.HXT7P) and high (strain KOY.PK2IC83) glucose uptake. (A) Growth curves and specific growth rates (μ) of CEN.PK cells cultures in SC medium (2% glucose). Cell viability was measured at 2- to 3-d intervals beginning the day cultures reached stationary phase (day 0) and is expressed as % of survival compared with survival at day 0 (100%). Values are means \pm SD of three independent experiments. Statistical significance (* $P < 0.05$) was determined by Student's t test. Growth curves represented are the results from a number of attempts, which showed similar trends.

During chronological aging yeast cells must deal with oxidative stress caused by H_2O_2 and O_2^- , and with extrinsic factors, such as acetic acid that results in cell death [78, 80, 204, 249]. For instance, it has been shown that different chronologically long-lived cell types and CR models, such as $\Delta sch9$, $\Delta cyr1-1$, as well as *SOD* overexpressing cells, are known to exhibit increased resistance to oxidative stress [20, 60]. On the other hand, oxidative stress has been suggested as a secondary effect of acetic acid induced cell death and a cause of chronologic aging [78, 80]. In this context, we tested the susceptibility of late-exponential cells submitted to CR, modelled either by reduction of glucose in the culture medium or by decreased glucose uptake, upon treatment with H_2O_2 [204] and acetic acid [80] (Fig. 25). The results demonstrated that low glucose uptake (KOY.TM6*P) confers higher resistance to both oxidative (Fig. 25A) and acid stresses (Fig. 25B) comparatively to those displaying intermediate (KOY.HXT7P) and, particularly significant compared with high (KOY.PK2IC83) glucose uptake. However, although displaying increased resistance to high concentrations of acetic acid (Fig.

25D), CR-cells demonstrated increases sensitivity to oxidative stress by H_2O_2 , when compared to non-CR cells (Fig 25C).

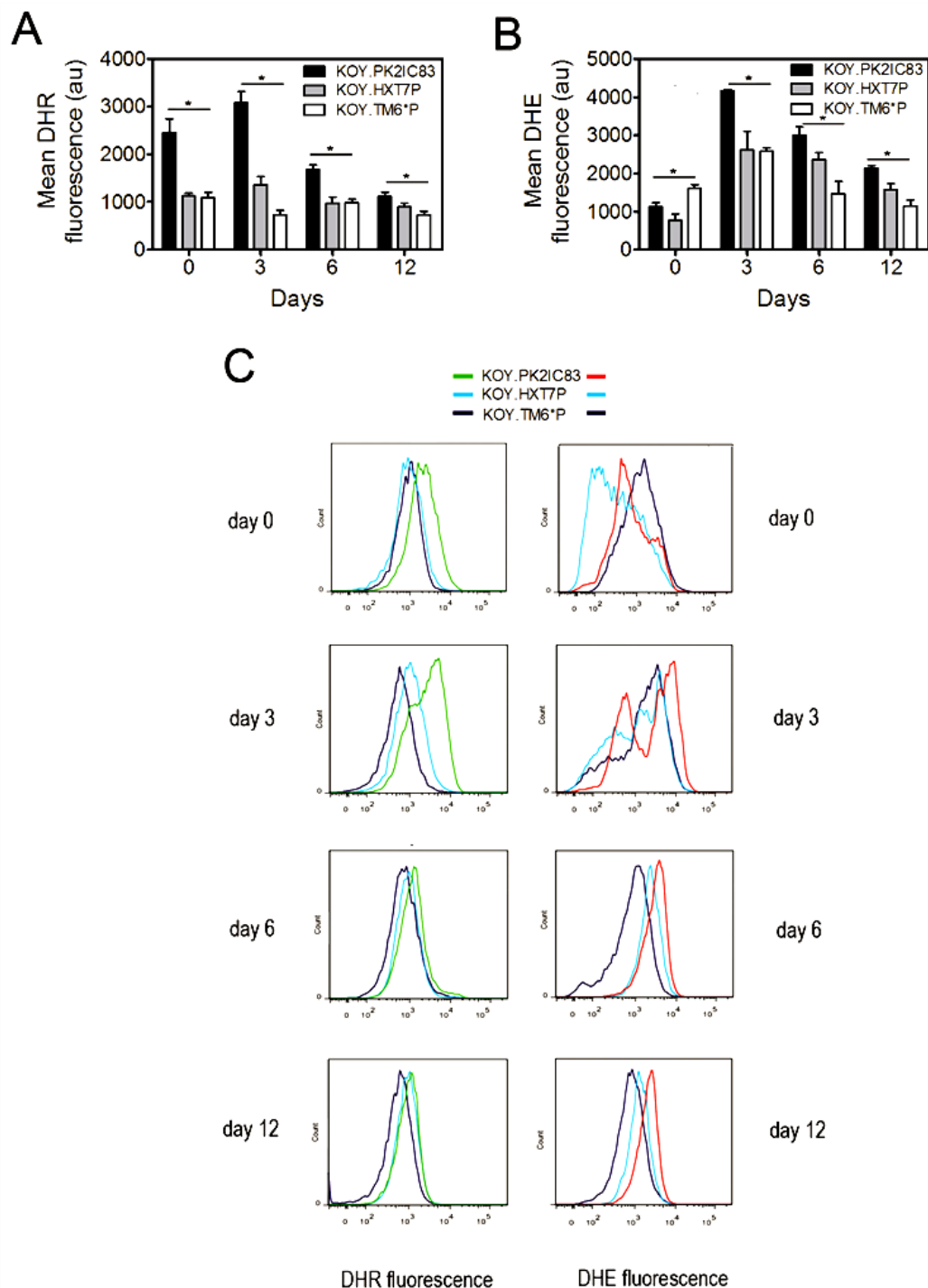


Figure 24 - Reduced glucose uptake into the cells (KOY.TM6*P) promotes CLS extension associated with decreased intracellular ROS accumulation. FACS measurements of (A and C) H_2O_2 (DHR fluorescence) and of (B and C) O_2^- (DHE fluorescence) in cells displaying high glucose (KOY.PK2IC83), intermediate (KOY.HXT7P) and low (KOY.TM6*P) uptake. Cell viability was measured at 2- to 3-d

intervals beginning the day cultures reached stationary phase (day 0) and is expressed as % of survival compared with survival at day 0 (100%). Values are means \pm SD of three independent experiments. Bar graphs indicate mean \pm SEM (%) fluorescence/cell measured in 30,000 cells/sample in three independent experiments. Statistical significance (* $P < 0.05$) was determined by Student's t test.

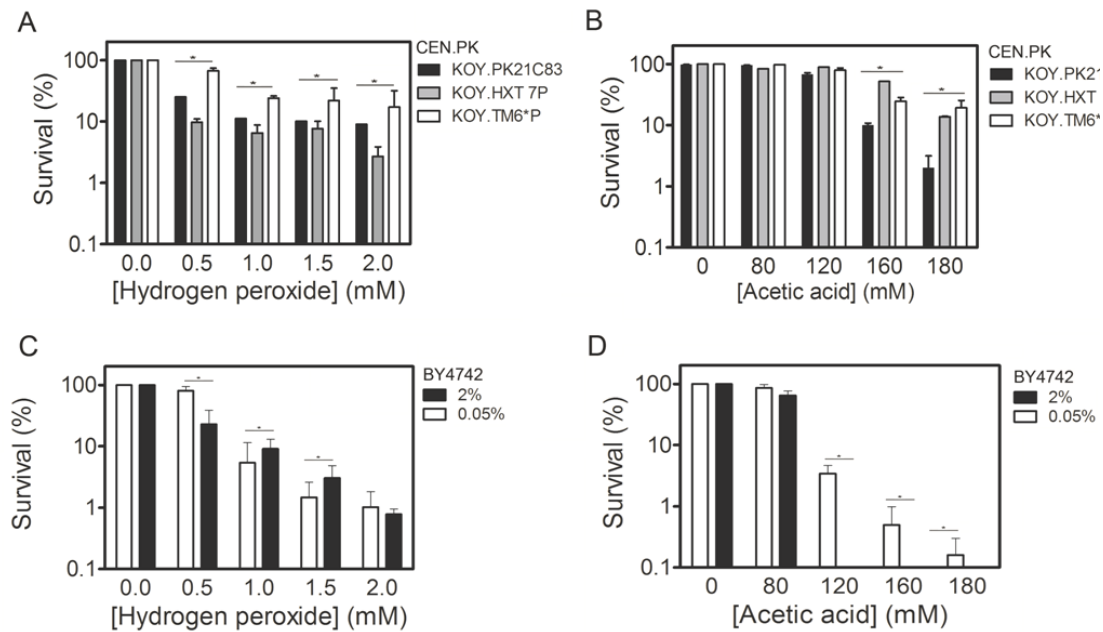


Figure 25- CR modelled by decreased glucose uptake (KOY.TM6*P) promotes resistance to both (A) oxidative and (B) acid stresses when compared to higher glucose uptake conditions (strains KOY.HXT7P and KOY.PK21C83). CR induces resistance to the lowest H₂O₂ concentrations tested (C) and to the highest concentrations of acetic acid (D). Viability was measured after 200 minutes of treatment with (A,C) H₂O₂ and (B,D) acetic acid during exponential phase and is expressed as % survival compared with survival of cells not submitted to each stress inducer (100%). Values are means \pm SD of three independent experiments. Bar graphs indicate mean \pm SEM (%) fluorescence/cell measured in 30,000 cells/sample in three independent experiments. Statistical significance (* $P < 0.05$) was determined by Student's t test. In A) and B) statistical significant differences are only noted between strains displaying low (KOY.TM6*P) and high (KOY.PK21C83) glucose uptake into the cell.

Overall, these results suggest that the reduction of glucose uptake into the cell may mimic CR effects in CLS extension by triggering a broadly acting mechanism, associated with decreases in the levels of ROS accumulation and enhanced stress protection [106, 194]. However, these results discarded previously suggested hormesis-

like effect for H_2O_2 in CLS-extension, as supported by the higher susceptibility of KOY.TM6*P cells to this specific forms of ROS. Decreased glucose uptake into the cell may trick the organism into a CR state and thereby activating the protective mechanisms that are induced in CR, including the activation of Sods. However, further studies are needed to establish hexose transporters as possible candidates as CRM and to identify similar, or parallel, route(s) whereby CR extends CLS in *S. cerevisiae*. For instance, it has been suggested that the PKA pathway controls glucose intake through the regulation of hexose transporters responsible for glucose import in *S. cerevisiae* [250]. Thus, it would be of particular interest to understand, for instance, if the involvement of glucose-sensing signaling pathways in *S. cerevisiae* chronological aging regulate specific steps of glucose metabolism. On the other hand, further studies are needed identify a role of ROS in the span-extending effects associated with decreased glucose consumption, metabolism and sensing. In this context, and as it will be presented, we further studied the involvement of mutations affecting glucose metabolism and signaling in *S. cerevisiae* CLS.

3.2.2 MUTATIONAL INACTIVATION OF SPECIFY STEPS OF GLYCOLYSIS EXTENDS *S. cerevisiae* CLS ASSOCIATED WITH DECREASES IN INTRACELLULAR ROS, PARTICULARLY H_2O_2

Several studies suggest that targeting glycolysis could invoke beneficial effects in lifespan similar to CR. For instance, pre-treatment of fetal hippocampal neurons with iodoacetate acid, which inhibits the glycolytic enzyme glyceraldehyde-3-phosphate (GAPDH), has shown potential as a CR mimetics providing protection against several stresses [197]. Also, increased expression of hexokinase 2, which might contribute to enhanced aerobic glycolysis, has been demonstrated in most immortalized and malignant cells [251]. In *C. elegans*, inhibition of glycolysis with 2-deoxyglucose (2-DOG) has been shown to promote significant increases in lifespan associated with a ROS-dependent induction of stress resistance [139]. In yeast, as Hxk2p acts in a signaling pathway important for maintaining glucose repression, it has also been linked to longevity control [196]. In addition, mutational inactivation in *HXX2* is known to extend yeast RLS, being considered a well established genetic model for studying the

CR effects in lifespan [56]. This suggestion was further supported by studies showing that the deletion of *SIR2* prevents lifespan extension by growth on low glucose [181] or in genetic models of CR including mutants in hexokinase 2 gene (*HXK2*) as well as in glucose-sensing genes involved in RAS-AC (*GPR1* and *GPA2*) and cAMP-PKA signaling (*CDC35*) [181]. However, little is known about the genetic mimetics of CR that could result in *S. cerevisiae* CLS extension.

In this context, we aimed to identify specific steps of glucose metabolism that could mimic CR-effects in CLS extension. The results presented indicate that all the mutants in the glycolytic pathway tested promoted the extension of CLS when compared to wild type strain (Fig. 26A).

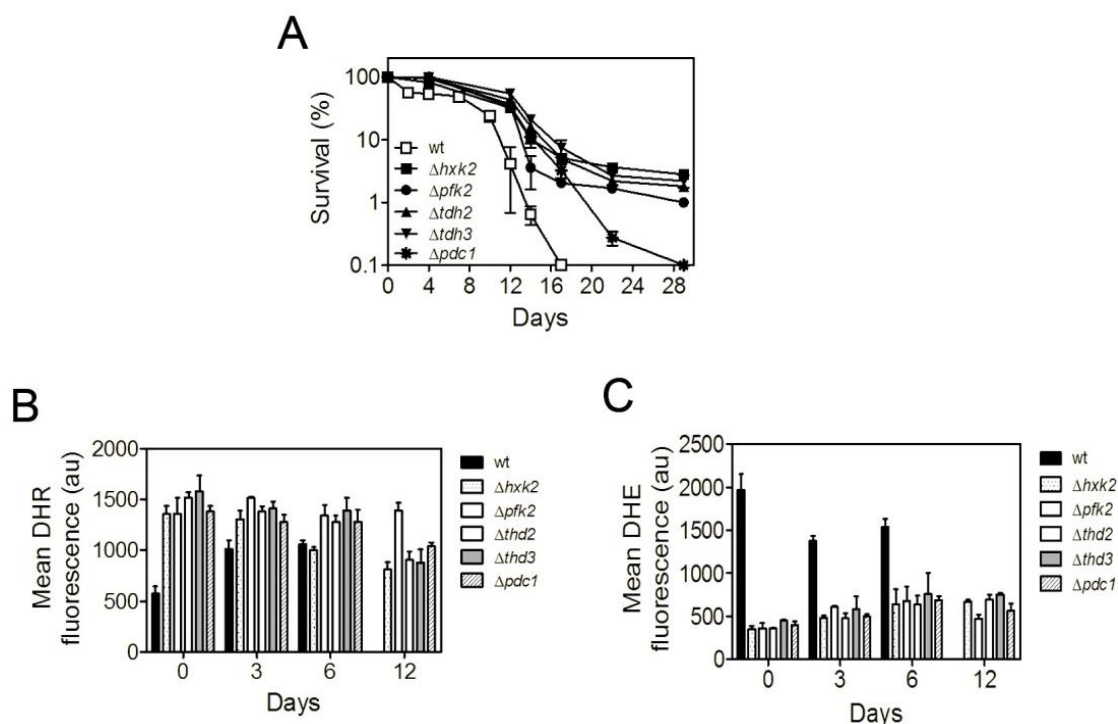


Figure 26 - Genetic inactivation of specific enzymes involved in glucose metabolism extends *S. cerevisiae* CLS by increasing intracellular H_2O_2 levels and decreasing O_2^- levels. (A) Survival of wild type, $\Delta hxxk2$, $\Delta pfk2$, $\Delta tdh2$, $\Delta tdh3$ and $\Delta pdc1$ cells assessed by cell viability, measured at 2- to 3-d intervals beginning the day cultures reached stationary phase (day 0) and is expressed as % of survival compared with survival at day 0 (100%). FACS measurements of (A) H_2O_2 (DHR fluorescence) and of (B) O_2^- (DHE fluorescence) in wild type, $\Delta hxxk2$, $\Delta pfk2$, $\Delta tdh2$, $\Delta tdh3$ and $\Delta pdc1$ cells. Bar graphs indicate mean \pm SEM (%) fluorescence/cell measured in 30,000 cells/sample in three independent experiments. Values of survival are means \pm SD of three independent experiments. With the exception of $\Delta hxxk2$ cells at day 3, all mutants showed statistically significant increases in intracellular H_2O_2 comparatively to wild type cells. Globally, statistically significant decreases in O_2^- levels were observed for all mutants in comparison to wild type cells.

The higher extension of the CLS was associated with deletion of genes that encode hexokinase (Hxk2p), phosphofructokinase (Pfk2p), and glyceraldehyde-3-phosphate dehydrogenase (GAPDH; Tdh2p and Tdh3p isoforms) (Fig. 26A). On the other hand, the abrogation of pyruvate decarboxylase (Pdc1p) extended CLS, although not so drastically when compared the other mutants. However, and contrary to that observed upon decreased glucose uptake, the results demonstrated that the CLS-extending effects globally observed in those mutants are associated with increases in the intracellular H_2O_2 levels (Fig. 26B) and decreases in O_2^- levels (Fig. 26C), as determined by staining cells with DHR and DHE, respectively. In addition, the CLS-extending effects associated with all these mutants were shown to be associated with increased resistance to both oxidative and acid stresses at all time points tested, with the exception of $\Delta pfhk2$ upon low doses of acetic acid (Fig. 27). These results suggest that CRM by targeting specific enzymes involved in glucose metabolism may promote oxidative metabolism and extend lifespan. Accordingly, previous findings showed that the deletion of *HXK2* extends lifespan similar to growth in 0.5% glucose and in association with a significant increased in the respiration rate (~3-fold) [56].

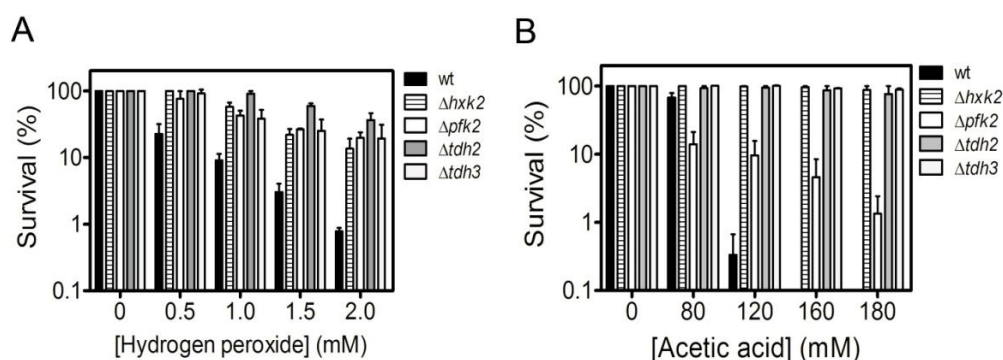


Figure 27 - Genetic inactivation of specific enzymes involved in glucose metabolism promotes resistance to both oxidative and acid stresses. Cell viability was measured after 200 minutes of treatment with (A) H_2O_2 and (B) acetic acid during exponential phase and is expressed as % survival compared with survival of cells not submitted to each stress inducer (100%). Values are means \pm SD of three independent experiments. Bar graphs indicate mean \pm SEM (%) fluorescence/cell measured in 30,000 cells/sample in three independent experiments. With the exception of $\Delta pfhk2$ cells treated with acetic acid (80 mM), all mutants showed statistically significant increases resistance to H_2O_2 and acetic acid comparatively to wild type cells.

Both CRM by reduction of glucose uptake and the abrogation of specific glycolytic enzymes were shown to impact CLS. In addition, an involvement of H₂O₂ in this effect was suggested within the abrogation the specific glycolytic enzymes tested. However, and contrary to CR- wild type cells, $\Delta h x k 2$, $\Delta p f k 2$, $\Delta t d h 2$ and $\Delta t d h 3$ cells showed increased resistance to H₂O₂ treatment. Thus, suggesting that H₂O₂ may be a key signalling molecule as previously suggested, however, its CLS-extending effects may depend on the concentrations that are perceived by the cells. The data suggest that CRM interventions aimed at decreasing ROS formation do not necessarily promote longevity and may rather reduce lifespan.

3.2.3 REDUCED GROWTH SIGNALING BY Rim15p INACTIVATION EXTENDS *S. cerevisiae* CHRONOLOGICAL LIFESPAN ASSOCIATED WITH INCREASES IN H₂O₂ LEVELS

There is a general agreement that nutrient-sensing pathways are responsive to nutrient deprivation, modulate longevity in evolutionarily different organisms and mediate at least various longevity benefits associated with CR [149]. New insights into the molecular mechanisms of CR have been provided by the development of many CR genetic models in which pro-growth glucose-regulated kinases have been deleted. For instance, the reduction of the activity of target of rapamycin (TOR) [53], protein kinase A (PKA) [56, 252] or Sch9p [53, 252] is known to resemble CR effect on both yeast RLS and CLS. Accordingly, in our model, the pharmacological inhibition of these pathways mimicked CR and induced a reversion in the death phenotype of non-CR wild type cells from day 7 on (Fig. 28). This effect was demonstrated to be independent of the pathway inhibited, suggesting that they may interconnect in CLS regulation. This question is not simply answered since these kinases have overlapping roles in regulating several cellular responses to nutrient exposure. As nutrients levels become limiting, reduced activity of these kinases leads to a reversal of these phenotypes with emphasis placed on oxidative stress response pathways, including ROS-detoxifying enzymes. For instance, in mammalian, both ROS and hyperactivation of the nutrient-sensing TOR-S6K kinase cascade have been associated to aging and age-related diseases as well as to the anti-aging effect of CR [253]. In yeast, it has been proposed that inhibition of TOR signaling causes derepression of respiration during growth in glucose [47]. Therefore, the subsequent increase in mitochondrial oxygen consumption is suggested to limit intracellular oxygen and ROS-mediated damage during glycolytic growth, leading to

CLS extension. Previous findings from our lab demonstrated that $\Delta tor1$ cells display increased survival rates associated lower intracellular ROS levels upon acid treatment [254], suggesting a causal involvement of the TOR pathway during acetic acid-induced apoptosis. However, the link between growth signaling, ROS and lifespan is complex and still remain controversial.

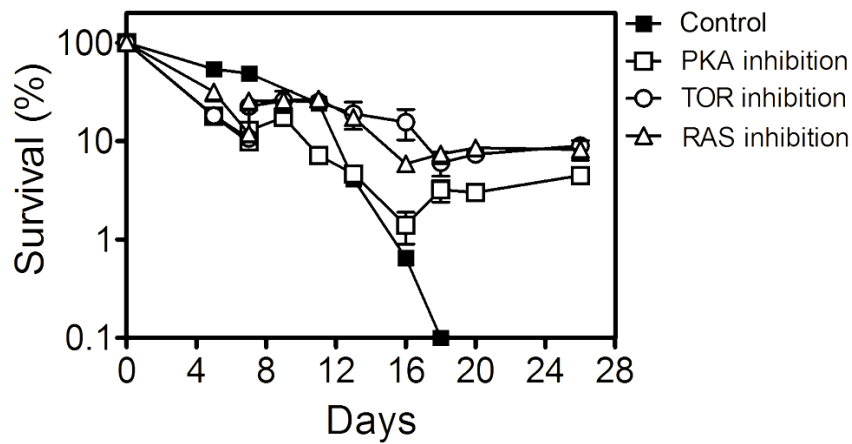


Figure 28 - Pharmacological inactivation of RAS, PKA and TOR kinases with manumycin, wortmannin and rapamycin, respectively, extends CLS in BY4742 wild type cells cultured in 2% glucose, comparatively to non-treated cells. Survival was assessed by cell viability, measured at 2- to 3-d intervals beginning the day cultures reached stationary phase (day 0) and is expressed as % of survival compared with survival at day 0 (100%). Values are means \pm SD of three independent experiments.

The nutrient-sensing signaling pathways involving Ras2p, Tor1p, and Sch9p are known to converge on the inhibition of Rim15p activity and its induction of Sod2p [54]. In this context, we aimed to study the involvement of glucose-sensing through Rim15p in CLS and oxidative stress (Fig. 29). As for wild type cells (Fig. 29 A and C), CR- $\Delta rim15$ cells were shown to accumulate higher intracellular H_2O_2 levels (Fig. 29B), and decreased O_2^- levels (Fig. 29D), when compared to non-CR conditions. Therefore, these results suggest that Rim15p might be not necessary to the H_2O_2 induction of Sods during the CLS-extending effects of CR, previously demonstrated in Section 3.1. Similarly, a Rim15p-independent mechanism in yeast CLS has also been suggested based on evidence showing that the inactivation of Sch9p, Tor1p and Ras2p which,

unlike CR, does not promote the reduction in O_2^- levels as a result in H_2O_2 increases and, thus, of activation of Sods [255].

Overall, these results suggest that the hormesis-like effect for H_2O_2 in CLS-extension may be independent of the regulation of CLS by nutrient-sensing pathways and, particularly, of Rim15p and its regulatory protective effect for entry in stationary phase. It has been observed that the CLS-extending effects associated with the reduced activity of nutrient-sensing signalling pathways are associated with increases in both respiration and cellular resistance to a variety of stresses [47, 55, 256]. An important unanswered question, however, is which downstream targets of these kinases are most important for the regulation of lifespan in yeast and other organisms.

The different CRM approaches described in this section suggest that a pro-longevity role of ROS, rather than a negative role recognized for many decades [1] may underlie the CLS-extending effects associated with decreased glucose consumption, metabolism and sensing. Accordingly, increasing evidence have suggested that decreasing ROS formation do not necessarily promote longevity and may rather reduce lifespan in multicellular eukaryotes (reviewed in [257]). Therefore, a better comprehension of the impact of growth signaling in ROS/oxidative stress as modulators of the aging process in the budding yeast *S. cerevisiae* may help to elucidate the regulation of such a complex and multifactorial process in higher eukaryotes.

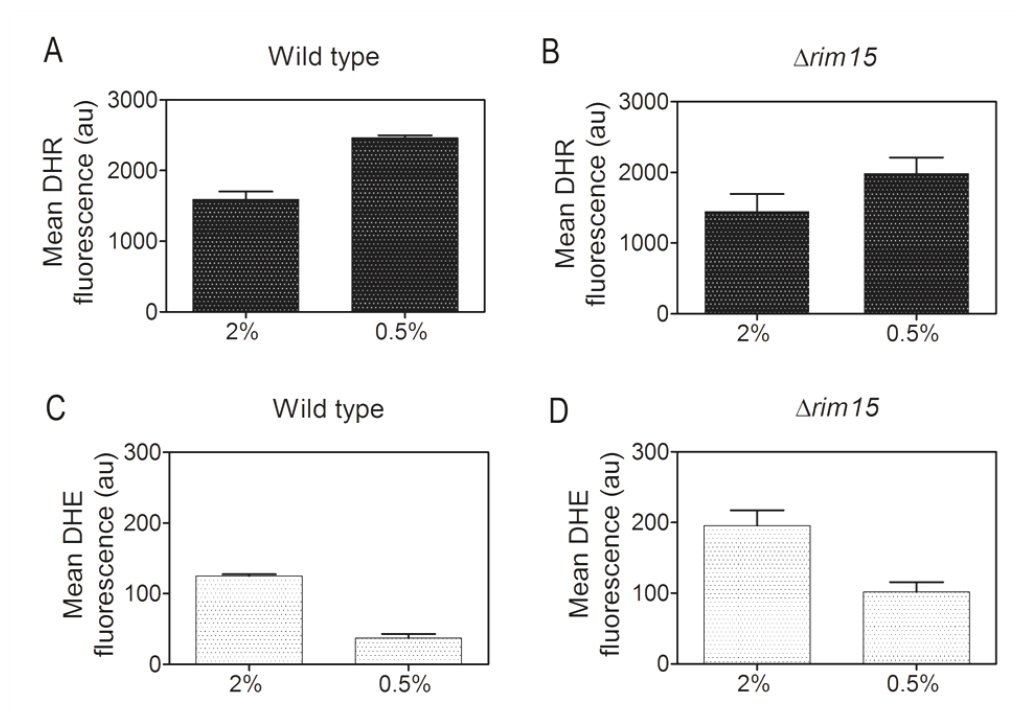


Figure 29 - Similar to wild type cells the inhibition of the growth signaling pathway Rim15p promoted increases in H_2O_2 (DHR fluorescence) (A and B) and a reduction in the intracellular O_2 accumulation (DHE fluorescence) levels (C and D), as demonstrated by FACS measurements. Bar graphs indicate mean \pm SEM (%) fluorescence/cell measured in 30,000 cells/sample in three independent experiments. Values of survival are means \pm SD of three independent experiments.

CHAPTER4.
CONCLUDING REMARKS
AND FUTURE PERSPECTIVES

4. CONCLUDING REMARKS AND FUTURE PERSPECTIVES

Since the pioneering observations by McCay and colleagues, in 1935, caloric restriction (CR) is a well established intervention that extends lifespan in a variety of model systems [101-105]. In this context, a lifespan regulatory network composed of parallel but partially connected signalling pathways controlled by nutrient-responsive pathways, sirtuins and oxidative stress regulation has been suggested [209-211, 258]. However, the mechanisms that trigger the outcomes of CR on lifespan have been difficult to establish. Initially, the background for the effects of CR was based on the "Rate of Living" theory proposed by Max Rubner in 1908. In that context, CR would extend lifespan by reducing the nutritive/caloric availability and, thus, the amount of energy metabolized. Some decades later Denham Harman provided a molecular perspective for the aging process suggesting that increases in the metabolic rate would favour the formation of free radicals and its cumulative damage to the cell and, ultimately, to the organism [1]. Based on the integration of both theories it has been suggested that CR functions by slowing metabolism and thereby slowing the generation of reactive oxygen species (ROS) [10, 106, 258].

Although it has been suggested that an inverse correlation between levels of mitochondrial ROS and lifespan exists [209-211, 258], a causative effect of ROS-induced oxidation in limiting lifespan has been difficult to establish due to inconsistent or null effects of antioxidants [104, 259]. In yeast, CR mimic by reducing the glucose concentration in the culture medium has been shown to extend both replicative lifespan (RLS) and chronological lifespan (CLS) [45, 56, 60, 212]. Apparently ROS may not limit RLS [172] but the pharmacological and genetic evidence provided until now still favour a role for ROS in both RLS and CLS [164]. Contrary to the general belief, our results demonstrated that the CLS-extending effects of CR are associated with an increase, rather than decrease, in the intracellular ROS levels. In a first approach, a pro-longevity role for H₂O₂ was suggested based on the combined use of probes that can distinguish between hydrogen peroxide (H₂O₂) and superoxide anions (O₂⁻). This hypothesis was further supported by the CLS extension observed after the genetic/pharmacological inactivation of H₂O₂-detoxifying systems, catalase and glutathione, and in chronological aged wild type cells treated with non-toxic concentrations of H₂O₂. Such involvement of H₂O₂ in CLS extension was further confirmed by the reduction of the intracellular H₂O₂ levels in cells overexpressing

CTA1. On the other hand, the pro-longevity role of H_2O_2 observed in catalase mutants, and in contrast to CR-cell cells, occurred associated with an increase in oxidative damage. These findings may challenge the Harman's theory, however, increased oxidative damage is well established in long-lived naked mole rats [136]. In this context, it has been suggested that a secondary stress response may be induced as a result of the primary response to an augment in ROS formation during increased mitochondrial metabolism, resulting in a reduction of the stress levels and an extension of lifespan [123, 260-263].

In yeast, an involvement of ROS in lifespan extension has been mainly based on the pharmacological inhibition of respiratory chain [164] and on the deletion of SOD genes [138, 213]. For instance, mutation of *SOD1* has been demonstrated to decrease yeast RLS [137] and accelerate chronological aging [58, 187]. Accordingly, it has been shown that the mutation of copper/zinc-containing SOD decreases lifespan in flies [264] and in mice [265]. Nevertheless, it was previously reported in yeast that, despite increases in the activity of both Sod enzymes, CR conditions were associated with ROS production [166]. Thus, suggesting that ROS may act as second messengers to regulate SOD activity. In agreement, increases of ROS levels were also associated to *C. elegans* longevity [139] and a paradoxical induction of stress response to increased metabolism has been further suggested in mice [146, 147]. On the other hand, it has been recently observed that glutathione-dependent *SOD1* activation is crucial for CLS extension by a mild oxidative stress pre-treatment [246]. However, none of those studies have addressed if a specific form of ROS have benefits for lifespan. Our results revealed that the mechanism whereby CR extends CLS involves the induction of Sod2p activity by H_2O_2 . Based on these results we suggest that Sods are, therefore, targets of a H_2O_2 -induced stress response triggered by CR that confers hormesis-like protective effects against aging by reducing the levels of O_2^- .

In this context of aging research, most studies have been highly compartmentalized and mainly concerned with mitochondria formation of ROS. Although mitochondria are the main source of ROS production it is nowadays well accepted that ROS are originated by a number of other cellular organelles besides mitochondria [109]. In this context, we assessed CLS in *rho0* cells in both CR and non-CR conditions. Our results showed that in non-CR conditions *rho0* cells have a reduced CLS comparatively to wild type cells, suggesting the protective role for this organelle in CLS. However, as for wild type cells, the CLS-extending effects of CR were shown to

be associated with increased intracellular ROS levels and, thus, suggesting that other ROS sources may be involved in CLS. The extension of CLS in cells lacking functional peroxisomes associated with an increase in intracellular ROS accumulation suggested an negative contribution of this organelle to CLS. However, peroxisomes were also shown to be required for the CLS-extending effects of moderate CR and, thus, calling into question a dual role for peroxisome and/or peroxisome-derived ROS, and particularly H₂O₂, in *S. cerevisiae* CLS extension.

Altogether, the results led us to theorize about a major involvement of increased H₂O₂ levels CLS extension, mimicking the effect of CR in cells grown in non-CR conditions and promoting their survival. On the other hand, while some ROS, such as O₂⁻, appear to be extremely detrimental to biological systems others, and especially H₂O₂, may be key signalling molecules depending on the concentrations that are perceived by the cells. In fact, H₂O₂ has been well recognized as an important signalling molecule [266, 267] that may influence cell proliferation, cell death and the expression of genes [268-270], besides to be involved in the activation of several nutrient signalling pathways. Data herein presented suggest that Rim15p is not necessary to the induction of Sods by H₂O₂ during the CLS-extending effects of CR. As for wild type, in $\Delta rim15$ cells the CLS-extending effects of CR were associated with H₂O₂ increases and O₂⁻ reduction. Also, although CR can extend CLS by inhibiting the accumulation of acetic acid [78], the hormesis-like mechanism by which H₂O₂ extends CLS was demonstrated in buffered medium. Thus, suggesting that such effect may be independent of an acetic acid-mediated mechanism. On the other hand, increased resistance to high acetic acid concentrations was observed in exponential CR-cells. Therefore, suggesting that additional mechanisms may exist whereby CR extends yeast CLS associated to redox signaling. For instance, in glucose limiting conditions, respiration-induced oxidative stress and ROS production were shown to extend fission yeast lifespan by inducing an adaptive response in a mitogen-activated protein (MAP) kinase Sty1-dependent manner [271]. Moreover, such adaptative mechanism was suggested to be associated with increases in stress defences by H₂O₂.

The impact of ROS and oxidative stress in *S. cerevisiae* CLS was further studied within CR mimetics by interfering with glucose metabolism and sensing signaling. A similar mechanism whereby increases in H₂O₂ promote the extension of CLS was suggested upon mutational inactivation of specific glycolytic enzymes including Hxk2p, Pfk2p and GAPDH, but not within the reduction of the glucose uptake. These

results are supported by existing evidence showing that deletion of *HXX2*, which is expected to mimic the effect of growth in low glucose, promotes increases in respiration rate and RLS extension [56]. On the other hand, Hxk2p has been linked to longevity control by acting in a signaling pathway important for maintaining glucose repression [196]. Accordingly, in *C. elegans*, the inhibition of glycolysis with 2-deoxy glucose was shown to induce respiration and increases lifespan [139], reflecting previous results in yeast [172]. In this context, our results suggest that CR mimetics (CRM), may operate in parallel mechanism(s) beyond those involving TOR-Sch9p and RAS-AC-PKA nutrient-sensing signaling pathways observed with general CR, to extend *S.cerevisiae* CLS (Fig. 1).

In contrast to the general belief that CR extends lifespan by reducing the production of ROS our data called into question a novel role for augmented ROS levels, and particularly H_2O_2 , in *S. cerevisiae* CLS extension. Although the exact action of hormetic levels of ROS and their interplay as signals in CR-mediated lifespan extension still remains elusive, it has been suggested it likely may be conserved in other organisms. For instance, low concentrations of H_2O_2 have already been associated with the extension of RLS in human skin keratinocytes, being this effect accompanied by an increase in telomere length [141]. On the other hand, the activation of Sods by H_2O_2 has been shown in cultured rat glomerular cells [272]. In addition, Sods were also implicated in telomere maintenance during RLS extension of mammalian cells [143] by counteracting the inhibition of telomere elongation by O_2^- [142]. A role for H_2O_2 in the inhibition of O_2^- was further suggested by the high levels of O_2^- and decreases in H_2O_2 in *SOD2*-defective mouse cells driven into quiescence by contact inhibition [237]. More recently, it was reported in a mouse model of inflammatory responses in the lung that genetic or pharmacological inactivation of catalase in neutrophils induces intracellular H_2O_2 that inhibits the O_2^- -dependent inflammatory responses of these cells [238, 239]. Thus, once more, proposing that H_2O_2 exerts its anti-inflammatory effects in mouse neutrophils by inducing Sods activity and reducing O_2^- -mediated inflammation.

Overall, these findings suggest mechanisms that challenge the validity of the "Free Radical Theory" and provide a different paradigm for understanding how oxidative stress impacts aging and health. For instance, it has been recently reported that administration of antioxidants may abrogate the advantageous effects of physical exercise in healthy humans, through inhibition of the ROS-mediated activation of endogenous antioxidant capacity [247]. Consistent with the hormesis hypothesis, the

ROS signal may induce ROS defence mechanisms which culminate in the extension of lifespan (Fig. 1).

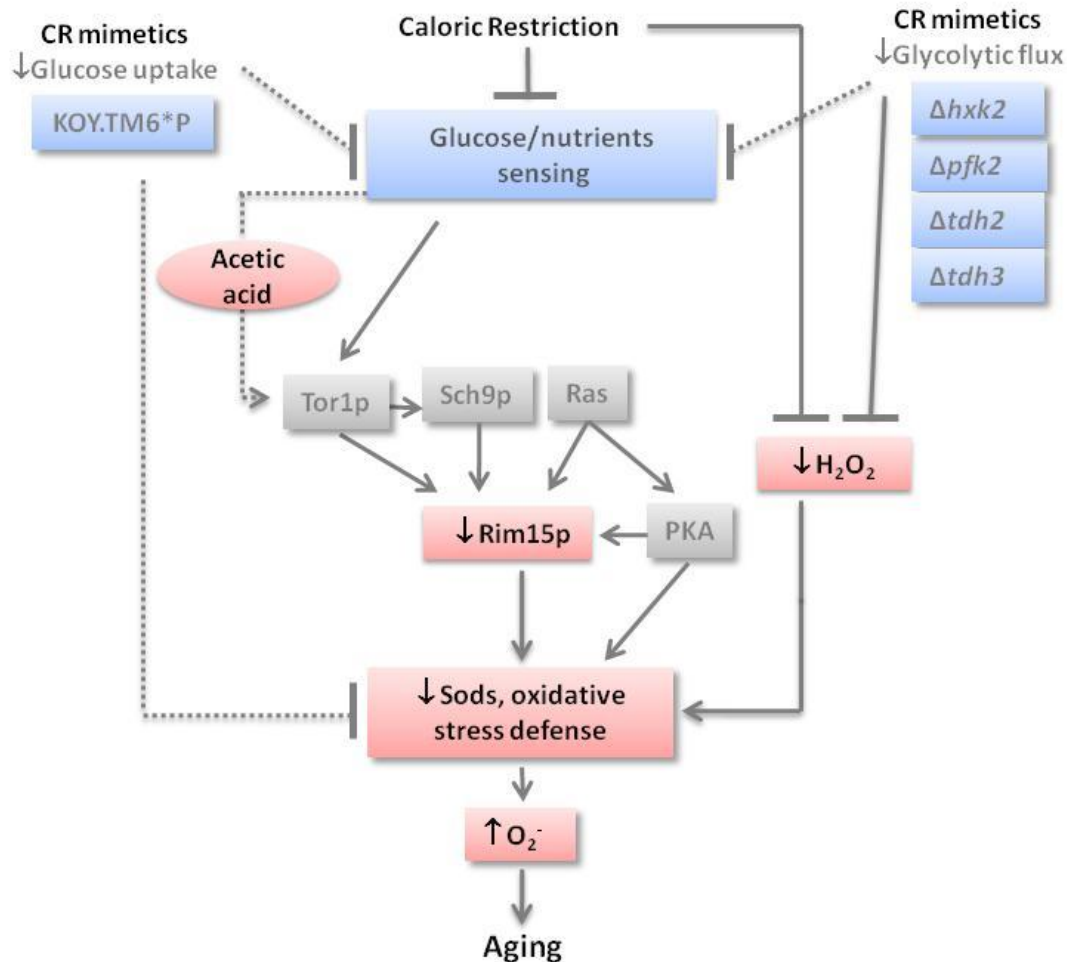


Figure 1. The CLS-extending effects of CR may be independent of the established CR signaling through the conserved Sch9p-, Tor1p-, and RAS-dependent pathways and of the induction of oxidative stress defenses by Rim15p [54]. As an alternative, CR may extend CLS by an hormesis-like mechanism in which CR induces H₂O₂ that activates Sods and reduces the levels of O₂⁻, ultimately resulting in increased lifespan. Furthermore, this mechanism is suggested to be independent of the acetic acid effects on CLS. A mechanism involving the CLS-extending effects of increased H₂O₂ levels is also suggested upon deletion of specific glycolytic enzymes, but discarded within reduced glucose uptake into the cell. Overall, it is suggested that different routes may mediate the CR-mediated extension in yeast CLS. (Figure from [255] with adaptations).

In this scenario, antioxidants may prevent this adaptive response and abolish the extension of lifespan. Thus, interventions aimed at decreasing ROS formation may not

necessarily promote longevity and may rather reduce lifespan. Due to the inconsistent effects of antioxidants and taking into consideration that ROS production may be a double-edged sword, the findings herein presented uncover a new link between ROS and longevity. In this context, it is still necessary to depict the molecular pathways that are mediating the ROS benefits in yeast lifespan in order to obtain a more complete understanding of how CR could be acting in extending longevity in higher organisms.

REFERENCES

REFERENCES

1. Harman, D., *Aging: a theory based on free radical and radiation chemistry*. J Gerontol, 1956. **11**(3): p. 298-300.
2. Flachsbarth, F., et al., *Association of FOXO3A variation with human longevity confirmed in German centenarians*. Proc Natl Acad Sci U S A, 2009. **106**(8): p. 2700-5.
3. Willcox, B.J., et al., *FOXO3A genotype is strongly associated with human longevity*. Proc Natl Acad Sci U S A, 2008. **105**(37): p. 13987-92.
4. Ding, S.L. and C.Y. Shen, *Model of human aging: recent findings on Werner's and Hutchinson-Gilford progeria syndromes*. Clin Interv Aging, 2008. **3**(3): p. 431-44.
5. Someya, S., et al., *Effects of caloric restriction on age-related hearing loss in rodents and rhesus monkeys*. Curr Aging Sci, 2010. **3**(1): p. 20-5.
6. Ramsey, J.J., et al., *Dietary restriction and aging in rhesus monkeys: the University of Wisconsin study*. Exp Gerontol, 2000. **35**(9-10): p. 1131-49.
7. Colman, R.J., et al., *Caloric restriction delays disease onset and mortality in rhesus monkeys*. Science, 2009. **325**(5937): p. 201-4.
8. Hastay, P. and J. Vijg, *Accelerating aging by mouse reverse genetics: a rational approach to understanding longevity*. Aging Cell, 2004. **3**(2): p. 55-65.
9. Jazwinski, S.M., *New clues to old yeast*. Mech Ageing Dev, 2001. **122**(9): p. 865-82.
10. Guarente, L. and C. Kenyon, *Genetic pathways that regulate ageing in model organisms*. Nature, 2000. **408**(6809): p. 255-62.
11. Kenyon, C., *The plasticity of aging: insights from long-lived mutants*. Cell, 2005. **120**(4): p. 449-60.
12. Carey, J.R. and F. Molleman, *Reproductive aging in tephritid fruit flies*. Ann N Y Acad Sci, 2010. **1204**: p. 139-48.
13. Kaeberlein, M., M. McVey, and L. Guarente, *The SIR2/3/4 complex and SIR2 alone promote longevity in Saccharomyces cerevisiae by two different mechanisms*. Genes Dev, 1999. **13**(19): p. 2570-80.
14. Jazwinski, S.M., *Longevity, genes, and aging: a view provided by a genetic model system*. Exp Gerontol, 1999. **34**(1): p. 1-6.
15. Bitterman, K.J., O. Medvedik, and D.A. Sinclair, *Longevity regulation in Saccharomyces cerevisiae: linking metabolism, genome stability, and heterochromatin*. Microbiol Mol Biol Rev, 2003. **67**(3): p. 376-99, table of contents.
16. Piper, P.W., *Long-lived yeast as a model for ageing research*. Yeast, 2006. **23**(3): p. 215-26.
17. Kaeberlein, M., C.R. Burtner, and B.K. Kennedy, *Recent developments in yeast aging*. PLoS Genet, 2007. **3**(5): p. e84.
18. Mortimer, R.K.J., J. R., *Life span of individual yeast cells*. Nature, 1959. **183**: p. 1751-1752.
19. Jazwinski, S.M., N.K. Egilmez, and J.B. Chen, *Replication control and cellular life span*. Exp Gerontol, 1989. **24**(5-6): p. 423-36.
20. Fabrizio, P., et al., *Regulation of longevity and stress resistance by Sch9 in yeast*. Science, 2001. **292**(5515): p. 288-90.
21. Fabrizio, P. and V.D. Longo, *The chronological life span of Saccharomyces cerevisiae*. Aging Cell, 2003. **2**(2): p. 73-81.

22. Fontana, L., L. Partridge, and V.D. Longo, *Extending healthy life span--from yeast to humans*. Science, 2010. **328**(5976): p. 321-6.
23. Kennedy, B.K., *The genetics of ageing: insight from genome-wide approaches in invertebrate model organisms*. J Intern Med, 2008. **263**(2): p. 142-52.
24. Partridge, L., et al., *Ageing in Drosophila: The role of the insulin/Igf and TOR signalling network*. Exp Gerontol, 2011. **46**(5): p. 376-81.
25. Longo, V.D. and C.E. Finch, *Evolutionary medicine: from dwarf model systems to healthy centenarians?* Science, 2003. **299**(5611): p. 1342-6.
26. Tissenbaum, H.A. and L. Guarente, *Model organisms as a guide to mammalian aging*. Dev Cell, 2002. **2**(1): p. 9-19.
27. Butler, R.N., et al., *Longevity genes: from primitive organisms to humans*. J Gerontol A Biol Sci Med Sci, 2003. **58**(7): p. 581-4.
28. Kenyon, C., et al., *A C. elegans mutant that lives twice as long as wild type*. Nature, 1993. **366**(6454): p. 461-4.
29. Kenyon, C.J., *The genetics of ageing*. Nature, 2010. **464**(7288): p. 504-12.
30. Gronke, S., et al., *Molecular evolution and functional characterization of Drosophila insulin-like peptides*. PLoS Genet, 2010. **6**(2): p. e1000857.
31. Tatar, M., et al., *A mutant Drosophila insulin receptor homolog that extends life-span and impairs neuroendocrine function*. Science, 2001. **292**(5514): p. 107-10.
32. Brown-Borg, H.M., *Hormonal regulation of longevity in mammals*. Ageing Res Rev, 2007. **6**(1): p. 28-45.
33. Bluher, M., B.B. Kahn, and C.R. Kahn, *Extended longevity in mice lacking the insulin receptor in adipose tissue*. Science, 2003. **299**(5606): p. 572-4.
34. Suh, Y., et al., *Functionally significant insulin-like growth factor I receptor mutations in centenarians*. Proc Natl Acad Sci U S A, 2008. **105**(9): p. 3438-42.
35. Amador-Noguez, D., et al., *Alterations in xenobiotic metabolism in the long-lived Little mice*. Aging Cell, 2007. **6**(4): p. 453-70.
36. Jia, K., D. Chen, and D.L. Riddle, *The TOR pathway interacts with the insulin signaling pathway to regulate C. elegans larval development, metabolism and life span*. Development, 2004. **131**(16): p. 3897-906.
37. Martin, D.E. and M.N. Hall, *The expanding TOR signaling network*. Curr Opin Cell Biol, 2005. **17**(2): p. 158-66.
38. Schmelzle, T. and M.N. Hall, *TOR, a central controller of cell growth*. Cell, 2000. **103**(2): p. 253-62.
39. Yang, Q. and K.L. Guan, *Expanding mTOR signaling*. Cell Res, 2007. **17**(8): p. 666-81.
40. Jacinto, E. and M.N. Hall, *Tor signalling in bugs, brain and brawn*. Nat Rev Mol Cell Biol, 2003. **4**(2): p. 117-26.
41. Kapahi, P., et al., *Regulation of lifespan in Drosophila by modulation of genes in the TOR signaling pathway*. Curr Biol, 2004. **14**(10): p. 885-90.
42. Bjedov, I., et al., *Mechanisms of life span extension by rapamycin in the fruit fly Drosophila melanogaster*. Cell Metab, 2010. **11**(1): p. 35-46.
43. Selman, C., et al., *Ribosomal protein S6 kinase 1 signaling regulates mammalian life span*. Science, 2009. **326**(5949): p. 140-4.
44. Loewith, R., et al., *Two TOR complexes, only one of which is rapamycin sensitive, have distinct roles in cell growth control*. Mol Cell, 2002. **10**(3): p. 457-68.
45. Powers, R.W., 3rd, et al., *Extension of chronological life span in yeast by decreased TOR pathway signaling*. Genes Dev, 2006. **20**(2): p. 174-84.

46. Harrison, D.E., et al., *Rapamycin fed late in life extends lifespan in genetically heterogeneous mice*. Nature, 2009. **460**(7253): p. 392-5.
47. Bonawitz, N.D., et al., *Reduced TOR signaling extends chronological life span via increased respiration and upregulation of mitochondrial gene expression*. Cell Metab, 2007. **5**(4): p. 265-77.
48. Kaeblerlein, M. and P. Kapahi, *Cell signaling. Aging is RSKy business*. Science, 2009. **326**(5949): p. 55-6.
49. Shih, D.M., et al., *Combined serum paraoxonase knockout/apolipoprotein E knockout mice exhibit increased lipoprotein oxidation and atherosclerosis*. J Biol Chem, 2000. **275**(23): p. 17527-35.
50. Sun, J., et al., *Divergent roles of RAS1 and RAS2 in yeast longevity*. J Biol Chem, 1994. **269**(28): p. 18638-45.
51. Wullschlegel, S., R. Loewith, and M.N. Hall, *TOR signaling in growth and metabolism*. Cell, 2006. **124**(3): p. 471-84.
52. Ruggero, D. and N. Sonenberg, *The Akt of translational control*. Oncogene, 2005. **24**(50): p. 7426-34.
53. Kaeblerlein, M., et al., *Regulation of yeast replicative life span by TOR and Sch9 in response to nutrients*. Science, 2005. **310**(5751): p. 1193-6.
54. Wei, M., et al., *Life span extension by calorie restriction depends on Rim15 and transcription factors downstream of Ras/PKA, Tor, and Sch9*. PLoS Genet, 2008. **4**(1): p. e13.
55. Pan, Y. and G.S. Shadel, *Extension of chronological life span by reduced TOR signaling requires down-regulation of Sch9p and involves increased mitochondrial OXPHOS complex density*. Aging (Albany NY), 2009. **1**(1): p. 131-45.
56. Lin, S.J., P.A. Defossez, and L. Guarente, *Requirement of NAD and SIR2 for life-span extension by calorie restriction in Saccharomyces cerevisiae*. Science, 2000. **289**(5487): p. 2126-8.
57. Wei, M., et al., *Tor1/Sch9-regulated carbon source substitution is as effective as calorie restriction in life span extension*. PLoS Genet, 2009. **5**(5): p. e1000467.
58. Longo, V.D., E.B. Gralla, and J.S. Valentine, *Superoxide dismutase activity is essential for stationary phase survival in Saccharomyces cerevisiae. Mitochondrial production of toxic oxygen species in vivo*. J Biol Chem, 1996. **271**(21): p. 12275-80.
59. Laun, P., et al., *Aged mother cells of Saccharomyces cerevisiae show markers of oxidative stress and apoptosis*. Mol Microbiol, 2001. **39**(5): p. 1166-73.
60. Fabrizio, P., et al., *SOD2 functions downstream of Sch9 to extend longevity in yeast*. Genetics, 2003. **163**(1): p. 35-46.
61. Fabrizio, P., et al., *Chronological aging-independent replicative life span regulation by Msn2/Msn4 and Sod2 in Saccharomyces cerevisiae*. FEBS Lett, 2004. **557**(1-3): p. 136-42.
62. Ashrafi, K., et al., *Passage through stationary phase advances replicative aging in Saccharomyces cerevisiae*. Proc Natl Acad Sci U S A, 1999. **96**(16): p. 9100-5.
63. Longo, V.D., *Ras: the other pro-aging pathway*. Sci Aging Knowledge Environ, 2004. **2004**(39): p. pe36.
64. Holzenberger, M., *The GH/IGF-I axis and longevity*. Eur J Endocrinol, 2004. **151 Suppl 1**: p. S23-7.
65. Yan, L., et al., *Type 5 adenylyl cyclase disruption increases longevity and protects against stress*. Cell, 2007. **130**(2): p. 247-58.

66. Sinclair, D.A. and L. Guarente, *Extrachromosomal rDNA circles--a cause of aging in yeast*. Cell, 1997. **91**(7): p. 1033-42.
67. Finkel, T., C.X. Deng, and R. Mostoslavsky, *Recent progress in the biology and physiology of sirtuins*. Nature, 2009. **460**(7255): p. 587-91.
68. Berdichevsky, A. and L. Guarente, *A stress response pathway involving sirtuins, forkheads and 14-3-3 proteins*. Cell Cycle, 2006. **5**(22): p. 2588-91.
69. Griswold, A.J., et al., *Sir2 mediates apoptosis through JNK-dependent pathways in Drosophila*. Proc Natl Acad Sci U S A, 2008. **105**(25): p. 8673-8.
70. Michan, S. and D. Sinclair, *Sirtuins in mammals: insights into their biological function*. Biochem J, 2007. **404**(1): p. 1-13.
71. Pearson, K.J., et al., *Resveratrol delays age-related deterioration and mimics transcriptional aspects of dietary restriction without extending life span*. Cell Metab, 2008. **8**(2): p. 157-68.
72. Beher, D., et al., *Resveratrol is not a direct activator of SIRT1 enzyme activity*. Chem Biol Drug Des, 2009. **74**(6): p. 619-24.
73. Morselli, E., et al., *Caloric restriction and resveratrol promote longevity through the Sirtuin-1-dependent induction of autophagy*. Cell Death Dis, 2010. **1**: p. e10.
74. Morselli, E., et al., *Spermidine and resveratrol induce autophagy by distinct pathways converging on the acetylproteome*. J Cell Biol, 2011. **192**(4): p. 615-29.
75. Dang, W., et al., *Histone H4 lysine 16 acetylation regulates cellular lifespan*. Nature, 2009. **459**(7248): p. 802-7.
76. Kaeblerlein, M., et al., *Sir2-independent life span extension by calorie restriction in yeast*. PLoS Biol, 2004. **2**(9): p. E296.
77. Burhans, W.C. and M. Weinberger, *Acetic acid effects on aging in budding yeast: are they relevant to aging in higher eukaryotes?* Cell Cycle, 2009. **8**(14): p. 2300-2.
78. Burtner, C.R., et al., *A molecular mechanism of chronological aging in yeast*. Cell Cycle, 2009. **8**(8): p. 1256-70.
79. Fabrizio, P., et al., *Sir2 blocks extreme life-span extension*. Cell, 2005. **123**(4): p. 655-67.
80. Ludovico, P., et al., *Saccharomyces cerevisiae commits to a programmed cell death process in response to acetic acid*. Microbiology, 2001. **147**(Pt 9): p. 2409-15.
81. Rose, M.R., et al., *Evolution of ageing since Darwin*. J Genet, 2008. **87**(4): p. 363-71.
82. Weinert, B.T. and P.S. Timiras, *Invited review: Theories of aging*. J Appl Physiol, 2003. **95**(4): p. 1706-16.
83. Arking, R., et al., *Genomic plasticity, energy allocations, and the extended longevity phenotypes of Drosophila*. Ageing Res Rev, 2002. **1**(2): p. 209-28.
84. Schneider, S.A., et al., *Stress resistance and longevity are not directly linked to levels of enzymatic antioxidants in the ponerine ant Harpegnathos saltator*. PLoS One, 2011. **6**(1): p. e14601.
85. Kanungo, M.S., *A model for ageing*. J Theor Biol, 1975. **53**(2): p. 253-61.
86. Puca, A.A., et al., *A genome-wide scan for linkage to human exceptional longevity identifies a locus on chromosome 4*. Proc Natl Acad Sci U S A, 2001. **98**(18): p. 10505-8.
87. Orgel, L.E., *The maintenance of the accuracy of protein synthesis and its relevance to ageing*. Proc Natl Acad Sci U S A, 1963. **49**: p. 517-21.

88. Musich, P.R. and Y. Zou, *Genomic instability and DNA damage responses in progeria arising from defective maturation of prelamin A*. Aging (Albany NY), 2009. **1**(1): p. 28-37.
89. Friedlander, R.M., *Apoptosis and caspases in neurodegenerative diseases*. N Engl J Med, 2003. **348**(14): p. 1365-75.
90. Zheng, J., et al., *Differential patterns of apoptosis in response to aging in Drosophila*. Proc Natl Acad Sci U S A, 2005. **102**(34): p. 12083-8.
91. Herker, E., et al., *Chronological aging leads to apoptosis in yeast*. J Cell Biol, 2004. **164**(4): p. 501-7.
92. Garigan, D., et al., *Genetic analysis of tissue aging in Caenorhabditis elegans: a role for heat-shock factor and bacterial proliferation*. Genetics, 2002. **161**(3): p. 1101-12.
93. Shen, J., et al., *A screen of apoptosis and senescence regulatory genes for life span effects when over-expressed in Drosophila*. Aging (Albany NY), 2009. **1**(2): p. 191-211.
94. Aubert, G. and P.M. Lansdorp, *Telomeres and aging*. Physiol Rev, 2008. **88**(2): p. 557-79.
95. Shiels, P.G., et al., *Analysis of telomere lengths in cloned sheep*. Nature, 1999. **399**(6734): p. 316-7.
96. Tomas-Loba, A., et al., *Telomerase reverse transcriptase delays aging in cancer-resistant mice*. Cell, 2008. **135**(4): p. 609-22.
97. Sharpless, N.E. and R.A. DePinho, *Telomeres, stem cells, senescence, and cancer*. J Clin Invest, 2004. **113**(2): p. 160-8.
98. Burtner, C.R. and B.K. Kennedy, *Progeria syndromes and ageing: what is the connection?* Nat Rev Mol Cell Biol, 2010. **11**(8): p. 567-78.
99. Lynn, W.S. and J.C. Wallwork, *Does food restriction retard aging by reducing metabolic rate?* J Nutr, 1992. **122**(9): p. 1917-8.
100. de Magalhaes, J.P., J. Costa, and G.M. Church, *An analysis of the relationship between metabolism, developmental schedules, and longevity using phylogenetic independent contrasts*. J Gerontol A Biol Sci Med Sci, 2007. **62**(2): p. 149-60.
101. Kirkwood, T.B. and D.P. Shanley, *Food restriction, evolution and ageing*. Mech Ageing Dev, 2005. **126**(9): p. 1011-6.
102. McCay, C.M., M.F. Cromwell, and L.A. Maynard, *The effect of retarded growth upon the length of life span and upon the ultimate body size*. J. Nutr. , 1935. **10**: p. 63-79.
103. Masoro, E.J., *Subfield history: caloric restriction, slowing aging, and extending life*. Sci Aging Knowledge Environ, 2003. **2003**(8): p. RE2.
104. Koubova, J. and L. Guarente, *How does calorie restriction work?* Genes Dev, 2003. **17**(3): p. 313-21.
105. Finch, C.E., M.C. Pike, and M. Witten, *Slow mortality rate accelerations during aging in some animals approximate that of humans*. Science, 1990. **249**(4971): p. 902-5.
106. Harman, D., *The aging process*. Proc Natl Acad Sci U S A, 1981. **78**(11): p. 7124-8.
107. Finkel, T. and N.J. Holbrook, *Oxidants, oxidative stress and the biology of ageing*. Nature, 2000. **408**(6809): p. 239-47.
108. Kyaw, M., et al., *Atheroprotective effects of antioxidants through inhibition of mitogen-activated protein kinases*. Acta Pharmacol Sin, 2004. **25**(8): p. 977-85.
109. Linnane, A.W., M. Kios, and L. Vitetta, *Healthy aging: regulation of the metabolome by cellular redox modulation and prooxidant signaling systems: the*

- essential roles of superoxide anion and hydrogen peroxide*. Biogerontology, 2007. **8**(5): p. 445-67.
110. Li, J.M. and A.M. Shah, *Endothelial cell superoxide generation: regulation and relevance for cardiovascular pathophysiology*. Am J Physiol Regul Integr Comp Physiol, 2004. **287**(5): p. R1014-30.
 111. Mueller, C.F., et al., *ATVB in focus: redox mechanisms in blood vessels*. Arterioscler Thromb Vasc Biol, 2005. **25**(2): p. 274-8.
 112. Lambert, A.J. and M.D. Brand, *Reactive oxygen species production by mitochondria*. Methods Mol Biol, 2009. **554**: p. 165-81.
 113. Terlecky, S.R., J.I. Koepke, and P.A. Walton, *Peroxisomes and aging*. Biochim Biophys Acta, 2006. **1763**(12): p. 1749-54.
 114. Aksam, E.B., et al., *Preserving organelle vitality: peroxisomal quality control mechanisms in yeast*. FEMS Yeast Res, 2009. **9**(6): p. 808-20.
 115. Titorenko, V.I. and S.R. Terlecky, *Peroxisome metabolism and cellular aging*. Traffic, 2011. **12**(3): p. 252-9.
 116. Zhang, D.X. and D.D. Gutterman, *Mitochondrial reactive oxygen species-mediated signaling in endothelial cells*. Am J Physiol Heart Circ Physiol, 2007. **292**(5): p. H2023-31.
 117. Harman, D., *The biologic clock: the mitochondria?* J Am Geriatr Soc, 1972. **20**(4): p. 145-7.
 118. Harman, D., *The biologic clock: the mitochondria?* J Am Geriatr Soc., 1972. **20**(4): p. 145-7.
 119. Beckman, K.B. and B.N. Ames, *The free radical theory of aging matures*. Physiol Rev, 1998. **78**(2): p. 547-81.
 120. Larsen, P.L., *Aging and resistance to oxidative damage in Caenorhabditis elegans*. Proc Natl Acad Sci U S A, 1993. **90**(19): p. 8905-9.
 121. Petriv, O.I. and R.A. Rachubinski, *Lack of peroxisomal catalase causes a progeric phenotype in Caenorhabditis elegans*. J Biol Chem, 2004. **279**(19): p. 19996-20001.
 122. Houthoofd, K., et al., *Life extension via dietary restriction is independent of the Ins/IGF-1 signalling pathway in Caenorhabditis elegans*. Exp Gerontol, 2003. **38**(9): p. 947-54.
 123. Johnson, T.E., et al., *Longevity genes in the nematode Caenorhabditis elegans also mediate increased resistance to stress and prevent disease*. J Inherit Metab Dis, 2002. **25**(3): p. 197-206.
 124. Van Raamsdonk, J.M. and S. Hekimi, *Deletion of the mitochondrial superoxide dismutase sod-2 extends lifespan in Caenorhabditis elegans*. PLoS Genet, 2009. **5**(2): p. e1000361.
 125. Doonan, R., et al., *Against the oxidative damage theory of aging: superoxide dismutases protect against oxidative stress but have little or no effect on life span in Caenorhabditis elegans*. Genes Dev, 2008. **22**(23): p. 3236-41.
 126. Parkes, T.L., et al., *Extension of Drosophila lifespan by overexpression of human SOD1 in motoneurons*. Nat Genet, 1998. **19**(2): p. 171-4.
 127. Sun, J. and J. Tower, *FLP recombinase-mediated induction of Cu/Zn-superoxide dismutase transgene expression can extend the life span of adult Drosophila melanogaster flies*. Mol Cell Biol, 1999. **19**(1): p. 216-28.
 128. Sun, J., et al., *Induced overexpression of mitochondrial Mn-superoxide dismutase extends the life span of adult Drosophila melanogaster*. Genetics, 2002. **161**(2): p. 661-72.

129. Tower, J., *Transgenic methods for increasing Drosophila life span*. Mech Ageing Dev, 2000. **118**(1-2): p. 1-14.
130. Orr, W.C. and R.S. Sohal, *Extension of life-span by overexpression of superoxide dismutase and catalase in Drosophila melanogaster*. Science, 1994. **263**(5150): p. 1128-30.
131. Sanz, A., et al., *Mitochondrial ROS production correlates with, but does not directly regulate lifespan in Drosophila*. Aging (Albany NY), 2010. **2**(4): p. 200-23.
132. Miwa, S., et al., *Lack of correlation between mitochondrial reactive oxygen species production and life span in Drosophila*. Ann N Y Acad Sci, 2004. **1019**: p. 388-91.
133. Schriner, S.E., et al., *Extension of murine life span by overexpression of catalase targeted to mitochondria*. Science, 2005. **308**(5730): p. 1909-11.
134. Perez, V.I., et al., *The overexpression of major antioxidant enzymes does not extend the lifespan of mice*. Aging Cell, 2009. **8**(1): p. 73-5.
135. Van Remmen, H., et al., *Life-long reduction in MnSOD activity results in increased DNA damage and higher incidence of cancer but does not accelerate aging*. Physiol Genomics, 2003. **16**(1): p. 29-37.
136. Andziak, B., et al., *High oxidative damage levels in the longest-living rodent, the naked mole-rat*. Aging Cell, 2006. **5**(6): p. 463-71.
137. Wawryn, J., et al., *Deficiency in superoxide dismutases shortens life span of yeast cells*. Acta Biochim Pol, 1999. **46**(2): p. 249-53.
138. Harris, N., et al., *Mnsod overexpression extends the yeast chronological (G(0)) life span but acts independently of Sir2p histone deacetylase to shorten the replicative life span of dividing cells*. Free Radic Biol Med, 2003. **34**(12): p. 1599-606.
139. Schulz, T.J., et al., *Glucose restriction extends Caenorhabditis elegans life span by inducing mitochondrial respiration and increasing oxidative stress*. Cell Metab, 2007. **6**(4): p. 280-93.
140. Groeger, G., C. Quiney, and T.G. Cotter, *Hydrogen peroxide as a cell-survival signaling molecule*. Antioxid Redox Signal, 2009. **11**(11): p. 2655-71.
141. Yokoo, S., et al., *Slow-down of age-dependent telomere shortening is executed in human skin keratinocytes by hormesis-like-effects of trace hydrogen peroxide or by anti-oxidative effects of pro-vitamin C in common concurrently with reduction of intracellular oxidative stress*. J Cell Biochem, 2004. **93**(3): p. 588-97.
142. Ksiazek, K., et al., *Mitochondrial dysfunction is a possible cause of accelerated senescence of mesothelial cells exposed to high glucose*. Biochem Biophys Res Commun, 2008. **366**(3): p. 793-9.
143. Serra, V., et al., *Extracellular superoxide dismutase is a major antioxidant in human fibroblasts and slows telomere shortening*. J Biol Chem, 2003. **278**(9): p. 6824-30.
144. Csiszar, A., et al., *Endothelial function and vascular oxidative stress in long-lived GH/IGF-deficient Ames dwarf mice*. Am J Physiol Heart Circ Physiol, 2008. **295**(5): p. H1882-94.
145. Dasgupta, J., et al., *Manganese superoxide dismutase protects from TNF-alpha-induced apoptosis by increasing the steady-state production of H2O2*. Antioxid Redox Signal, 2006. **8**(7-8): p. 1295-305.

146. Speakman, J.R., et al., *Uncoupled and surviving: individual mice with high metabolism have greater mitochondrial uncoupling and live longer*. Aging Cell, 2004. **3**(3): p. 87-95.
147. Speakman, J.R., *Body size, energy metabolism and lifespan*. J Exp Biol, 2005. **208**(Pt 9): p. 1717-30.
148. Weindruch, R., et al., *The retardation of aging in mice by dietary restriction: longevity, cancer, immunity and lifetime energy intake*. J Nutr, 1986. **116**(4): p. 641-54.
149. Kennedy, B.K., K.K. Steffen, and M. Kaeberlein, *Ruminations on dietary restriction and aging*. Cell Mol Life Sci, 2007. **64**(11): p. 1323-8.
150. Jiang, J.C., et al., *An intervention resembling caloric restriction prolongs life span and retards aging in yeast*. FASEB J, 2000. **14**(14): p. 2135-7.
151. Kaeberlein, M. and B.K. Kennedy, *Large-scale identification in yeast of conserved ageing genes*. Mech Ageing Dev, 2005. **126**(1): p. 17-21.
152. Vanfleteren, J.R. and B.P. Braeckman, *Mechanisms of life span determination in Caenorhabditis elegans*. Neurobiol Aging, 1999. **20**(5): p. 487-502.
153. Partridge, L., M.D. Piper, and W. Mair, *Dietary restriction in Drosophila*. Mech Ageing Dev, 2005. **126**(9): p. 938-50.
154. Mattson, M.P., *Energy intake, meal frequency, and health: a neurobiological perspective*. Annu Rev Nutr, 2005. **25**: p. 237-60.
155. Fontana, L. and S. Klein, *Aging, adiposity, and calorie restriction*. JAMA, 2007. **297**(9): p. 986-94.
156. Suzuki, M., B.J. Wilcox, and C.D. Wilcox, *Implications from and for food cultures for cardiovascular disease: longevity*. Asia Pac J Clin Nutr, 2001. **10**(2): p. 165-71.
157. Coschigano, K.T., et al., *Assessment of growth parameters and life span of GHR/BP gene-disrupted mice*. Endocrinology, 2000. **141**(7): p. 2608-13.
158. Holzenberger, M., et al., *IGF-1 receptor regulates lifespan and resistance to oxidative stress in mice*. Nature, 2003. **421**(6919): p. 182-7.
159. Lee, J.H., et al., *Sestrins at the crossroad between stress and aging*. Aging (Albany NY), 2010. **2**(6): p. 369-74.
160. Bartke, A., et al., *Extending the lifespan of long-lived mice*. Nature, 2001. **414**(6862): p. 412.
161. Clancy, D.J., et al., *Dietary restriction in long-lived dwarf flies*. Science, 2002. **296**(5566): p. 319.
162. Koizumi, A., R. Weindruch, and R.L. Walford, *Influences of dietary restriction and age on liver enzyme activities and lipid peroxidation in mice*. J Nutr, 1987. **117**(2): p. 361-7.
163. Sreekumar, R., et al., *Effects of caloric restriction on mitochondrial function and gene transcripts in rat muscle*. Am J Physiol Endocrinol Metab, 2002. **283**(1): p. E38-43.
164. Barros, M.H., et al., *Higher respiratory activity decreases mitochondrial reactive oxygen release and increases life span in Saccharomyces cerevisiae*. J Biol Chem, 2004. **279**(48): p. 49883-8.
165. Kharade, S.V., et al., *Mrg19 depletion increases S. cerevisiae lifespan by augmenting ROS defence*. FEBS Lett, 2005. **579**(30): p. 6809-13.
166. Agarwal, S., et al., *Caloric restriction augments ROS defense in S. cerevisiae, by a Sir2p independent mechanism*. Free Radic Res, 2005. **39**(1): p. 55-62.
167. Piper, P.W., N.L. Harris, and M. MacLean, *Preadaptation to efficient respiratory maintenance is essential both for maximal longevity and the*

- retention of replicative potential in chronologically ageing yeast.* Mech Ageing Dev, 2006. **127**(9): p. 733-40.
168. Selman, C., et al., *Life-long vitamin C supplementation in combination with cold exposure does not affect oxidative damage or lifespan in mice, but decreases expression of antioxidant protection genes.* Mech Ageing Dev, 2006. **127**(12): p. 897-904.
 169. Tapia, P.C., *Sublethal mitochondrial stress with an attendant stoichiometric augmentation of reactive oxygen species may precipitate many of the beneficial alterations in cellular physiology produced by caloric restriction, intermittent fasting, exercise and dietary phytonutrients: "Mitohormesis" for health and vitality.* Med Hypotheses, 2006. **66**(4): p. 832-43.
 170. Masoro, E.J. and S.N. Austad, *The evolution of the antiaging action of dietary restriction: a hypothesis.* J Gerontol A Biol Sci Med Sci, 1996. **51**(6): p. B387-91.
 171. Kaerberlein, M., et al., *Genes determining yeast replicative life span in a long-lived genetic background.* Mech Ageing Dev, 2005. **126**(4): p. 491-504.
 172. Lin, S.J., et al., *Calorie restriction extends Saccharomyces cerevisiae lifespan by increasing respiration.* Nature, 2002. **418**(6895): p. 344-8.
 173. Kaerberlein, M., et al., *High osmolarity extends life span in Saccharomyces cerevisiae by a mechanism related to calorie restriction.* Mol Cell Biol, 2002. **22**(22): p. 8056-66.
 174. Anderson, R.M., et al., *Yeast life-span extension by calorie restriction is independent of NAD fluctuation.* Science, 2003. **302**(5653): p. 2124-6.
 175. Lamming, D.W., et al., *HST2 mediates SIR2-independent life-span extension by calorie restriction.* Science, 2005. **309**(5742): p. 1861-4.
 176. Murakami, C.J., et al., *A method for high-throughput quantitative analysis of yeast chronological life span.* J Gerontol A Biol Sci Med Sci, 2008. **63**(2): p. 113-21.
 177. Kaerberlein, M., et al., *Increased life span due to calorie restriction in respiratory-deficient yeast.* PLoS Genet, 2005. **1**(5): p. e69.
 178. Lin, S.J. and L. Guarente, *Increased life span due to calorie restriction in respiratory-deficient yeast.* PLoS Genet, 2006. **2**(3): p. e33; author reply e34.
 179. Easlon, E., et al., *The dihydrolipoamide acetyltransferase is a novel metabolic longevity factor and is required for calorie restriction-mediated life span extension.* J Biol Chem, 2007. **282**(9): p. 6161-71.
 180. Anderson, R.M., et al., *Nicotinamide and PNC1 govern lifespan extension by calorie restriction in Saccharomyces cerevisiae.* Nature, 2003. **423**(6936): p. 181-5.
 181. Kaerberlein, M., et al., *Saccharomyces cerevisiae SSD1-V confers longevity by a Sir2p-independent mechanism.* Genetics, 2004. **166**(4): p. 1661-72.
 182. Lin, S.J., et al., *Calorie restriction extends yeast life span by lowering the level of NADH.* Genes Dev, 2004. **18**(1): p. 12-6.
 183. Koc, A., et al., *Methionine sulfoxide reductase regulation of yeast lifespan reveals reactive oxygen species-dependent and -independent components of aging.* Proc Natl Acad Sci U S A, 2004. **101**(21): p. 7999-8004.
 184. Aguilaniu, H., et al., *Asymmetric inheritance of oxidatively damaged proteins during cytokinesis.* Science, 2003. **299**(5613): p. 1751-3.
 185. Aguilaniu, H., et al., *Protein oxidation in G0 cells of Saccharomyces cerevisiae depends on the state rather than rate of respiration and is enhanced in pos9 but not yap1 mutants.* J Biol Chem, 2001. **276**(38): p. 35396-404.

186. Jakubowski, W., T. Bilinski, and G. Bartosz, *Oxidative stress during aging of stationary cultures of the yeast Saccharomyces cerevisiae*. Free Radic Biol Med, 2000. **28**(5): p. 659-64.
187. Longo, V.D., et al., *Mitochondrial superoxide decreases yeast survival in stationary phase*. Arch Biochem Biophys, 1999. **365**(1): p. 131-42.
188. Jazwinski, S.M., *The retrograde response links metabolism with stress responses, chromatin-dependent gene activation, and genome stability in yeast aging*. Gene, 2005. **354**: p. 22-7.
189. Powers, T., et al., *Yeast TOR signaling: a mechanism for metabolic regulation*. Curr Top Microbiol Immunol, 2004. **279**: p. 39-51.
190. Hardwick, J.S., et al., *Rapamycin-modulated transcription defines the subset of nutrient-sensitive signaling pathways directly controlled by the Tor proteins*. Proc Natl Acad Sci U S A, 1999. **96**(26): p. 14866-70.
191. Shamji, A.F., F.G. Kuruvilla, and S.L. Schreiber, *Partitioning the transcriptional program induced by rapamycin among the effectors of the Tor proteins*. Curr Biol, 2000. **10**(24): p. 1574-81.
192. Finley, L.W. and M.C. Haigis, *The coordination of nuclear and mitochondrial communication during aging and calorie restriction*. Ageing Res Rev, 2009. **8**(3): p. 173-88.
193. Beck, T. and M.N. Hall, *The TOR signalling pathway controls nuclear localization of nutrient-regulated transcription factors*. Nature, 1999. **402**(6762): p. 689-92.
194. Ingram, D.K., et al., *Calorie restriction mimetics: an emerging research field*. Aging Cell, 2006. **5**(2): p. 97-108.
195. Ingram, D.K. and G.S. Roth, *Glycolytic inhibition as a strategy for developing calorie restriction mimetics*. Exp Gerontol, 2011. **46**(2-3): p. 148-54.
196. Ahuatz, D., et al., *The glucose-regulated nuclear localization of hexokinase 2 in Saccharomyces cerevisiae is Mig1-dependent*. J Biol Chem, 2004. **279**(14): p. 14440-6.
197. Guo, Z., et al., *Iodoacetate protects hippocampal neurons against excitotoxic and oxidative injury: involvement of heat-shock proteins and Bcl-2*. J Neurochem, 2001. **79**(2): p. 361-70.
198. Sablina, A.A., et al., *The antioxidant function of the p53 tumor suppressor*. Nat Med, 2005. **11**(12): p. 1306-13.
199. Elbing, K., et al., *Role of hexose transport in control of glycolytic flux in Saccharomyces cerevisiae*. Appl Environ Microbiol, 2004. **70**(9): p. 5323-30.
200. Chang, J.Y. and W.A. Schroeder, *Reaction of 3-amino-1:2:4-triazole with bovine liver catalase and human erythrocyte catalase*. Arch Biochem Biophys, 1972. **148**(2): p. 505-8.
201. Margoliash, E., A. Novogrodsky, and A. Schejter, *Irreversible reaction of 3-amino-1:2:4-triazole and related inhibitors with the protein of catalase*. Biochem J, 1960. **74**: p. 339-48.
202. Griffith, O.W. and A. Meister, *Potent and specific inhibition of glutathione synthesis by buthionine sulfoximine (S-n-butyl homocysteine sulfoximine)*. J Biol Chem, 1979. **254**(16): p. 7558-60.
203. Elskens, M.T., C.J. Jaspers, and M.J. Penninckx, *Glutathione as an endogenous sulphur source in the yeast Saccharomyces cerevisiae*. J Gen Microbiol, 1991. **137**(3): p. 637-44.
204. Madeo, F., et al., *Oxygen stress: a regulator of apoptosis in yeast*. J Cell Biol, 1999. **145**(4): p. 757-67.

205. Qin, Y., M. Lu, and X. Gong, *Dihydrorhodamine 123 is superior to 2,7-dichlorodihydrofluorescein diacetate and dihydrorhodamine 6G in detecting intracellular hydrogen peroxide in tumor cells*. Cell Biol Int, 2008. **32**(2): p. 224-8.
206. Conyers, S.M. and D.A. Kidwell, *Chromogenic substrates for horseradish peroxidase*. Anal Biochem, 1991. **192**(1): p. 207-11.
207. Flohe, L. and F. Otting, *Superoxide dismutase assays*. Methods Enzymol, 1984. **105**: p. 93-104.
208. Levine, R.L., et al., *Carbonyl assays for determination of oxidatively modified proteins*. Methods Enzymol, 1994. **233**: p. 346-57.
209. Merry, B.J., *Oxidative stress and mitochondrial function with aging--the effects of calorie restriction*. Aging Cell, 2004. **3**(1): p. 7-12.
210. Sohal, R.S., *Oxidative stress hypothesis of aging*. Free Radic Biol Med, 2002. **33**(5): p. 573-4.
211. Barja, G., *Endogenous oxidative stress: relationship to aging, longevity and caloric restriction*. Ageing Res Rev, 2002. **1**(3): p. 397-411.
212. Reverter-Branchat, G., et al., *Oxidative damage to specific proteins in replicative and chronological-aged Saccharomyces cerevisiae: common targets and prevention by calorie restriction*. J Biol Chem, 2004. **279**(30): p. 31983-9.
213. Fabrizio, P., et al., *Superoxide is a mediator of an altruistic aging program in Saccharomyces cerevisiae*. J Cell Biol, 2004. **166**(7): p. 1055-67.
214. Crow, J.P., *Dichlorodihydrofluorescein and dihydrorhodamine 123 are sensitive indicators of peroxynitrite in vitro: implications for intracellular measurement of reactive nitrogen and oxygen species*. Nitric Oxide, 1997. **1**(2): p. 145-57.
215. Glebska, J. and W.H. Koppenol, *Peroxynitrite-mediated oxidation of dichlorodihydrofluorescein and dihydrorhodamine*. Free Radic Biol Med, 2003. **35**(6): p. 676-82.
216. Kooy, N.W., J.A. Royall, and H. Ischiropoulos, *Oxidation of 2',7'-dichlorofluorescein by peroxynitrite*. Free Radic Res, 1997. **27**(3): p. 245-54.
217. Cathcart, R., E. Schwieters, and B.N. Ames, *Detection of picomole levels of hydroperoxides using a fluorescent dichlorofluorescein assay*. Anal Biochem, 1983. **134**(1): p. 111-6.
218. Henderson, L.M. and J.B. Chappell, *Dihydrorhodamine 123: a fluorescent probe for superoxide generation?* Eur J Biochem, 1993. **217**(3): p. 973-80.
219. Schell-Steven, A., et al., *Identification of a novel, intraperoxisomal pex14-binding site in pex13: association of pex13 with the docking complex is essential for peroxisomal matrix protein import*. Mol Cell Biol, 2005. **25**(8): p. 3007-18.
220. Aksam, E.B., et al., *A peroxisomal lon protease and peroxisome degradation by autophagy play key roles in vitality of Hansenula polymorpha cells*. Autophagy, 2007. **3**(2): p. 96-105.
221. Farre, J.C., et al., *PpAtg30 tags peroxisomes for turnover by selective autophagy*. Dev Cell, 2008. **14**(3): p. 365-76.
222. Petrova, V.Y., et al., *Dual targeting of yeast catalase A to peroxisomes and mitochondria*. Biochem J, 2004. **380**(Pt 2): p. 393-400.
223. Legakis, J.E., et al., *Peroxisome senescence in human fibroblasts*. Mol Biol Cell, 2002. **13**(12): p. 4243-55.
224. Izawa, S., Y. Inoue, and A. Kimura, *Importance of catalase in the adaptive response to hydrogen peroxide: analysis of acatalasaemic Saccharomyces cerevisiae*. Biochem J, 1996. **320** (Pt 1): p. 61-7.

225. Lushchak, V.I. and D.V. Gospodaryov, *Catalases protect cellular proteins from oxidative modification in Saccharomyces cerevisiae*. Cell Biol Int, 2005. **29**(3): p. 187-92.
226. Ishii, K., et al., *Prevention of mammary tumorigenesis in acatalasemic mice by vitamin E supplementation*. Jpn J Cancer Res, 1996. **87**(7): p. 680-4.
227. Rao, G., et al., *Effect of dietary restriction on the age-dependent changes in the expression of antioxidant enzymes in rat liver*. J Nutr, 1990. **120**(6): p. 602-9.
228. Benov, L. and I. Fridovich, *Superoxide dependence of the toxicity of short chain sugars*. J Biol Chem, 1998. **273**(40): p. 25741-4.
229. Ludovico, P., et al., *Cytochrome c release and mitochondria involvement in programmed cell death induced by acetic acid in Saccharomyces cerevisiae*. Mol Biol Cell, 2002. **13**(8): p. 2598-606.
230. Magherini, F., et al., *Different carbon sources affect lifespan and protein redox state during Saccharomyces cerevisiae chronological ageing*. Cell Mol Life Sci, 2009. **66**(5): p. 933-47.
231. Takeda, K., et al., *Synergistic roles of the proteasome and autophagy for mitochondrial maintenance and chronological lifespan in fission yeast*. Proc Natl Acad Sci U S A, 2010. **107**(8): p. 3540-5.
232. Harris, N., et al., *Overexpressed Sod1p acts either to reduce or to increase the lifespans and stress resistance of yeast, depending on whether it is Cu(2+)-deficient or an active Cu,Zn-superoxide dismutase*. Aging Cell, 2005. **4**(1): p. 41-52.
233. Godon, C., et al., *The H2O2 stimulon in Saccharomyces cerevisiae*. J Biol Chem, 1998. **273**(35): p. 22480-9.
234. Gasch, A.P., et al., *Genomic expression programs in the response of yeast cells to environmental changes*. Mol Biol Cell, 2000. **11**(12): p. 4241-57.
235. Yoshioka, T., et al., *Induction of manganese superoxide dismutase by glucocorticoids in glomerular cells*. Kidney Int, 1994. **45**(1): p. 211-9.
236. Rohrdanz, E., et al., *The influence of oxidative stress on catalase and MnSOD gene transcription in astrocytes*. Brain Res, 2001. **900**(1): p. 128-36.
237. Sarsour, E.H., et al., *Manganese superoxide dismutase activity regulates transitions between quiescent and proliferative growth*. Aging Cell, 2008. **7**(3): p. 405-17.
238. Zmijewski, J.W., et al., *Antiinflammatory effects of hydrogen peroxide in neutrophil activation and acute lung injury*. Am J Respir Crit Care Med, 2009. **179**(8): p. 694-704.
239. Mitra, S. and E. Abraham, *Participation of superoxide in neutrophil activation and cytokine production*. Biochim Biophys Acta, 2006. **1762**(8): p. 732-41.
240. Fabrizio, P. and V.D. Longo, *The chronological life span of Saccharomyces cerevisiae*. Methods Mol Biol, 2007. **371**: p. 89-95.
241. Rockenfeller, P. and F. Madeo, *Apoptotic death of ageing yeast*. Exp Gerontol, 2008. **43**(10): p. 876-81.
242. Delori, F.C. and C.K. Dorey, *In Vivo Technique for Autofluorescent Lipopigments*. 1998. p. 229-243.
243. Terman, A., et al., *Ageing of cardiac myocytes in culture: oxidative stress, lipofuscin accumulation, and mitochondrial turnover*. Ann N Y Acad Sci, 2004. **1019**: p. 70-7.
244. Rattan, S.I., *Hormesis in aging*. Ageing Res Rev, 2008. **7**(1): p. 63-78.
245. Nisoli, E., et al., *Calorie restriction promotes mitochondrial biogenesis by inducing the expression of eNOS*. Science, 2005. **310**(5746): p. 314-7.

246. Mannarino, S.C., et al., *Requirement of glutathione for Sod1 activation during lifespan extension*. Yeast, 2011. **28**(1): p. 19-25.
247. Ristow, M., et al., *Antioxidants prevent health-promoting effects of physical exercise in humans*. Proc Natl Acad Sci U S A, 2009. **106**(21): p. 8665-70.
248. Mattison, J.A., et al., *Calorie restriction in rhesus monkeys*. Exp Gerontol, 2003. **38**(1-2): p. 35-46.
249. Fabrizio, P., L. Li, and V.D. Longo, *Analysis of gene expression profile in yeast aging chronologically*. Mech Ageing Dev, 2005. **126**(1): p. 11-6.
250. Kim, J.H. and M. Johnston, *Two glucose-sensing pathways converge on Rgt1 to regulate expression of glucose transporter genes in Saccharomyces cerevisiae*. J Biol Chem, 2006. **281**(36): p. 26144-9.
251. Rempel, A., et al., *Glucose catabolism in cancer cells: amplification of the gene encoding type II hexokinase*. Cancer Res, 1996. **56**(11): p. 2468-71.
252. Longo, V.D., *The Ras and Sch9 pathways regulate stress resistance and longevity*. Exp Gerontol, 2003. **38**(7): p. 807-11.
253. Pani, G., *P66SHC and ageing: ROS and TOR?* Aging (Albany NY), 2010. **2**(8): p. 514-8.
254. Almeida, B., et al., *Yeast protein expression profile during acetic acid-induced apoptosis indicates causal involvement of the TOR pathway*. Proteomics, 2009. **9**(3): p. 720-32.
255. Weinberger, M., et al., *Growth signaling promotes chronological aging in budding yeast by inducing superoxide anions that inhibit quiescence*. Aging (Albany NY), 2010. **2**(10): p. 709-26.
256. Lavoie, H. and M. Whiteway, *Increased respiration in the sch9Delta mutant is required for increasing chronological life span but not replicative life span*. Eukaryot Cell, 2008. **7**(7): p. 1127-35.
257. Bjelakovic, G., et al., *Mortality in randomized trials of antioxidant supplements for primary and secondary prevention: systematic review and meta-analysis*. JAMA, 2007. **297**(8): p. 842-57.
258. Sohal, R.S. and R. Weindruch, *Oxidative stress, caloric restriction, and aging*. Science, 1996. **273**(5271): p. 59-63.
259. Barja, G., *Aging in vertebrates, and the effect of caloric restriction: a mitochondrial free radical production-DNA damage mechanism?* Biol Rev Camb Philos Soc, 2004. **79**(2): p. 235-51.
260. Vanfleteren, J.R., *Oxidative stress and ageing in Caenorhabditis elegans*. Biochem J, 1993. **292** (Pt 2): p. 605-8.
261. Houthoofd, K., et al., *No reduction of metabolic rate in food restricted Caenorhabditis elegans*. Exp Gerontol, 2002. **37**(12): p. 1359-69.
262. Sinclair, D.A., *Toward a unified theory of caloric restriction and longevity regulation*. Mech Ageing Dev, 2005. **126**(9): p. 987-1002.
263. Zarse, K., et al., *Impaired respiration is positively correlated with decreased life span in Caenorhabditis elegans models of Friedreich Ataxia*. FASEB J, 2007. **21**(4): p. 1271-5.
264. Phillips, J.P., et al., *Null mutation of copper/zinc superoxide dismutase in Drosophila confers hypersensitivity to paraquat and reduced longevity*. Proc Natl Acad Sci U S A, 1989. **86**(8): p. 2761-5.
265. Elchuri, S., et al., *CuZnSOD deficiency leads to persistent and widespread oxidative damage and hepatocarcinogenesis later in life*. Oncogene, 2005. **24**(3): p. 367-80.

- 266. Linnane, A.W., M. Kios, and L. Vitetta, *The essential requirement for superoxide radical and nitric oxide formation for normal physiological function and healthy aging*. Mitochondrion, 2007. **7**(1-2): p. 1-5.
- 267. Adler, V., et al., *Role of redox potential and reactive oxygen species in stress signaling*. Oncogene, 1999. **18**(45): p. 6104-11.
- 268. Cai, H., et al., *Akt-dependent phosphorylation of serine 1179 and mitogen-activated protein kinase kinase/extracellular signal-regulated kinase 1/2 cooperatively mediate activation of the endothelial nitric-oxide synthase by hydrogen peroxide*. Mol Pharmacol, 2003. **63**(2): p. 325-31.
- 269. Chen, K., et al., *c-Jun N-terminal kinase activation by hydrogen peroxide in endothelial cells involves SRC-dependent epidermal growth factor receptor transactivation*. J Biol Chem, 2001. **276**(19): p. 16045-50.
- 270. Cai, H. and D.G. Harrison, *Endothelial dysfunction in cardiovascular diseases: the role of oxidant stress*. Circ Res, 2000. **87**(10): p. 840-4.
- 271. Zuin, A., et al., *Lifespan extension by calorie restriction relies on the Sty1 MAP kinase stress pathway*. EMBO J, 2010. **29**(5): p. 981-91.
- 272. Yoshioka, T., et al., *Oxidants induce transcriptional activation of manganese superoxide dismutase in glomerular cells*. Kidney Int, 1994. **46**(2): p. 405-13.

ATTACHMENTS

ATTACHMENT I

Mesquita A., Weinberger M., Silva A., Sampaio-Marques B., Almeida B., Leão C., Costa V., Rodrigues F., Burhans W.C., Ludovico P.. Caloric restriction or catalase inactivation extends yeast chronological lifespan by inducing H₂O₂ and superoxide dismutase activity. Proc Natl Acad Sci US A. 2010 Aug 24;107(34):15123-8.

Caloric restriction or catalase inactivation extends yeast chronological lifespan by inducing H₂O₂ and superoxide dismutase activity

Ana Mesquita^a, Martin Weinberger^b, Alexandra Silva^a, Belém Sampaio-Marques^a, Bruno Almeida^a, Cecília Leão^a, Vítor Costa^{c,d}, Fernando Rodrigues^a, William C. Burkans^{b,1}, and Paula Ludovico^{a,1}

^aInstituto de Investigação em Ciências da Vida e Saúde (ICVS), Escola de Ciências da Saúde, Universidade do Minho, Campus de Gualtar, 4710-057 Braga, Portugal; ^bDepartment of Molecular and Cellular Biology, Roswell Park Cancer Institute, Buffalo, NY 14263; ^cInstituto de Biologia Molecular e Celular (IBMC), Universidade do Porto, 4150-180 Porto, Portugal; and ^dInstituto de Ciências Biomédicas Abel Salazar (ICBAS), Departamento de Biologia Molecular, Universidade do Porto, 4099-003 Porto, Portugal

Edited* by Fred Sherman, University of Rochester School of Medicine and Dentistry, Rochester, NY, and approved July 23, 2010 (received for review April 1, 2010)

The free radical theory of aging posits oxidative damage to macromolecules as a primary determinant of lifespan. Recent studies challenge this theory by demonstrating that in some cases, longevity is enhanced by inactivation of oxidative stress defenses or is correlated with increased, rather than decreased reactive oxygen species and oxidative damage. Here we show that, in *Saccharomyces cerevisiae*, caloric restriction or inactivation of catalases extends chronological lifespan by inducing elevated levels of the reactive oxygen species hydrogen peroxide, which activate superoxide dismutases that inhibit the accumulation of superoxide anions. Increased hydrogen peroxide in catalase-deficient cells extends chronological lifespan despite parallel increases in oxidative damage. These findings establish a role for hormesis effects of hydrogen peroxide in promoting longevity that have broad implications for understanding aging and age-related diseases.

aging | hydrogen peroxide | hormesis | antioxidant enzymes | oxidative damage

The longstanding free radical theory has guided investigations into the causes and consequences of aging for more than 50 y (1). However, the results of a number of recent studies have failed to provide support for the free radical theory or suggest that this theory is at best incomplete (2). Studies of naked mole rats, for example, demonstrated that this extremely long-lived rodent exhibits high levels of oxidative damage compared with mice or rats, whose lifespans are $\approx 1/10$ that of naked mole rats (3). In addition, caloric restriction (CR), which extends the lifespans of a variety of eukaryotic organisms, promotes longevity in *Caenorhabditis elegans* by a mechanism that involves increased oxidative stress (4). In fact, in contrast to the destructive effects of reactive oxygen species (ROS), recent evidence indicates that in mammals, hydrogen peroxide (H₂O₂) and other forms of ROS function as essential secondary messengers in the regulation of a variety of physiological processes (reviewed in ref. 5). For example, H₂O₂ activates pro-survival signaling pathways mediated by p53, NF- κ B, AP-1, and other molecules (6). Furthermore, increases in the intracellular steady-state production of H₂O₂ by *SOD2* overexpression can block the activation of cellular processes required for programmed cell death (7). However, a causal relationship between CR and effects on oxidative stress has been difficult to establish.

To better understand how CR impacts oxidative stress and longevity in the model organism *Saccharomyces cerevisiae*, in this study we examined intracellular levels of H₂O₂ and superoxide anions (O₂⁻), which are two forms of ROS implicated in aging in all eukaryotes, under CR and other conditions. Our findings indicate that CR or inactivation of catalases extends chronological lifespan (CLS) by inducing elevated levels of H₂O₂, which activate superoxide dismutases that inhibit the accumulation of O₂⁻. These findings establish a role for hormesis effects of H₂O₂ in promoting

longevity induced by CR conditions that are likely to be conserved in complex eukaryotes. In catalase-deficient cells, increased H₂O₂ extends CLS despite parallel increases in oxidative damage. This violates a fundamental tenet of the free radical theory that posits oxidative damage as a primary determinant of aging.

Results

Caloric Restriction or Inactivation of Catalases Extends *S. cerevisiae* Chronological Lifespan by Increasing Intracellular Levels of H₂O₂. CLS of budding yeast is determined by measuring the survival of non-dividing stationary phase cells, which is impacted by conserved factors that affect aging of postmitotic cells of complex eukaryotes, including humans (8). As reported previously (9), CR by decreasing the concentration of glucose extended CLS of budding yeast (Fig. 1A). Surprisingly, however, the CLS-extending effects of CR were accompanied by an increase in the fraction of cells containing high levels of intracellular ROS, detected by staining cells with dihydrorhodamine 123 (DHR) (Fig. 1B and Fig. S1). CR-induced increases in ROS were also detected by staining cells with 2',7'-dichlorodihydrofluorescein diacetate (H₂DCF-DA) (Fig. S2). CR also induced the activity of the peroxisomal catalase Cta1p, as well as the cytosolic catalase Ctt1p (Fig. S3), which are the two main H₂O₂ scavenging enzymes in this organism. However, increased catalase activity did not contribute to the CLS-extending effects of CR, because CLS was also extended by mutational inactivation of *CTA1* and the longer CLS of Δ *cta1* cells was extended further by CR (Fig. 1C). Similar results were obtained upon mutational inactivation of *CTT1* or pharmacological inhibition of the synthesis of glutathione, which scavenges H₂O₂ (Fig. S4). These findings identify H₂O₂ as a form of intracellular ROS induced by CR in stationary phase budding yeast cells and establish that catalase activity or glutathione synthesis inhibits longevity in the chronological aging model.

The longer CLS of Δ *cta1* cells was accompanied by an increased fraction of cells containing high levels of intracellular H₂O₂ under non-CR conditions (Fig. 1C and D). Under CR conditions, the fraction of Δ *cta1* cells exhibiting high intracellular levels of H₂O₂ was similar to CR wild-type cells or non-CR Δ *cta1* cells at day 6 and lower at day 12 (Fig. 1D). Increased levels of H₂O₂ were also detected in Δ *ctt1* and in Δ *cta1 Δ *ctt1* compared with wild-type cells*

Author contributions: V.C., W.C.B., and P.L. designed research; A.M., M.W., A.S., B.S.-M., W.C.B., and P.L. performed research; M.W., B.S.-M., B.A., C.L., V.C., F.R., W.C.B., and P.L. analyzed data; and F.R., W.C.B., and P.L. wrote the paper.

The authors declare no conflict of interest.

*This Direct Submission article had a prearranged editor.

¹To whom correspondence may be addressed. E-mail: wburkans@buffalo.edu or pludovico@icsaude.uminho.pt

This article contains supporting information online at www.pnas.org/lookup/suppl/doi:10.1073/pnas.1004432107/-DCSupplemental.

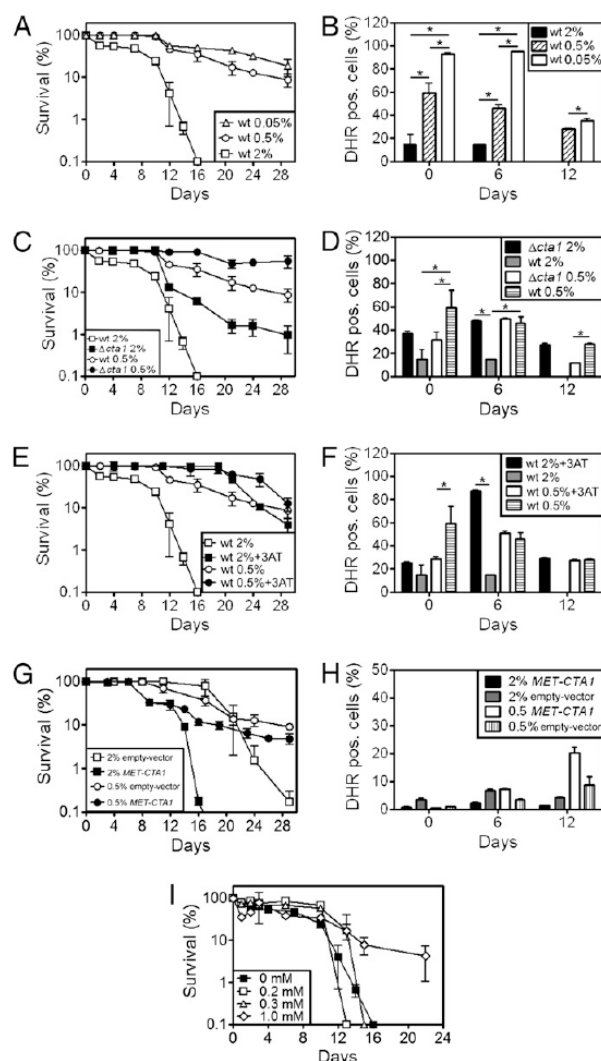


Fig. 1. Caloric restriction (CR) or inactivation of catalases extends *Saccharomyces cerevisiae* chronological lifespan by increasing intracellular levels of H_2O_2 . Survival of (A) wild-type (BY4742) cells, (C) $\Delta cta1$ cells, (E) wild-type cells in the absence or presence of the catalase inhibitor 10 mM 3-amino-1,2,4-triazole (3AT), and (G) wild-type cells transformed with an empty vector or a plasmid that overexpresses *CTA1* ("MET-CTA1"). (I) Effects of ectopic exposure of wild-type cells to indicated concentrations of H_2O_2 . Cell viability was measured at 2- to 3-d intervals beginning the day cultures achieved stationary phase (day 0) and is expressed as % survival compared with survival at day 0 (100%). Percentage of cells exhibiting high levels of intracellular ROS detected by FACS measurements of fluorescence of the probe dihydrorhodamine 123 (DHR) in (B) wild-type cells, (D) $\Delta cta1$ cells, (F) wild-type cells in the absence or presence of 3AT, and (H) wild-type cells transformed with an empty vector or a plasmid that overexpresses *CTA1* ("MET-CTA1"). Three to five biological replicates of each experiment were performed. Survival and DHR positive cell values are mean \pm SD or mean \pm SEM, respectively, in all experiments. Statistical significance ($*P < 0.05$) was determined by Student's *t*-test.

(Fig. S5). Pharmacological inactivation of catalases by 3-amino-1,2,4-triazole (3AT) also extended CLS, and CR extended the CLS of 3AT-treated cells even further (Fig. 1E). Treatment with 3AT also increased the fraction of cells containing high levels of intracellular H_2O_2 (Fig. 1F). However, CR did not increase the

fraction of 3AT-treated cells containing high intracellular levels of H_2O_2 further (Fig. 1F). Overexpression of *CTA1* had effects opposite to those associated with inactivation of catalases—it decreased CLS in non-CR and CR cells (Fig. 1G) and reduced the fraction of cells containing high levels of intracellular H_2O_2 (Fig. 1H). However, the fraction of cells containing high intracellular levels of H_2O_2 was also reduced (albeit to a lesser extent) in cells harboring an empty vector. This may reflect effects of the different medium required to maintain plasmids in these but not other experiments.

These observations suggest that H_2O_2 promotes longevity in the budding yeast CLS model. To address this possibility directly, we asked whether ectopic application of H_2O_2 over a range of concentrations from 0 to 1 mM would extend CLS of non-CR wild-type cells. The lowest H_2O_2 concentrations tested did not alter CLS compared with cells that were not exposed to H_2O_2 (Fig. 1I). In contrast, exposure to 1 mM H_2O_2 resulted in a significant increase in longevity (Fig. 1I). Overall these results indicate that H_2O_2 extends CLS of budding yeast and is an important component of the CLS-extending effects of CR.

CR is known to extend CLS by inhibiting the accumulation of acetic acid in culture medium (10). As reported earlier, buffering medium to eliminate acetic acid also extends CLS (10, 11). However, CR increased intracellular H_2O_2 in experiments performed in buffered medium (Fig. S6). This suggests that some of the CLS-extending effects of CR occur independently of reduced levels of acetic acid in medium. Furthermore, the CLS-extending effects of increased H_2O_2 detected in catalase mutants occurred in the absence of a change in medium pH compared with cultures of wild-type cells (Table S1). This establishes that the effects of increased H_2O_2 on CLS can occur independently of changes in levels of acetic acid in culture medium.

Elevated H_2O_2 Levels Induced by CR or Inactivation of Catalases Are Accompanied by a Reduction in Levels of Superoxide Anions. To determine whether CR or other experimental manipulations also increase levels of superoxide anions, we measured O_2^- levels in stationary phase cells using dihydroethidium (DHE), which can detect O_2^- (12). In non-CR conditions, O_2^- levels increased in wild-type cells from day 0 to day 3 of stationary phase, whereas H_2O_2 levels remained unchanged (Fig. 2A). However, CR caused a significant reduction in O_2^- levels compared with levels in non-CR cells, despite a pronounced increase in H_2O_2 in the same cells (Fig. 2A). Similar to the effects of CR in wild-type cells, O_2^- levels were decreased and H_2O_2 levels were increased in $\Delta cta1$ compared with wild-type cells at day 0 and day 3 of stationary phase (Fig. 2A). O_2^- levels in stationary phase $\Delta cta1$ cells were also reduced by CR conditions, comparable to the effects of CR on stationary phase wild-type cells (Fig. 2A). The reduction in O_2^- levels in CR $\Delta cta1$ cells was accompanied by an increase in H_2O_2 at day 0 (Fig. 2A). Treatment of wild-type cells with 3AT or inactivation of both catalases ($\Delta cta1ctt1$ cells) also reduced O_2^- levels at the same time that it increased intracellular H_2O_2 in the same cells (Fig. 2B and Fig. S5B). These findings suggest that the longevity-promoting effects of intracellular H_2O_2 in CR conditions or when catalases are inactivated are related to inhibition of the accumulation of O_2^- . Although buffering medium to eliminate the effects of acetic acid also inhibits the accumulation of O_2^- in wild-type cells in stationary phase (11), CR reduced levels of O_2^- in buffered medium (Fig. S6). Therefore, CR inhibition of O_2^- accumulation is mediated by both acetic acid-dependent and -independent mechanisms.

Induction of Superoxide Dismutase Activity by Intracellular H_2O_2 . Ectopic application of sublethal concentrations of H_2O_2 in budding yeast induces the transcription of genes encoding both the cytosolic Cu/Zn-dependent and the mitochondrial Mn-dependent superoxide dismutases *SOD1* and *SOD2* (13, 14) as well as an increase in levels of the corresponding proteins (13). Ectopic H_2O_2

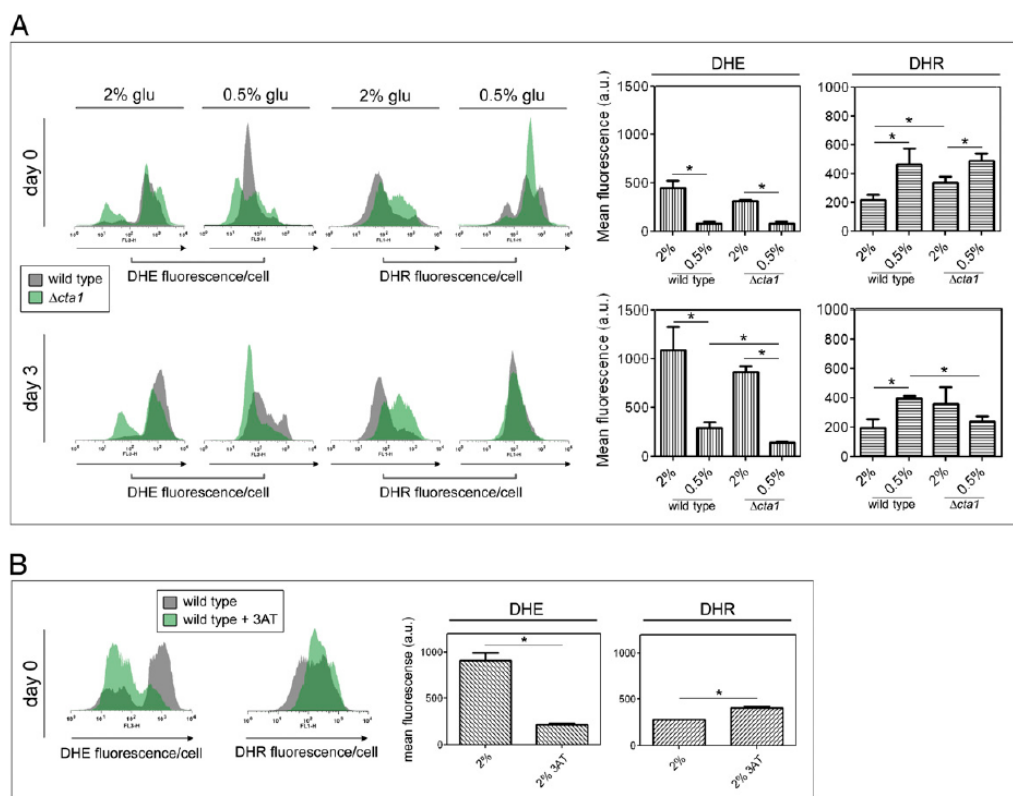


Fig. 2. The longevity-promoting effects of high intracellular H_2O_2 levels induced by CR or inactivation of catalases are accompanied by a reduction in the chronological age-dependent accumulation of superoxide anions. (A) FACS measurements of superoxide anions using the probe dihydroethidium (DHE) in parallel with measurements of H_2O_2 using dihydrorhodamine 123 (DHR) in wild-type (gray histograms) and Δcta1 (green histograms) cells at day 0 and day 3 of stationary phase. Bar graphs indicate mean \pm SD fluorescence/cell (arbitrary units) measured in 25,000 cells/sample in three independent experiments. (B) FACS measurements of superoxide anions (DHE) and H_2O_2 (DHR) in wild-type cells in the absence (gray histograms) or presence (green histograms) of 10 mM 3-amino-1,2,4-triazole (3AT) at day 0 of stationary phase. Bar graphs indicate mean \pm SD fluorescence/cell (arbitrary units) as described above. Statistical significance (* $P < 0.05$) was determined by Student's *t*-test.

also induces transcription of the superoxide dismutase *sodA* in *Escherichia coli* (15) and the transcription and activity of MnSOD, but not Cu/Zn-SOD in rat cells (16). To determine whether induction of Sod1p and/or Sod2p activity underlies the reduction in O_2^- levels that accompanies increases in intracellular H_2O_2 , we measured the activities of Sod1p and Sod2p under CR and non-CR conditions in wild-type and ΔCTA1 mutant cells. CR or ΔCTA1 deletion resulted in minor increases in Sod1p activity at day 0 that were not detected at day 3 of stationary phase (Fig. 3A and B). However, at day 6 both CR and deletion of CTA1 increased the activity of Sod1p (Fig. 3A and B). CR or deletion of CTA1 increased the activity of Sod2p at day 0 compared with wild-type cells in non-CR conditions (Fig. 3A and B). Larger increases in Sod2p activity were induced by CR conditions in wild-type cells at day 3 and day 6 (Fig. 3A and B). Deletion of CTA1 also induced large increases in Sod2p activity at day 3 and day 6 under non-CR conditions and under CR conditions at day 3 (Fig. 3A and B). Similar observations were made in Δctl1 cells at these same time points (Fig. S7). Exposure of wild-type cells to 1 mM H_2O_2 also resulted in an increase in Sod2p but not Sod1p activity (Fig. 3C). These findings indicate that intracellular H_2O_2 induced by CR or by inactivation of catalase activity or ectopic exposure to H_2O_2 induces superoxide dismutase activity in budding yeast, especially Sod2p activity. The more robust induction of Sod2p activity in these experiments is consistent with earlier reports that ectopic

exposure to H_2O_2 induces higher levels of Sod2p compared with Sod1p (13, 16, 17).

Effects of Increased H_2O_2 Induced by Caloric Restriction or by Inactivation of CTA1 on Oxidative Damage to Macromolecules. According to the free radical theory, oxidative damage to macromolecules is a primary factor in aging. Our observations show that under different experimental conditions, H_2O_2 levels are increased, whereas O_2^- levels are decreased in the same cells (Fig. 2). To determine the overall impact these divergent changes in different types of ROS have on oxidative damage, we examined levels of protein carbonylation, which is a form of oxidative damage, under different experimental conditions. Protein carbonylation was increased in Δcta1 cells compared with wild-type cells at day 0 of stationary phase (Fig. 4A). A similar increase in protein carbonylation was observed in stationary phase Δctl1 cells at this time point (Fig. S8). CR conditions also increased protein carbonylation in wild-type cells at day 0. Nevertheless, CR conditions decreased protein carbonylation in wild-type and Δcta1 cells at day 6 (Fig. 4A).

We also measured changes in cellular autofluorescence, which is produced by global oxidative damage to proteins and lipids (18, 19). Similar to the increased protein carbonylation detected in Δcta1 compared with wild-type cells, autofluorescence of Δcta1 cells was increased at day 0 and day 3 (Fig. 4). Comparable results were obtained in Δctl1 cells (Fig. S8). In contrast, CR conditions

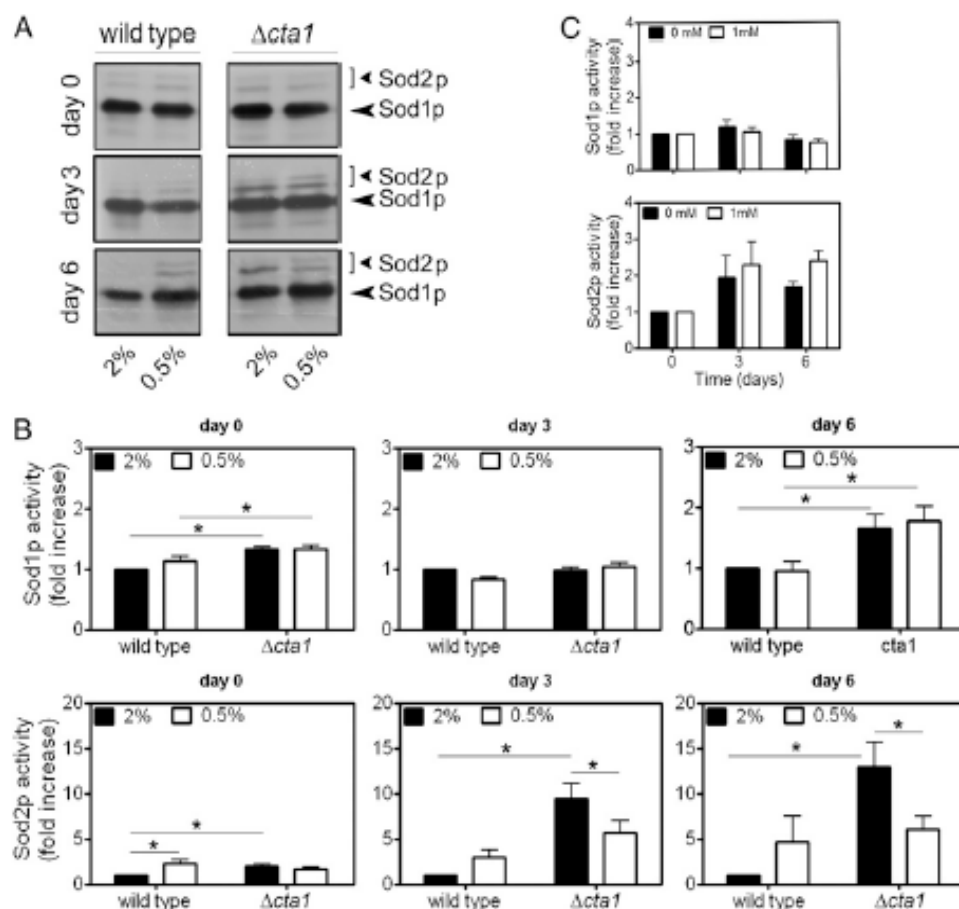


Fig. 3. Induction of superoxide dismutase activity by intracellular H_2O_2 . (A) In situ determination of superoxide dismutase activity in stationary phase wild-type and $\Delta cta1$ cells measured as previously described. MnSOD (Sod2p) activity was assessed in the presence of 2 mM potassium cyanide, which inhibits Sod1p, but not Sod2p activity (Fig. S7B). (B) Quantification of fold increases in Sod1p and Sod2p activity under indicated conditions in wild-type and $\Delta cta1$ cells. Sod1p and Sod2p activity at each time point was normalized to activity in wild-type cells under non-CR conditions (2% glucose). (C) Quantification of fold increases in Sod1p and Sod2p activity in wild-type cells after ectopic exposure to 1 mM H_2O_2 . Sod1p and Sod2p activity at each time point was normalized to activity in wild-type cells under non-CR conditions (2% glucose). Values indicate mean \pm SEM from three independent experiments. Statistical significance (* P < 0.05) was determined by Student's t -test.

led to a reduction in autofluorescence of wild-type cells at these time points, similar to the effects of CR on protein carbonylation in wild-type cells at day 6 (Fig. 4). CR conditions also reduced the autofluorescence of $\Delta cta1$ (Fig. 4B) and $\Delta ctt1$ cells (Fig. S8). Together, these findings establish that CR extends CLS in parallel with a reduction in oxidative damage to macromolecules in stationary phase budding yeast cells despite the induction of higher levels of H_2O_2 . In contrast, the CLS-extending effects of inactivating catalases are accompanied by parallel increases in levels of both H_2O_2 and oxidative damage, especially under non-CR conditions.

Discussion

Our study leads to the surprising conclusions that despite the induction of catalase activity by CR conditions that promote longevity, catalases are proaging factors in the budding yeast chronological aging model and both CR and catalase inactivation promote longevity in this model by inducing oxidative stress in the form of H_2O_2 . Although previous studies showed that glucose restriction increases ROS that promote longevity both in budding yeast (20) and in *C. elegans* (4), specific types of ROS were not identified in these studies. In our study, the effects of genetic or

pharmacological inactivation of catalases, catalase overexpression, and ectopic exposure to H_2O_2 combined with the use of probes that can distinguish between H_2O_2 and O_2^- definitively establish H_2O_2 as a longevity-promoting form of ROS induced by CR. The absence of toxic effects of H_2O_2 in these experiments reflects the well-documented dual roles of ROS in both survival and cell death pathways reported in other systems. Although H_2O_2 can induce programmed cell death (21), the intracellular concentrations that induce the beneficial hormesis-like effects in our study are likely to be far less than the concentrations that induce toxic effects. Furthermore, stationary phase cells are more resistant to H_2O_2 and other stresses compared with cells in exponential phase growth.

Our study also shows that the mechanism by which H_2O_2 exerts its prolongevity effects in budding yeast involves H_2O_2 induction of SOD activity. Hormesis theories posit that mild oxidative and other stresses induce adaptive responses that protect against further increases in stress (22). Our data identify SODs as targets of a H_2O_2 -induced stress response triggered by CR that confers hormesis-like protective effects against aging by reducing levels of O_2^- . This is consistent with previous reports that overexpression of SODs extends budding yeast CLS (23, 24). Although

promotes longevity despite increased oxidative damage to macromolecules by inducing superoxide dismutases that reduce levels of O_2^- . This mechanism likely underlies recent findings that challenge the validity of the free radical theory and provides a different paradigm for understanding how oxidative stress impacts aging and health.

Materials and Methods

Strains, Media, Chronological Lifespan, and Treatments. *S. cerevisiae* strain BY4742 cells (MAT α his3 Δ 1 leu2 Δ 0 lys2 Δ 0 ura3 Δ 0) and the respective knockouts in the *CTT1* and *CTA1* genes (European *Saccharomyces cerevisiae* Archive for Functional Analysis, EUROSCARF) were used for all experiments. Cell stocks were maintained in YEPD agar medium containing 0.5% yeast extract, 1% peptone, 2% agar, and 2% glucose. All experiments were performed in synthetic complete (SC) medium containing glucose as a carbon source and 0.67% yeast nitrogen base without amino acids (Difco Laboratories) supplemented with excess amino acids and bases for which the strains

were auxotrophic (50 μ g/mL histidine, 50 μ g/mL lysine, 300 μ g/mL leucine, and 100 μ g/mL uracil) with the exception that uracil was absent from medium in experiments that used the *CTA1* overexpressing strain, the control strain transformed with an empty vector or the double mutant *CTA1CTT1*. CLS was measured in different conditions as described in Supplementary Information. Construction of the *CTA1* overexpressing strain or the double mutant *CTA1CTT1* strain, treatment with pharmacological inhibitors of catalases or glutathione synthesis, measurements of intracellular reactive oxygen species, oxidative damage and SOD activity were performed using standard techniques: details are provided in Supplementary Information. Statistical analysis was performed according to the description in *SI Materials and Methods*.

ACKNOWLEDGMENTS. This work was supported by Fundação para a Ciência e Tecnologia, Portugal Grant PTDC/AGR-ALI/71460/2006, and National Cancer Institute Cancer Center Support Grant (P30 CA016056) to Roswell Park Cancer Institute. A.M., A.S., and B.S.-M. have fellowships from Fundação para a Ciência e Tecnologia (SFRH/BD/32464/2006, SFRH/BD/33125/2007, and SFRH/BD/41674/2007, respectively).

- Harman D (1956) Aging: A theory based on free radical and radiation chemistry. *J Gerontol* 11:298–300.
- Blagosklonny MV (2008) Aging: ROS or TOR. *Cell Cycle* 7:3344–3354.
- Andziak B, et al. (2006) High oxidative damage levels in the longest-living rodent, the naked mole-rat. *Aging Cell* 5:463–471.
- Schulz TJ, et al. (2007) Glucose restriction extends *Caenorhabditis elegans* life span by inducing mitochondrial respiration and increasing oxidative stress. *Cell Metab* 6:280–293.
- Linnane AW, Kios M, Vitetta L (2007) Healthy aging: Regulation of the metabolome by cellular redox modulation and prooxidant signaling systems: the essential roles of superoxide anion and hydrogen peroxide. *Biogerontology* 8:445–467.
- Groeger G, Quiney C, Cotter TG (2009) Hydrogen peroxide as a cell-survival signaling molecule. *Antioxid Redox Signal* 11:2655–2671.
- Dasgupta J, et al. (2006) Manganese superoxide dismutase protects from TNF- α -induced apoptosis by increasing the steady-state production of H_2O_2 . *Antioxid Redox Signal* 8:1295–1305.
- Madia F, Gattazzo C, Fabrizio P, Longo VD (2007) A simple model system for age-dependent DNA damage and cancer. *Mech Ageing Dev* 128:45–49.
- Weinberger M, et al. (2007) DNA replication stress is a determinant of chronological lifespan in budding yeast. *PLoS ONE* 2:e748.
- Burner CR, Murakami CJ, Kennedy BK, Kaerberlein M (2009) A molecular mechanism of chronological aging in yeast. *Cell Cycle* 8:1256–1270.
- Burhans WC, Weinberger M (2009) Acetic acid effects on aging in budding yeast: Are they relevant to aging in higher eukaryotes? *Cell Cycle* 8:2300–2302.
- Benov L, Szejnberg L, Fridovich I (1998) Critical evaluation of the use of hydroethidine as a measure of superoxide anion radical. *Free Radic Biol Med* 25:826–831.
- Godon C, et al. (1998) The H_2O_2 stimulin in *Saccharomyces cerevisiae*. *J Biol Chem* 273:22480–22489.
- Gasch AP, et al. (2000) Genomic expression programs in the response of yeast cells to environmental changes. *Mol Biol Cell* 11:4241–4257.
- Semchyshyn H (2009) Hydrogen peroxide-induced response in *E. coli* and *S. cerevisiae*: Different stages of the flow of the genetic information. *Cent Eur J Biol* 4:142–153.
- Yoshioka T, et al. (1994) Oxidants induce transcriptional activation of manganese superoxide dismutase in glomerular cells. *Kidney Int* 46:405–413.
- Röhrdanz E, Schmuck G, Ohler S, Kahl R (2001) The influence of oxidative stress on catalase and MnSOD gene transcription in astrocytes. *Brain Res* 900:128–136.
- Delori FC, Dorey CK (1998) In vivo technique for autofluorescent lipopigments. *Methods Mol Biol* 108:229–243.
- Terman A, Dalen H, Eaton JW, Neuzil J, Brunk UT (2004) Aging of cardiac myocytes in culture: Oxidative stress, lipofuscin accumulation, and mitochondrial turnover. *Ann N Y Acad Sci* 1019:70–77.
- Agarwal S, Sharma S, Agrawal V, Roy N (2005) Caloric restriction augments ROS defense in *S. cerevisiae*, by a Sir2p independent mechanism. *Free Radic Res* 39:55–62.
- Madeo F, et al. (1999) Oxygen stress: A regulator of apoptosis in yeast. *J Cell Biol* 145:757–767.
- Gems D, Partridge L (2008) Stress-response hormones and aging: “That which does not kill us makes us stronger.” *Cell Metab* 7:200–203.
- Harris N, et al. (2005) Overexpressed Sod1p acts either to reduce or to increase the lifespans and stress resistance of yeast, depending on whether it is Cu(2+)-deficient or an active Cu,Zn-superoxide dismutase. *Aging Cell* 4:41–52.
- Fabrizio P, Fletcher SD, Minois N, Vaupel JW, Longo VD (2004) Chronological aging-independent replicative life span regulation by Msn2/Msn4 and Sod2 in *Saccharomyces cerevisiae*. *FEBS Lett* 557:136–142.
- Yokoo S, Furumoto K, Hiyama E, Miwa N (2004) Slow-down of age-dependent telomere shortening is executed in human skin keratinocytes by hormesis-like-effects of trace hydrogen peroxide or by anti-oxidative effects of pro-vitamin C in common concurrently with reduction of intracellular oxidative stress. *J Cell Biochem* 93:588–597.
- Passos JF, et al. (2007) Mitochondrial dysfunction accounts for the stochastic heterogeneity in telomere-dependent senescence. *PLoS Biol* 5:e110.
- Serra V, von Zglinicki T, Lorenz M, Saretzki G (2003) Extracellular superoxide dismutase is a major antioxidant in human fibroblasts and slows telomere shortening. *J Biol Chem* 278:6824–6830.
- Sarsour EH, Venkataraman S, Kalen AL, Oberley LW, Goswami PC (2008) Manganese superoxide dismutase activity regulates transitions between quiescent and proliferative growth. *Aging Cell* 7:405–417.
- Zmijewski JW, et al. (2009) Antiinflammatory effects of hydrogen peroxide in neutrophil activation and acute lung injury. *Am J Respir Crit Care Med* 179:694–704.
- Mitra S, Abraham E (2006) Participation of superoxide in neutrophil activation and cytokine production. *Biochim Biophys Acta* 1762:732–741.

Supporting Information

Mesquita et al. 10.1073/pnas.1004432107

SI Materials and Methods

Chronological Lifespan. Caloric restriction (CR) was accomplished by reducing the glucose concentration from 2 to 0.5% or 0.05% in the initial culture medium. pH values of all of the conditions were monitored during chronological lifespan (CLS) experiments. For growth in buffered medium, a citrate phosphate buffer (64.2 mM Na_2HPO_4 and 17.9 mM citric acid) adjusted to pH 6.0 was added to the medium before inoculation. In a standard experiment, overnight cultures were grown in SC medium containing these different concentrations of glucose and then inoculated into flasks containing medium with the same concentration of glucose at a volume ratio of 1:3. These cultures were then incubated at 26 °C with shaking at 150 rpm. Cultures reached stationary phase 2–3 d later and this was considered day 0 of CLS. Survival was assessed by counting colony-forming units (CFUs) after 2 d of incubation of culture aliquots at 26 °C on YEPD agar plates beginning at day 0 of CLS (when viability was considered to be 100%) and then again every 2–3 d until less than 0.01% of the cells in the culture were viable.

Construction of the *CTA1* Overexpressing and *CTA1CTT1* Double Mutant Strains. To construct the *CTA1* overexpressing strain, *CTA1* was amplified by PCR with the following primers: F (CCGGTCTAGAATGTCGAAATTGGGACAAGA) and R (CCGG-AAGCTTGGAGTTACTCGAAAGCTCAG) using genomic DNA isolated from *Saccharomyces cerevisiae* wild-type cells as template. The resulting fragment was cloned into the XbaI–HindIII site of the plasmid pUG35 (EUROSCARF), producing the plasmid pUG35CTA1. The wild-type *S. cerevisiae* strain BY4742 was transformed by the lithium acetate method with plasmid pUG35CTA1 to produce the strain overexpressing *CTA1* (“*MET-CTA1*”) or with the plasmid pUG35 to produce the “empty-vector” control strain.

Double *CTA1CTT1* mutant cells were obtained by *CTT1* disruption in the $\Delta cta1$ strain. A deletion fragment, containing *URA3* gene and *CTT1* flanking regions, was amplified by PCR using genomic DNA isolated from W303 $\Delta ctt1::URA3$ cells and the following primers: F (ATGGGGATAGAACCTCCGTTAT) and R (GAATTTAAAGTTTCTCTGCTGG). Cells were transformed by electroporation and $\Delta cta1 ctt1$ mutants were selected in minimal medium lacking uracil. Gene disruption was confirmed by the analysis of catalase activity in a native gel. Double mutants lacking both Cta1p and Ctt1p activity were selected.

Pharmacological Inhibition of Catalases and Glutathione Synthesis. Pharmacological inhibition of catalase was accomplished by treating cells beginning at day 0 of CLS with 10 mM 3-amino-1,2,4-triazole (3AT) (Sigma), which binds covalently to the active center of the active tetrameric heme-containing form of catalases (1, 2). Pharmacological inhibition of glutathione synthesis was accomplished by treating cells at day 0 with 1 mM L-buthionine-sulfoximine (BSO) (Sigma), which indirectly inhibits glutathione synthesis by interacting with γ -glutamylcysteine synthetase (3). The ectopic effects of hydrogen peroxide on CLS were assessed by treating non-CR (2% glucose) wild-type cells with 0, 0.2, 0.3, and 1 mM H_2O_2 (Merck) beginning at day 0 of CLS and survival was measured as described before.

FACS Analysis of Intracellular Reactive Oxygen Species. Levels of intracellular ROS were measured using dihydrorhodamine 123 (DHR) or 2',7'-dichlorodihydrofluorescein diacetate ($\text{H}_2\text{DCF-DA}$) (Molecular Probes), compounds that are capable of detecting H_2O_2 (4). Briefly, aliquots were taken at selected time points and

DHR was added to a final concentration of 15 $\mu\text{g/mL}$ and cells were incubated for 90 min at 26 °C. For $\text{H}_2\text{DCF-DA}$ staining cells were incubated with a final concentration of 10 μM for 90 min at 30 °C. Cells were then washed twice in PBS and analyzed by flow cytometry. FACS analysis used an EPICS XL-MCL (Beckman–Coulter) flow cytometer equipped with a 15 mW argon laser emitting at 488 nm. The green fluorescence was collected through a 488-nm blocking filter, a 550-nm long-pass dichroic with a 525 nm band pass. Data acquired from a minimum of 30,000 cells per sample at low flow rate were analyzed with the Multigraph software included in the system II software for the EPICS XL-MCL version 1.0. Intracellular superoxide anions were measured using dihydroethidium (DHE) (Molecular Probes). Aliquots of cells were collected at indicated time points and DHE was added to a final concentration of 5 μM from a 5-mM stock in DMSO. After incubation for 10 min at 30 °C, cells were washed once with 0.5 mL PBS, resuspended in 50 μL PBS, and added to 1 mL PBS. After briefly sonicating the suspension, DHE signals were measured using a FACSCaliber2 flow cytometer (BD-Biosciences) with a 488-nm excitation laser. Signals from 25,000 cells/sample were captured in FL3 (>670 nm) at a flow rate of 5,000 cells/s. FACS measurements of DHR signals presented in Fig. 2 were measured similar to the DHR measurements described for Fig. 1 except that a FACSCaliber flow cytometer was used to capture signals in FL1 (530 nm \pm 15 nm) from 25,000 cells/sample at a flow rate of 5,000 cells/s. Data collected with the FACSCaliber2 flow cytometer were processed with FlowJo software (Tree Star) and quantified with WinList software (Verity Software House).

Protein Extract Preparation, Superoxide Dismutase, and Catalase Activity Assays. For determination of catalase and superoxide dismutase activities, yeast extracts were prepared in 25 mM Tris buffer (pH 7.4) containing a mixture of protease inhibitors. Protein content of cellular extracts was estimated by the method of Lowry using BSA as a standard.

Catalase activity was determined as in ref. 5. Briefly, 30 μg of proteins were separated by native PAGE and catalase activity was analyzed in situ in the presence of 3,3'-diaminobenzidine tetrahydrochloride (Sigma), using the H_2O_2 /peroxidase system. The gel was incubated in horseradish peroxidase (Sigma) (50 $\mu\text{g/mL}$) in 50 mM potassium phosphate buffer (pH 6.7) for 45 min. H_2O_2 was then added to a final concentration of 5 mM and incubation was continued for 10 min. The gel was then rapidly rinsed twice with distilled water and incubated in 0.5 mg/mL diaminobenzidine in 50 mM potassium phosphate buffer until staining was complete.

Superoxide dismutase activities were measured on the basis of their ability to inhibit reduction of nitro blue tetrazolium to formazan in nondenaturing polyacrylamide gels (6). Sod2p activity was distinguished from Sod1p activity on the basis of the ability of 2 mM cyanide to inhibit Sod1p, but not Sod2p. Quantification of band intensities was performed by densitometry using Quantity One Basic software from Bio-Rad.

Determination of Oxidative Damage. To measure levels of carbonylated proteins, samples of total cell protein were derivatized by mixing aliquots with one volume of 12% (wt/vol) SDS and two volumes of 20 mM 2,4-dinitrophenylhydrazine in 10% (vol/vol) trifluoroacetic acid (a blank control was treated with two volumes of 10% (vol/vol) trifluoroacetic acid alone) (7). After incubation for 30 min at room temperature in the dark, samples were neutralized and proteins (0.15 μg) were slot blotted onto a poly-

vinylidene fluoride membrane (Hybond-PVDF, GE Healthcare). The PVDF membrane was probed with rabbit IgG anti-DNP (Dako) (1:5,000 dilution) and goat anti-rabbit IgG linked to horseradish peroxidase (Sigma) (1:5,000 dilution) by standard techniques. Detection of derivatized proteins was accomplished by chemiluminescence, using reagents contained in a RPN 2109 kit (GE Healthcare). The membranes were exposed to a Hybond-ECL film (GE Healthcare) for 15 s to 1 min, and the film was developed. Quantitative analysis of carbonyls was performed by densitometry using Quantity One Basic software from Bio-Rad.

1. Chang JY, Schroeder WA (1972) Reaction of 3-amino-1,2,4-triazole with bovine liver catalase and human erythrocyte catalase. *Arch Biochem Biophys* 148:505–508.
2. Margoliash E, Novogrodsky A, Schejter A (1960) Irreversible reaction of 3-amino-1,2,4-triazole and related inhibitors with the protein of catalase. *Biochem J* 74:339–348.
3. Griffith OW, Meister A (1979) Potent and specific inhibition of glutathione synthesis by buthionine sulfoximine (S-n-butyl homocysteine sulfoximine). *J Biol Chem* 254:7558–7560.

Autofluorescence signals indicating oxidative damage to proteins and lipids were collected from 25,000 cells/sample using a FACSCaliber2 flow cytometer as described above for DHE measurements, except that cells were not stained with DHE after the PBS wash step.

Statistical Analysis. Data are reported as mean values of at least three independent assays and presented as mean \pm SD or mean \pm SEM. The arithmetic means are given with SD with 95% confidence value. Statistical analyses were carried out using Student's *t*-test. **P* < 0.05 was considered statistically significant.

4. Qin Y, Lu M, Gong X (2008) Dihydrorhodamine 123 is superior to 2,7-dichlorodihydrofluorescein diacetate and dihydrorhodamine 6G in detecting intracellular hydrogen peroxide in tumor cells. *Cell Biol Int* 32:224–228.
5. Aebi H (1984) Catalase in vitro. *Methods Enzymol* 105:121–126.
6. Flohé L, Otting F (1984) Superoxide dismutase assays. *Methods Enzymol* 105:93–104.
7. Levine RL, Williams JA, Stadtman ER, Shacter E (1994) Carbonyl assays for determination of oxidatively modified proteins. *Methods Enzymol* 233:346–357.

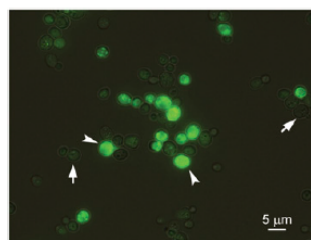


Fig. S1. Determination of dihydrorhodamine 123 (DHR) positive cells containing high levels of ROS. Photomicrograph of DHR-stained *Saccharomyces cerevisiae* wild-type cells (BY4742) from day 3 of stationary phase cultures under caloric restriction (CR) conditions (0.5% glucose). Arrowheads indicate cells displaying bright green fluorescence and correspond to cells with high intracellular ROS levels, designated DHR positive cells. Arrows indicate cells that did not stain with DHR. Cells were visualized by epifluorescence microscopy using an Olympus BX61 microscope equipped with a high-resolution DP70 digital camera and an Olympus PlanApo 60 \times /oil objective, with a numerical aperture of 1.42. Total magnification 600 \times . (Bar, 5 μ m.)

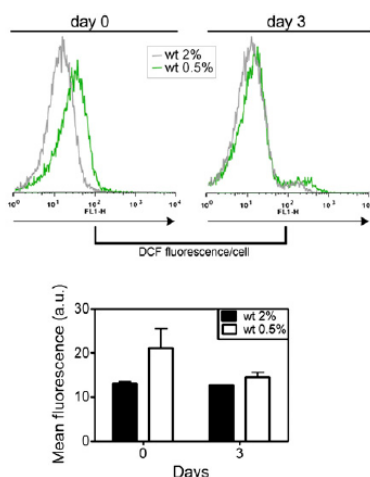


Fig. S2. Increased levels of ROS in caloric-restricted *Saccharomyces cerevisiae* wild-type cells. FACS measurements of intracellular ROS using the probe H₂DCF-DA at day 0 and day 3 of stationary phase (histograms). Bar graphs indicate mean \pm SD fluorescence/cell (arbitrary units) measured in 30,000 cells/sample in three independent experiments.

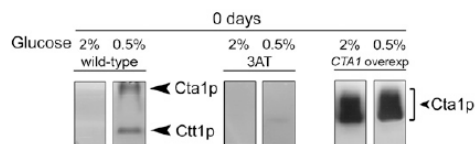


Fig. S3. Caloric restriction of stationary phase cells induces the activity of the peroxisomal catalase *CTA1*, as well as the cytosolic catalase *CTT1*. Catalase activities of wild-type *Saccharomyces cerevisiae* (BY4742) cells were increased by CR conditions beginning at day 0 of stationary phase. The pharmacological inhibition of catalase with 10 mM 3-amino-1,2,4-triazole (3AT) resulted in complete inhibition of CR-induced Cta1p and Ctt1p activity. Overexpression of *CTA1* resulted in a substantial increase in Cta1p activity.

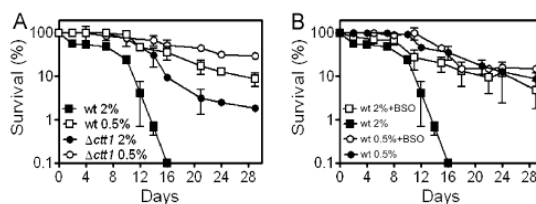


Fig. S4. CLS was also extended by mutational inactivation of *CTT1* or upon inhibition of glutathione synthesis, and the longer CLS detected under these conditions was extended further by CR. Survival of (A) wild-type (BY4742) and $\Delta ctt1$ cells and (B) wild-type cells in the absence or presence of 1 mM L-buthionine-sulfoximine (BSO), which indirectly inhibits glutathione synthesis. Cell viability was measured every 2–3 d starting at day 0 when cultures reached the stationary phase. Three to five biological replicates of each experiment were performed and measurements were made in three samples per experiment. Survival values indicate mean \pm SD of all experiments. Statistical significance ($*P < 0.05$) was determined by Student's *t* test.

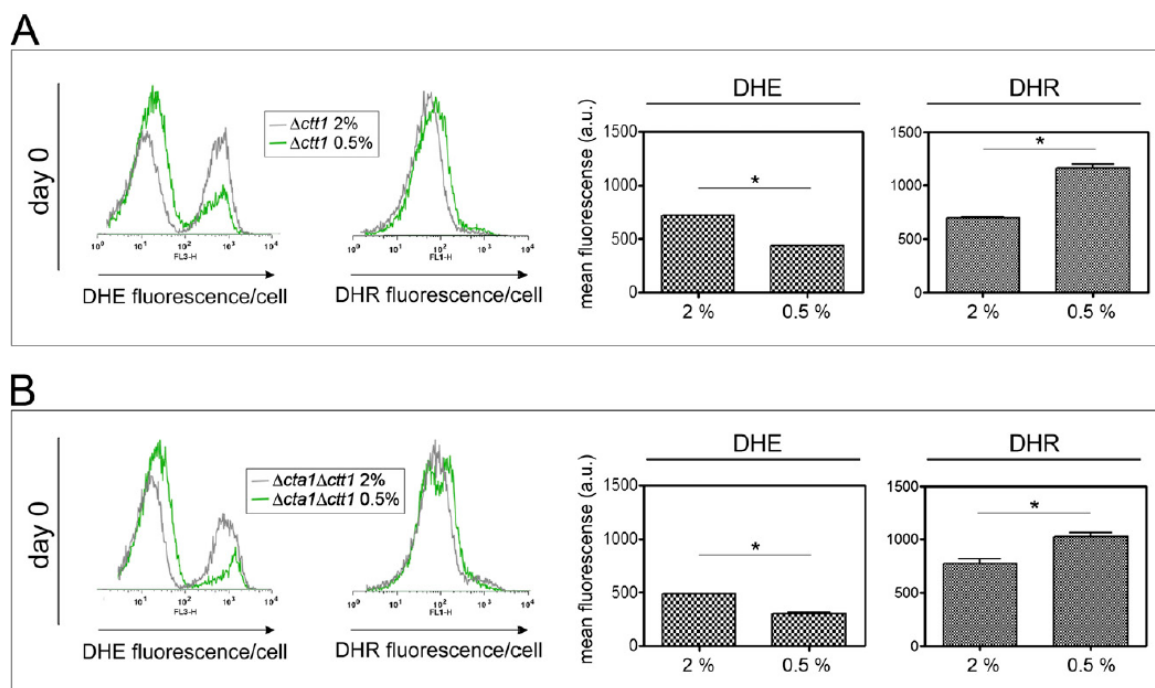


Fig. S5. Abrogation of *CTT1* or of both catalases (*CTA1CTT1*) mimics the CR longevity-promoting effects associated with high intracellular H_2O_2 levels and reduction in the chronological age-dependent accumulation of superoxide anions. FACS measurements of superoxide anions using dihydroethidium (DHE) in parallel with measurements of H_2O_2 using dihydrorhodamine 123 (DHR) at day 0 of CLS in $\Delta ctt1$ (A) and $\Delta cta1\Delta ctt1$ (B) cells. Bar graphs indicate mean \pm SD fluorescence/cell (arbitrary units) measured in 30,000 cells/sample in three independent experiments. Statistical significance ($*P < 0.05$) was determined by Student's *t* test.

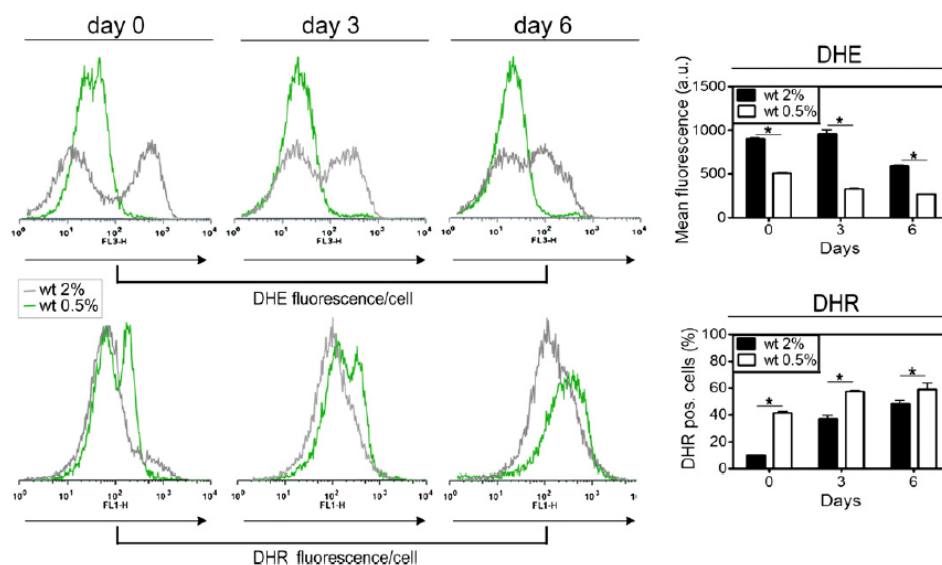


Fig. S6. CR-induced increases in intracellular H_2O_2 accompanied by a reduction in the accumulation of superoxide anions occurs independently of changes in levels of acetic acid as demonstrated in cells cultured in buffered medium. FACS measurements of superoxide anions using dihydroethidium (DHE) in parallel with measurements of H_2O_2 using dihydrorhodamine 123 (DHR) in wild-type cells cultured in buffered medium (citrate phosphate buffer, pH 6.0) at days 0, 3, and 6 of stationary phase. Bar graphs indicate mean \pm SD fluorescence/cell (arbitrary units) measured in 30,000 cells/sample in three independent experiments. Statistical significance (* $P < 0.05$) was determined by Student's t test.

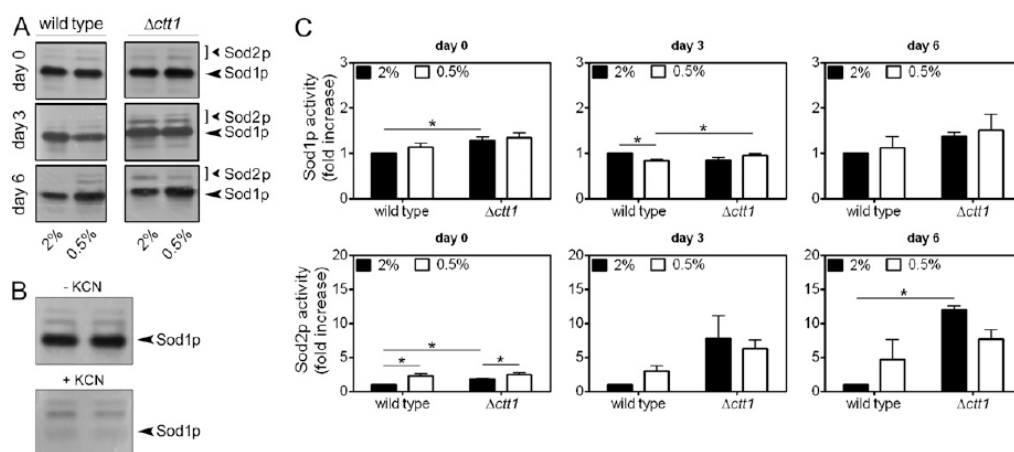


Fig. S7. Induction of superoxide dismutase activity in $\Delta ctt1$ cells. (A) In situ determination of superoxide dismutase activities, as previously described (6), in stationary phase wild-type and $\Delta ctt1$ cells. (B) MnSOD (Sod2p) activity detected in the presence of 2 mM potassium cyanide, which inhibits Sod1p activity. (C) Quantification of fold increase in Sod1p and Sod2p activity in wild-type and $\Delta ctt1$ cells. Sod1p and Sod2p activities measured at each time point were normalized to the activity of wild-type cells under non-CR conditions (2% glucose). Values indicate mean \pm SEM from three independent experiments. Statistical significance (* $P < 0.05$) was determined by Student's t test.

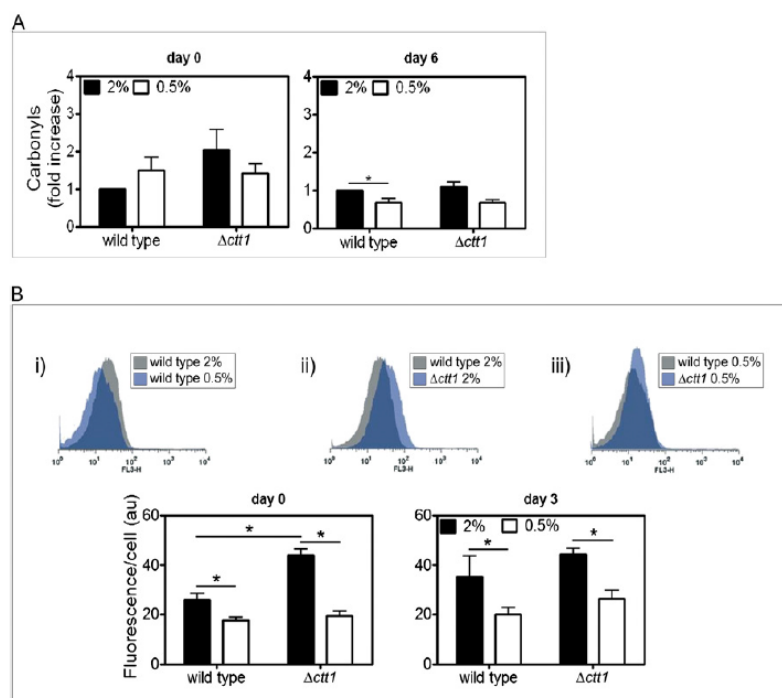


Fig. S8. Increased H_2O_2 in $\Delta ctt1$ cells is associated with higher levels of oxidative damage despite the increased longevity of these cells. (A) Oxidative damage was measured as the fold increase in levels of oxidized proteins (carbonyls) (7) in stationary phase wild-type and $\Delta ctt1$ cells under non-CR and CR conditions. The levels of carbonyls measured at each time point were normalized to those of wild-type cells under non-CR conditions (2% glucose). (B) Determination of oxidative damage to proteins and lipids indicated by autofluorescence of stationary phase wild-type and $\Delta ctt1$ cells under non-CR and CR conditions. Histograms are representative of data collected at day 3. Values indicate mean \pm SEM from three independent experiments. Statistical significance ($*P < 0.05$) was determined by Student's t test.

Table S1. pH of aging cultures

	SC 2%	SC 0.5%
BY4742	2.95 (\pm 0.02)	3.16 (\pm 0.02)
BY4742 $\Delta cta1$	2.93 (\pm 0.01)	3.10 (\pm 0.03)
BY4742 $\Delta ctt1$	2.93 (\pm 0.00)	3.26 (\pm 0.06)
BY4742 $\Delta cta1ctt1$	2.96 (\pm 0.00)	3.16 (\pm 0.01)

Cells were inoculated into the indicated medium and pH was measured at 72 h of aging. Data are presented as mean pH of three biological replicates with SD in parentheses. SC, synthetic complete medium.

ATTACHMENT II

Almeida B., Buttner S., Ohlmeier S., Silva A., Mesquita A., Sampaio-Marques B., Osório N.S., Kollau A., Mayer B., Leão C., Laranjinha J., Rodrigues F., Madeo F., Ludovico P.. NO-mediated apoptosis in yeast. *J Cell Sci.* 2007 Sep 15;120(Pt 18):3279-88.

NO-mediated apoptosis in yeast

Bruno Almeida¹, Sabrina Buttner², Steffen Ohlmeier³, Alexandra Silva¹, Ana Mesquita¹, Belém Sampaio-Marques¹, Nuno S. Osório¹, Alexander Kollau⁴, Bernhard Mayer⁴, Cecília Leão¹, João Laranjinha⁵, Fernando Rodrigues¹, Frank Madeo² and Paula Ludovico^{1,*}

¹Life and Health Sciences Research Institute (ICVS), School of Health Sciences, University of Minho, Campus de Gualtar, 4710-057 Braga, Portugal

²Institute for Molecular Biosciences, Universitätsplatz 2, A-8010 Graz, Austria

³Proteomics Core Facility, Biocenter Oulu, Department of Biochemistry, University of Oulu, Oulu, Finland

⁴Department of Pharmacology and Toxicology, KFUG, Universitätsplatz 2, A-8010 Graz, Austria

⁵Faculty of Pharmacy and Center for Neurosciences and Cell Biology, University of Coimbra, 3000 Coimbra, Portugal

*Author for correspondence (e-mail: pludovico@icsaude.uminho.pt)

Accepted 18 July 2007

Journal of Cell Science 120, 3279–3288 Published by The Company of Biologists 2007

doi:10.1242/jcs.010926

Summary

Nitric oxide (NO) is a small molecule with distinct roles in diverse physiological functions in biological systems, among them the control of the apoptotic signalling cascade. By combining proteomic, genetic and biochemical approaches we demonstrate that NO and glyceraldehyde-3-phosphate dehydrogenase (GAPDH) are crucial mediators of yeast apoptosis. Using indirect methodologies and a NO-selective electrode, we present results showing that H₂O₂-induced apoptotic cells synthesize NO that is associated to a nitric oxide synthase (NOS)-like activity as demonstrated by the use of a classical NOS kit assay. Additionally, our results show that yeast GAPDH is a target of extensive proteolysis upon H₂O₂-induced apoptosis and undergoes S-nitrosation. Blockage of NO synthesis with N^ω-nitro-L-arginine methyl ester leads to a decrease of

GAPDH S-nitrosation and of intracellular reactive oxygen species (ROS) accumulation, increasing survival. These results indicate that NO signalling and GAPDH S-nitrosation are linked with H₂O₂-induced apoptotic cell death. Evidence is presented showing that NO and GAPDH S-nitrosation also mediate cell death during chronological life span pointing to a physiological role of NO in yeast apoptosis.

Supplementary material available online at
<http://jcs.biologists.org/cgi/content/full/120/18/3279/DC1>

Key words: Yeast apoptosis, Nitric oxide, S-nitrosation, Glyceraldehyde-3-phosphate dehydrogenase, L-arginine, Reactive oxygen species

Introduction

Nitric oxide (NO) is a highly diffusible free radical with dichotomous regulatory roles in numerous physiological and pathological events (Ignarro et al., 1987; Nathan, 1992) being recognized as an intra- and inter-cellular signalling molecule in both animals and plants (Delledonne, 2005). Diverse cellular functions can be directly or indirectly affected by NO through posttranslational modification of proteins, of which the most widespread and functionally relevant one is S-nitrosation, defined as the covalent attachment of NO to the thiol side chain of a cysteine (Cys) (Hess et al., 2005). NO also controls the apoptotic signalling cascade by regulating the expression of several genes, mitochondrial dysfunction, and caspase activity/activation (Brune et al., 1995; Kroncke et al., 1995). Nonetheless, the mechanisms underlying the NO-mediated inhibition of apoptosis are not clearly understood, although it is well known that S-nitrosation is a crucial event to permanently maintain human caspases in an inactive form (Choi et al., 2002). Recent work demonstrated that like mammalian caspases, metacaspases, which are apoptosis-executing caspase-like proteases in yeast (Madeo et al., 2002) and plants (Suarez et al., 2004), can be kept inactive through S-nitrosation of one Cys residue (Belenghi et al., 2007). Nevertheless, a second catalytic Cys residue, highly conserved in all known metacaspases but absent in all members of caspases, can rescue the first S-nitrosated catalytic site even in

the presence of high NO levels (Belenghi et al., 2007). In addition, S-nitrosation has been shown to regulate the function of an increasing number of intracellular proteins (Stamler et al., 2001), among them glyceraldehyde-3-phosphate dehydrogenase (GAPDH), a key glycolytic enzyme that when S-nitrosated translocates to the nucleus, triggering apoptosis in mammalian cells (Hara et al., 2005).

The origin of NO in yeast cells is still a matter of debate essentially because of the lack of mammalian nitric oxide synthase (NOS) orthologues in the yeast genome, as previously observed in plants. Recently, Castello and coworkers (Castello et al., 2006) showed that yeast cells are capable of producing NO in mitochondria under hypoxic conditions. This production is nitrite dependent through cytochrome c oxidase and is influenced by YHb, a flavohaemoglobin NO oxidoreductase (Castello et al., 2006). Furthermore, results from our group showed that treatment of yeast cells with menadione leads to NO production dependent on intracellular L-arginine levels, suggesting the existence of an enzyme with NOS-like activity (Osorio et al., 2007). Supporting the relevance of NO in yeast physiology and pathophysiology is the presence of various cellular defences against nitrosative stress. Several molecules, such as peroxiredoxins, thioredoxins and the flavohaemoglobin, prompt yeast cells to face nitrosative stress (Liu et al., 2000; Wong et al., 2002). Moreover, when nitrosative stress is exogenously imposed it is sufficient to inactivate GAPDH

(Sahoo et al., 2003). However, the role of NO and its relevance in yeast apoptosis has never been explored.

Using proteomic, genetic and biochemical approaches we found evidence suggesting the intervention of NO and GAPDH in yeast H_2O_2 -activated apoptotic pathway. NO production upon H_2O_2 treatment is dependent on intracellular L-arginine content and contributes to the generation of intracellular reactive oxygen species (ROS). GAPDH, the levels of which increase in total cellular extracts of H_2O_2 -induced apoptotic cells, becomes fragmented and S-nitrosated, possibly acting as an apoptotic trigger. Chronologically aged cells also display increased NO production and GAPDH S-nitrosation, as well as a correlation between intracellular levels of superoxide anion and NO production, thereby suggesting a physiological role of NO in the signalling of yeast apoptosis.

Results

H_2O_2 , as a ROS, triggers a stress response in *Saccharomyces cerevisiae* by activating a number of stress-induced pathways that might lead to alterations of gene expression, protein modification and translocation, growth arrest or apoptosis. Using 2-D gel electrophoresis coupled to mass spectrometry we analyzed both the mitochondrial and total cellular proteome of H_2O_2 -induced apoptotic cells, identifying increased levels of several stress-related proteins (Fig. 1, Table 1). An acidic form of the thiol-specific peroxiredoxin, Ahp1p (Lee et al., 1999), previously described as the active form (Prouzet-Mauleon et al., 2002), and two spots of the thioredoxin peroxidase, Tsa1p (Garrido and Grant, 2002), were induced upon H_2O_2 treatment (Fig. 1, Table 1). Under the same conditions, increased levels of two mitochondrial stress-related proteins, Prx1p, a thioredoxin peroxidase (Pedrajas et al., 2000), and Ilv5p, required for the maintenance of mitochondrial DNA (Zelenaya-Troitskaya et al., 1995) were also detected (Fig. 1, Table 1).

NO is synthesized by an L-arginine-dependent process during H_2O_2 -induced apoptosis

Taking into account that molecules such as peroxiredoxins and thioredoxins are known to play a role against both oxidative and nitrosative stress in several organisms, including yeast (Barr and Gedamu, 2003; Missall and Lodge, 2005; Wong et al., 2002; Wong et al., 2004), we questioned whether H_2O_2 might be inducing nitrosative stress due to an endogenous production of NO. Therefore, we performed several experiments in order to measure NO production in yeast cells dying by an apoptotic process triggered by H_2O_2 . Given that NO is a diffusible free radical rapidly oxidized to nitrate and nitrite (Palmer et al., 1987), an indirect measurement of NO production by monitoring nitrate and nitrite formation was performed. The obtained results supported the hypothesis of NO production since nitrate concentrations increased upon exposure to H_2O_2 (Fig. 2A). Additionally, flow cytometric quantification of cells stained with the NO indicator 4-amino-5-methylamino-2',7'-difluorescein (DAF-FM) diacetate revealed that a high percentage of H_2O_2 -treated cells contain high NO and/or reactive nitrogen species (RNS) levels, which decreased when a non-metabolized L-arginine analogue, N ω -nitro-L-arginine methyl ester (L-NAME), was added (Fig. 2B). Nonetheless, Balcerczyk and coworkers (Balcerczyk et al., 2005) have shown that NO quantitative determination by DAF-

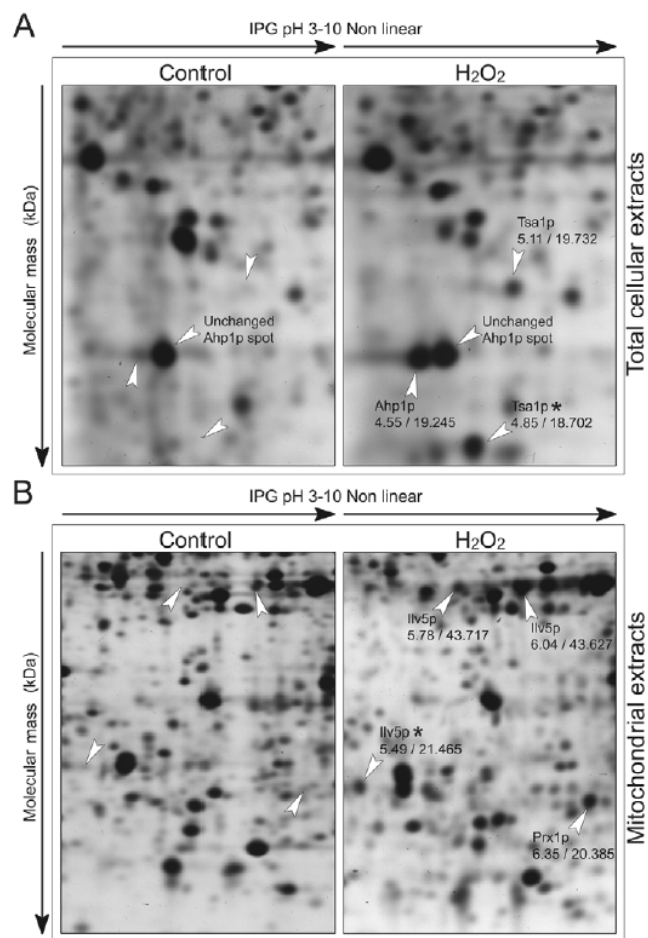


Fig. 1. The levels of stress response proteins are increased in both total and purified mitochondrial extracts from H_2O_2 -induced apoptotic cells. Comparison of protein expression levels in total cellular (A) and purified mitochondrial extracts (B) of untreated (control) and H_2O_2 -treated wild-type *S. cerevisiae* cells. Selected regions of the 2-D gel (isoelectric point/molecular mass) are shown enlarged and the position of altered protein spots are marked with an arrowhead. Putative protein fragments are marked with an asterisk. The apparent isoelectric points and molecular masses of the proteins were calculated with Melanie 3.0 (GeneBio) using identified proteins with known parameters as references.

FM in the presence of ROS is overestimated, indicating that DAF-FM is a fairly specific NO probe. Thus, to support the hypothesis of NO production in H_2O_2 -apoptosing cells we investigated NO synthesis *in vivo* using a NO-selective electrode (AmiNO-700). After H_2O_2 stimulus, yeast cells produced NO (Fig. 2C), the concentration of which increased in the medium following sigmoid-type kinetics. In fact, NO production was shown to be dependent of H_2O_2 concentration as indicated by the rate of NO production inferred from the curves during the initial linear periods (Fig. 2D). These results were further confirmed using a different NO-selective electrode (ISO-NO; World Precision Instruments; data not shown). Moreover, the results obtained with the NO-selective electrode supported that NO synthesis is L-arginine dependent

Table 1. Proteins of mitochondrial and total cellular extracts with detected expression changes upon H₂O₂ treatment

Proteins identified	Spots	Function	Expression level*	Theoretical pI/mol. mass (kDa)	Experimental pI/mol. mass (kDa)
Total cellular proteome					
Stress response					
Ahp1	1	Thiol-specific peroxiredoxin	Up	5.01/19.115	4.55/19.245
Tsa1	2	Thioredoxin peroxidase	Up	5.03/21.458	4.85/18.702
			Up		5.11/19.732
Carbohydrate metabolism					
Adh1	1	Alcohol dehydrogenase	Up	6.26/36.692	5.68/42.191
Eno2	2	Enolase II	Up	5.67/46.783	5.45/45.268
			Up		5.97/43.214
Tdh2	1	Glyceraldehyde-3-phosphate dehydrogenase, isozyme 2	Up	6.49/35.716	5.89/18.980
Tdh3	5	Glyceraldehyde-3-phosphate dehydrogenase, isozyme 3	Up	6.46/35.747 (5.83/29.513)	5.57/31.420
			Up		5.54/20.168
			Up		5.78/20.188
			Up		5.72/19.118
			Up		5.60/37.475
Amino acid biosynthesis					
His4	1	Involved in histidine biosynthesis	Down	5.18/87.721	5.15/97.957
Unknown function					
Ycl026c-b	1	Hypothetical protein	Up	6.43/20.994	6.05/19.989
Mitochondrial proteome					
Ilv5	3	Acetohydroxyacid reductoisomerase	Up	9.10/44.368 (6.31/39.177)	5.49/21.465
			Up		6.04/43.627
			Up		5.78/43.717
Prx1	1	Mitochondrial peroxiredoxin	Up	8.97/29.496	6.35/20.385
Tdh3	1	Glyceraldehyde-3-phosphate dehydrogenase, isozyme 3	Up	6.46/35.747 (5.83/29.513)	6.44/37.008
Ycl026c-b	1	Hypothetical protein	Up	6.43/20.994	6.14/19.749

*An expression change was considered significant if the intensity of the corresponding spot differed reproducibly more than threefold.

Protein function was obtained from SGD (<http://www.yeastgenome.org/>). Theoretical pI (isoelectric point) and molecular mass (kDa) were calculated with the Compute pI/kDa tool (http://ca.expasy.org/tools/pi_tool.html).

since pre-incubation with L-NAME or D-arginine partially inhibited its synthesis (Fig. 2C). T80, time at which NO concentration is 80% of the maximal concentration, was 368.81 seconds for 4 mM of H₂O₂ and 384.52 and 403.38 seconds when cells were pre-incubated with D-arginine or L-NAME, respectively. Given the evidence supporting the synthesis of NO being dependent on L-arginine, we decided to use a classical method to detect a putative nitric oxide synthase (NOS)-like activity. Using a NOS assay kit that measures the formation of [³H]citrulline from L-[³H]arginine, we observed that H₂O₂-induced apoptotic yeast cells increased NOS-like activity in a H₂O₂ dose-dependent manner, concurrent with the previously observed NO production (Fig. 3A). Additionally, analysis of intracellular amino acid concentrations in yeast cells revealed that upon treatment there was a twofold increase in L-arginine concentration, which might be crucial for NO production upon H₂O₂-induced apoptosis (Fig. 3B). In fact, pre-incubation of cells grown in SC medium with L-arginine is sufficient to increase their susceptibility to H₂O₂ (data not shown). However, pre-incubation of cells with tyrosine, methionine, or glutamine, whose intracellular concentrations were also found to increase after H₂O₂ treatment (Fig. 3B), did not increase cellular susceptibility to this oxidative agent (data not shown). Moreover, results showing that pre-incubation with L-NAME rendered yeast cells resistant to H₂O₂ (Fig. 4A), further supported the hypothesis that NO synthesis occurs during, and accounts for, H₂O₂-induced apoptosis. In fact,

cellular protection conferred by L-NAME was shown to be specific since it did not result in a cell-death-resistant phenotype when challenged with acetic acid (Fig. 4B). Also, rather than having a protective effect on cells dying by Bax heterologous expression, L-NAME actually increases Bax toxicity (Fig. 4C). In accordance with the specificity of NO production during H₂O₂-induced apoptosis, pre-incubation with L-NAME dramatically decreased the intracellular levels of ROS (Fig. 4D). Supporting the suggested correlation between NO production and the increase of ROS, cell treatment with the NO donor DETA/NO, previously used to induce nitrosative stress in yeast cells (Horan et al., 2006), resulted in intracellular ROS accumulation (data not shown).

Altogether our results demonstrated that upon H₂O₂-induced apoptosis, NO is produced in yeast cells by an L-arginine-dependent mechanism pointing to the requirement of a yet unknown protein with a NOS-like activity. Moreover, NO is presented herein as an important apoptotic regulator that correlates with the intracellular ROS levels generated during H₂O₂-induced apoptosis.

NO is produced during chronological life span leading to an increase of superoxide anion levels

In order to unravel the possible role of NO in a physiological scenario of yeast apoptosis, we evaluated its production during chronological life span. Our results demonstrated that chronologically aged cells (10 days) display more than a

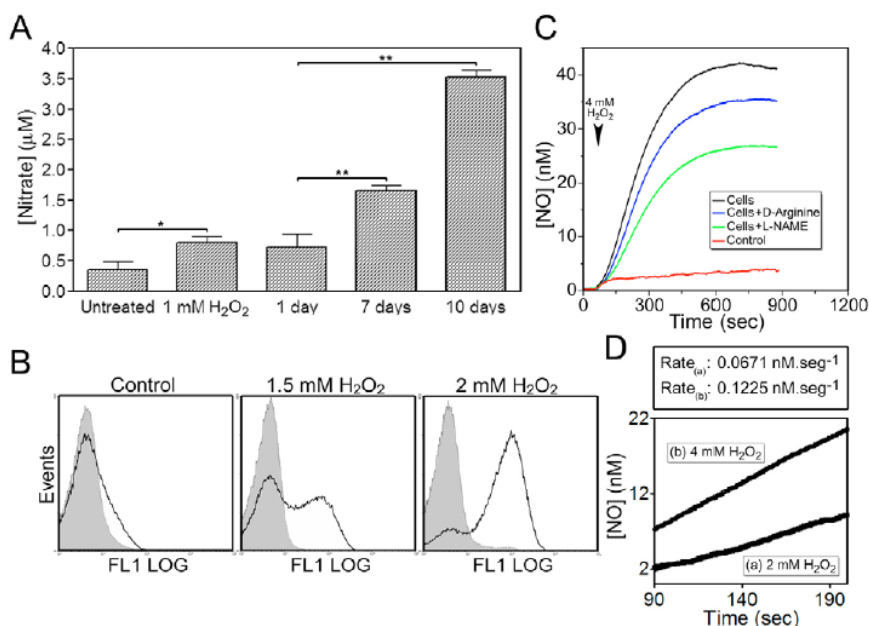


Fig. 2. Yeast cells synthesize NO upon apoptosis induction, which is dependent on L-arginine. (A) NO production in untreated, H₂O₂-treated and chronologically aged cells was indirectly assessed through measurement of nitrite and nitrate concentrations as described in Materials and Methods. * $P \leq 0.05$ versus untreated cells, ** $P \leq 0.03$ versus 1-day-old cells; t -test, $n=3$. (B) NO production in untreated and H₂O₂-treated (1.5 and 2.0 mM) cells assessed by flow cytometric quantification of cells stained with the NO indicator DAF-FM diacetate, in the absence (white area under the peak) or presence (shaded area) of the non-metabolized L-arginine analogue L-NAME. The data are presented in the form of frequency histograms displaying relative fluorescence (x axis) against the number of events analyzed (y axis). (C) Direct measurement of L-arginine-dependent NO production upon H₂O₂-induced apoptosis. NO production was recorded with a NO-selective electrode (AmiNO-700) upon addition of 4 mM H₂O₂ to 5×10^8 wild-type cells (black line) or to wild-type cells pre-incubated with the non-metabolized D-arginine (blue line) or L-NAME (green line). A control experiment without cells was also recorded and is represented as a red line. (D) Rate of NO production is H₂O₂ dependent. 2 mM or 4 mM of H₂O₂ was added to 5×10^8 wild-type cells and NO production assessed using the NO-selective electrode (AmiNO-700). Data presented correspond to the linear part of the NO production curve. Rate of NO production was calculated from the slope.

fivefold increase in NO generation, as indirectly determined by an increase in nitrate concentrations, which directly correlated with aging time (Fig. 2A). Given the limitations of assessing NO production by a NO-selective electrode with a chronic stimulus such as aging, and aiming to address the consequences of the indirect observation of NO production, we also evaluated distinct cellular parameters in the presence of oxyhaemoglobin (OxyHb), a compound that scavenges NO and is considered a major route of its catabolism (Kelm et al., 1996; Pietraforte et al., 1995; Wennmalm et al., 1992), representing a gold standard test for the involvement of NO in a biological process (Ignarro et al., 1987; Joshi et al., 2002). Cells in the presence of OxyHb revealed a faster growth (Fig. 5A) and a delay in cell death induced during chronological life span (Fig. 5B), both of which are OxyHb dose dependent.

Superoxide anion, which is generated during chronological life span, is known to play a major role in the age-associated death of yeast and other eukaryotic cells (Fabrizio et al., 2004). In mammalian cells, superoxide anion interacts with NO

leading to the formation of peroxynitrite (Packer et al., 1996), a RNS that enhances mitochondrial dysfunction, triggering an increased production of intracellular ROS levels (Zamzami et al., 1995). Following this line of thought, we evaluated the intracellular levels of superoxide anion during chronological life span in the presence of OxyHb. Our results demonstrated a decrease in superoxide anion production during chronological life span, which was inversely correlated to OxyHb concentrations (Fig. 5C). Overall, these results point to the occurrence of NO synthesis during chronologic life span and a role for NO during physiological apoptotic cell death. Moreover, NO is suggested to mediate superoxide anion production probably due to the action of intracellular RNS.

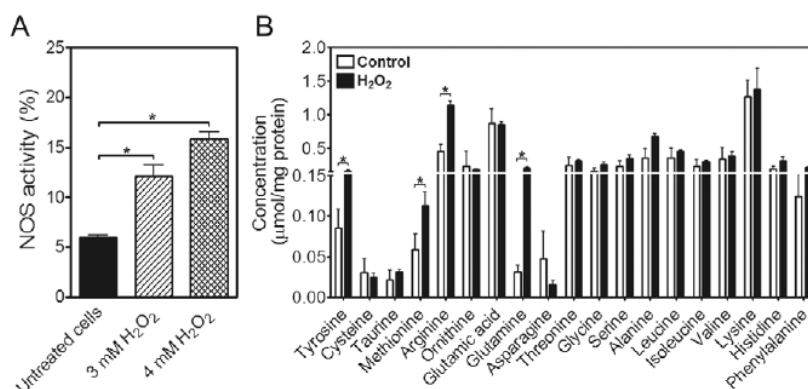
GAPDH is S-nitrosated during yeast apoptosis

Analysis of mitochondrial and total cellular proteome of H₂O₂-induced apoptotic cells revealed several GAPDH alterations, particularly of the Tdh3p isoenzyme (Fig. 6, Table 1). Upon H₂O₂ exposure, Tdh3p was detected within five spots of increased intensity, three of them corresponding to putative protein fragments, one to the mature protein with the putative mitochondrial import signal sequence removed (see Fig. S1 in supplementary material), and one corresponding to a new isoform of the complete Tdh3p with a lower isoelectric point. Tdh2p was also detected as a putative protein fragment (Fig. 6, Table 1; Fig. S1 in supplementary material), indicating that both GAPDH isoenzymes

might be targets for proteolysis. In yeast, GAPDH, particularly the Tdh3p isoform, is normally found in the cytoplasm, the nuclei or the mitochondria depending on the physiological conditions (Ohlmeier et al., 2004). Interestingly, a new form of Tdh3p with a lower isoelectric point was detected in mitochondrial extracts (Fig. 6, Table 1), suggesting the occurrence of a posttranslational modification upon H₂O₂ treatment.

S-nitrosation promoted by NO has been shown to regulate GAPDH, a glycolytic protein extensively implicated in mammalian apoptosis (reviewed by Chuang et al., 2005). Besides NO production, our results revealed several different alterations of GAPDH upon H₂O₂-induced apoptosis, which prompted us to investigate whether GAPDH S-nitrosation and its involvement in apoptosis were probably conserved in yeast cells. The first approach explored the contribution of GAPDH isoenzymes (Tdh2p and Tdh3p) that, from the proteomic assay, were found to be altered during yeast cell death. Exposure of both *TDH2*- and *TDH3*-disrupted cells to apoptotic inducing

Fig. 3. H_2O_2 -induced apoptotic cells display NOS-like activity. (A) NOS activity assessed in untreated and H_2O_2 -treated wild-type cells. The radioactivity obtained from a negative control consisting of yeast extract boiled for 20 minutes was subtracted from all the samples to remove background radioactivity. Data are expressed as the percentage conversion of L-[^3H]arginine to [^3H]citrulline. * $P \leq 0.03$ versus untreated cells; t -test, $n=4$. (B) Intracellular amino acid concentrations of untreated (control) and H_2O_2 -treated wild-type cells. * $P \leq 0.05$ versus untreated cells; t -test, $n=3$.



concentrations of H_2O_2 revealed an increase in the survival rate compared to that of wild-type cells (Fig. 7A), reflecting a putative role of GAPDH in the apoptotic process. Remarkably, $\Delta tdh2$ and $\Delta tdh3$ cells also displayed a reduction in intracellular ROS upon H_2O_2 -induced apoptosis (Fig. 7B), suggesting the involvement of GAPDH in ROS generation during apoptotic cell death.

As a posttranslationally modified form of Tdh3p was detected in the mitochondria of H_2O_2 -treated cells (Fig. 6, Table 1), we questioned if the concurrent synthesis of NO was promoting GAPDH S-nitrosation and its translocation to mitochondria. However, mass spectrometry analysis revealed that the observed mitochondrial GAPDH posttranslational modified form corresponds to an oxidation rather than an S-nitrosation of the protein (data not shown). Nevertheless, by immunoprecipitating GAPDH from cellular extracts with an anti-nitrosocysteine (CSNO) antibody, we demonstrated that GAPDH suffers a dose-dependent increase of S-nitrosation upon exposure to H_2O_2 (Fig. 8A,B). To support the

observation of the occurrence of GAPDH S-nitrosation, cells were treated with the NO donor DETA/NO. The results showed that GAPDH also suffers S-nitrosation upon exposure to the NO donor, discarding a possible artefact of H_2O_2 treatment. Interestingly, treatment with H_2O_2 after pre-incubation with L-NAME resulted in a reduction in the amount of S-nitrosated GAPDH to control levels (Fig. 8C,D), associated with an increased survival rate of yeast cells (Fig. 4A). Furthermore, chronologically aged cells displayed increased GAPDH S-nitrosation (Fig. 8C,D), pointing to a role of NO and GAPDH in the signalling of yeast apoptosis.

In summary, the occurrence of GAPDH S-nitrosation reinforces the fact that during yeast apoptotic cell death, induced by H_2O_2 or age-associated, NO is produced, which is dependent on intracellular L-arginine content, and that, as in mammalian cells, it is responsible for the signalling and execution of the process through GAPDH action (Hara et al., 2005). These results show yeast to be a valuable model for

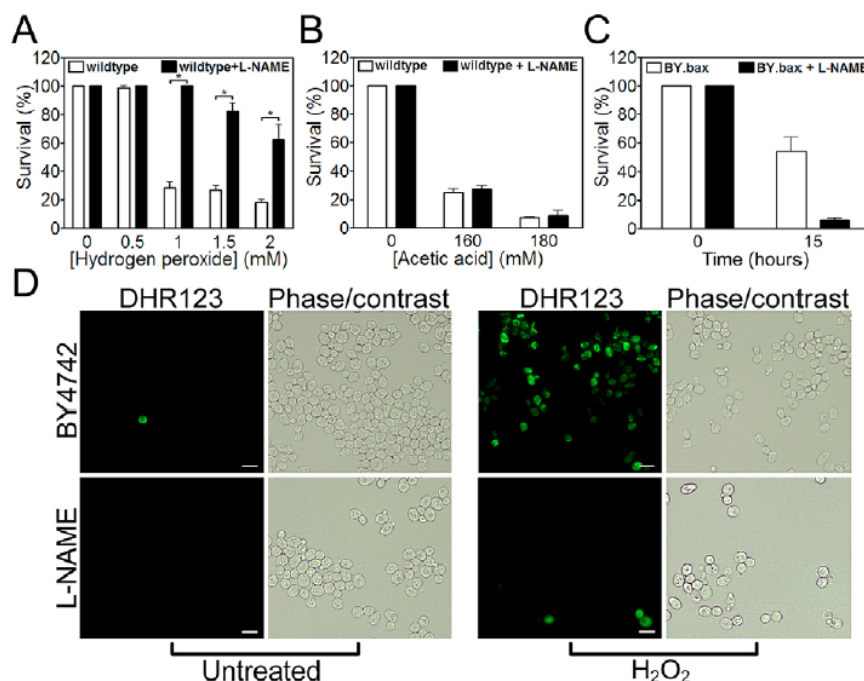


Fig. 4. Inhibition of NO production by L-NAME protects yeast cells from H_2O_2 , but not from mammalian Bax expression, or acetic acid-induced apoptosis.

(A) Comparison of the survival rate of wild-type cells upon H_2O_2 treatment with or without pre-incubation with L-NAME in order to inhibit NO production. * $P \leq 0.03$ versus wild type; t -test, $n=3$.

(B) Comparison of the survival of wild-type cells upon acetic acid-induced apoptosis with or without pre-incubation with L-NAME. (C) Comparison of the survival of yeast cells (strain BY.bax) upon Bax expression for 15 hours (apoptotic inducing conditions), with or without pre-incubation with L-NAME.

(D) Epifluorescence and phase-contrast micrographs of untreated and H_2O_2 -treated (1.5 mM) wild-type cells, with or without pre-incubation with L-NAME, stained with dihydrorhodamine 123 (DHR123) as an indicator of high intracellular ROS accumulation. Bars, 5 μm.

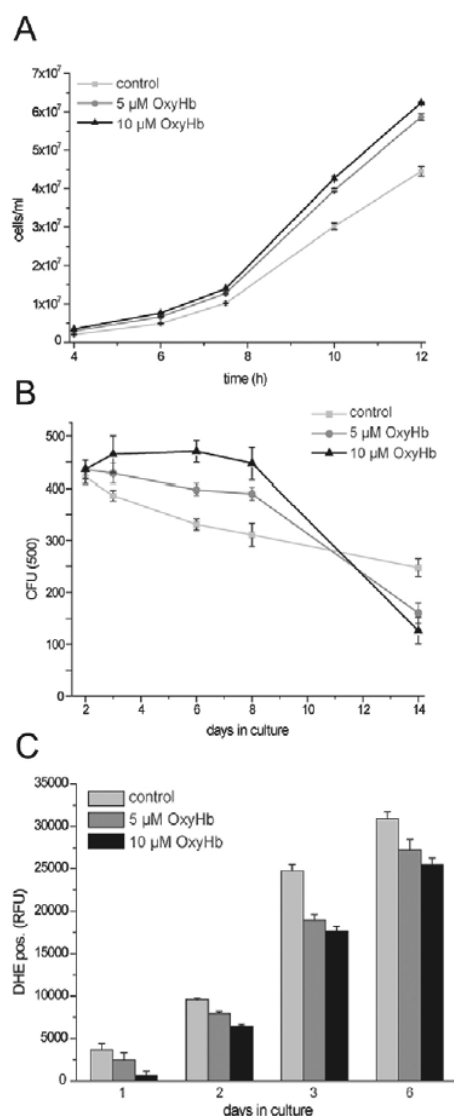


Fig. 5. NO scavenged by OxyHb is associated with a delay in cell death during chronological life span and to decreased levels of superoxide anion. (A) Growth curve of wild-type cells after addition of indicated concentrations of OxyHb. (B) Survival determined by clonogenicity during chronological aging of wild-type cells with or without addition of OxyHb, at the indicated concentrations on day 0. (C) Quantification (fluorescence) of ROS accumulation using dihydroethidium (DHE) staining during chronological aging of wild-type cells with or without OxyHb treatment.

studying the role of GAPDH in apoptosis and also open new frontiers for the study of NO role in yeast physiology.

Discussion

Apoptosis can be triggered by several different signals through different sub-programs controlled by a complex network of regulators and effectors. A large fraction of these apoptotic events depends on newly synthesized proteins, posttranslational modifications and translocation to specific cellular compartments (Ferri and Kroemer, 2001; Porter, 1999;

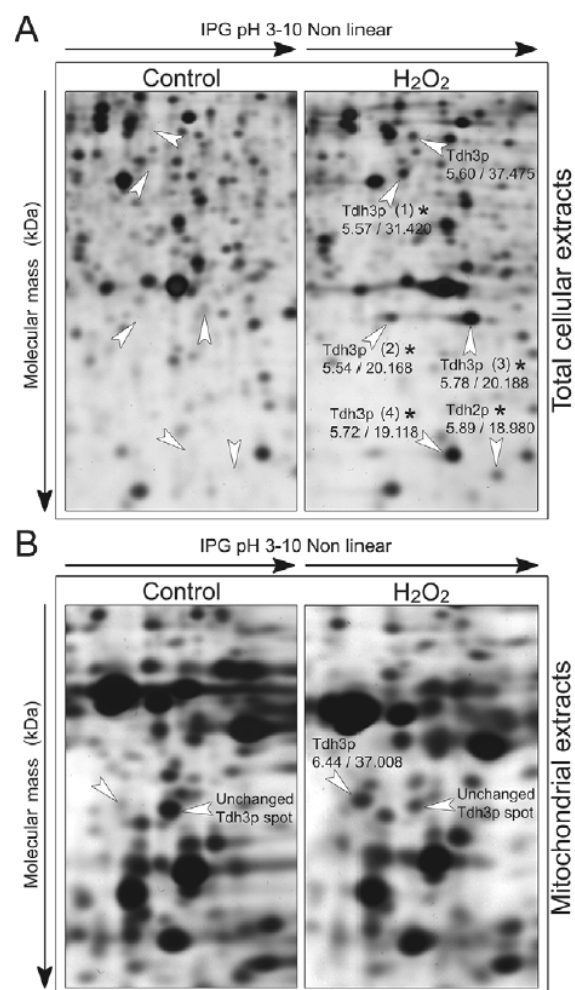


Fig. 6. GAPDH is extensively fragmented in H₂O₂-induced apoptotic cells. Comparison of protein expression levels in total cellular (A) and purified mitochondrial extracts (B) of untreated (control) and H₂O₂-treated wild-type cells. Selected regions of the 2-D gel (isoelectric point/molecular mass) are shown enlarged and the position of altered protein spots are marked with an arrowhead. The apparent isoelectric points and molecular masses of the proteins were calculated with Melanie 3.0 (GeneBio) using identified proteins with known parameters as a reference. Putative protein fragments are marked with an asterisk. Tdh3p fragments are numbered 1 to 4. For each Tdh3p and Tdh2p fragment, matched peptides obtained after trypsin digestion and used for identification of the proteins, as well as the amino acids specific for Tdh3p and Tdh2p, are shown in Fig. S1 in supplementary material.

Thiede and Rudel, 2004). Taking this into consideration, the analysis of cellular proteome under apoptotic conditions might produce useful information for the identification of apoptotic regulators and effectors. In our work, we examined the total and mitochondrial proteome of H₂O₂-induced apoptotic yeast cells. Proteomic analysis revealed the activation of stress-induced pathways through the increased levels of proteins previously described to be involved in both oxidative and nitrosative stresses. In addition, different posttranslationally modified forms of GAPDH were shown to be present at

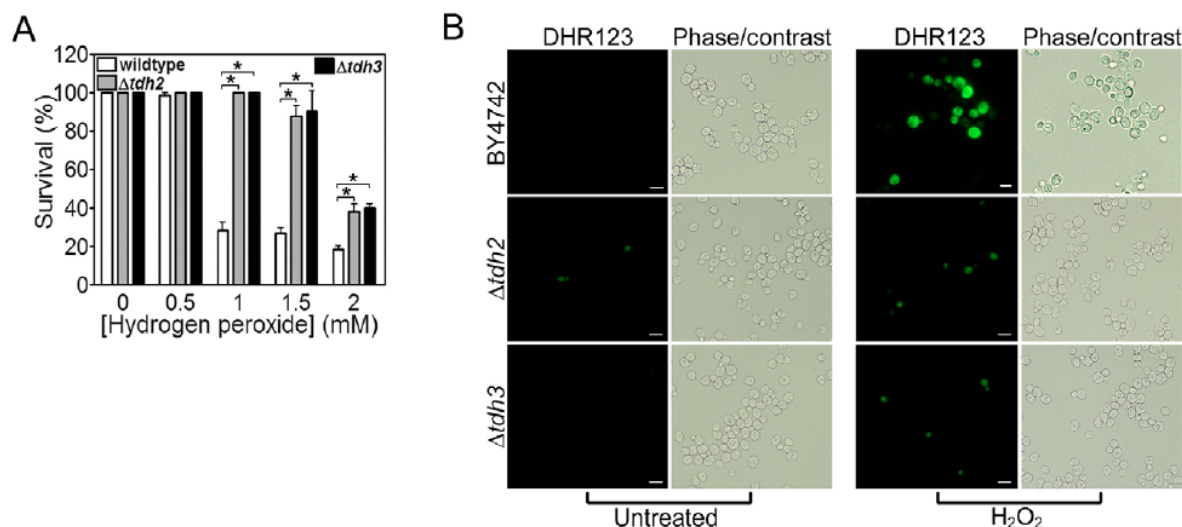


Fig. 7. Deletion of GAPDH isoform 2 and 3 prevents H_2O_2 -induced apoptosis. (A) Comparison of the survival of wild-type, $\Delta tdh2$ and $\Delta tdh3$ cells upon H_2O_2 treatment, $*P \leq 0.03$ versus wild type, t -test, $n=3$. (B) Epifluorescence and phase-contrast micrographs of untreated and H_2O_2 -treated (1.5 mM) wild-type, $\Delta tdh2$ and $\Delta tdh3$ cells, stained with dihydrorhodamine 123 (DHR123) as an indicator of high intracellular ROS accumulation. Bar, 5 μ m.

increased levels, indicating that the activation of oxidative and nitrosative stress-induced pathways might have led to increased protein modifications, culminating in apoptotic cell death.

The observation of a nitrosative stress response, together with previous reports on endogenous NO production in yeast (Osorio et al., 2007), prompted us to examine the possibility of NO synthesis under H_2O_2 treatment. Our results show that H_2O_2 induces nitrosative stress as demonstrated by the indirect (measurement of nitrate concentration) and direct (NO-selective electrode and a NO-sensitive probe) detection of elevated intracellular NO levels, as well as by the detection of a NOS-like activity (classical methods used for mammalian cells). NO synthesis was found to be dependent on L-arginine and could be inhibited by the non-metabolized L-arginine

analogous, L-NAME. The endogenous NO synthesis during H_2O_2 -induced apoptosis, herein observed in yeast cells, has been previously described in mammalian cells, in which H_2O_2 activates endothelial NOS (Thomas et al., 2002), pointing to the conservation of some basic biochemical pathways activated/affected by H_2O_2 . It is also clear that NO levels are mediating the apoptotic cell death occurring during chronological life span. Given that a common feature of apoptotic cell death induced by H_2O_2 or age-associated cell death is the generation of ROS, and bearing in mind that menadione was found to promote endogenous NO synthesis (Osorio et al., 2007), the relevance of NO in yeast apoptotic programs is reinforced, pointing to the conservation of links between ROS and RNS (Espey et al., 2000). Nevertheless, the origin of NO in yeast cells is still unclear, mainly due to the lack of mammalian NOS orthologues in the yeast genome. Although Castello and coworkers (Castello et al., 2006) showed that yeast cell mitochondria are capable of NO synthesis independently of a NOS-like activity, our results,

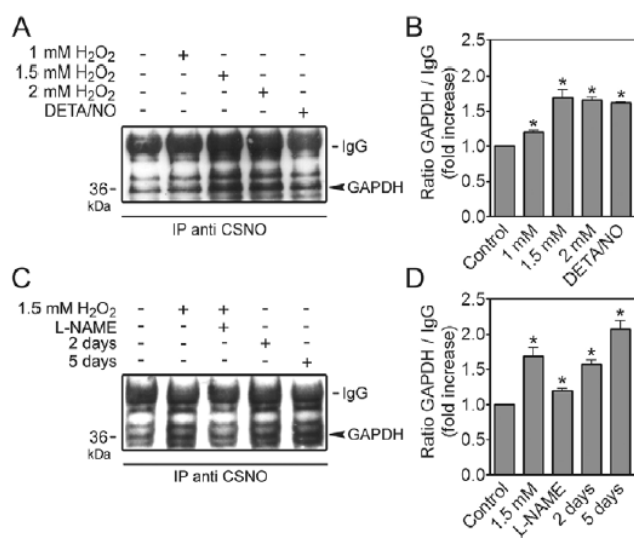


Fig. 8. GAPDH is S-nitrosated during H_2O_2 -induced apoptosis. (A) Detection of S-nitrosated GAPDH by immunoprecipitation using an anti-CSNO antibody in cell extracts from untreated cells, H_2O_2 -treated (1.0, 1.5 and 2.0 mM) cells and cells treated for 200 minutes with 2 mM of the NO donor diethylenetriamine/NO (DETA/NO). (B) Quantification of band intensity from A by densitometry. Band intensities were normalized to the intensity of IgG bands. Data express the GAPDH/IgG fold change in comparison to control (lane 1). $*P \leq 0.05$ versus control, t -test, $n=3$. (C) Immunoprecipitation of S-nitrosated GAPDH with an anti-CSNO antibody from cellular extracts of untreated, H_2O_2 -treated (1.5 mM), either in the absence or presence of L-NAME, or chronologically aged cultures (2 and 5 days). (D) Quantification of band intensity from C by densitometry. Band intensities were normalized to the intensity of IgG bands. Data express the GAPDH/IgG fold change in comparison to control (lane 1). $*P \leq 0.05$ versus control, t -test, $n=3$.

together with the physiological role of NO, point to the presence of a yet unknown protein(s) with NOS-like activity in yeast. Plants, like yeast, do not have a protein with sequence similarity to known mammalian-type NOS but display a NOS-like activity, indicating the presence of an enzyme structurally unrelated to those of their mammalian counterparts.

Diverse cellular functions can be affected by NO through posttranslational modification, particularly S-nitrosation of GAPDH, a key glycolytic enzyme that undergoes S-nitrosation and translocates to the nucleus, triggering apoptosis in mammalian cells (Hara et al., 2005). Our results show that following H₂O₂ stimulus, yeast GAPDH is a target of extensive proteolysis as revealed by the number of identified fragments. Further studies concerning the elucidation of the functional relationship of GAPDH fragmentation with its apoptotic role will be crucial for the understanding of the evolutionarily conserved multifunction of GAPDH.

GAPDH has been previously described to suffer different posttranslational modifications upon an oxidative stress insult, both as a target (Magherini et al., 2007) and as the most abundant yeast S-thiolated protein in response to H₂O₂ challenge (Shenton and Grant, 2003). Surprisingly, only the Tdh3p and not the Tdh2p GAPDH isoenzyme is modified (Grant et al., 1999). In addition, GAPDH Tdh3p isoenzyme was also described as suffering a redox-dependent and reversible S-glutathiolation (reviewed by Klatt and Lamas, 2000), with the formation of proteins with different mixed disulfides probably encompassing NO-dependent S-nitrosation of protein thiol groups. In this study we show that H₂O₂ or the NO donor DETA/NO lead to GAPDH S-nitrosation, revealing that yeast GAPDH is both S-nitrosated and S-glutathionylated as described for mammalian cells (Giustarini et al., 2005). This evidenced interrelationship between S-glutathiolation, thiol oxidation and nitrosation points to the formation of proteins with different mixed disulfides as a mechanism that integrates signalling by both oxidative and nitrosative stimuli (reviewed by Klatt and Lamas, 2000). Our results concerning NO synthesis, GAPDH fragmentation and S-nitrosation, together with the fact that ROS/RNS-induced S-glutathiolation is involved in the modulation of signal transduction pathways such as the regulation of proteolytic processing, ubiquitination and degradation of proteins (Klatt and Lamas, 2000), pinpoint yeast as an attractive model to uncover the emerging roles for ROS/RNS. Moreover, the role of GAPDH S-nitrosation seems to be of extreme importance for the yeast apoptotic process, since the blockage of GAPDH S-nitrosation by L-NAME is associated with decreased amounts of ROS within the cells, suggesting that S-nitrosated GAPDH also concurs with ROS generation, although by a mechanism that is still elusive, as it is in mammalian cells (Puttonen et al., 2006).

Altogether, our findings bring new insights into the evolutionarily conserved apoptotic pathways. Similarly to higher eukaryotes, yeast cells undergo apoptosis mediated by NO signalling, which places yeast as a powerful tool in the study of the mechanisms that determine cellular sensitivity to NO and for the elucidation of NO pro- and anti-apoptotic functions. Moreover, the finding that S-nitrosated GAPDH is involved in yeast apoptosis raises the possibility of future investigations using yeast cells to screen for drugs that directly act against S-nitrosated GAPDH.

Materials and Methods

Strains, media and treatments

S. cerevisiae strain BY4742 (*MAT α his3 Δ 1 leu2 Δ 0 lys2 Δ 0 ura3 Δ 0*) and the respective knockouts in the *TDH2* and *TDH3* genes (EUROSCARF, Frankfurt, Germany) were used. For H₂O₂ treatment, yeast cells were grown until the early stationary growth phase in liquid YPD medium containing glucose (2%, w/v), yeast extract (0.5%, w/v) and peptone (1%, w/v). Cells were then harvested and suspended (10⁷ cells/ml) in fresh YPD medium followed by the addition of 0.5, 1.0, 1.5 and 2.0 mM H₂O₂ and incubation for 200 minutes at 26°C with stirring (150 r.p.m.), as previously described (Madero et al., 1999). After treatment, 300 cells were spread on YPD agar plates and viability was determined by counting colony-forming units (c.f.u.) after 2 days of incubation at 26°C. For proteomic analysis, experiments were performed in YPD medium and an equitoxic dose of H₂O₂ was used which induced 50% of apoptotic cell death, as evaluated by TUNEL assay after 200 minutes (data not shown). For determination of NOS activity and kinetic measurement of NO production with the NO-selective electrode, cells were treated for a shorter period using higher H₂O₂ concentrations (3 and 4 mM) in order to induce 50% of apoptotic cell death. For acetic acid treatment, yeast cells were grown until the early stationary growth phase as described previously (Ludovico et al., 2002), harvested and suspended in YPD medium (pH 3.0 set with HCl) containing 0, 160 and 180 mM of acetic acid. Treatments were carried out for 200 minutes at 26°C. Viability was determined by c.f.u. counts as described above.

For determination of chronological life span and growth rates, cells were grown on synthetic complete (SC) medium containing glucose (2%, w/v), yeast nitrogen base (Difco) (0.17%, w/v), (NH₄)₂SO₄ (0.5%, w/v) and 30 mg/l of all amino acids (except 80 mg/l histidine and 200 mg/l leucine), 30 mg/l adenine and 320 mg/l uracil. For chronological aging experiments, cells were inoculated to an OD₆₀₀=0.1, oxyhaemoglobin (OxyHb) was added at the indicated concentrations (day 0) and viability was determined by counting c.f.u. For determination of proliferation rates, cells were inoculated to 5×10⁵ cells/ml, OxyHb was added and cell number was determined using a CASY cell counter.

Bax expression was induced as described before (Madero et al., 1999). In brief, strain BY4742 was transformed with plasmid pSD10.a-Bax (Madero et al., 1999), which contains murine bax under the control of a hybrid GAL1-10/CYC1 promoter; originating strain BY.bax. Individual clones were pre-grown overnight in SC medium with glucose (2%, w/v) until exponential growth phase. To induce bax expression, cells were washed three times with water and resuspended in SC medium with galactose (2%, w/v). Cells were then incubated at 26°C with stirring (150 r.p.m.) for 15 hours. Viability was determined by c.f.u. counts as described above.

2-D gel electrophoresis

For analysis of total cell extracts, cells were collected and washed twice with 2 ml TE buffer (1 mM EDTA, 0.1 M Tris-HCl pH 7.5, complete mini protease inhibitor; Roche Applied Science, Mannheim, Germany). Cells were disrupted using a French Press with 900 p.s.i. (62.1 bar) and the cell lysate centrifuged. For analysis of mitochondrial extracts, cells were collected and mitochondria isolated and purified as previously described (Meisinger et al., 2000). Protein concentrations were determined with a commercially available kit (RotiNanquant, C. Roth, Karlsruhe, Germany) and protein aliquots of total cell extracts, as well as mitochondrial extracts, (100 µg, 600 µg) were stored at -20°C. For two dimensional (2-D) gel electrophoresis the protein pellet was resuspended in urea buffer [8 M urea, 2 M thiourea, 1% (w/v) CHAPS, 20 mM 1,4-dithio-DL-threitol, 0.8% (v/v) carrier ampholytes], and complete mini protease inhibitor. The protein separation was done as previously described (Gorg et al., 1995). Briefly, the protein solution was adjusted with urea buffer to a final volume of 350 µl and in-gel rehydration performed overnight. Isoelectric focusing was carried out in IPG strips (pH 3-10, non linear, 18 cm; Amersham Biosciences, Uppsala, Sweden) with the Multiphor II system (Amersham Biosciences) under paraffin oil for 55 kVh. SDS-PAGE was done overnight in 12.5% T, 2.6% C polyacrylamide gels using the Ettan DALT II system (Amersham Biosciences) at 1-2 W per gel and 12°C. The gels were silver stained and analyzed with the 2-D PAGE image analysis software Melanie 3.0 (GeneBio, Geneva, Switzerland). The apparent isoelectric points (pI) and molecular masses (in kDa) of the proteins were calculated with Melanie 3.0 (GeneBio) using identified proteins with known parameters as a reference. An expression change was considered significant if the intensity of the corresponding spot reproducibly differed more than threefold.

Identification of altered proteins by mass spectrometry

Excised spots were in-gel digested and identified from the peptide fingerprints as described elsewhere (Gorg et al., 1995). Proteins were identified with the ProFound database, version 2005.02.14 (<http://prowl.rockefeller.edu/prowl/cgi/profound.exe>) using the parameters: 20 ppm; 1 missed cut; MH⁺; +C₂H₂O₂@C (Complete), +O@M (Partial). The identification of a protein was accepted if the peptides (mass tolerance 20 ppm) covered at least 30% of the complete sequence. Sequence coverage between 30% and 20% or sequence coverage below 20% for protein fragments was only accepted if at least two main peaks of the mass spectrum matched with the sequence and the number of weak-intensity peaks was clearly

reduced. The spot-specific peptides in the mass spectrum were also analyzed to confirm which parts of the corresponding protein sequence matched with these peptides, indicating putative fragmentation. This comparison reveals that spots presenting putative fragments lacked peptides observed in the mass spectrum of the whole protein. Thus, the spot position observed by 2-D gel electrophoresis and the specific peptides in the corresponding mass spectrum were analyzed to define the spot as intact protein or putative fragment. Distinction between GAPDH isoform 2 and 3 (Tdh2p and Tdh3p) was possible by the identification of amino acids present in the matched peptides that are specific for each GAPDH isoform.

Epifluorescence microscopy and flow cytometry analysis

Images were acquired using an Olympus BX61 microscope equipped with a high-resolution DP70 digital camera and using an Olympus PlanApo 60 \times oil objective, with a numerical aperture of 1.42. All the samples were suspended in PBS and visualized at room temperature.

Flow cytometry assays were performed on an EPICS XL-MCL flow cytometer (Beckman-Coulter Corporation, USA), equipped with an argon-ion laser emitting a 488 nm beam at 15 mW. Twenty thousand cells per sample were analyzed. The data were analyzed with the Multigraph software included in the system II acquisition software for the EPICS XL/XL-MCL version 1.0.

Assessment of intracellular reactive oxygen species (ROS)

Free intracellular ROS were detected with dihydrorhodamine 123 (DHR123) (Molecular Probes, Eugene, OR, USA). DHR123 was added from a 1 mg/ml stock solution in ethanol, to 5×10^6 cells/ml suspended in PBS, reaching a final concentration of 15 μ g/ml. Cells were incubated for 90 minutes at 30°C in the dark, washed in PBS and visualized by epifluorescence microscopy. For dihydroethidium (DHE) staining, 5×10^6 cells were harvested by centrifugation, resuspended in 250 μ l of 2.5 μ g/ml DHE in PBS and incubated in the dark for 5 minutes. Relative fluorescence units (RFU) were determined using a fluorescence reader (Tecan, GeniusPROTM).

Indirect assessment of NO levels through nitrate concentration measurement

Nitrite and nitrate concentration was measured spectrophotometrically using the Griess-reagent. Sodium nitrite (0, 1.0, 2.0, 3.0, 5.0, 10, 15, 20 μ M) was used as standard. For the reagent, 20 mg *N*-1-naphthylethylenediamine dihydrochloride, 200 mg sulfanilamide and 2.8 g HCl (36%) was dissolved in 17.2 g water. Individual supernatant samples (100 μ l) were mixed with 100 μ l reagent and the concentration recorded. For nitrate concentration, 100 μ l of vanadium (III) chloride (8 mg/ml 1 M HCl) was added, thus reducing any existent nitrate to nitrite. After incubation (90 minutes at 37°C) the concentration was recorded again. Nitrate concentration was calculated as the difference between the two measurements. Since NO is a diffusible free radical rapidly oxidized to nitrate and nitrite, the nitrate concentration obtained was assumed to be correlated to the amount of NO synthesized by the cells.

Direct assessment of NO levels

Intracellular NO levels upon H₂O₂ treatment, with or without the inhibition of NO production by the non-metabolized L-arginine analogue, N_G-nitro-L-arginine methyl ester (L-NAME; Sigma-Aldrich) were assessed by flow cytometry using the NO-sensitive probe 4-amino-5-methylamino-2',7'-difluorescein (DAF-FM) diacetate (Molecular Probes, Eugene, OR, USA). After treatment, 3×10^7 cells were harvested, washed and suspended in PBS, pH 7.4. Cells were then incubated for 30 minutes at room temperature, with DAF-FM diacetate (5 μ M).

NO production was kinetically measured using the AmiNO-700 Nitric Oxide Sensor with inNO Model-T – Nitric Oxide Measuring System (Innovative Instruments, Inc., Florida, USA). This NO electrode is specific to NO and has the detection limit of 0.1 nM, which is 20 times more sensitive than that of the ISO-NO electrode (World Precision Instruments, Florida, USA). For NO measurement, 5×10^8 cells (with or without pre-incubation with D-arginine or L-NAME, to inhibit NO production) were washed, resuspended in 3 ml of Tris buffer (10 mM Tris-HCl, pH 7.4) and transferred to a recording cell chamber with agitation, under aerobic conditions, followed by addition of 4 mM H₂O₂. A negative control consisting of Tris buffer without cells was also included to exclude possible H₂O₂ interferences with the electrode. Amperometric currents originated from the oxidation of NO at the electrode surface were recorded at +0.9 V. The electrode was calibrated in 100 mM KI-H₂SO₄ with stock solutions of nitrite according to the manufacturer's instructions.

Inhibition of NO production

For inhibition of NO production, cells were pre-incubated, for 1 hour, with L-NAME (200 mM) in YPD medium or pre-incubated for 1 hour with 0.4 mg/ml D-arginine. A high concentration of L-NAME was used throughout the work because of the presence of a cell wall in yeast cells.

Determination of NOS activity

The conversion of L-[³H]arginine to [³H]citrulline (NOS activity) was monitored using a highly sensitive Nitric Oxide Synthase Assay Kit (Calbiochem) with minor

changes from the supplied protocol. Untreated or H₂O₂-treated yeast cells were harvested, washed in double-distilled water and resuspended in 25 mM Tris-HCl, pH 7.4; 1 mM EDTA and 1 mM EGTA. Yeast protein extracts were obtained by vortexing in the presence of 1 g of glass beads and used immediately after. 10 μ l of protein extract (2 μ g/ μ l) were added to 40 μ l of reaction buffer with 1 μ Ci of L-[³H]arginine (60 Ci/mmol), 6 μ M tetrahydrobiopterin, 2 μ M FAD, 2 μ M FMN, 1 mM NADPH, 0.6 mM CaCl₂ in 50 mM Tris-HCl, pH 7.4. After 60 minutes of incubation, 400 μ l of EDTA buffer (50 mM Hepes pH 5.5, 5 mM EDTA) were added. In order to separate L-arginine from citrulline, 100 μ l of equilibrated L-arginine-binding resin was added and samples were applied to spin cup columns and centrifuged. Citrulline quantification was performed by liquid scintillation spectroscopy of the flow-through. The radioactivity obtained from a negative control consisting of yeast extract boiled for 20 minutes was subtracted from all the samples to remove background radioactivity. Data are expressed as the percentage of conversion of L-[³H]arginine to [³H]citrulline and represent the average of four independent experiments.

Quantification of intracellular amino acids

For the intracellular amino acid quantification, untreated and H₂O₂-treated cells were disrupted as described above. Proteins were removed from the samples by TCA precipitation followed by sulfosalicylic acid clean-up and filtration. Samples were then analyzed by ion exchange column chromatography followed by post-column ninhydrin derivatization on an automated amino acid analyzer (Biochrome 30, Amersham Pharmacia Biotech, Cambridge, UK).

Detection of S-nitrosated GAPDH

S-nitrosated GAPDH was detected by immunoprecipitation with an anti-nitrosocysteine (CSNO) antibody. Briefly, untreated, H₂O₂-treated with or without pre-incubation with L-NAME, and aged cells were disrupted using glass beads as previously described (Gourlay et al., 2003). As a positive control, cellular nitrosative stress was induced by the NO donor (Cahuana et al., 2004; Horan et al., 2006) diethylenetriamine/NO (DETA/NO, Sigma-Aldrich). The treatment with a NO donor facilitated the increase of intracellular NO levels allowing the determination of GAPDH S-nitrosation independent of H₂O₂. Thus, cells were incubated for 200 minutes with 2 mM of DETA/NO. One mg of cell lysate was mixed with rabbit anti-S-nitrosocysteine antibody (Sigma-Aldrich) at a dilution of 1:160 and incubated at 4°C with rotation for 4 hours. Protein G plus/protein A-agarose beads were added and rotated overnight at 4°C. Immunoprecipitated proteins were then resolved on a 10% SDS gel and transferred to a PVDF membrane before being probed with a monoclonal mouse anti-GAPDH antibody (MAB474, Chemicon) at a dilution of 1:200. A horseradish peroxidase-conjugated anti-mouse IgG secondary antibody was used (Chemicon) at a dilution of 1:5000 and detected by enhanced chemiluminescence.

Statistical analysis

The arithmetic means are given with standard deviation with 95% confidence value. Statistical analyses were carried out using independent samples *t*-test analysis. A *P* value less than 0.05 was considered to denote a significant difference.

We thank M. Teixeira da Silva, Tiago Fleming Outeiro, Elsa Logarinho, Agostinho Almeida and Ulrich Bergmann for all the helpful suggestions and for critical reading of the manuscript. We are grateful to Eeva-Liisa Stefanus for excellent assistance. This work was supported by a grant from FCT-Fundação para a Ciência e a Tecnologia (POCI/BIA-BCM/57364/2004). B.A. has a fellowship from FCT (SFRH/BD/15317/2005). We are also grateful to FWF for a Lipotox grant to F.M. and B.M. and for grant no. S-9304-B05 to F.M. and S.B.

References

- Balcerczyk, A., Soszynski, M. and Bartosz, G. (2005). On the specificity of 4-amino-5-methylamino-2',7'-difluorofluorescein as a probe for nitric oxide. *Free Radic. Biol. Med.* 39, 327-335.
- Barr, S. D. and Gedamu, L. (2003). Role of peroxidoxins in *Leishmania chagasi* survival. Evidence of an enzymatic defense against nitrosative stress. *J. Biol. Chem.* 278, 10816-10823.
- Belenghi, B., Romero-Puertas, M. C., Vercammen, D., Brackener, A., Inze, D., Delledonne, M. and Van Breusegem, F. (2007). Metacaspase activity of *Arabidopsis thaliana* is regulated by S-nitrosylation of a critical cysteine residue. *J. Biol. Chem.* 282, 1352-1358.
- Brune, B., Messmer, U. K. and Sandau, K. (1995). The role of nitric oxide in cell injury. *Toxicol. Lett.* 82-83, 233-237.
- Cahuana, G. M., Tejedo, J. R., Jimenez, J., Ramirez, R., Sobrino, F. and Bedoya, F. J. (2004). Nitric oxide-induced carbonylation of Bcl-2, GAPDH and ANT precedes apoptotic events in insulin-secreting RINm5F cells. *Exp. Cell Res.* 293, 22-30.
- Castello, P. R., David, P. S., McClure, T., Crook, Z. and Poyton, R. O. (2006). Mitochondrial cytochrome oxidase produces nitric oxide under hypoxic conditions:

- implications for oxygen sensing and hypoxic signaling in eukaryotes. *Cell Metab.* **3**, 277-287.
- Choi, B. M., Pae, H. O., Jang, S. I., Kim, Y. M. and Chung, H. T. (2002). Nitric oxide as a pro-apoptotic as well as anti-apoptotic modulator. *J. Biochem. Mol. Biol.* **35**, 116-126.
- Chuang, D. M., Hough, C. and Senatorov, V. V. (2005). Glyceraldehyde-3-phosphate dehydrogenase, apoptosis, and neurodegenerative diseases. *Annu. Rev. Pharmacol. Toxicol.* **45**, 269-290.
- Delledonne, M. (2005). NO news is good news for plants. *Curr. Opin. Plant Biol.* **8**, 390-396.
- Espey, M. G., Miranda, K. M., Feelisch, M., Fukuto, J., Grisham, M. B., Vitek, M. P. and Wink, D. A. (2000). Mechanisms of cell death governed by the balance between nitrosative and oxidative stress. *Ann. N. Y. Acad. Sci.* **899**, 209-221.
- Fabrizio, P., Battistella, L., Vardavas, R., Gattazzo, C., Liou, L. L., Diaspro, A., Dossen, J. W., Gralla, E. B. and Longo, V. D. (2004). Superoxide is a mediator of an altruistic aging program in *Saccharomyces cerevisiae*. *J. Cell Biol.* **166**, 1055-1067.
- Ferri, K. F. and Kroemer, G. (2001). Organelle-specific initiation of cell death pathways. *Nat. Cell Biol.* **3**, E255-E263.
- Garrido, E. O. and Grant, C. M. (2002). Role of thioredoxins in the response of *Saccharomyces cerevisiae* to oxidative stress induced by hydroperoxides. *Mol. Microbiol.* **43**, 993-1003.
- Giustarini, D., Milzani, A., Aldini, G., Carini, M., Rossi, R. and Dalle-Donne, I. (2005). S-nitrosation versus S-glutathionylation of protein sulphydryl groups by S-nitroso-glutathione. *Antioxid. Redox Signal.* **7**, 930-939.
- Gorg, A., Boguth, G., Obermaier, C., Posch, A. and Weiss, W. (1995). Two-dimensional polyacrylamide gel electrophoresis with immobilized pH gradients in the first dimension (IPG-Dalt): the state of the art and the controversy of vertical versus horizontal systems. *Electrophoresis* **16**, 1079-1086.
- Gourlay, C. W., Dewar, H., Warren, D. T., Costa, R., Satish, N. and Ayscough, K. R. (2003). An interaction between Sla1p and Sla2p plays a role in regulating actin dynamics and endocytosis in budding yeast. *J. Cell Sci.* **116**, 2551-2564.
- Grant, C. M., Quinn, K. A. and Dawes, I. W. (1999). Differential protein S-thiolation of glyceraldehyde-3-phosphate dehydrogenase isoenzymes influences sensitivity to oxidative stress. *Mol. Cell Biol.* **19**, 2650-2656.
- Hara, M. R., Agrawal, N., Kim, S. F., Cascio, M. B., Fujimuro, M., Ozeki, Y., Takahashi, M., Cheah, J. H., Tankou, S. K., Hester, L. D. et al. (2005). S-nitrosylated GAPDH initiates apoptotic cell death by nuclear translocation following Siah1 binding. *Nat. Cell Biol.* **7**, 665-674.
- Hess, D. T., Matsumoto, A., Kim, S. O., Marshall, H. E. and Stamler, J. S. (2005). Protein S-nitrosylation: purview and parameters. *Nat. Rev. Mol. Cell Biol.* **6**, 150-166.
- Horan, S., Bourges, I. and Meunier, B. (2006). Transcriptional response to nitrosative stress in *Saccharomyces cerevisiae*. *Yeast* **23**, 519-535.
- Ignarro, L. J., Buga, G. M., Wood, K. S., Byrns, R. E. and Chaudhuri, G. (1987). Endothelium-derived relaxing factor produced and released from artery and vein is nitric oxide. *Proc. Natl. Acad. Sci. USA* **84**, 9265-9269.
- Joshi, M. S., Ferguson, T. B., Jr, Han, T. H., Hyduke, D. R., Liao, J. C., Rassaf, T., Bryan, N., Feelisch, M. and Lancaster, J. R., Jr (2002). Nitric oxide is consumed, rather than conserved, by reaction with oxyhemoglobin under physiological conditions. *Proc. Natl. Acad. Sci. USA* **99**, 10341-10346.
- Kelm, M., Preik, M., Hafner, D. J. and Strauer, B. E. (1996). Evidence for a multifactorial process involved in the impaired flow response to nitric oxide in hypertensive patients with endothelial dysfunction. *Hypertension* **27**, 346-353.
- Klatt, P. and Lamas, S. (2000). Regulation of protein function by S-glutathiolation in response to oxidative and nitrosative stress. *Eur. J. Biochem.* **267**, 4928-4944.
- Kroncke, K. D., Fehsel, K. and Kolb-Bachofen, V. (1995). Inducible nitric oxide synthase and its product nitric oxide, a small molecule with complex biological activities. *Biol. Chem. Hoppe-Seyler* **376**, 327-343.
- Lee, J., Spector, D., Godon, C., Labarre, J. and Toledano, M. B. (1999). A new antioxidant with alkyl hydroperoxide defense properties in yeast. *J. Biol. Chem.* **274**, 4537-4544.
- Liu, L., Zeng, M., Hausladen, A., Heitman, J. and Stamler, J. S. (2000). Protection from nitrosative stress by yeast flavohemoglobin. *Proc. Natl. Acad. Sci. USA* **97**, 4672-4676.
- Ludovico, P., Rodrigues, F., Almeida, A., Silva, M. T., Barrientos, A. and Corte-Real, M. (2002). Cytochrome c release and mitochondria involvement in programmed cell death induced by acetic acid in *Saccharomyces cerevisiae*. *Mol. Biol. Cell* **13**, 2598-2606.
- Madeo, F., Frohlich, E., Ligr, M., Grey, M., Sigrist, S. J., Wolf, D. H. and Frohlich, K. U. (1999). Oxygen stress: a regulator of apoptosis in yeast. *J. Cell Biol.* **145**, 757-767.
- Madeo, F., Herker, E., Maldener, C., Wissing, S., Lachelt, S., Herlan, M., Fehr, M., Lauber, K., Sigrist, S. J., Wesselborg, S. et al. (2002). A caspase-related protease regulates apoptosis in yeast. *Mol. Cell* **9**, 911-917.
- Magherini, F., Tani, C., Gamberi, T., Caselli, A., Bianchi, L., Bini, L. and Modesti, A. (2007). Protein expression profiles in *Saccharomyces cerevisiae* during apoptosis induced by H₂O₂. *Proteomics* **7**, 1434-1445.
- Meisinger, C., Sommer, T. and Pfanner, N. (2000). Purification of *Saccharomyces cerevisiae* mitochondria devoid of microsomal and cytosolic contaminations. *Anal. Biochem.* **287**, 339-342.
- Missall, T. A. and Lodge, J. K. (2005). Thioredoxin reductase is essential for viability in the fungal pathogen *Cryptococcus neoformans*. *Eukaryotic Cell* **4**, 487-489.
- Nathan, C. (1992). Nitric oxide as a secretory product of mammalian cells. *FASEB J.* **6**, 3051-3064.
- Ohlmeier, S., Kastaniotis, A. J., Hiltunen, J. K. and Bergmann, U. (2004). The yeast mitochondrial proteome, a study of fermentative and respiratory growth. *J. Biol. Chem.* **279**, 3956-3979.
- Osoorio, N. S., Carvalho, A., Almeida, A. J., Padilla-Lopez, S., Leao, C., Laranjinha, J., Ludovico, P., Pearce, D. A. and Rodrigues, F. (2007). Nitric oxide signaling is disrupted in the yeast model for Batten disease. *Mol. Biol. Cell* **18**, 2755-2767.
- Packer, M. A., Porteous, C. M. and Murphy, M. P. (1996). Superoxide production by mitochondria in the presence of nitric oxide forms peroxynitrite. *Biochem. Mol. Biol. Int.* **40**, 527-534.
- Palmer, R. M., Ferrige, A. G. and Moncada, S. (1987). Nitric oxide release accounts for the biological activity of endothelium-derived relaxing factor. *Nature* **327**, 524-526.
- Pedrajas, J. R., Miranda-Vizuete, A., Javanmard, N., Gustafsson, J. A. and Spyrou, G. (2000). Mitochondria of *Saccharomyces cerevisiae* contain one-conserved cysteine type peroxiredoxin with thioredoxin peroxidase activity. *J. Biol. Chem.* **275**, 16296-16301.
- Pietraforte, D., Mallozzi, C., Scorza, G. and Minetti, M. (1995). Role of thiols in the targeting of S-nitroso thiols to red blood cells. *Biochemistry* **34**, 7177-7185.
- Porter, A. G. (1999). Protein translocation in apoptosis. *Trends Cell Biol.* **9**, 394-401.
- Prouzet-Mauleon, V., Monribot-Espagne, C., Boucherie, H., Lagniel, G., Lopez, S., Labarre, J., Garin, J. and Lauquin, G. J. (2002). Identification in *Saccharomyces cerevisiae* of a new stable variant of alkyl hydroperoxide reductase 1 (Ahp1) induced by oxidative stress. *J. Biol. Chem.* **277**, 4823-4830.
- Puttonen, K. A., Lehtonen, S., Raasmaja, A. and Mannisto, P. T. (2006). A prolyl oligopeptidase inhibitor, Z-Pro-Prolinal, inhibits glyceraldehyde-3-phosphate dehydrogenase translocation and production of reactive oxygen species in CV1-P cells exposed to 6-hydroxydopamine. *Toxicol. In Vitro* **20**, 1446-1454.
- Sahoo, R., Sengupta, R. and Ghosh, S. (2003). Nitrosative stress on yeast: inhibition of glyoxalase-I and glyceraldehyde-3-phosphate dehydrogenase in the presence of GSNO. *Biochem. Biophys. Res. Commun.* **302**, 665-670.
- Shenton, D. and Grant, C. M. (2003). Protein S-thiolation targets glycolysis and protein synthesis in response to oxidative stress in the yeast *Saccharomyces cerevisiae*. *Biochem. J.* **374**, 513-519.
- Stamler, J. S., Lamas, S. and Fang, F. C. (2001). Nitrosylation: the prototypic redox-based signaling mechanism. *Cell* **106**, 675-683.
- Suarez, M. F., Filonova, L. H., Smertenko, A., Savenkov, E. I., Clapham, D. H., von Arnold, S., Zhivotovsky, B. and Bozhkov, P. V. (2004). Metacaspase-dependent programmed cell death is essential for plant embryogenesis. *Curr. Biol.* **14**, R339-R340.
- Thiede, B. and Rudel, T. (2004). Proteomic analysis of apoptotic cells. *Mass Spectrom. Rev.* **23**, 333-349.
- Thomas, S. R., Chen, K. and Keaney, J. F., Jr (2002). Hydrogen peroxide activates endothelial nitric-oxide synthase through coordinated phosphorylation and dephosphorylation via a phosphoinositide 3-kinase-dependent signaling pathway. *J. Biol. Chem.* **277**, 6017-6024.
- Wennmalm, A., Benthin, G. and Petersson, A. S. (1992). Dependence of the metabolism of nitric oxide (NO) in healthy human whole blood on the oxygenation of its red cell haemoglobin. *Br. J. Pharmacol.* **106**, 507-508.
- Wong, C.-M., Zhou, Y., Ng, R. W., Kung, H.-f. and Jin, D. Y. (2002). Cooperation of yeast peroxiredoxins Tsa1p and Tsa2p in the cellular defense against oxidative and nitrosative stress. *J. Biol. Chem.* **277**, 5385-5394.
- Wong, C. M., Siu, K. L. and Jin, D. Y. (2004). Peroxiredoxin-null yeast cells are hypersensitive to oxidative stress and are genomically unstable. *J. Biol. Chem.* **279**, 23207-23213.
- Zamzami, N., Marchetti, P., Castedo, M., Decaudin, D., Macho, A., Hirsch, T., Susin, S. A., Petit, P. X., Mignotte, B. and Kroemer, G. (1995). Sequential reduction of mitochondrial transmembrane potential and generation of reactive oxygen species in early programmed cell death. *J. Exp. Med.* **182**, 367-377.
- Zelenaya-Troitskaya, O., Perlman, P. S. and Butow, R. A. (1995). An enzyme in yeast mitochondria that catalyzes a step in branched-chain amino acid biosynthesis also functions in mitochondrial DNA stability. *EMBO J.* **14**, 3268-3276.

ATTACHMENT III

Weinberger M., Mesquita A., Carroll T., Marks L., Yang H., Zhang Z., Ludovico P., Burhans W.C.. Growth signaling promotes chronological aging in budding yeast by inducing superoxide anions that inhibit quiescence. *Aging* (Albany NY). 2010 Oct;2(10):709-26.

Growth signaling promotes chronological aging in budding yeast by inducing superoxide anions that inhibit quiescence

Martin Weinberger¹, Ana Mesquita², Timothy Carroll¹, Laura Marks¹, Hui Yang³, Zhaojie Zhang³, Paula Ludovico², and William C. Burkans¹

¹ Department of Molecular and Cellular Biology, Roswell Park Cancer Institute, Buffalo, NY 14263, USA

² Instituto de Investigação em Ciências da Vida e Saúde (ICVS), Escola de Ciências da Saúde, Universidade do Minho, Campus de Gualtar, 4710-057 Braga, Portugal

³ Department of Zoology and Physiology, University of Wyoming, Laramie, WY 82071, USA

Key words: oxidative stress, replication stress, lifespan, caloric restriction, hydrogen peroxide

Received: 10/14/10; **accepted:** 10/25/10; **published on line:** 10/27/10

Corresponding author: William C. Burkans, PhD; **E-mail:** wburhans@buffalo.edu

Copyright: © Weinberger et al. This is an open-access article distributed under the terms of the Creative Commons Attribution License, which permits unrestricted use, distribution, and reproduction in any medium, provided the original author and source are credited

Abstract: Inhibition of growth signaling pathways protects against aging and age-related diseases in parallel with reduced oxidative stress. The relationships between growth signaling, oxidative stress and aging remain unclear. Here we report that in *Saccharomyces cerevisiae*, alterations in growth signaling pathways impact levels of superoxide anions that promote chronological aging and inhibit growth arrest of stationary phase cells in G0/G1. Factors that decrease intracellular superoxide anions in parallel with enhanced longevity and more efficient G0/G1 arrest include genetic inactivation of growth signaling pathways that inhibit Rim15p, which activates oxidative stress responses, and downregulation of these pathways by caloric restriction. Caloric restriction also reduces superoxide anions independently of Rim15p by elevating levels of H₂O₂, which activates superoxide dismutases. In contrast, high glucose or mutations that activate growth signaling accelerate chronological aging in parallel with increased superoxide anions and reduced efficiency of stationary phase G0/G1 arrest. High glucose also activates DNA damage responses and preferentially kills stationary phase cells that fail to arrest growth in G0/G1. These findings suggest that growth signaling promotes chronological aging in budding yeast by elevating superoxide anions that inhibit quiescence and induce DNA replication stress. A similar mechanism likely contributes to aging and age-related diseases in complex eukaryotes.

INTRODUCTION

Inhibition of growth signaling by caloric restriction (CR) or mutational inactivation of conserved insulin/IGF-1-like and Target of Rapamycin (TOR) signaling pathways prolongs the lifespans of eukaryotic organisms as diverse as yeasts and humans. In complex eukaryotes, inhibition of growth signaling also protects against age-related diseases, including cancer, cardiovascular disease and neurodegenerative disorders [1]. The lifespan-extending effects of reduced growth signaling occur in parallel with the induction of oxidative stress responses that reduce levels of reactive oxygen species (ROS) and oxidative damage to macro-

molecules. This is consistent with the longstanding free radical theory of aging, which posits oxidative damage to macromolecules as a primary determinant of lifespan [2].

A number of recent studies have investigated the impact of conserved growth signaling pathways on chronological lifespan (CLS) in the model organism *Saccharomyces cerevisiae* (budding yeast). CLS of this organism is determined by measuring the length of time cells maintain viability or reproductive capacity after nutrient depletion induces a stationary phase growth arrest. Growth arrest in stationary phase mimics the quiescent, postmitotic state that occurs in higher

eukaryotes when growth-signaling pathways are downregulated during differentiation. The results of many of these studies support the free radical theory. For example, CLS is extended by inactivation of the budding yeast *SCH9* gene encoding a homologue of the mammalian AKT protein [3]. Stationary phase *sch9Δ* cells express elevated levels of the Mn-dependent superoxide dismutase Sod2p [4] and exhibit lower levels of superoxide anions (O_2^-) [5]. CLS is also extended by inactivation of the mammalian Ras homologue *RAS2* via a mechanism that depends on Sod2p [4] and by inactivation of conserved TOR growth signaling pathways, which also leads to a reduction in levels of O_2^- [5, 6]. When active, Tor1p, Sch9p and Ras2p inhibit the Rim15p kinase and its induction of superoxide dismutases and other oxidative stress defenses, and reduced signaling through these pathways in calorie-restricted cells extends CLS in a Rim15p-dependent fashion [7]. CR or inactivation of catalases also extends CLS by inducing elevated levels of hydrogen peroxide (H_2O_2), which inhibits the accumulation of intracellular O_2^- by activating superoxide dismutases [8]. Conversely, a shorter CLS in concert with elevated levels of O_2^- have been detected in stationary phase budding yeast cells in which the cAMP phosphodiesterase Pde2p has been inactivated [9]. Pde2 inhibits Ras2p-dependent growth signaling, which is constitutively active in *pde2Δ* cells [10].

All of these findings are consistent with a role for oxidative stress produced in association with growth signaling through highly conserved AKT, TOR and RAS-dependent pathways as an important pro-aging factor in the budding yeast chronological aging model. Similar connections have been established between levels of ROS and growth signaling through AKT, mTOR and RAS-dependent pathways in more complex eukaryotes [11]. However, the mechanisms by which oxidative stress is increased by growth signaling and promotes aging remain unclear. For example, although some of the CLS-extending effects of CR in budding yeast depend on the induction of oxidative and other stress defenses by Rim15p, CR also extends CLS via an Sch9p, Ras2p and Rim15p-independent mechanism [7]. Furthermore, it was recently reported that chronological aging is caused by toxic effects of acetic acid that accumulate in the medium of stationary phase cultures. According to this model, CR or deletion of *SCH9* or *RAS2* extend CLS independently of effects on oxidative stress by inhibiting the accumulation of acetic acid (in the case of CR) or by creating resistance to acetic acid toxicity via unknown mechanisms (in the case of the deletion of *SCH9* or *RAS2*) [12]. In addition, inactivation of catalases extends CLS in parallel with increased levels of oxidative damage to proteins and other macromolecules despite a reduction

in intracellular O_2^- [8]. Although this latter finding is consistent with the model that O_2^- shortens CLS, it is not consistent with the free radical theory postulate that oxidative damage to macromolecules is a primary cause of aging.

DNA replication stress – i.e., inefficient DNA replication that causes DNA damage – in stationary phase budding yeast cells that fail to arrest in G0/G1 is an additional factor determining CLS of budding yeast. Growth arrest in G0/G1 prevents replication stress that arises when stationary phase cells arrest growth in S phase instead [13]. Experimental manipulations that shorten CLS and inhibit stationary phase growth arrest in G0/G1 include constitutive activation of Ras2p [13, 14] and mutational inactivation of Rim15p [15]. In contrast, CR or mutational inactivation of Ras2p or Sch9p promote a more frequent G0/G1 arrest of stationary phase budding yeast cells in concert with an extended CLS [13]. CR was also recently shown to extend the CLS of fission yeast (*S. pombe*) in association with more frequent growth arrest in G0/G1 [16].

To better understand the effects of growth signaling and CR on aging and how they relate to both oxidative and replication stress, in this study we examined levels of ROS in budding yeast stationary phase cells under a variety of experimental conditions in parallel with measurements of CLS and the frequency with which stationary phase cells growth arrest in G0/G1. Our findings indicate that in general, growth signaling enhances the age-dependent accumulation of O_2^- , and inhibition of growth signaling inhibits O_2^- accumulation. Furthermore, the reduction in O_2^- induced by elevated H_2O_2 in calorie-restricted cells occurs independently of Rim15p. Although CR inhibits the accumulation of acetic acid in stationary phase cultures under some conditions, it can also reduce intracellular levels of O_2^- and extend CLS in the absence of changes in levels of acetic acid. Factors that enhance the accumulation of O_2^- independently of acetic acid include elevated concentrations of glucose, which block the accumulation of H_2O_2 and selectively kill cells that fail to arrest in G0/G1 in stationary phase. Together, these findings suggest that growth signaling promotes aging in the chronological aging model in part by inducing O_2^- that inhibit the growth arrest of stationary phase cells in G0/G1, thus leading to DNA replication stress.

RESULTS

Caloric restriction or inactivation of growth signaling pathways reduces superoxide anions in stationary phase cells and enhances G0/G1 arrest

Chronological lifespan experiments require the establish-

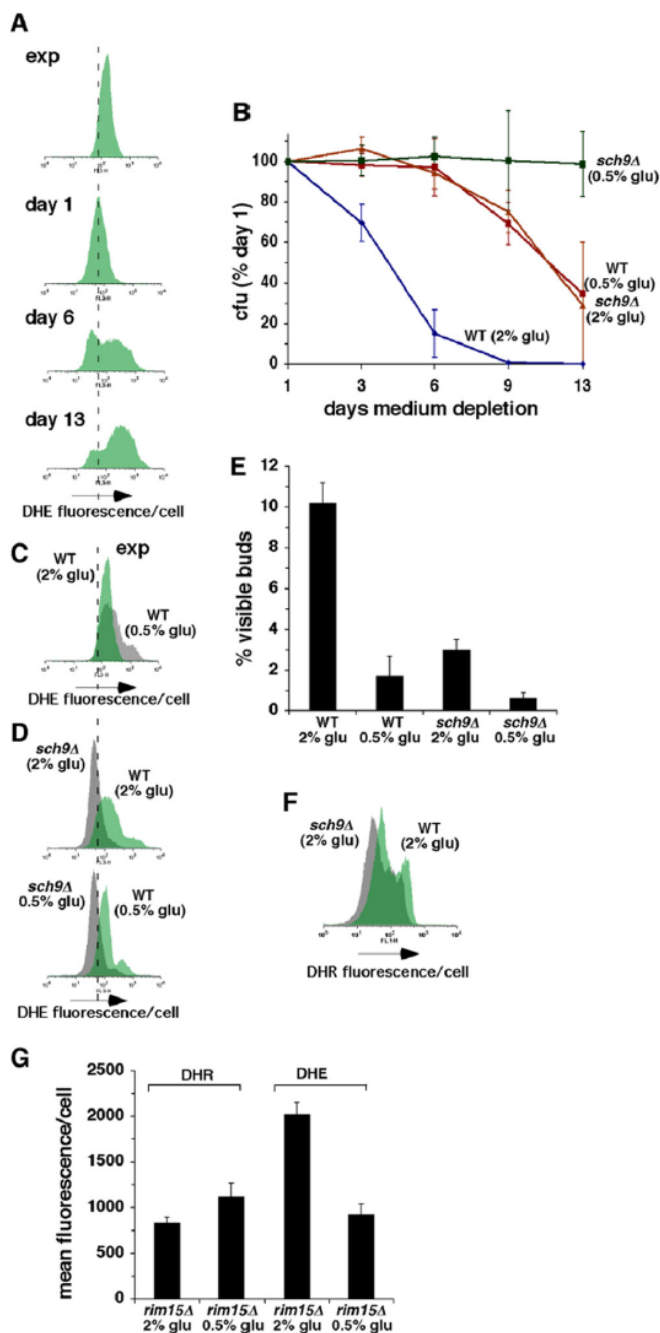


Figure 1. Inhibition of growth signaling pathways prolongs CLS in concert with reduced O_2^- and more frequent growth of stationary phase cells in G0/G1. (A) Levels of O_2^- detected by dihydroethidium (DHE) fluorescence in exponential cultures and stationary phase wild type cells. In this and subsequent figures, dashed vertical line through flow cytometry histograms provides an arbitrarily chosen reference point for comparing related histograms. (B) Effects of caloric restriction and/or inactivation of Sch9p on CLS. (C) Effect of caloric restriction on levels of O_2^- detected by DHE fluorescence in exponential cultures of wild type cells. (D) Effects of caloric restriction and/or inactivation of Sch9p on levels of O_2^- detected by DHE fluorescence in stationary phase cells at day 3 of medium depletion. (E) Effects of caloric restriction and/or inactivation of Sch9p on the fraction of stationary phase cells that failed to arrest in G0/G1 as measured by counting cells with visible buds at day 3 of medium depletion. (F) Levels of H_2O_2 detected in stationary phase wild type and *sch9Δ* cells by dihydrorhodamine 123 (DHR) fluorescence at day 3. (G) Levels of H_2O_2 detected by DHR fluorescence and O_2^- detected by DHE fluorescence in *rim15Δ* cells at day 3.

ment of exponentially dividing cultures of cells that eventually deplete nutrients from the medium, leading to entry into a non-dividing stationary phase state a few days later. Compared to exponential cultures, intracellular levels of O_2^- detected by the fluorescent probe dihydroethidium (DHE), which can detect superoxide [17], initially declined during the few days of experiments but then gradually accumulated with time in stationary phase (Figure 1A). The chronological age-dependent accumulation of O_2^- occurred in parallel with loss of reproductive capacity as measured by colony-forming units (Figure 1B; “WT 2% glu”). As reported earlier [18], both the accumulation of O_2^- and loss of reproductive capacity in stationary phase cells were accompanied by an increase in cell death as measured by uptake of the membrane-impermeable DNA stain propidium iodide (PI) (Figure S1), which does not stain viable cells with intact membranes. The rate of cell death was accelerated in cells with visible buds that failed to exit the cell cycle in stationary phase compared to cells without visible buds (Figure S1). This is consistent with an earlier report that a subpopulation of stationary phase cells that includes all budded cells exhibits elevated levels of apoptosis [19].

Also similar to earlier reports [13, 20], CR by reducing the initial concentration of glucose in growth medium from 2% to 0.5% extended the CLS of wild type cells (Figure 1B). Although CR initially increased O_2^- in exponential cultures at the start of CLS experiments (Figure 1C), it led to a reduction in O_2^- in stationary phase cultures three days later (Figure 1D; compare “WT 0.5% glu” with “WT 2% glu”). This decrease was detected in association with a decrease in the fraction of cells that failed to arrest in G0/G1 as indicated by visible buds (Figure 1E). In the absence of CR, CLS was lengthened to a similar extent (compared to CR) in a strain from which the *SCH9* gene had been deleted, and CR extended the CLS of *sch9Δ* cells even further (Figure 1B). Similar to the effects of CR, the CLS-extending effects of inactivating Sch9p in 2% glucose medium were also accompanied by a decrease in O_2^- , and inactivation of Sch9p decreased levels of O_2^- in calorie-restricted cells even further (Figure 1D). A reduc-

tion in intracellular O_2^- in *sch9Δ* cells was recently reported by others as well [5] and is consistent with a previous report that expression of the superoxide dismutase Sod2p is elevated in *sch9Δ* cells [4]. Inactivation of Sch9p also led to a decrease in the fraction of stationary phase cells that failed to arrest growth in G0/G1 as was reported earlier [13], and this fraction was reduced further by CR of *sch9Δ* cells (Figure 1E). Similar quantitative effects on efficiency of G0/G1 arrest in stationary phase in parallel with changes in CLS and O_2^- were observed in medium containing 2% glucose or 0.5% glucose in cells from which *TOR1* had been deleted (Figure S2). Culturing cells in rich medium (YPD) rather than defined medium (SC), which also promotes more frequent growth arrest of stationary phase cells in G0/G1 [13], also reduced levels of O_2^- compared to cells cultured in SC (Figure S3).

Growth signaling pathways that depend on Sch9p, Tor1p and Ras2p converge on inhibition of Rim15p kinase activity that activates Sod2p and other stress responses, which are induced when these growth signaling pathways are genetically ablated or attenuated by CR [21]. Sod1p and Sod2p activity are also induced

by H_2O_2 that accumulates to higher levels in calorie-restricted cells or when catalases have been inactivated [8]. Intracellular levels of H_2O_2 detected with the fluorescent probe dihydrorhodamine 123 were slightly reduced in stationary phase *sch9Δ* compared to wild type cells (Figure 1F; “DHR”). Therefore, unlike CR, inactivation of Sch9 does not reduce levels of O_2^- by inducing elevated levels of H_2O_2 that activate SODs. Moreover, CR increased H_2O_2 and reduced O_2^- levels in stationary phase *rim15Δ* cells (Figure 1G), similar to its effects in wild type cells [8]. Thus, the reduction in O_2^- levels detected in calorie-restricted cells reflects both Rim15p-dependent effects downstream of reduced signaling by Sch9p, Tor1p and Ras2p that do not depend on increased H_2O_2 , as well as Rim15p-independent effects related to H_2O_2 induction of SODs. Rim15p-independent effects of CR on levels of O_2^- are consistent with an earlier report of Rim15p-independent effects of CR on CLS [7]. Together, these findings reveal the existence of a quantitative relationship between CLS extension, reduction in intracellular levels of O_2^- by Rim15p-dependent and -independent mechanisms and more efficient growth arrest of stationary phase cells in G0/G1 when growth signaling is inhibited.

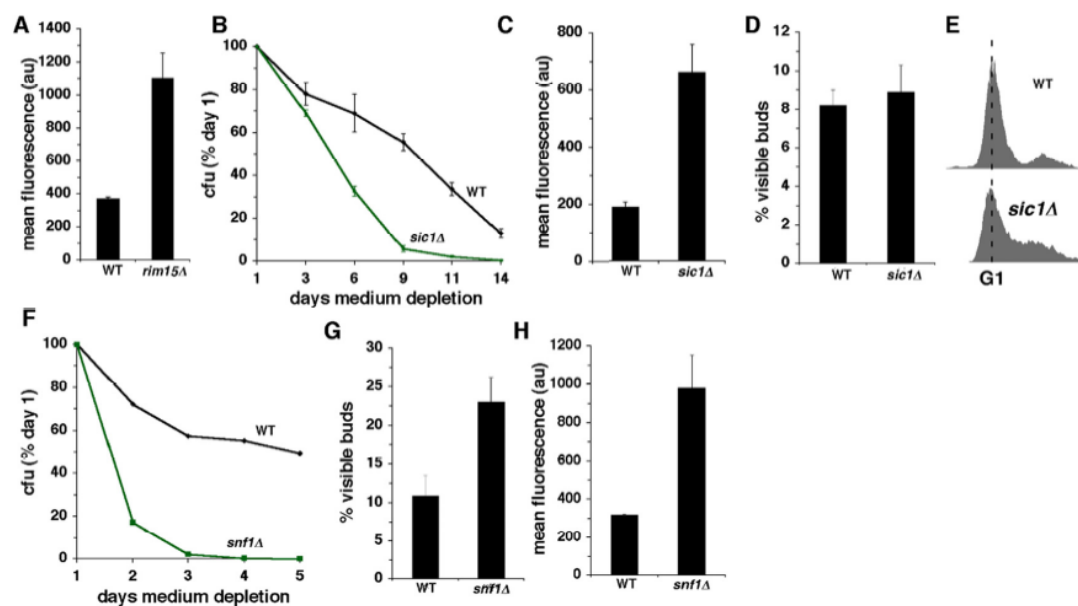


Figure 2. Constitutive activation of growth signaling pathways shortens CLS in concert with increased O_2^- and less frequent growth of stationary phase cells in G0/G1. (A) Levels of O_2^- detected by DHE fluorescence in wild type and *rim15Δ* cells at day 3 of medium depletion. (B) CLS of wild type and *sic1Δ* cells. (C–D) Levels of DHE fluorescence (C) and fraction of cells with visible buds (D) in wild type and *sic1Δ* cells. Measurements depicted in panels C and D were made at day 3 of medium depletion. (E) DNA content of wild type and *sic1Δ* cells at day 3 of medium depletion. (F–H) Effects of inactivating Snf1p on CLS (F), fraction of cells with visible buds (G) and levels of O_2^- detected by DHE fluorescence. (H) Measurements depicted in panels G and H were made at day 3 of medium depletion.

Constitutive activation of growth signaling elevates superoxide anions and inhibits stationary phase G0/G1 arrest

In mammals, sustained mitogenic signaling by RAS, AKT and other oncogenes increases levels of O_2^- and other forms of ROS [22] and induces replication stress in cells that growth arrest in S phase instead of G0/G1 during differentiation [23]. Similar increases in O_2^- [9] and a reduced frequency of stationary phase growth arrest in G0/G1 phase [13, 14] have been described for budding yeast cells expressing constitutively active Ras2p. As noted above, RAS- and AKT-related pathways that signal growth in response to nutrients in budding yeast converge on inhibition of Rim15p kinase activity [21]. In addition to exhibiting a shorter CLS, *rim15Δ* cells fail to arrest in G0/G1 when they enter stationary phase [13, 24]. Stationary phase *rim15Δ* cells also exhibit higher levels of O_2^- compared to wild type cells (Figure 2A).

The mammalian cyclin-dependent kinase inhibitor p27 blocks entry into S phase when mitogenic growth signaling is downregulated in mammalian cells [25]. Sic1p, the budding yeast homologue of p27, similarly inhibits entry of budding yeast cells into S phase when they enter into a nutrient depletion-induced stationary phase growth arrest [26]. As reported earlier [27], inactivation of Sic1p shortens CLS (Figure 2B). Similar to the effects of the constitutively active Ras2 or deletion of *RIM15*, the shorter CLS of *sic1Δ* cells is accompanied by increased O_2^- (Figure 2C). Although in this strain background (W303), deletion of *SIC1* did not increase the number of cells with visible buds (Figure 2D), budding is uncoupled from DNA replication in *sic1Δ* cells in some genetic backgrounds [26]. Measurements of DNA content by flow cytometry confirmed that a large fraction of stationary phase W303 *sic1Δ* cells were growth-arrested in S phase, despite a low frequency of buds (Figure 2E). Uncoupling of budding from DNA replication was not observed, however, in *sic1Δ* cells in a different genetic background (CEN.PK). *sic1Δ* cells in this background arrested growth in stationary phase with a substantial increase in the fraction of cells with visible buds (Figure S4).

Snf1p is a conserved AMP kinase that regulates budding yeast metabolism in response to glucose [28]. In mammals, AMPK inhibits mTOR signaling [28] and is required for a “metabolic checkpoint” that drives cells into G1 in response to reduced glucose concentrations [29], similar to the more frequent stationary phase growth arrest in G0/G1 imposed by CR during nutrient depletion of budding yeast cells [13]. In addition to

exhibiting a shorter CLS compared to wild type cells (Figure 2F), stationary phase *snf1Δ* cells also arrested in G0/G1 less frequently (Figure 2G) and exhibited elevated levels of O_2^- (Figure 2H). These findings establish a strong correlation between enhanced growth signaling, increased intracellular levels of O_2^- and less efficient G0/G1 arrest in stationary phase related to glucose metabolism.

Enhanced growth signaling by high glucose shortens CLS in parallel with increased superoxide anions, less efficient G0/G1 arrest and increased DNA damage in stationary phase cells

High glucose accelerates aging in *C. elegans* [30] and hyperglycemia and/or excess calorie intake are risk factors for a number of age-related diseases. High glucose activates AKT in mammalian cells [31], and similar to enhanced mitogenic signaling by oncogenes [32, 33], increased growth signaling by elevated levels of glucose promotes senescence in parallel with DNA damage and increased ROS [34, 35]. To determine whether growth signaling by high glucose might trigger related events and accelerate chronological aging in budding yeast, we examined the effects of increasing the concentration of glucose in medium to 10% from the standard 2% (in these experiments, 2% glucose medium also contained 8% sorbitol, a non-metabolized sugar, in order to maintain equivalent osmolarity). Culturing cells in SC medium containing 10% glucose shortened CLS compared to CLS in medium containing 2% glucose (Figure 3A). The shorter CLS of 10% glucose SC cultures is likely accompanied by DNA damage and/or DNA replication stress, because loss of reproductive capacity was dramatically reduced in cells harboring mutations in the DNA damage/DNA replication stress response proteins Mec1p or Rad53p (Figure 3B). Cells cultured in 10% glucose SC medium also exhibited increased levels of intracellular O_2^- (Figure 3C). This increase occurred in parallel with a reduction in intracellular levels of H_2O_2 in 10% glucose compared to 2% glucose cultures (Figure 3D). Since levels of H_2O_2 are also increased in 0.5% compared to 2% glucose cultures [8], this suggests that glucose inhibits the accumulation of H_2O_2 in stationary phase cells in a dose-dependent fashion. The shorter CLS and increased O_2^- detected in 10% compared to 2% glucose SC cultures was not related to increased medium acidity, because in the genetic background of the strains employed in these experiments (DBY746), the pH of stationary phase cultures established in 10% glucose was not significantly different from the pH of 2% glucose cultures (Table 1). Unexpectedly, the fraction of stationary phase cells with visible buds in 10% glucose SC cultures was reduced rather than increased

compared to 2% glucose SC cultures (Figure 3E). This likely reflects the accelerated death of dividing cells in SC medium containing 10% glucose (see below).

Similar to the effects of elevated glucose in SC medium, wild type cells cultured in 10% glucose YPD medium exhibited a shorter CLS and increased O_2^- levels compared to cells cultured in 2% glucose YPD (Figure 3F-G). However, in contrast to the reduced fraction of cells with visible buds detected in 10% glucose SC (Figure 3E), a substantial increase in the fraction of visibly budded cells was detected in YPD cultures established in 10% glucose (Figure 3H). As was the case for 10% glucose SC medium, the effects of 10% glucose in YPD medium were unrelated to changes in

medium acidity, because the pH of these cultures did not differ significantly from the pH of YPD cultures established in 2% glucose (Table 1). Similar to the effects of inactivating Sch9p in cells cultured in 2% glucose SC (Figure 1B-D), Sch9p inactivation extended CLS, reduced O_2^- and lowered the fraction of budded cells detected in wild type cells cultured in 10% glucose YPD (Figure 3F-H). Since the CLS-shortening effects of 10% compared to 2% glucose are not related to acetic acid, we conclude that inactivation of Sch9p reduces O_2^- levels, enhances stationary phase G0/G1 arrest and extends CLS in 10% glucose medium by inhibiting glucose-dependent growth signaling, and not by causing resistance to acetic acid.

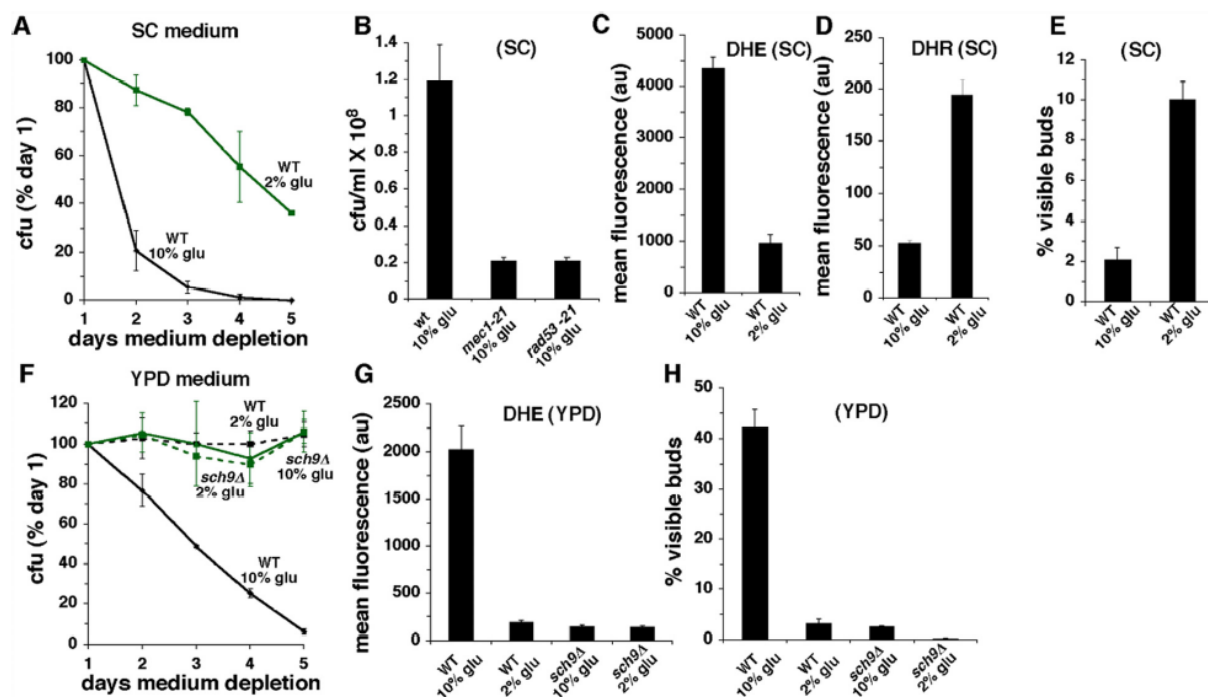


Figure 3. Effects of high glucose (10%) in SC or YPD medium. (A) CLS of wild type cells in SC medium initially containing 2% or 10% glucose. (B) Reproductive capacity after 2 days of medium depletion of wild type, *mec1-21* or *rad53-21* cells cultured in SC medium containing 10% glucose. (C) Levels of O_2^- detected by DHE fluorescence in SC cultures of wild type cells at day 3. (D) Levels of H_2O_2 detected by DHR fluorescence in SC cultures of wild type cells at day 3. (E) Fraction of cells with visible buds in SC cultures at day 3 of medium depletion. (F) CLS of wild type and *sch9Δ* cells in YPD medium initially containing 2% or 10% glucose. (G) Levels of O_2^- detected by DHE fluorescence in YPD cultures at day 3. (H) Fraction of cells with visible buds in YPD cultures at day 3.

Table 1. pH day 5 medium depletion

Strain	SC 10% glucose	SC 2% glucose	YPD 10% glucose	YPD 2% glucose
DBY746	3.32 (±0.2)	3.38 (±0.03)	4.72 (±0.11)	4.79 (±0.09)
BY4742	3.19 (±0.02)	3.79 (±0.59)		
BY4741	3.18 (±0.06)	4.17 (±0.07)		
W303	3.17 (±0.01)	3.57 (±0.01)		

Wild type cells cultured in 2% glucose YPD medium also exhibited reduced levels of O_2^- compared to 2% glucose SC cultures (Figure S3; also compare “WT 2% glu” in Figure 3C with “WT 2% glu” in Figure 3G). This likely reflects a reduced amount of acetic acid in stationary phase YPD cultures compared to SC cultures, because the pH of stationary phase YPD medium is substantially higher than the pH of SC medium (Table 1). Furthermore, unlike in 2% glucose SC cultures (Figure 1B-C), in 2% glucose YPD cultures *sch9Δ* cells did not exhibit a longer CLS or reduced levels of O_2^- compared to wild type cells (Figure 3F-G). This suggests that in 2% glucose SC cultures, inactivation of *SCH9* extends CLS by inhibiting acetic acid induction of O_2^- .

High glucose causes more frequent apoptotic elimination of dividing compared to non-dividing cells

The findings described in previous sections indicate that both glucose and acetic acid shorten CLS in concert with elevated levels of O_2^- and less efficient growth arrest of stationary phase cells in G0/G1. However, the reduced fraction of budded cells detected in 10% glucose compared to 2% glucose SC cultures (Figure 3E) is not consistent with a general relationship between enhanced growth signaling, increased O_2^- and less efficient G0/G1 arrest. Budding yeast cells die in stationary phase by an apoptosis-like mechanism [36, 37]. The substantial increase in the fraction of stationary phase wild type cells with visible buds in 10% glucose YPD (Figure 3H) raised the possibility that the reduced fraction of budded cells in 10% glucose SC might be related to the very short CLS observed in

these cultures and frequent apoptotic elimination of budded cells. Consistent with this possibility, PI staining of cells in 10% glucose SC stationary phase cultures revealed a 6-fold increase in the fraction of visibly budded cells that were dying compared to cells that did not have visible buds (Figure 4A). This is substantially larger than the ~2-fold increase in budded compared to unbudded cells that stain with PI in 2% glucose SC cultures (Figure S1).

Furthermore, at day 2 of medium depletion, cells in 10% glucose SC cultures were more frequently undergoing apoptosis compared to cells in 2% glucose SC indicated by increased apoptotic degradation of DNA. In fact almost all the cells in 10% glucose cultures harbored substantially less than the complete G1 complement of DNA required for continued viability (Figure 4B). Electron microscopic visualization of stationary phase cells cultured in 2% glucose YPD medium revealed that some cells exhibited fragmented nuclei indicative of apoptosis as well as an irregular cell shape indicating deterioration of the cell wall structure (Figure 4C and D). This contrasted with the appearance of intact nuclei and cell walls in non-apoptosing cells (Figure 4E). In some cases, disruption of the cell wall structure was detected at specific sites in apoptosing cells (Figure 4D; arrow) that may correspond to the location of a bud that broke off in cells undergoing apoptosis. A decline in numbers of cells in 10% glucose SC stationary phase cultures from day 1 to day 3 measured by counting particles (Figure 4F) confirmed that similar to mammalian cells, budding yeast cells undergoing apoptosis eventually are completely destroyed. We conclude that high glucose

reduces the efficiency of G0/G1 arrest in stationary phase and preferentially kills dividing cells, and that the reduced number of cells with visible buds in 10% glucose SC cultures is caused by the specific and rapid apoptotic destruction of cells that failed to arrest growth in G0/G1.

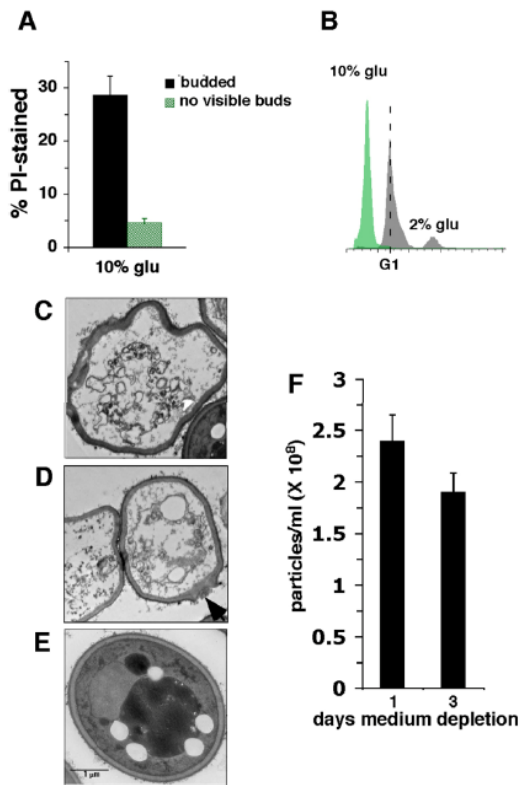


Figure 4. Effects of SC medium containing 10% or 2% glucose on cell death in stationary phase. (A) % wild type cells cultured in 10% glucose SC medium stained with propidium iodide (PI) at day 2 of medium depletion. (B) DNA content of wild type cells cultured in 10% or 2% glucose SC medium at day 2 of stationary phase. Dotted line marks cells with a G1 content of DNA. (C-E) Electron micrographs of stationary phase cells cultured in 2% glucose SC medium undergoing apoptosis (C and D) or not undergoing apoptosis (E). (F) Number of particles in 10% glucose SC cultures at day 1 and 3 of medium depletion.

Superoxide anions inhibit stationary phase G0/G1 arrest

The inverse relationship between levels of O_2^- and the frequency with which cells arrest in G0/G1 when they

enter stationary phase under a variety of experimental conditions (summarized in Table 2) suggests that O_2^- inhibits G0/G1 arrest. To test this hypothesis, we examined the effects of experimental manipulations that directly alter levels of O_2^- independently of changes in growth signaling pathways. *sod2Δ* cells exhibited a significantly shorter CLS (Figure 5A; [38]) accompanied by increased O_2^- (Figure 5B) and less efficient G0/G1 arrest (Figure 5C) in stationary phase. Sod2p expression is elevated in *sch9Δ* cells, and deletion of *SOD2* from *sch9Δ* cells partially suppresses their longevity phenotype ([4]; Figure 5D). *sch9Δ sod2Δ* double mutant cells also exhibited an intermediate level of O_2^- compared to wild type or *sch9Δ* cells (Figure 5E) accompanied by a stationary phase G0/G1 arrest that was intermediate between that of wild type and *sch9Δ* cells (Figure 5F). Thus, a quantitative relationship exists between levels of O_2^- and frequency of G0/G1 arrest in *sod2Δ*, *sch9Δ sod2Δ* and wild type cells.

We also asked whether treatment of cells with the antioxidant N-acetylcysteine (NAC) would extend CLS and increase the efficiency of stationary phase G0/G1 arrest in association with reduced levels of superoxide. Surprisingly, NAC shortened CLS in a dose-dependent fashion in wild type, but not *sch9Δ* cells (Figure 5G). The shorter CLS conferred by NAC in wild type cells occurred in concert with dose-dependent increases rather than decreases in levels of O_2^- (Figure 5H). Similar pro-oxidant effects of the antioxidants α -tocopherol and coenzyme Q10 were recently reported in budding yeast [39], and induction of O_2^- by NAC has been reported in mammalian cells as well [40]. Increased O_2^- in wild type cells exposed to NAC was accompanied by a parallel dose-dependent increase in the fraction of cells with visible buds (Figure 5I). NAC-induced increases in O_2^- and frequency of G0/G1 arrest in stationary phase were absent in *sch9Δ* cells (Figure 5H and I; “*sch9Δ*”). The absence of NAC effects in *sch9Δ* cells expressing elevated levels of Sod2p [4] suggests that in wild type cells, the effects of NAC are related to increased amounts of O_2^- and not to unrelated toxic effects of this compound. In contrast, cells in which the catalases Cta1p or Ctt1p had been inactivated, which exhibit reduced levels of O_2^- in stationary phase and a longer CLS [8], also exhibited fewer visible buds (Figure 5J). Similarly, cells treated with the antioxidant glutathione (GSH) also exhibited fewer visible buds (Figure 5K) in concert with reduced levels of O_2^- (Figure 5L). We conclude that O_2^- inhibits growth arrest of stationary phase cells in G0/G1.

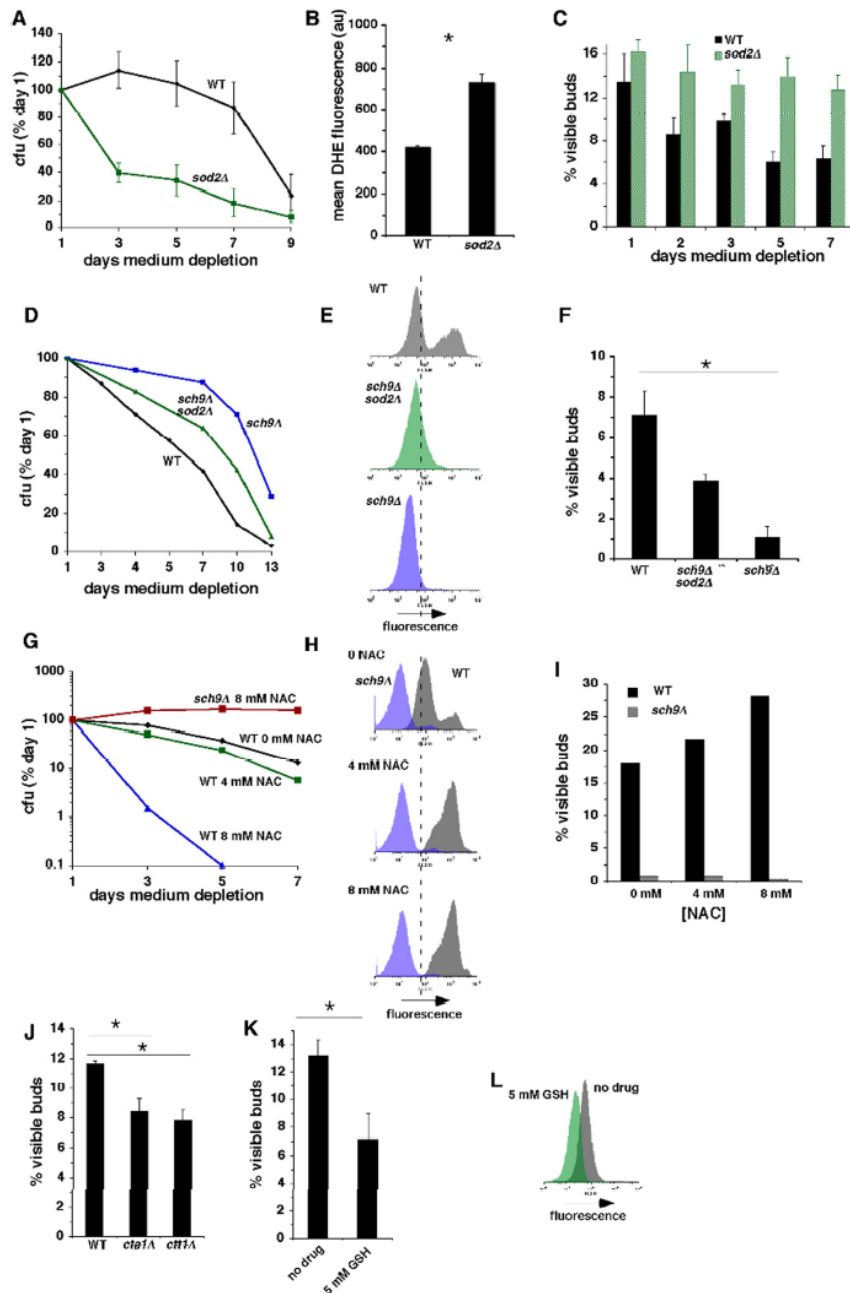


Figure 5. O₂⁻ inhibits growth arrest of stationary phase cells in G0/G1 in parallel with a shorter CLS. (A) CLS of wild type and *sod2Δ* cells in 2% glucose SC medium. (B) Levels of O₂⁻ in wild type and *sod2Δ* cells detected by DHE fluorescence at day 3 of medium depletion. (C) Fraction of cells with visible buds in wild type and *sod2Δ* cells at indicated times of medium depletion. (D) CLS of wild type, *sch9Δ* and *sch9Δ sod2Δ* cells. (E) Levels of O₂⁻ detected by DHE fluorescence in wild type, *sch9Δ* and *sch9Δ sod2Δ* cells at day 3 of medium depletion. (F) Fraction of cells with visible buds in wild type, *sch9Δ* and *sch9Δ sod2Δ* cells at day 3 of medium depletion. (G) Dose-dependent effects of NAC on CLS in wild type and *sch9Δ* cells. (H and I) Dose-dependent effects of NAC on O₂⁻ detected by DHE (H) and fraction of cells with visible buds (I) in wild type and *sch9Δ* cells at day 3 of medium depletion. (J) Fraction of cells with visible buds in wild type cells and the catalase mutants *cta1Δ* and *ctt1Δ* at day 3 of medium depletion. (K) Fraction of cells with visible buds at day 3 of medium depletion that were treated or not treated with the anti-oxidant GSH beginning at day 0. (L) Effect of GSH in wild type cells on levels of O₂⁻ indicated by DHE fluorescence at day 3 of medium depletion.

DISCUSSION

Growth signaling and superoxide anions in the chronological aging model

Our findings reveal that under a variety of experimental conditions, an inverse relationship exists between budding yeast CLS and intracellular levels of O_2^- (summarized in Table 2) that points to O_2^- accumulating downstream of growth signaling as a primary cause of chronological aging. A role for growth signaling-induced O_2^- in chronological aging is consistent with earlier reports that CR extends CLS in part by downregulating Tor1p-, Ras2p- and Sch9p-dependent growth signaling pathways that inhibit the Rim15p kinase and its induction of oxidative stress defenses ([7]; Figure 6). Our findings also indicate that the Rim15p-independent extension of CLS by CR reported earlier [7] is related to the induction of H_2O_2 that reduces O_2^- (Figure 1G) by activating SODs [8] independently of Rim15p (Figure 6).

Burtner et al. [12] recently proposed that the primary cause of chronological aging in budding yeast is toxic effects of acetic acid that are not caused by oxidative stress, and that inactivation of Sch9 or Ras2 protect against acetic acid toxicity through unknown mechanisms rather than reduced growth signaling. Our data are consistent with a role for acetic acid toxicity as a determinant of CLS in 2% glucose medium. However, acetic acid causes O_2^- to accumulate in stationary phase cells, because buffering SC medium to a higher pH, which extends CLS, reduces levels of O_2^- [18]. O_2^- levels are similarly reduced in cells in YPD (Figure S3), which in addition to maintaining a higher medium pH (Table 1) exhibit a longer CLS (Figure 3; [13]). O_2^- accumulating in stationary phase cells is toxic, because experimental manipulations that directly elevate O_2^- levels (inactivation of Sod2p or exposure to NAC) shorten CLS (Figure 5).

Acetic acid [41] and/or intracellular acidification [42] induce the same TOR- and RAS-dependent growth signaling pathways induced by glucose, and the induction of O_2^- by acetic acid is likely a consequence of acetic acid-induced growth signaling. A role for RAS-dependent growth signaling in acetic acid toxicity is consistent with an earlier report that the enhanced stationary phase viability of *ras1Δ* and/or *ras2Δ* cells cultured in SC medium is absent in YPD cultures or in SC cultures buffered to a higher pH [43]. Our finding that CLS extension in *sch9Δ* compared to wild type cells cultured in 2% glucose SC (Figure 1B; [3]) is similarly absent when these cells are cultured in 2% glucose YPD, (Figure 3F), which also maintains a

higher pH, suggests that acetic acid also triggers Sch9p-dependent growth signaling pathways. Therefore, the protective effects against acetic acid toxicity in unbuffered 2% glucose medium associated with inactivating Ras1p, Ras2p and Sch9p are likely due to downregulation of growth signaling by acetic acid and consequent upregulation of SODs and other oxidative stress defenses by Rim15p (Figure 6).

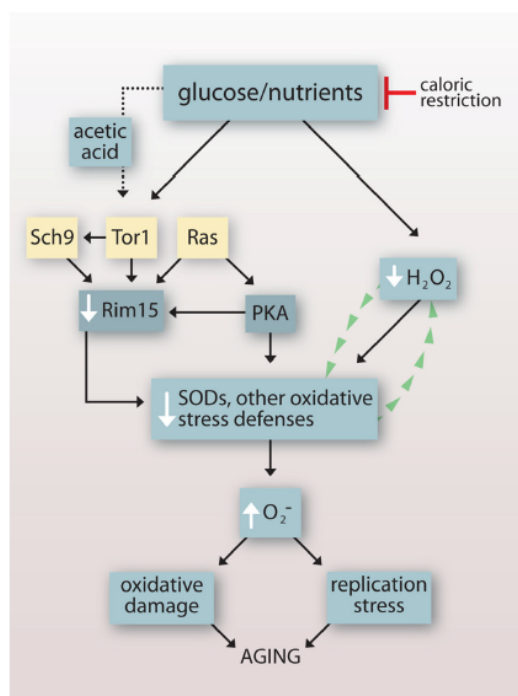


Figure 6. Impact of growth signaling pathways and caloric restriction on chronological lifespan in budding yeast.

Glucose and other nutrients signal growth through conserved Sch9p-, Tor1p- and Ras-dependent pathways that inhibit Rim15p and its induction of oxidative stresses defenses, leading to elevated O_2^- that cause oxidative damage and DNA replication stress. Acetic acid induces O_2^- by activating the same pathways. Caloric restriction attenuates signaling through these pathways and also induces H_2O_2 that activates SODs and reduces levels of O_2^- independently of Rim15p. In caloric restriction conditions, H_2O_2 that accumulates as a byproduct of increased SOD activity might stimulate SOD activity further by a self-amplifying mechanism.

Burtner et al. also proposed that the effects of acetic acid on CLS are specific for this form of acid [12]. However, deletion of *RAS1* and *RAS2* also protects against acid stress induced by hydrochloric acid [43]. Furthermore, Ras2p-dependent growth signaling is triggered by the acidifying protonophore 2,4-

dinitrophenol [42]. Low pH also induces AKT activity in human cells [44, 45], and as we noted earlier [18], growth signaling by low pH that depends on RAS, AKT and other oncogenes underlies a number of pathological states in humans, including cancer. Thus, acetic acid toxicity in budding yeast corresponds to a conserved mitogen-like response to low pH, and not just acetic acid, that mimics the sustained activation of oncogenes in complex eukaryotes.

Superoxide anions and effects of enhanced growth signaling by high glucose

In mammalian cell cultures, high levels of glucose that mimic the effects of hyperglycemia induce DNA damage, AKT-dependent growth signaling, increased O_2^- and senescence [31, 34, 35, 46]. Each of these effects has been implicated in aging and age-related diseases linked to hyperglycemia and/or excess calorie intake, including cancer, diabetes and cardiovascular disease. High glucose also promotes aging in *C. elegans* in association with increased O_2^- [30]. The induction of elevated O_2^- and a shorter CLS by glucose signaling has been implicated in aging in the fission yeast *S. pombe* as well [47]. The increased levels of O_2^- (Figure 3C and G) and shorter CLS (Figure 3A and F) induced by 10% glucose in either SC or YPD medium establish budding yeast as an additional model for investigating the effects

of elevated glucose on aging and age-related diseases. These effects are mediated in part by Sch9p-dependent signaling by glucose because in 10% glucose YPD cultures, *sch9Δ* cells exhibit a longer CLS and less O_2^- compared to wild type cells (Figure 3) in the absence of changes in pH compared to 2% glucose YPD cultures.

Changes in levels of acetic acid also do not play a role in the CLS-extending effects of increased H_2O_2 induced by CR [8]. The longer CLS in 2% compared to 10% glucose SC or YPD cultures in the absence of a change in medium pH reveals an additional mechanism by which CR extends CLS in budding yeast related to reduced growth signaling by glucose rather than acetic acid. CR is most often defined in yeast experiments as a decrease in the glucose content of medium below 2%. However, in their natural environment yeasts are likely exposed to higher concentrations of glucose and other sugars that trigger growth signaling. For example, the glucose and fructose content of grapes can exceed 13% [48] and the sugar content of overripe plantains approaches 27% [49]. Thus, culturing cells in 2% compared to 10% glucose medium can be considered a physiologically relevant form of CR that depends on reduced growth signaling by glucose rather than acetic acid. This form of CR is broadly relevant to CR in complex eukaryotes.

Table 2. Summary of effects of experimental manipulations that impact CLS on superoxide anions and frequency of G0/G1 arrest in stationary phase

Experiment	Superoxide anions	G0/G1 arrest
Longer CLS:		
Deletion of <i>SCH9</i>	↓	↑
Deletion of <i>TOR1</i>	↓	↑
Deletion of <i>RAS2</i>	n.d.	↑
Caloric restriction	↓	↑
Buffering pH to 6.0	↓	↑
GSH	↓	↑
Deletion of <i>CTA1</i>	↓	↑
Deletion of <i>CTT1</i>	↓	↑
Shorter CLS:		
Deletion of <i>PDE2</i>	↑	↓
Deletion of <i>SNF1</i>	↑	↓
Deletion of <i>RIM15</i>	↑	↓
Deletion of <i>SIC1</i>	↑	↓
Deletion of <i>SOD2</i>	↑	↓
High glucose	↑	↓
N-acetylcysteine	↑	↓

Growth signaling, superoxide anions and DNA replication stress

The longstanding free radical theory of aging predicts that the pro-aging effects of O_2^- are caused by oxidative damage to macromolecules. However, the reduced levels of O_2^- and extended CLS produced by inactivation of catalases are accompanied by increased, rather than decreased oxidative damage [8]. Conversely, the shorter CLS detected in *sod2Δ* and other cells harboring defective oxidative stress defenses is not accompanied by general increases in oxidative damage to macromolecules [50, 51]. A similar disconnect between oxidative damage and longevity is observed in naked mole rats, which exhibit a ~10-fold longer lifespan compared to mice despite the presence of high levels of oxidative damage [52]. This suggests that the pro-aging effects of oxidative stress are not always a direct consequence of oxidative damage.

The inverse relationship between CLS and levels of O_2^- we detected under a variety of experimental conditions is accompanied by a similar inverse relationship between levels of O_2^- and frequency of G0/G1 arrest in stationary phase (Table 2). This points to an alternative, but not mutually exclusive possibility - that the age-promoting effects of O_2^- are related in part to inhibition by O_2^- of growth arrest of stationary phase cells in G0/G1, leading to more frequent growth arrest in S phase instead, where cells suffer replication stress. The inhibitory effects on G0/G1 arrest in stationary phase of experimental manipulations that more directly impact levels of O_2^- compared to alterations in growth signaling pathways (Figure 5) are consistent with this model.

Based on measurements of the fraction of stationary phase cells with visible buds, Madia et al. proposed that the effects on chronological aging related to replication stress are minor compared to other pro-aging factors [53]. In fact, the magnitude of inhibitory effects on G0/G1 arrest in stationary phase related to O_2^- is larger than suggested by counting cells with visible buds in stationary phase, for several reasons. First, cells die in stationary phase cultures via an apoptosis-like mechanism ([36]; Figure 4B-D) that eventually destroys cells (Figure 4F). The preferential death of cells that failed to arrest in G0/G1 (Figures. S1 and 4A) leads to underestimates of the fraction of these cells. Second, our data suggest that as the budding yeast cell wall deteriorates during apoptosis, buds break off of mother cells (Figure 4D), which would lead to additional underestimates of the fraction of cells with visible buds. Third, cells in early S phase with small buds are difficult to distinguish microscopically from unbudded cells that have truly arrested in G0/G1. Consequently,

at least some of the dying cells that do not have visible buds in stationary phase in our experiments have not arrested in G0/G1.

According to a recent study, treatment of cells with low levels of hydroxyurea, which inhibits a protein essential for DNA replication (ribonucleotide reductase) shortens CLS by 20 – 27% [54]. Furthermore, increased apoptosis of stationary phase cells harboring a mutation in the replication stress protein Mec1 is suppressed by ectopic expression of the *RNR1* gene encoding ribonucleotide reductase [13]. Therefore, in principle, replication stress caused by reduced dNTP pools can substantially shorten CLS. Replication stress as a determinant of CLS is consistent with the observation that stationary phase cells that fail to arrest in G0/G1 die faster than unbudded cells (Figures S1;[18]). The rate at which dividing cells die in stationary phase is accelerated further when growth signaling and levels of O_2^- are enhanced by high glucose (Figure 4A), which also triggers DNA damage responses (Figure 3B). These findings suggest that the toxic effects of O_2^- in stationary phase cells are caused in part by DNA damage specifically in cells that failed to growth arrest in G0/G1.

A role for replication stress in chronological aging is also consistent with an earlier report by Allen et al. that non-quiescent stationary phase cells separated from denser quiescent cells by density gradients more frequently undergo apoptosis and exhibit elevated expression of genes encoding proteins that respond to replication stress [19]. It is not consistent with the results of a recent genetic screen that identified budding yeast deletion mutants that exhibit an extended CLS in the absence of more frequent stationary phase growth arrest in G0/G1 [55]. However, this screen also failed to identify the numerous deletion strains with inactivated growth signaling pathways, including *sch9Δ*, that were previously reported to have an extended CLS. In fact, in this recently published study, *ras2Δ* cells that earlier studies indicated are long-lived in the CLS model exhibited a substantially shorter CLS compared to wild type cells.

Replication stress as a determinant of CLS also is not consistent with the recent claim by Madia et al. [53] that the denser fraction of stationary phase cells, which according to Allen et al. [19] are quiescent and exhibit fewer signs of genome instability-promoting replication stress, paradoxically exhibit an elevated mutation frequency compared to “non-quiescent” cells [53]. We note that the experiments of Allen et al. employed YPD medium, which prolongs CLS compared to CLS in SC medium (Figure 3; [13]) and maintains a fraction of

quiescent cells exhibiting a higher density for weeks [19]. In contrast, Madia et al. employed SC medium in their experiments. Close inspection of the data in Figure 2 of Madia et al. indicates that although a denser fraction of cells initially accumulated at day 1 of stationary phase in their experiments, unlike the experiments of Allen et al., this fraction declined and the fraction of less dense non-quiescent cells increased during the next several days of stationary phase. Furthermore, the number of stationary phase cells in S phase increased during this same period of time (Madia et al., Figure S1A). Although the fraction of budded cells in both “quiescent” and “non-quiescent” fractions continues to decline with increasing time in stationary phase despite an overall increase in cells in S phase, this likely reflects the specific apoptotic destruction of budded cells. In fact, flow cytometry measurements by Madia et al. of the DNA content of “quiescent” and “non-quiescent” wild type cells clearly indicate that at the three and five day stationary phase time points they employed to measure mutation frequency in their experiments, most of the wild type cells they defined as “quiescent” that exhibited a higher mutation frequency also harbored significantly more DNA compared to “non-quiescent” wild type cells, and thus were more frequently in S phase (Figure S1B of Madia et al.; compare “Lower Fraction” (quiescent) histograms with “Upper Fraction” (non-quiescent) histograms at each time point). Thus, in contrast to the experiments of Allen et al., the initially denser cells Madia et al. refer to as “quiescent” do not remain quiescent for more than a few days, most likely due to increased growth signaling by the larger amounts of acetic acid accumulating in SC medium compared to the YPD medium employed in the experiments of Allen et al. In the absence of nutrients required for efficient DNA replication in stationary phase cultures, entry of these cells into S phase is a recipe for replication stress and mutations.

Growth signaling, replication stress and aging in complex organisms

The induction of insulin/IGF-1-like growth signaling pathways that depend on RAS, AKT, mTOR and other oncogenic proteins has been implicated in aging and a number of age-related diseases in humans, including many for which hyperglycemia and/or excess calorie intake are risk factors. In addition to elevated levels of ROS, DNA replication stress has been implicated in some of these diseases as well. For example, sustained oncogenic signaling that leads to growth arrest in S phase has been implicated in the senescent state of preneoplastic cells [33]. Similarly, inappropriate activation of growth signaling pathways in tauopathies and other neurodegenerative disorders promotes

unscheduled entry of postmitotic neurons into S phase [56], where these cells also likely undergo replication stress. Thus, as in budding yeast, growth signaling may impact aging in more complex organisms, including humans, by inducing replication stress, in addition to oxidative stress.

As in budding yeast, replication stress in mammalian cells may be related to O_2^- inhibition of quiescence. Consistent with this possibility, MnSOD-defective mouse cells driven into a non-dividing state by contact inhibition exhibit elevated levels of O_2^- , a higher fraction of S phase cells and increased apoptosis [40]. Furthermore, O_2^- induced by hyperglycemia [57] or by a metabolite of polychlorinated biphenyls that cause cancer [58] inhibit DNA replication. These findings have important implications for understanding aging and age-related diseases. For example, although DNA replication stress now is generally accepted as a factor that contributes to tumorigenesis downstream of oncogene activation, it is not considered to be an initiating event [59]. However, high glucose inhibits progression of endothelial cells through S phase [60], and as in our yeast experiments, also induces DNA damage in human mesothelial cells [34]. It is possible, therefore, that hyperglycemia and other factors can initiate tumorigenesis by inducing replication stress that leads to mutational activation of oncogenes.

This model does not explain all facets of aging, which is multifactorial and exceedingly complex. A compelling argument can be made, for example, that autophagy is an important component of lifespan regulation in all eukaryotes [61]. Even here, however, our model may be relevant – in budding yeast, CLS extension by spermidine, which activates autophagy, is accompanied by reduced levels of O_2^- and more frequent arrest of stationary phase cells in G0/G1 [62]. Overall, our results provide a framework for investigating the role of growth signaling and oxidative stress in aging that accommodates recent evidence pointing to pro-aging factors other than oxidative damage. They also suggest a novel mechanism by which normal aging can be impacted by diet and other environmental factors.

METHODS

Strains employed in these studies are listed in Table S1. To assess CLS 50 ml cultures were inoculated with 1% (v/v) of a fresh overnight culture in either SC or YPD. SC was supplemented as described [63]. In experiments that employed media that initially contained 10% glucose, control 2% glucose cultures also contained 8% sorbitol to maintain equivalent osmolarity. Determination of chronological life span, fraction of budded

cells, flow cytometry measurements of DNA content and measurements of dihydroethidium (DHE) and dihydrorhodamine 123 (DHR) were as described previously [8, 13]. N-acetylcysteine (NAC) and glutathione (GSH) were dissolved in growth medium, filter sterilized and added to cultures from 100mM (NAC) or 250mM (GSH) stocks at the start of experiments. Propidium iodide (PI) was used to assess viability of cells by mixing a 2µl of cells with an equal volume of 1mM PI on a microscope slide and examining the slide with a fluorescence microscope equipped with a Texas Red filter. Non-fluorescent cells were scored as intact (live) and fluorescent cells were scored as dead. The total number of cells in cultures was determined by particle counts using a Petroff Hauser counting chamber.

Samples for transmission electron microscopy were prepared according to [64]. Briefly, cells cultured at 30°C in YPD medium for 3 to 5 days were harvested by gentle centrifugation, washed in phosphate buffered saline (PBS) (pH=7.2), resuspended in 2.5%(v/v) glutaraldehyde in PBS and fixed for 40 min at room temperature. Cells were further fixed by 2% freshly prepared potassium permanganate in water for 1 hour at room temperature. Fixed cells were dehydrated with 30%, 50%, 75%, 85%, 95%, and 100% ethanol. Cells were transitioned with propylene oxide, infiltrated in Spurr resin (Electron Microscopy Sciences, PA). Resin was polymerized at 65°C overnight in the oven. 60 nm ultrathin sections were cut with a diamond knife, stained with 2% uranyl acetate and lead citrate and examined using a Hitachi H-7000 electron microscope, equipped with a 4K × 4K cooled CCD digital camera (Gatan, Inc., CA).

Values presented in graphs that contain error bars represent means and standard deviations from three or more independent experiments. Other results are representative of at least three independent experiments. Statistical analyses were performed using Student's *t*-test. *P* < 0.05 was considered statistically significant.

ACKNOWLEDGEMENTS

This research was supported by a National Cancer Institute Cancer Center Support Grant (P30 CA016056) to Roswell Park Cancer Institute and a fellowship to A.M. from Fundação para a Ciência e Tecnologia (SFRH/BD/32464/2006). We are grateful to Molly Burhans for preparation of Figure 6.

CONFLICT OF INTERESTS STATEMENT

The authors have no conflicts of interest to declare.

REFERENCES

- Burhans WC and Weinberger M. DNA replication stress, genome instability and aging. *Nucleic Acids Res.* 2007; 35:7545-7456.
- Harman D. Aging: a theory based on free radical and radiation chemistry. *J Gerontol.* 1956; 11: 298-300.
- Fabrizio P, Pozza F, Pletcher SD, Gendron CM and Longo VD. Regulation of longevity and stress resistance by Sch9 in yeast. *Science.* 2001; 292:288-290.
- Fabrizio P, Liou LL, Moy VN, Diaspro A, Valentine JS, Gralla EB and Longo VD. SOD2 functions downstream of Sch9 to extend longevity in yeast. *Genetics.* 2003; 163: 35-46.
- Pan Y and Shadel GS. Extension of chronological life span by reduced TOR signaling requires down-regulation of Sch9p and involves increased mitochondrial OXPHOS complex density. *Aging.* 2009; 1: 131-145.
- Bonawitz ND, Chatenay-Lapointe M, Pan Y and Shadel GS. Reduced TOR signaling extends chronological life span via increased respiration and upregulation of mitochondrial gene expression. *Cell Metab.* 2007; 5: 265-277.
- Wei M, Fabrizio P, Hu J, Ge H, Cheng C, Li L and Longo VD. Life span extension by calorie restriction depends on Rim15 and transcription factors downstream of Ras/PKA, Tor, and Sch9. *PLoS Genet.* 2008; 4: e13.
- Mesquita A, Weinberger M, Silva A, Sampaio-Marques B, Almeida B, Leao C, Costa V, Rodrigues F, Burhans WC and Ludovico P. Caloric restriction or catalase inactivation extends yeast chronological lifespan by inducing H₂O₂ and superoxide dismutase activity. *Proc Natl Acad Sci U S A.* 2010; 107: 15123-15128.
- Gourlay CW and Ayscough KR. Actin-induced hyperactivation of the Ras signaling pathway leads to apoptosis in *Saccharomyces cerevisiae*. *Mol Cell Biol.* 2006; 26: 6487-6501.
- Sass P, Field J, Nikawa J, Toda T and Wigler M. Cloning and characterization of the high-affinity cAMP phosphodiesterase of *Saccharomyces cerevisiae*. *Proc Natl Acad Sci U S A.* 1986; 83: 9303-9307.
- Burhans WC and Heintz NH. The cell cycle is a redox cycle: linking phase-specific targets to cell fate. *Free Radic Biol Med.* 2009; 47: 1282-1293.
- Burtner CR, Murakami CJ, Kennedy BK and Kaeblerlein M. A molecular mechanism of chronological aging in yeast. *Cell Cycle* 2009; 8: 1256-70.
- Weinberger M, Feng L, Paul A, Smith DL, Hontz RD, Smith JS, Vujcic M, Singh KK, Huberman J and Burhans WC. DNA replication stress is a determinant of chronological lifespan in budding yeast. *PLOS One.* 2007; 2: e748.
- Kataoka T, Powers S, McGill C, Fasano O, Strathern J, Broach J and Wigler M. Genetic analysis of yeast RAS1 and RAS2 genes. *Cell.* 1984; 37:437-445.
- Swinnen E, Wanke V, Roosen J, Smets B, Dubouloz F, Pedruzzi I, Cameroni E, De Virgilio C and Winderickx J. Rim15 and the crossroads of nutrient signalling pathways in *Saccharomyces cerevisiae*. *Cell Div.* 2006; 1:3.
- Chen BR and Runge KW. A new *Schizosaccharomyces pombe* chronological lifespan assay reveals that caloric restriction promotes efficient cell cycle exit and extends longevity. *Exp Gerontol.* 2009; 44:493-502.

17. Benov L, Sztajnberg L and Fridovich I. Critical evaluation of the use of hydroethidine as a measure of superoxide anion radical. *Free Radic Biol Med.* 1998; 25: 826-831.
18. Burhans WC and Weinberger M. Acetic acid effects on aging in budding yeast: are they relevant to aging in higher eukaryotes? *Cell Cycle.* 2009; 8: 2300-2302.
19. Allen C, Buttner S, Aragon AD, Thomas JA, Meirelles O, Jaetao JE, Benn D, Ruby SW, Veenhuis M, Madeo F and Werner-Washburne M. Isolation of quiescent and nonquiescent cells from yeast stationary-phase cultures. *J Cell Biol* 2006; 174: 89-100.
20. Smith DL, McClure JM, Matecic M and Smith JS. Calorie restriction extends the chronological life span of *Saccharomyces cerevisiae* independently of the sirtuins. *Ageing Cell.* 2007; in press.
21. Cameroni E, Hulo N, Roosen J, Winderickx J and De Virgilio C. The novel yeast PAS kinase Rim 15 orchestrates G0-associated antioxidant defense mechanisms. *Cell Cycle.* 2004; 3: 462-468.
22. Courtois-Cox S, Jones SL and Cichowski K. Many roads lead to oncogene-induced senescence. *Oncogene.* 2008; 27: 2801-2809.
23. Di Micco R, Fumagalli M, Cicalese A, Piccinin S, Gasparini P, Luise C, Schurra C, Garre M, Nuciforo PG, Bensimon A, Maestro R, Pelicci PG and d'Adda di Fagnana F. Oncogene-induced senescence is a DNA damage response triggered by DNA hyper-replication. *Nature.* 2006; 444: 638-642.
24. Pedruzzi I, Dubouloz F, Cameroni E, Wanke V, Roosen J, Winderickx J and De Virgilio C. TOR and PKA signaling pathways converge on the protein kinase Rim15 to control entry into G0. *Mol Cell.* 2003; 12: 1607-1613.
25. Chu IM, Hengst L and Slingerland JM. The Cdk inhibitor p27 in human cancer: prognostic potential and relevance to anticancer therapy. *Nat Rev Cancer* 2008; 8: 253-267.
26. Schneider BL, Yang Q-H and Futcher AB. Linkage of replication to start by the cdk inhibitor *sic1*. *Science.* 1996; 272: 560-562.
27. Zinzalla V, Graziola M, Mastriani A, Vanoni M and Alberghina L. Rapamycin-mediated G1 arrest involves regulation of the Cdk inhibitor *Sic1* in *Saccharomyces cerevisiae*. *Mol Microbiol.* 2007; 63: 1482-1494.
28. Hardie DG, Carling D and Carlson M. The AMP-activated/SNF1 protein kinase subfamily: metabolic sensors of the eukaryotic cell? *Annu Rev Biochem.* 1998; 67: 821-855.
29. Jones RG, Plas DR, Kubek S, Buzzai M, Mu J, Xu Y, Birnbaum MJ and Thompson CB. AMP-activated protein kinase induces a p53-dependent metabolic checkpoint. *Mol Cell.* 2005; 18: 283-293.
30. Schlotterer A, Kukudov G, Bozorgmehr F, Hutter H, Du X, Oikonomou D, Ibrahim Y, Pfisterer F, Rabbani N, Thornalley P, Sayed A, Fleming T, Humpert P, Schwenger V, Zeier M, Hamann A, Stern D, Brownlee M, Bierhaus A, Nawroth P and Morcos M. *C. elegans* as model for the study of high glucose-mediated life span reduction. *Diabetes.* 2009; 58: 2450-2456.
31. Sheu ML, Ho FM, Chao KF, Kuo ML and Liu SH. Activation of phosphoinositide 3-kinase in response to high glucose leads to regulation of reactive oxygen species-related nuclear factor-kappaB activation and cyclooxygenase-2 expression in mesangial cells. *Mol Pharmacol.* 2004; 66: 187-196.
32. d'Adda di Fagnana F. Living on a break: cellular senescence as a DNA-damage response. *Nat Rev Cancer.* 2008; 8: 512-522.
33. Halazonetis TD, Gorgoulis VG and Bartek J. An oncogene-induced DNA damage model for cancer development. *Science.* 2008; 319: 1352-1355.
34. Ksiazek K, Passos JF, Olijslagers S and von Zglinicki T. Mitochondrial dysfunction is a possible cause of accelerated senescence of mesothelial cells exposed to high glucose. *Biochem Biophys Res Commun.* 2008; 366: 793-799.
35. Yokoi T, Fukuo K, Yasuda O, Hotta M, Miyazaki J, Takemura Y, Kawamoto H, Ichijo H and Ogiwara T. Apoptosis signal-regulating kinase 1 mediates cellular senescence induced by high glucose in endothelial cells. *Diabetes* 2006; 55: 1660-5.
36. Herker E, Jungwirth H, Lehmann KA, Maldener C, Frohlich KU, Wissing S, Buttner S, Fehr M, Sigrist S and Madeo F. Chronological aging leads to apoptosis in yeast. *J Cell Biol.* 2004; 164: 501-507.
37. Fabrizio P, Battistella L, Vardavas R, Gattazzo C, Liou LL, Diaspro A, Dossen JW, Gralla EB and Longo VD. Superoxide is a mediator of an altruistic aging program in *Saccharomyces cerevisiae*. *J Cell Biol.* 2004; 166: 1055-1067.
38. Fabrizio P, Pletcher SD, Minois N, Vaupel JW and Longo VD. Chronological aging-independent replicative life span regulation by *Msn2/Msn4* and *Sod2* in *Saccharomyces cerevisiae*. *FEBS Lett.* 2004; 557: 136-142.
39. Lam YT, Stocker R and Dawes IW. The lipophilic antioxidants alpha-tocopherol and coenzyme Q10 reduce the replicative lifespan of *Saccharomyces cerevisiae*. *Free Radic Biol Med.* 49:237-244.
40. Sarsour EH, Venkataraman S, Kalen AL, Oberley LW and Goswami PC. Manganese superoxide dismutase activity regulates transitions between quiescent and proliferative growth. *Ageing Cell.* 2008; 7: 405-417.
41. Almeida B, Ohlmeier S, Almeida AJ, Madeo F, Leao C, Rodrigues F and Ludovico P. Yeast protein expression profile during acetic acid-induced apoptosis indicates causal involvement of the TOR pathway. *Proteomics.* 2009; 9: 720-732.
42. Colombo S, Ma P, Cauwenberg L, Winderickx J, Crauwels M, Teunissen A, Nauwelaers D, de Winder JH, Gorwa MF, Colavizza D and Thevelein JM. Involvement of distinct G-proteins, *Gpa2* and *Ras*, in glucose- and intracellular acidification-induced cAMP signalling in the yeast *Saccharomyces cerevisiae*. *EMBO J* 1998; 17: 3326-3341.
43. Lastauskiene E and Citavicius D. Influence of RAS genes on yeast *Saccharomyces cerevisiae* cell viability in acid environment. *Biologija.* 2008; 54: 150-155.
44. Martinez D, Vermeulen M, Trevani A, Ceballos A, Sabatte J, Gamberale R, Alvarez ME, Salamone G, Tanos T, Coso OA and Geffner J. Extracellular acidosis induces neutrophil activation by a mechanism dependent on activation of phosphatidylinositol 3-kinase/Akt and ERK pathways. *J Immunol.* 2006; 176: 1163-1171.
45. Flacke JP, Kumar S, Kostin S, Reusch HP and Ladilov Y. Acidic preconditioning protects endothelial cells against apoptosis through p38- and Akt-dependent Bcl-xL overexpression. *Apoptosis.* 2009; 14: 90-96.
46. Lee YJ and Han HJ. Troglitazone ameliorates high glucose-induced EMT and dysfunction of SGLTs through PI3K/Akt, GSK-3(beta), Snail1, and (beta)-catenin in renal proximal tubule cells. *Am J Physiol Renal Physiol.* 2010; 298: 1263-1275.
47. Roux AE, Leroux A, Alaamery MA, Hoffman CS, Chartrand P, Ferbeyre G and Rokeach LA. Pro-aging effects of glucose signaling through a G protein-coupled glucose receptor in fission yeast. *PLoS Genet.* 2009; 5: e1000408.

48. Varandas S, Teixeira MJ, Marques JC, Aguiar A, Alves A and Bastos MSM. Glucose and fructose levels on grape skin: interference in *Lobesia botrana* behavior. *Anal. Chim. Acta.* 2004; 513: 351-355.
49. Marriott J, Robinson M., Karikari, S.K. Starch and sugar transformation during the ripening of plantains and bananas. *Journal of the Science of Food and Agriculture.* 2006; 32: 1021-1026.
50. O'Brien KM, Dirmeier R, Engle M and Poyton RO. Mitochondrial protein oxidation in yeast mutants lacking manganese-(MnSOD) or copper- and zinc-containing superoxide dismutase (CuZnSOD): evidence that MnSOD and CuZnSOD have both unique and overlapping functions in protecting mitochondrial proteins from oxidative damage. *J Biol Chem.* 2004; 279: 51817-51827.
51. Demir AB and Koc A. Assessment of chronological lifespan dependent molecular damages in yeast lacking mitochondrial antioxidant genes. *Biochem Biophys Res Commun.* 400: 106-110.
52. Andziak B, O'Connor TP, Qi W, DeWaal EM, Pierce A, Chaudhuri AR, Van Remmen H and Buffenstein R. High oxidative damage levels in the longest-living rodent, the naked mole-rat. *Aging Cell.* 2006; 5: 463-471.
53. Madia F, Wei M, Yuan V, Hu J, Gattazzo C, Pham P, Goodman MF and Longo VD. Oncogene homologue Sch9 promotes age-dependent mutations by a superoxide and Rev1/Polzeta-dependent mechanism. *J Cell Biol.* 2009; 186: 509-523.
54. Palermo V, Cundari E, Mangiapelo E, Falcone C and Mazzoni C. Yeast *Ism* pro-apoptotic mutants show defects in S phase entry and progression. *Cell Cycle.* 2010; 9: 3991-6.
55. Fabrizio P, Hoon S, Shamalasab M, Galbani A, Wei M, Giaever G, Nislow C and Longo VD. Genome-wide screen in *Saccharomyces cerevisiae* identifies vacuolar protein sorting, autophagy, biosynthetic, and tRNA methylation genes involved in life span regulation. *PLoS Genet.* 6: e1001024.
56. Herrup K and Yang Y. Cell cycle regulation in the postmitotic neuron: oxymoron or new biology? *Nat Rev Neurosci.* 2007; 8: 368-378.
57. Zanetti M, Zwacka R, Engelhardt J, Katusic Z and O'Brien T. Superoxide anions and endothelial cell proliferation in normoglycemia and hyperglycemia. *Arterioscler Thromb Vasc Biol.* 2001; 21: 195-200.
58. Chaudhuri L, Sarsour EH and Goswami PC. 2-(4-Chlorophenyl)benzo-1,4-quinone induced ROS-signaling inhibits proliferation in human non-malignant prostate epithelial cells. *Environ Int.* 2010; 36:924-930.
59. Luo J, Solimini NL and Elledge SJ. Principles of cancer therapy: oncogene and non-oncogene addiction. *Cell.* 2009; 136: 823-837.
60. Lorenzi M, Cagliero E and Toledo S. Glucose toxicity for human endothelial cells in culture. Delayed replication, disturbed cell cycle, and accelerated death. *Diabetes.* 1985; 34: 621-627.
61. Madeo F, Tavernarakis N and Kroemer G. Can autophagy promote longevity? *Nat Cell Biol.* 12: 842-846.
62. Eisenberg T, Knauer H, Schauer A, Buttner S, Ruckenstein C, Carmona-Gutierrez D, Ring J, Schroeder S, Magnes C, Antonacci L, Fussi H, Deszcz L, et al. Induction of autophagy by spermidine promotes longevity. *Nat Cell Biol.* 2009; 11: 1305-1314.
63. Fabrizio P, Gattazzo C, Battistella L, Wei M, Cheng C, McGrew K and Longo VD. Sir2 blocks extreme life-span extension. *Cell.* 2005; 123: 655-6676.
64. Yang H, Ren Q and Zhang Z. Chromosome or chromatin condensation leads to meiosis or apoptosis in stationary yeast (*Saccharomyces cerevisiae*) cells. *FEMS Yeast Res.* 2006; 6: 1254-1263.

SUPPLEMENTARY FIGURES

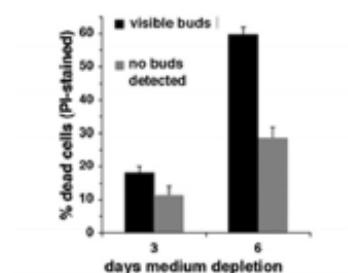


Figure S1. Identification of dead or dying cells in stationary phase by staining with the membrane-impermeable dye propidium iodide.

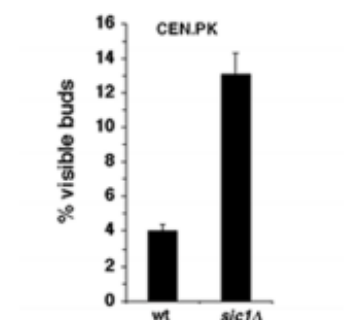


Figure S3. Inactivation of Sic1 inhibits growth arrest of stationary phase in G0/G1 in the CEN.PK background.

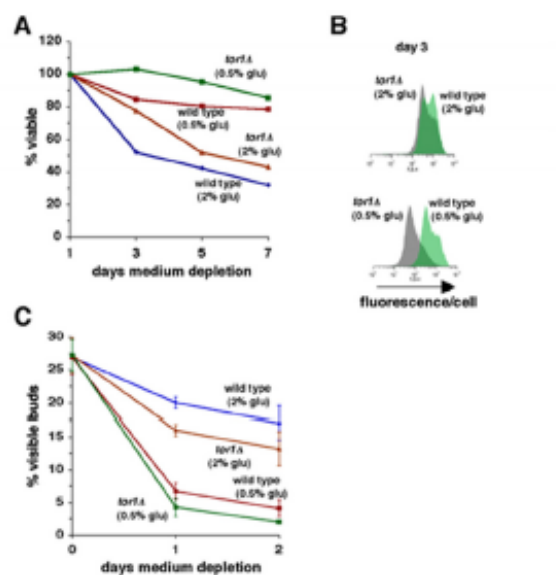


Figure S2. Effect of inactivation of TOR1 and/or caloric restriction on CLS (A), levels of superoxide anions detected by DHE (B) and fraction of cells that fail to arrest in G0/G1 stationary phase (C).

Table S1. Strains employed in this study

Strain	Genotype	Source
DBY746	<i>MATa leu2-3,112 his3Δ1 trp1-2889 ura3-52</i>	V. Longo Fabrizio et al Genetics 163:35, 2003)
DBY746 <i>rim15Δ</i>	<i>MATa leu2-3,112 his3Δ1 trp1-2889 ura3-52 rim15Δ::TRP1</i>	Constructed by inserting Xho-Sal fragment from pSR117 (see Fabrizio et al Genetics 163:35, 2003)
DBY746 <i>sch9Δ</i> (PF102)	<i>MATa leu2-3,112 his3Δ1 trp1-2889 ura3-52 sch9::URA3</i>	see Fabrizio et al Genetics 163:35, 2003
DBY746 <i>sch9Δ rim15Δ</i>	<i>MATa leu2-3,112 his3Δ1 trp1-2889 ura3-52 sch9::URA3 rim15::LEU2</i>	Paola Fabrizio (see Science 292:288 2001)
BY4741	<i>MATa his3Δ leu2Δ met15Δ ura3Δ</i>	Open Biosystems
BY4741 <i>sic1Δ</i>	<i>MATa his3Δ leu Δ met15Δ uraΔ ΔYRL079W</i>	Open Biosystems
BY4741 <i>snf1Δ</i>	<i>MATa his3Δ leu2Δ met15Δ ura3Δ ΔYDR477W</i>	Open Biosystems
BY 4742	<i>MATalpha his3Δ1 leu2Δ lys2Δ0 ura3Δ</i>	Paula Ludovico
BY 4742 <i>cta1Δ</i>	<i>MATalpha his3Δ leu2Δ lys2Δ ura3Δ cta1Δ</i>	Paula Ludovico
BY 4742 <i>ctt1Δ</i>	<i>MATalpha his3Δ leu2Δ lys2Δ ura3Δ ctt1Δ</i>	Paula Ludovico
W303-1A	<i>MATa ade2-1 ura3-1 his3-11 trp1-1 leu2-3 can1-100</i>	Bruce Stillman
MTy767 (W303 <i>sic1Δ</i>)	<i>MATa ade2-1 ura3-1 his3-11 trp1-1 leu2-3 can1-100 sic1::URA3</i>	Mike Tyers
Y604 (W303 <i>mec1-21</i>)	<i>MATa ade2-1 ura3-1 his3-11 trp1-1 leu2-3 can1-100 mec1-21</i>	Steve Elledge
W303 <i>rad53-21</i>	<i>MATa ade2-1 ura3-1 his3-11 trp1-1 leu2-3 can1-100 rad53-21</i>	Steve Elledge

